ISSN 0021-9673

VOL. 655 NO. 1 NOVEMBER 26, 1993

21st Sci. Meet. of the Spanish Group of Chromatography and Related Techniques Granada, October 21–23, 1992

JOURNAL OF CHROMATOGRAPHY A

INCLUDING ELECTROPHORESIS AND OTHER SEPARATION METHODS

SYMPOSIUM VOLUMES

JOURNAL OF CHROMATOGRAPHY A

INCLUDING ELECTROPHORESIS AND OTHER SEPARATION METHODS

Scope. The *Journal of Chromatography A* publishes papers on all aspects of **chromatography, electrophoresis** and related methods. Contributions consist mainly of research papers dealing with chromatographic theory, instrumental developments and their applications. In the *Symposium volumes*, which are under separate editorship, proceedings of symposia on chromatography, electrophoresis and related methods are published. *Journal of Chromatography B: Biomedical Applications* —This journal, which is under separate editorship, deals with the following aspects: developments in and applications of chromatographic and electrophoretic techniques related to clinical diagnosis or alterations during medical treatment; screening and profiling of body fluids or tissues related to the analysis of active substances and to metabolic disorders; drug level monitoring and pharmacokinetic studies; clinical toxicology; forensic medicine; veterinary medicine; occupational medicine; results from basic medical research with direct consequences in clinical practice.

Submission of Papers. The preferred medium of submission is on disk with accompanying manuscript (see *Electronic manuscripts* in the Instructions to Authors, which can be obtained from the publisher, Elsevier Science Publishers B.V., P.O. Box 330, 1000 AH Amsterdam, Netherlands). Manuscripts (in English; *four* copies are required) should be submitted to: Editorial Office of *Journal of Chromatography A*, P.O. Box 681, 1000 AR Amsterdam, Netherlands, Telefax (+31-20) 5862 304, or to: The Editor of *Journal of Chromatography B: Biomedical Applications*, P.O. Box 681, 1000 AR Amsterdam, Netherlands. Review articles are invited or proposed in writing to the Editors who welcome suggestions for subjects. An outline of the proposed review should first be forwarded to the Editors for preliminary discussion prior to preparation. Submission of an article is understood to imply that the article is original and unpublished and is not being considered for publication elsewhere. For copyright regulations, see below.

Publication information. *Journal of Chromatography A* (ISSN 0021-9673): for 1994 Vols. 652–682 are scheduled for publication. *Journal of Chromatography B: Biomedical Applications* (ISSN 0378-4347): for 1994 Vols. 652–662 are scheduled for publication. Subscription prices for *Journal of Chromatography A*, *Journal of Chromatography B: Biomedical Applications* or a combined subscription are available upon request from the publisher. Subscriptions are accepted on a prepaid basis only and are entered on a calendar year basis. Issues are sent by surface mail except to the following countries where air delivery via SAL is ensured: Argentina, Australia, Brazil, Canada, China, Hong Kong, India, Israel, Japan, Malaysia, Mexico, New Zealand, Pakistan, Singapore, South Africa, South Korea, Taiwan, Thailand, USA. For all other countries airmail rates are available upon request. Claims for missing issues must be made within six months of our publication (mailing) date. Please address all your requests regarding orders and subscription queries to: Elsevier Science Publishers, Journal Department, P.O. Box 211, 1000 AE Amsterdam, Netherlands. Tel.: (+31-20) 5803 642; Fax: (+31-20) 5803 598. Customers in the USA and Canada wishing information on this and other Elsevier journals, please contact Journal Information Center, Elsevier Science Publishing Co. Inc., 655 Avenue of the Americas, New York, NY 10010, USA, Tel. (+1-212) 633 3750, Telefax (+1-212) 633 3764.

Abstracts/Contents Lists published in Analytical Abstracts, Biochemical Abstracts, Biological Abstracts, Chemical Abstracts, Chemical Titles, Chromatography Abstracts, Current Awareness in Biological Sciences (CABS), Current Contents/Life Sciences, Current Contents/Physical, Chemical & Earth Sciences, Deep-Sea Research/Part B: Oceanographic Literature Review, Excerpta Medica, Index Medicus, Mass Spectrometry Bulletin, PASCAL-CNRS, Referativnyi Zhurnal, Research Alert and Science Citation Index.

US Mailing Notice. *Journal of Chromatography A* (ISSN 0021-9673) is published weekly (total 52 issues) by Elsevier Science Publishers (Sara Burgerhartstraat 25, P.O. Box 211, 1000 AE Amsterdam, Netherlands). Annual subscription price in the USA US$ 5132.25 (US$ price valid in North, Central and South America only) including air speed delivery. Second class postage paid at Jamaica, NY 11431. **USA POSTMASTERS**: Send address changes to *Journal of Chromatography A*, Publications Expediting, Inc., 200 Meacham Avenue, Elmont, NY 11003. Airfreight and mailing in the USA by Publications Expediting.

See inside back cover for Publication Schedule, Information for Authors and information on Advertisements.

0021-9673/93/$06.00

For Contents see p. VII.

JOURNAL OF CHROMATOGRAPHY A

VOL. 655 (1993)

JOURNAL OF CHROMATOGRAPHY A

INCLUDING ELECTROPHORESIS AND OTHER SEPARATION METHODS

SYMPOSIUM VOLUMES

ELSEVIER

AMSTERDAM — LONDON — NEW YORK — TOKYO

The Alhambra from the Albaycin

0021-9673/93/$06.00

Printed in the Netherlands

SYMPOSIUM ISSUE

21ST SCIENTIFIC MEETING OF THE GROUP OF CHROMATOGRAPHY AND RELATED TECHNIQUES OF THE SPANISH ROYAL SOCIETY OF CHEMISTRY

Granada (Spain), October 21–23, 1992

Guest Editors

E. GELPÍ
(Barcelona)

J.O. GRIMALT
(Barcelona)

CONTENTS

21ST SCIENTIFIC MEETING OF THE SPANISH GROUP OF CHROMATOGRAPHY AND RELATED TECHNIQUES, GRANADA, OCTOBER 21–23, 1992

Journal of Chromatography A, 655 (1993) 1
Elsevier Science Publishers B.V., Amsterdam

CHROM. 25 644

Foreword

The 21st Annual Scientific Meeting of the Grupo de Cromatografía y Técnicas Afines (GCTA or the Group of Chromatography and Related Techniques) of the Spanish Royal Society of Chemistry was held from October 21 to 23 in Granada, Andalucia, south Spain. This historically rich city contains some of the most beautiful remains of the Arab civilization which ruled this region until the end of the XV Century.

The meeting took place in the brand new Palacio de Exposiciones y Congresos, a few months after its opening. It was the 21st in a series of yearly meetings which have taken place since the constitution of GCTA whose membership, from academia and industry in Spain, now approaches 700. On this occasion, it was attended by 170 chromatographers who presented a total of 128 communications and had the opportunity of listening to interesting invited lectures by W. König (Enantioselective GC), T.E. Beesley (Chiral separation by HPLC), J.W. Dolan (Troubleshooting nightmares in HPLC), S. Trestianu (Large volume sample injection in capillary GC) and J. Segura (Analytical developments for doping control in the Olympic Games). These scientific presentations were completed by poster sessions and round table discussions (analysis of volatile organic compounds, SCF extraction, sample handling for chromatography).

The scientific content of forty-one of the communications presented at this meeting and selected by us were developed into full manuscripts and submitted for publication in the *Journal of Chromatography*. Of these, a total of 40 have been accepted after the usual review procedures and 22 of them are collected in this issue. The present issue is similar to that corresponding to the previous Donostia-San Sebastian Meeting in 1991 (Vol. 607, No. 2) and represents another milestone witnessing the progress of the chromatographic sciences in Spain. We always thought that there was more chromatographic activity in our country than was reflected in the number of journal publications from Spanish laboratories. These collective issues have certainly encouraged a substantial amount of activity to come to light.

We would like to thank the Organizing Committee for their efforts to ensure an enjoyable meeting, both from a scientific and a social viewpoint. We wish, particularly, to express our thanks and congratulations to Drs. Juan Carlos Orte and Manuel Miro (Faculty of Pharmacy, University of Granada) who, as secretaries of the event, demonstrated high organizational skills. We also thank the 20 companies active in the field of chromatography who participated in the Technical Exhibition and provided an excellent updated summary of the new instruments, columns and other complements which have recently been developed in separation science.

Emilio Gelpí
Barcelona (Spain) Joan O. Grimalt

Journal of Chromatography A, 655 (1993) 3–9
Elsevier Science Publishers B.V., Amsterdam

CHROM. 25 001

Solution properties of polyelectrolytes

IX☆. Quantitative dependence on eluent ionic strength of elution volumes in aqueous size-exclusion chromatography

Rosa García, Iolanda Porcar, Agustín Campos, Vicente Soria and Juan E. Figueruelo*

Departament de Química Física, Universitat de València, E-46100 Burjassot, València (Spain)

ABSTRACT

Quantitative evaluation of elution volumes (V_e) of polyelectrolytes in salt-containing eluents was performed, taking into account electric double-layer effects and the effective radius of polyions, and assuming that polyelectrolytes behave as rigid hydrodynamic spheres and that the geometry of gel pores is cylindrical. A polynomial V_e dependence on ionic strength (I) was obtained, namely a second order one in $I^{-1/2}$. The semi-empirical polynomial coefficients depend on column characteristics, namely V_0 (interstitial volume), V_p (total pore volume) and a (mean pore radius), as well as on effective coil radius (R_η) and on k (a parameter related to the electric effects). Fair correlations between predicted and measured elution volumes for uncharged polymers hold, at least for the polyelectrolyte–gel systems tested here: polyelectrolytes poly(L-glutamic acid), sodium poly(styrene sulphonate) and poly(acrylic acid); gels Spherogel TSK PW4000 and Ultrahydrogel 250.

INTRODUCTION

Aqueous size-exclusion chromatography (ASEC) has become a useful analytical and preparative technique for separating macromolecules of different size, shape and charge. However, several problems associated with ASEC, termed non-exclusion or secondary effects, usually interfere with a pure size-exclusion mechanism.

According to Barth [1], secondary effects can be divided into two types, ionic and adsorption effects. Ion-exchange, ion-inclusion, ion-exclusion and intramolecular electrostatic effects are of the first type, and hydrogen bonding, hydrophobic and attractive ionic interactions are of the second type. A considerable literature on these effects exists [2–4].

Electrolyte-containing eluents are often used for the total suppression or minimization of the ionic effects. However, when the ionic strength of the eluent increases, the elution profile for a given polyelectrolyte becomes broader, so that a poorer resolution is achieved experimentally; the reasons for this behaviour are still unclear [5].

The use of salt-containing eluents affects the solution properties of the polyion as well as its elution volume in ASEC. On the one hand, the intrinsic viscosity of a polyelectrolyte decreases sharply with increasing ionic strength [6–9], as would be expected by the increasing screening of polyion charge. On the other hand, the shrink-

* Corresponding author.
☆ For part VIII, see ref. 21.

0021-9673/93/$06.00

age of the coil with increasing ionic strength is not the only effect responsible for the shifts towards higher elution volumes of polyelectrolyte occurring in ASEC in the presence of extra salts. Other effects, such as the diminution of charge density on a gel surface in the presence of salts, should also be taken into account [10]. However, to date, a quantitative evaluation of each contribution has not been undertaken.

In this context, considerable efforts have been made to quantify the aforementioned ASEC secondary effects, most of them based on experimental evidence obtained with model charged polymers on packing materials of very different nature. The model of Dubin and co-workers [11–13] to predict ion-exclusion effects based on the reduction in the pore volume accessible to polyions deserves mention. They calculate a repulsion volume as a function of an electrostatic potential of the stationary phase. An empirical correlation between the repulsion volume and eluent ionic strength based on the Debye–Hückel theory has also been proposed by Mori [14]. Styring and co-workers [15,16] have established a semi-empirical approach that takes into account exclusively the electrostatic double layer around the polyion and proposes a linear dependence of the elution volumes with the inverse of the square root of the ionic strength (I). Recently, Potschka [17] has reported on the ionic strength dependency of elution in SEC of DNA, proteins and viruses, and has found that chromatographic radii of these macromolecules increase linearly with $I^{-1/2}$. We have also reported an empirical relationship in terms of polymer-support compatibility accounting for solute–matrix attractive/repulsive interactions [10]. It makes use of the thermodynamic formalism previously developed for uncharged polymers [18,19]. Finally, Hoagland [20] has formulated a theoretical treatment on electrostatic interactions of rod-like polyelectrolytes with repulsive, charged surfaces.

In this paper, the dependence on ionic strength of elution volumes of polyions in ASEC is studied. Shifts in elution volumes are quantitatively interpreted in terms of coil dimensions, as defined by hydrodynamic effective radii, mean pore radius of gel and electrical double-layer effects. Chromatographic data reported in an earlier paper [21], for sodium poly(styrene sulphonate), poly(acrylic acid) and poly(L-glutamic acid) at different ionic strengths, have been used to test the validity of the proposed semi-empirical equation.

EXPERIMENTAL

Chemical and reagents

Dextran samples purchased from Pharmacia (Uppsala, Sweden) with nominal molar masses of 10 000, 17 700, 40 000, 66 900, 83 300, 170 000, 500 000 and 2 000 000 g mol^{-1}, were used as the standards for uncharged polymers. The chromatographic low-molar-mass range was covered by poly(ethylene oxide) (PEO) standards with molar masses 2000 and 4000 g mol^{-1}, from Fluka (Darmstadt, Germany). The polyelectrolytes tested were samples of poly(L-glutamic acid) (PGA) from Sigma (St. Louis, MO, USA), sodium poly(styrene sulphonate) (PSS) from Pressure Chemical (Pittsburgh, PA, USA) and poly(acrylic acid) (PAA) from Aldrich (Milwaukee, WI, USA). Their nominal molar masses (in g mol^{-1}) and the code used along the paper were: 13 600 (PGA-1), 43 000 (PGA-2), 77 800 (PGA-3), 1600 (PSS-1), 16 000 (PSS-2), 31 000 (PSS-3), 88 000 (PSS-4), 177 000 (PSS-5), 5000 (PAA-1), 90 000 (PAA-2) and 250 000 (PAA-3). All samples showed polydispersities lower than 1.1.

Solvents used for viscometric measurements and as eluents in SEC were buffers made up from sodium dihydrogenphosphate and disodium hydrogenphosphate for pH 7.0 and from sodium acetate and acetic acid for pH 5.0. Desired ionic strengths were adjusted from 0.005 to 0.20 M. Reagents used in the preparation of buffers were analytical grade from Merck (Darmstadt, Germany).

Viscosities

Intrinsic viscosity values $[\eta]$ fro uncharged polymers in pure water at 25.0 ± 0.1°C were evaluated through the viscometric equations $[\eta] = 97.8 \cdot 10^{-3} M^{0.50}$ ml g^{-1} for dextran [22] and $[\eta] = 2.0 + 0.016\ M^{0.76}$ ml g^{-1} for PEO [23], where M stands for molar mass. The effects of

ionic strength and pH on the viscosity of non-ionic polymers were neglected [11].

Viscosity measurements of polyelectrolyte samples at 25.0 ± 0.1°C were performed with an automatic AVS 440 Ubbelohde-type capillary viscometer from Schott Geräte (Hofheim, Germany). Details of the experimental conditions and procedure have been reported previously [21].

Chromatography

The liquid chromatographic equipment has been described elsewhere [21]. The columns used were an Ultrahydrogel 250 (UHG-250) packed with hydroxylated poly(methacrylate)-based gel of 250 Å nominal pore size and 30 × 0.78 cm I.D. from Waters (Milford, MA, USA), and a Spherogel TSK PW4000 packed with hydroxylated polyether copolymer of 500 Å nominal pore diameter and 30 × 0.75 cm. I.D. from Beckman Instruments (Galway, Ireland). Experimental details for obtaining chromatograms of samples and their elution volumes have been reported in an earlier paper [21]. Exclusion volumes, V_0, and total column volumes, V_T, were 5.48 and 10.46 ml for the UHG-250 column, and 5.15 and 10.40 ml for the TSK one, as determined with blue dextran ($M = 2\,000\,000$ g mol^{-1}) and ^2H_2O, respectively.

RESULTS AND DISCUSSION

Intrinsic viscosity, $[\eta]_I$, like other properties of polyelectrolytes in aqueous solution, follows a linear dependence with the inverse square root of the ionic strength:

$$[\eta]_I = [\eta]_\infty + SI^{-1/2} \quad (1)$$

where $[\eta]_I$ stands for the intrinsic viscosity at ionic strength I, $[\eta]_\infty$ is the intrinsic viscosity extrapolated at infinite ionic strength and S is related to the stiffness (or the flexibility) of the macromolecule according to the Odijk's treatment [24]. Plots of eqn. 1 for the polyelectrolyte–gel systems studied in this work have been reported previously [21], and all of them exhibit a good linear correlation.

The hydrodynamic radius or effective radius of neutral polymers, R_η, and of polyelectrolytes, R'_η, are related to the hydrodynamic volume, $M[\eta]$, through [25]:

$$R_\eta = \left(\frac{3 \cdot 10^{23} M[\eta]}{\pi N_A}\right)^{1/3} \quad (2a)$$

and

$$R'_\eta = \left(\frac{3 \cdot 10^{23} M[\eta]_I}{\pi N_A}\right)^{1/3} \quad (2b)$$

respectively, where M is the macromolecule molar mass and N_A Avogadro's number. Units for R_η are Å if $[\eta]$ is in ml g^{-1}.

On the other hand, Styring and co-workers [15,16] proposed a model to explain the variation in elution volumes of polyelectrolytes with ionic strength. This model, based on the assumption that the polyion electric double-layer thickness in the Gouy–Chapman approximation varies with $I^{-1/2}$, as $[\eta]_I$ does, leads to:

$$R'_\eta = R_\eta + kI^{-1/2} \quad (3)$$

where k is a constant in which the double-layer parameters are enclosed, and the intercept values should correspond to the physical (or geometrical) radius of the uncharged polyelectrolyte due to the screening of charges by the counterions occurring along the chain at high ionic strength, that is when $I \rightarrow \infty$.

Eqn. 3 plots for PGA, PSS and PAA are shown in Fig. 1a–c. As can be seen, all systems show excellent linear dependencies. The slope, k, accounts for the electrostatic repulsive effect, and its value increases with the molar mass of sample (or with the charge of the macromolecule).

The elution volumes in SEC of a neutral polymer, V_e [26], and of a polyelectrolyte, V'_e [11], can be respectively written as:

$$V_e = V_0 + K_{SEC} V_p \quad (4a)$$

$$V'_e = V_0 + K'_{SEC} V_p \quad (4b)$$

where V_0 is the interstitial packing volume and V_p is the total pore volume. K_{SEC} represents the partition coefficient when the steric mechanism is the only one accounting for solute separation, and the partition coefficient K'_{SEC} takes into

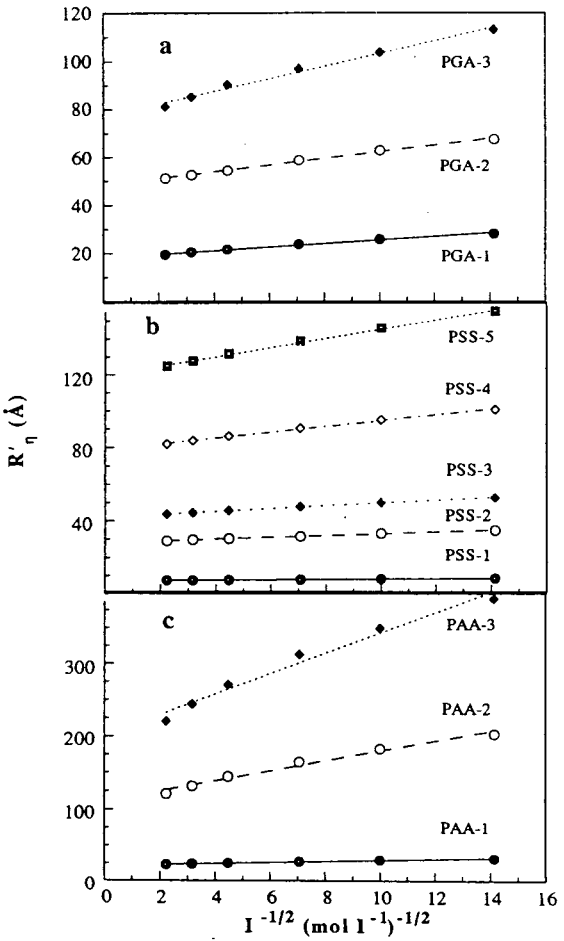

Fig. 1. Effective radius, R'_η, dependence on ionic strength, I, for different polyelectrolytes: (a) poly(L-glutamic acid), PGA; (b) poly(styrene sulphonate), PSS; (c) poly(acrylic acid), PAA.

account steric and other secondary mechanisms. Thus, $K'_{SEC} < 1$ when solute–gel electrostatic interactions become important and $K'_{SEC} > 1$ if adsorption of solute onto the stationary phase occurs. By analogy with the expression of Casassa [27] derived for the permeation of spheres in cylindrical cavities, K_{SEC} and K'_{SEC} can be written as:

$$K_{SEC} = \left(\frac{a - R_\eta}{a}\right)^2 \quad (5a)$$

$$K'_{SEC} = \left(\frac{a - R'_\eta}{a}\right)^2 \quad (5b)$$

with a standing for the mean pore radius of cylinder. By substitution of R'_η given by eqn. 3 into eqn. 5b and further introduction of the obtained K'_{SEC} in eqn. 4b, Styring *et al.* [16] found the following V'_e dependence with I:

$$V'_e = V_\infty - k_{el} I^{-1/2} \quad (6)$$

where V_∞ stands for the elution volume of a polyanion when $I \rightarrow \infty$, *e.g.* when it becomes an uncharged polymer (or when the solute–gel repulsive interactions disappear), and k_{el} is a constant containing double-layer parameters, cylinder pore radius and total pore volume.

V'_e *vs.* $I^{-1/2}$ plots are depicted in Fig. 2 for PGA in TSK PW4000 (Fig. 2a) and PGA in UHG-250 (Fig. 2b) columns, both at pH 7.0. As can be seen, the expected eqn. 6 dependence is not followed by the systems so far represented, as also occurs with Mori's data on PSS in an FPG(500 + 170) porous glass column [14], as shown in Fig. 3. Similar results have also been found for the PSS–UHG-250, PAA–TSK

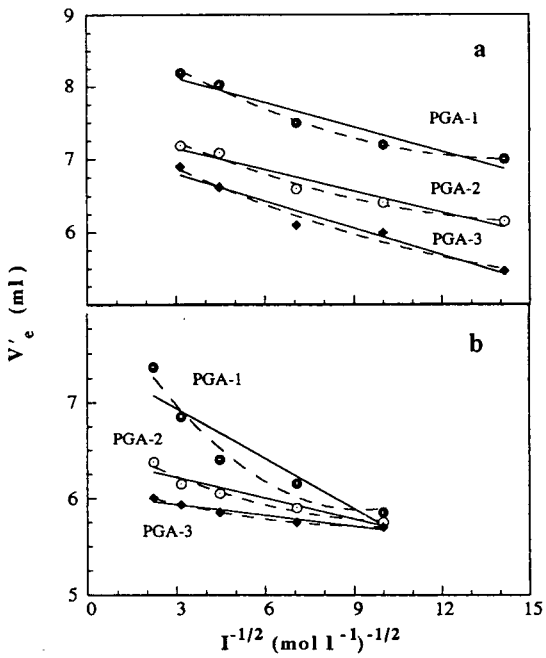

Fig. 2. Elution volume dependence on ionic strength for PGA at pH 7.0 on TSK PW4000 (a) and UHG-250 (b) columns. Points stand for experimental data, solid lines for fits according to eqn. 6 and dashed lines according to eqn. 8.

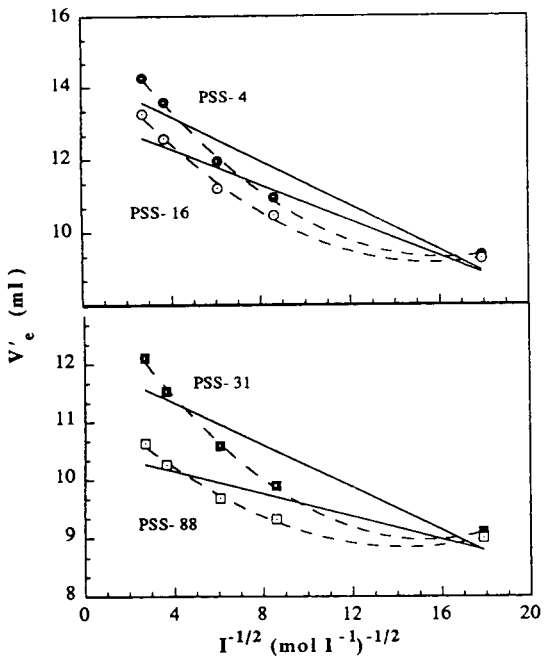

Fig. 3. Elution volume dependence on ionic strength for PSS (4, 16, 31 and 88 refer to molecular masses 4000, 16 000, 31 000 and 88 000, respectively) at pH 8.0 on an FPG(500 + 170) porous glass column (data extracted from Fig. 1 in ref. 14). Symbols as in Fig. 2.

PW4000 and PAA–UHG-250 polyelectrolyte–gel systems here studied and with other systems described previously [12,14,28].

A repetition of the above Styring manipulation, that is substitution of R'_η give by eqn. 3 into eqn. 5b with expansion now of the square term and final substitution of K'_{SEC} into eqn. 4b, leads to:

$$V'_e = V_0 + \left(\frac{a - R_\eta}{a}\right)^2 V_p - 2\left(\frac{a - R_\eta}{a}\right)\frac{k}{a} V_p I^{-1/2} + \frac{k^2}{a^2} V_p I^{-1} \quad (7)$$

or its simplified from (compare with eqns. 4a and 5a):

$$V'_e = V_e - AI^{-1/2} + BI^{-1} \quad (8)$$

where V_e is the elution volume of a polyion when $I \rightarrow \infty$ (equivalent to the V_∞ defined in ref. 16) and A and B are constants accounting for electrostatic effects (through k) and for the characteristics of packings (through a and V_p).

When an ion-exclusion effect is the main mechanism governing SEC of polyanions, not a first-order V'_e dependence on $I^{-1/2}$, as claimed by Styring *et al.* [15], is obeyed, but a second-order one in agreement with eqn. 8 and the experimental results depicted in Figs. 2 and 3. In order to confirm that predicted V_e values obtained from eqn. 8 are more appropriate than those predicted by means of eqn. 6, in Fig. 4 both sets of V_e values are shown as "universal" calibration plots log $M[\eta]_\infty$ *vs.* V_e for the same systems as in Fig. 2, together with the reference curve for dextran (neutral polymer). As can be observed, predicted V_e values from eqn. 8 practically coincide with the reference calibration curve, which seems to indicate that polyelectrolyte becomes a neutral polymer, as expected, and it elutes by a steric mechanism. However, the data predicted by eqn. 6 describe far from ideal SEC behaviour,

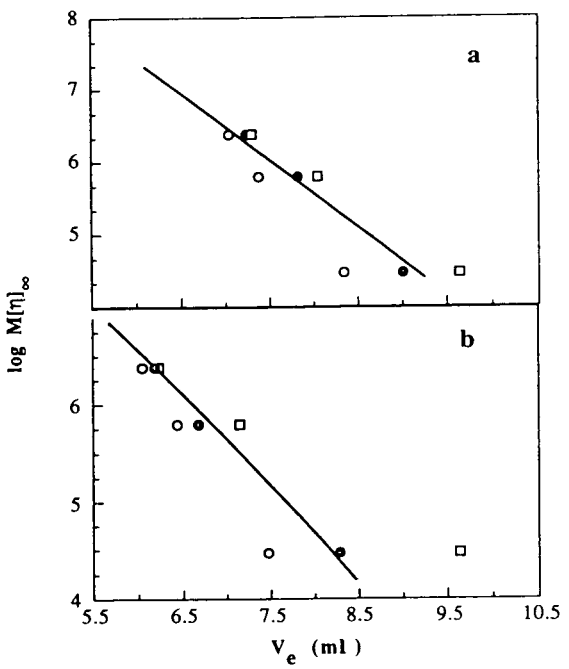

Fig. 4. Universal calibration plots for uncharged polymers. Solid line is the experimental calibration curve (dextran and PEO). Points stand for predicted values from data on PGA–TSK PW4000 (a) and on PGA–UHG-250 (b) systems: ○ = from eqn. 6; ● = from eqn. 8; □ = assuming spherical pore geometry.

the more so the lower the molar mass of samples. Universal calibration graphs for PSS in an FPG(500 + 170) column together with the reference pullulan one [14] are shown in Fig. 5. Again, the best prediction of elution volumes when $I \rightarrow \infty$ is achieved through the intercepts of eqn. 8, as is also the case for the other systems tested so far. Therefore, V_e' dependence on ionic strength seems to obey to a second-order polynomial on $I^{-1/2}$, at least in the range of low to moderate ionic strength, whereas electrostatic factors are the dominant ones in the SEC mechanism.

On the other hand, some comments on the assumption made about the geometry of pores deserves to be made. Exponent 2 in eqn. 5 indicates that the most likely pore shape is cylindrical. If a spherical geometry is assumed, the above-mentioned exponent should be 3, and therefore an expression for V_e' dependent on $I^{-3/2}$ should be obtained. When fitting the experimental data to a third-order polynomial on $I^{-1/2}$, the corresponding intercepts yield overestimated values of V_e and theoretical calibration plots appear on the right-hand side of the reference one, as shown, as an example, in Figs. 4 and 5.

As a conclusion, a geometrical model in which the polymers are treated as rigid equivalent hydrodynamic spheres (see eqn. 2) and the pores as well-defined cylinders (see eqn. 5) seems to be the most appropriate to describe polyanion elution in aqueous SEC. However, the aforementioned treatment is intended to be a first approximation to the real problem, since it essentially neglects the potential due to the surface of the stationary phase, although this last contribution does not seem to be significant in organic-based hydrophilic gels, as it is the present case. A most rigorous treatment is currently in progress.

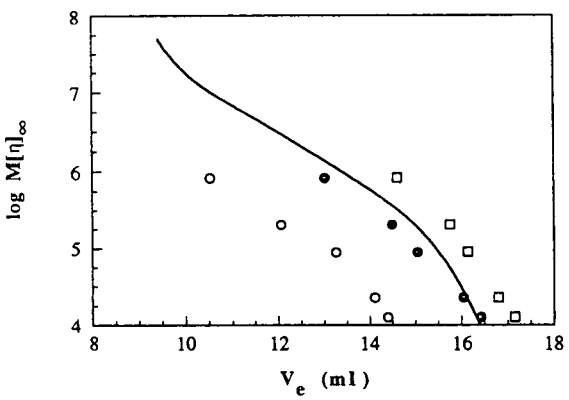

Fig. 5. Universal calibration plots for uncharged polymers. Solid line is the experimental calibration curve (pullulan). Points stand for predicted values from data on a PSS–FPG(500 + 170) system (see ref. 14). Symbols as in Fig. 4.

ACKNOWLEDGEMENTS

This work was partially supported by Grant No. PB91-0808 from DGICYT (Spain). One of the authors (I.P.) was a recipient of a long-term fellowship from Ministerio de Educación y Ciencia (Spain). We are also grateful to the Secretaría de Estado de Universidades (Spain; Grant No. OP90-0042) and to the Conselleria d'Educació i Ciència (Generalitat Valenciana, Spain) for computer support.

REFERENCES

1 H.G. Barth, *J. Chromatogr. Sci.*, 18 (1980) 409.
2 H.G. Barth and J.W. Mays (Editors), *Modern Methods of Polymer Characterization*, Wiley-Interscience, New York, 1991.
3 K.M. Gooding and F.E. Regnier, in K.M. Gooding and F.E. Regnier (Editors), *HPLC of Biological Macromolecules (Chromatographic Sciences Series*, Vol. 51), Marcel Dekker, New York, 1990, Ch. 3.
4 H.G. Barth and B.E. Boyes, *Anal. Chem.*, 64 (1992) 428R.
5 B. Stenlund, *Adv. Chromatogr.* 14 (1974) 37.
6 T. Okubo, *J. Phys. Chem.*, 93 (1989) 6860.
7 J. Cohen and Z. Priel, *Macromolecules*, 22 (1989) 2356.
8 W.F. Reed, S. Ghosh, G. Medjahdi and J. François, *Macromolecules*, 24 (1991) 6189.
9 J.L.M. Ganter, M. Milas and M. Rinaudo, *Polymer*, 33 (1992) 113.
10 E. Pérez-Payá, L. Braco, C. Abad, V. Soria and A. Campos, *J. Chromatogr.*, 548 (1991) 93.
11 P.L. Dubin and M.M. Tecklenburg, *Anal. Chem.*, 57 (1985) 275.
12 P.L. Dubin C.M. Speck and J.I. Kapland, *Anal. Chem.*, 60 (1988) 895.
13 P.L. Dubin, R.M. Larter, C.J. Wu and J.I. Kaplan, *J. Phys. Chem.*, 94 (1990) 7243.
14 S. Mori, *Anal. Chem.*, 61 (1989) 530.
15 M.G. Styring, C.J. Davison, C. Price and C. Booth, *J. Chem. Soc., Faraday Trans. I*, 80 (1984) 3051.

16 M.G. Styring, H.H. Teo, C. Price and C. Booth, *Eur. Polym. J.*, 24 (1988) 333.
17 M. Potschka, *Macroomolecules*, 242 (1991) 5023.
18 R. Tejero, R. Gavara, C. Gómez, B. Celda and A. Campos, *Polymer*, 28 (1987) 1455.
19 R. García, B. Celda, V. Soria, R. Tejero and A. Campos, *Polymer*, 31 (1990) 1694.
20 D.A. Hoagland, *Macromolecules*, 23 (1990) 2781.
21 R. García, I. Porcar, V. Soria, A. Campos and J.E. Figueruelo, *J. Chromatogr. A*, 655 (1993) in press.
22 F.R. Senti, N.N. Hellmann, N.H. Ludwing, G.E. Babcock, R. Tobin, C.A. Class and B. Lamberts, *J. Polym. Sci.*, 17 (1955) 527.
23 H.G. Elias, *Kunst.-Plast.*, 4 (1961) 1.
24 T. Odijk, *Biopolymers*, 18 (1979) 3111.
25 J. Janca, *Adv. Chromatogr.*, 19 (1981) 37.
26 E.F. Cassasa, *Sep. Sci.*, 6 (1971) 305.
27 E.F. Cassasa, *J. Phys. Chem.*, 75 (1971) 3929.
28 V. Soria, A. Campos, R. García, M.J. Parets, L. Braco and C. Abad, *J. Liq. Chromatogr.*, 13 (1990) 1785.

Journal of Chromatography A, 655 (1993) 11–20
Elsevier Science Publishers B.V., Amsterdam

CHROM. 25 088

Thermodynamic characterization of Superox 20M by inverse gas chromatography

E. Fernández-Sánchez, A. Fernández-Torres, J.A. García-Domínguez* and E. López de Blas☆

Instituto de Química Física "Rocasolano", CSIC, Serrano 119, 28006 Madrid (Spain)

ABSTRACT

Inverse gas chromatographic experiments carried out between 80 and 140°C were used to characterize Superox 20M deposited on glass capillary columns, using 28 substances belonging to five different chemical types. No absorption in the gas–liquid interphase was observed except in three cases corresponding to the highest molecular masses. The thermodynamic parameters of solution and mixing and the Flory–Huggins solute–stationary phase interaction parameter were measured. The dependences of all magnitudes on temperature and chain length were also calculated, and conclusions on the relationship between their values and the chromatographic behaviour of the solutes in the stationary phase were drawn. The solubility parameter of Superox 20M was measured between 80 and 140°C and was found to have a linear dependence on temperature. Values at 50, 64 and 280°C were deduced.

INTRODUCTION

Poly(ethylene oxide)s are among the most popular stationary phases for gas chromatography (GC). They have been used for years in the analysis of all kind of oxygenated compounds, and they are probably the most widely used polar stationary phases today. Carbowaxes and Superoxes are both poly(ethylene oxide)s, the latter, with higher molecular mass and without catalytic residues, having been prepared with capillary columns in mind. This type of polymer has been considered as "preferred stationary phases" [1,2]. The effect of immobilization on the phase transition of Superox 20M and therefore on the minimum allowed operating temperature (MAOT) has already been studied [3]. We report here a study of Superox 20M, at temperatures above its melting point, using capillary columns, involving the thermodynamic characterization of the polymer and its interactions with certain chemical functions, based on the chromatographic behaviour of various substances belonging to five different families.

Inverse gas chromatography (IGC), introduced in 1967 by Kiselev [4] and later developed in theory and methods mainly by Smidsrod and Guillet [5], is the term applied to a technique which uses GC as it is normally known by analysts, but with the interest focused on the substance which is used as the stationary phase in the chromatographic column. With this aim, selected solutes are injected into the chromatograph and information on the thermodynamic parameters of the solute–stationary phase system is deduced from the chromatographic retention parameters measured. The term "inverse" refers to the fact that, in conventional analytical GC, the type of sample to be analysed determines the selection of the most convenient stationary phase, whereas in IGC studies, the solutes are chosen so that the appropriate information on the stationary phase may be obtained.

* Corresponding author.
☆ Present address: Coritel SA, Pl. Pablo Picasso s/n, Edificio Serantes, 28020 Madrid, Spain.

0021-9673/93/$06.00

EXPERIMENTAL

Three glass capillary columns (drawn from borosilicate glass in a Shimadzu GBM-1B machine) with Superox 20M (Alltech, Deerfield, IL, USA) as stationary phase were prepared by the procedure described previously [3]: column tube deactivated from Carbowax 20M (Hewlett-Packard) and no immobilization of the polymer. The dimensions of the three columns are given in Table I.

The samples used were ethylbenzene from Aldrich (Gillingham, Dorset, UK), 2-heptanone, 2-octanone and 1-hexanol from Aldrich Chemie (Steinhein, Germany), 1-butanol and 2-pentanone from BDH (Poole, UK), *n*-heptane, *n*-octane, benzene and 1-pentanol from Carlo Erba (Milan, Italy), *n*-decane, *n*-dodecane, 2-pentanone, methyl formate, methyl acetate, methyl hexanoate, methyl heptanoate and methyl octanoate from Fluka (Buchs, Switzerland), acetone, *n*-hexane and propylbenzene from Merck-Schuchard (Germany), toluene from Merck (Darmstadt, Germany), propanol, from Probus (Barcelona, Spain), methanol from Riedel-de Haën (Seelze, Germany), *n*-nonane and *n*-undecane from Sigma (St. Louis, MO, USA), methyl butyrate from UCB (Brussels, Belgium) and pentylbenzene, synthesized in the laboratories of the Institute of General Organic Chemistry, CSIC (Madrid, Spain).

Two gas chromatographs (Hewlett-Packard HP-5890A) with flame ionization detectors and capillary column injectors, were modified to measure the carrier gas head pressure by means of pressure transducers (WIKA Tronic 891.13.500, Alexander Wiegand GmbH, Klingenberg, Germany). Atmospheric pressure was checked with a mercury barometer (precision 0.2 mmHg; 1 mmHg = 133.322 Pa). The density of Superox 20M at different temperatures was measured with a pycnometric procedure. Chromatograms were measured at 80, 100, 120 and 140°C.

TABLE I

DIMENSIONS OF THE THREE CAPILLARY COLUMNS

Parameter	Column		
	1	2	3
Length (m)	22.46	24.88	24.88
Inner diameter (mm)	0.259	0.287	0.287
Film thickness (μm)	0.275	0.151	0.351

DATA REDUCTION

Specific retention volumes (V_g) were calculated in the usual manner [6]. Activity coefficients at infinite dilution based on mass fraction, Ω_1^∞, were calculated according to the expression of Guillet and co-workers [7,8]. Vapour pressures were deduced using Antoine coefficients from various sources [9,10]. Second viral coefficients of *n*-alkanes were calculated by the method of O'Connell and Prausnitz [11]; for other substances, values were inter- or extrapolated from literature values corresponding to other temperatures [12]. Densities of the solutes were calculated according to the pertinent equation [13,14]. Molar volumes were deduced from molecular mass and density values.

Flory–Huggins interaction parameters, $\chi_{1,2}^\infty$ were calculated from the known expression [7,8,15]. Partial molar enthalpies of solution, ΔH_s, mixing, ΔH_m, and vaporization, ΔH_v, were deduced in each instance from experimental results [16]. Partial molar free energies of mixing were calculated from activity coefficients at infinite dilution [15]. Partial molar free energies of solution at infinite dilution were calculated from experimental values of V_g [15].

Solubility parameters of the solutes were deduced from the known expression, using the experimentally determined enthalpies of vaporization. Solubility parameters of the polymers used as stationary phases were deduced from a plot based on the expression of Price *et al.* [8]. The FORTRAN programs necessary to obtain the values of the different parameters were run on a personal computer.

The equations used for these calculations are given in the Appendix.

RESULTS AND DISCUSSION

Plots of V_g *versus* the inverse of the volume of the stationary phase in the column show that the values are equivalent, indicating no adsorption

of the solutes at any temperature (*i.e.*, the values are independent of the stationary phase loading) except for *n*-dodecane, *n*-pentylbenzene and methyl octanoate, which presented slightly lower values of V_g at higher loadings. In these three cases, the V_g values were corrected to infinite film thickness. All other figures presented here correspond to the experimental values obtained on the column made with the thickest film (column 3). Plots of values of log V_g *versus* $1/T$ showed correlation coefficients of 0.9999 or better in the three columns for all the solutes tested.

Solute–polymer interaction parameters ($\chi^{\infty}_{1,2}$)

The value of the Flory–Huggins solute–stationary phase interaction parameter, $\chi^{\infty}_{1,2}$, may be considered as an indicator of the behaviour of the solute as a solvent of the stationary phase, high values corresponding to substances that behave as poor solvents. Experimental values are given in Table II. Values of $\chi^{\infty}_{1,2}$ deduced from IGC experiments are averages of all possible interactions encountered in the solute–stationary phase system. It is clear that *n*-alkanes show values of $\chi^{\infty}_{1,2}$ that are much higher than those corresponding to other solutes. Therefore, it may be deduced that alkanes are poor solvents of Superox 20M, whereas alcohols, aromatics, esters and ketones may be considered as good solvents. Table II also shows that for any given homologous series, the solubility decreases with increasing chain length, as would be expected from the values obtained in the case of the *n*-alkanes.

The dependence of $\chi^{\infty}_{1,2}$ on temperature may be observed from examination of Table II. In some instances the points seem to fit a linear correlation, whereas in others the points describe a second-degree curve. As an example, Fig. 1 shows this dependence for *n*-alkanes and ketones and the fact that the values of $\chi^{\infty}_{1,2}$ decrease with increasing temperature. For all solutes tested, miscibility with the stationary phase increases with increasing temperature, indicating that solutes are leaving their upper critical solution temperature (UCST) [17,18], below which phase separation should occur in high-concentration solutions. The Flory–Huggins interaction parameter, $\chi^{\infty}_{1,2}$, has the physical meaning of a residual free energy [19] with a parabolic dependence on temperature between two values corresponding to the UCST and to the lower critical solution temperature (LCST) above which, again, phase separation takes place. The minimum of the curve corresponds to the region of maximum solubility. The trend of the values of $\chi^{\infty}_{1,2}$ indicates that all solutes will reach their maximum solubility in the stationary phase at temperatures above 140°C. Experiments with IGC are carried out under concentration conditions that are far from those where the critical conditions are satisfied (high solute concentration), but the shape of the curves is a good indication of the

TABLE II

SOLUTE–POLYMER INTERACTION PARAMETER, $\chi^{\infty}_{1,2}$, AT DIFFERENT TEMPERATURES

Solute	Temperature (K)			
	353	373	393	413
n-Hexane	1.32	1.09	0.91	0.72
n-Heptane	1.50	1.28	1.11	0.93
n-Octane	1.67	1.45	1.28	1.09
n-Nonane	1.82	1.59	1.44	1.23
n-Decane	1.97	1.72	1.56	1.35
n-Undecane	2.11	1.86	1.68	1.47
n-Dodecane	2.26	2.00	1.80	1.59
Benzene	−0.22	−0.28	−0.29	−0.34
Toluene	−0.04	−0.10	−0.11	−0.17
Ethylbenzene	0.14	0.07	0.07	0.02
n-Propylbenzene	0.29	0.22	0.20	0.15
n-Pentylbenzene	0.64	0.51	0.44	0.36
Methyl formate	−0.03	−0.08	0.01	−0.15
Methyl acetate	−0.07	−0.16	−0.18	−0.27
Methyl butyrate	0.10	0.05	0.04	−0.04
Methyl hexanoate	0.33	0.31	0.31	0.28
Methyl heptanoate	0.39	0.29	0.25	0.19
Methyl octanoate	0.50	0.37	0.30	0.23
2-Butanone	0.08	0.00	−0.05	−0.12
2-Pentanone	0.15	0.07	0.02	−0.07
2-Heptanone	0.32	0.24	0.20	0.12
2-Octanone	0.77	0.58	0.45	0.30
Methanol	0.42	0.27	0.12	−0.03
Ethanol	0.36	0.23	0.14	−0.04
n-Propanol	0.22	0.10	0.01	−0.14
n-Butanol	0.19	0.05	0.02	−0.16
n-Pentanol	0.11	0.01	−0.03	−0.11
n-Hexanol	0.18	0.04	0.00	−0.09

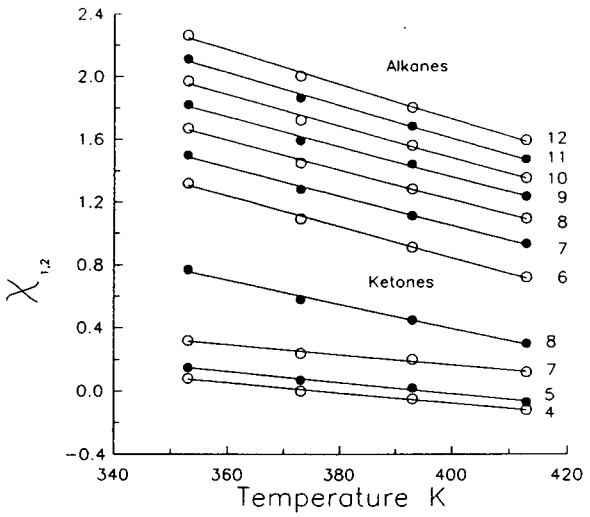

Fig. 1. Dependence of the value of the solute–polymer interaction parameter, $\chi^{\infty}_{1,2}$, on temperature on Superox 20M for *n*-alkanes and ketones. The figures on the right represent the number of carbon atoms in the solute molecule.

temperature zone of the system in the corresponding solute–polymer solution diagram.

The dependence of the value of $\chi^{\infty}_{1,2}$ on the chain length of a homologous series may best be observed from Fig. 2. *n*-Alkanes, aromatics and esters show a linear dependence of solubility on chain length, if methyl formate is excluded. The slope of the lines (the contribution of the methylene group to the value of $\chi^{\infty}_{1,2}$) is a measure of the deterioration of solubility due to the addition of one methylene group to the chain. This contribution is similar with *n*-alkanes and aromatic hydrocarbons, and smaller with methyl esters, indicating that the contribution of the methylene group to $\chi^{\infty}_{1,2}$ depends on the "active" radical attached to the hydrocarbon chain in the homologous series. In all these cases the solubility deteriorates with the addition of methylene groups, as expected.

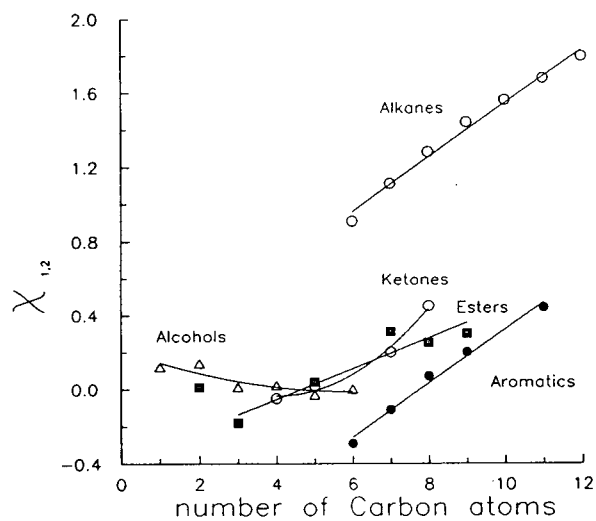

Fig. 2. Variation of the value of the solute–polymer interaction parameter, $\chi^{\infty}_{1,2}$, with chain length for each homologous series.

The effect of the addition of a methylene group to the chain of alcohols and ketones is not as uniform. In the former, there seems to be a maximum in solubility round *n*-butanol or *n*-pentanol, indicating that for these chain lengths stronger specific interactions are produced between the alcohols and Superox 20M. Alcohols should interact fairly strongly with this stationary phase, but their strong autoassociation competes with the association with Superox 20M, making them poorer solvents of the polymer than expected. This is particularly important in the case of the smaller molecules, producing the peculiar behaviour observed. When ketones are considered, solubility deteriorates with increase in chain length, but the deterioration (in terms of the change in the value of $\chi^{\infty}_{1,2}$ per methylene group) seems to increase with increasing chain length, as may be deduced from the rate at which the values of $\chi^{\infty}_{1,2}$ change.

Thermodynamic parameters of mixing

Partial molar enthalpies and free energies of mixing are given in Table III. Ideal solutions should have values of the partial molar enthalpy of mixing of zero. The value of ΔH_m is a measure of the departure of the system from ideality. It can be seen that the solute–polymer systems considered here show parallelism between the values of $\chi^{\infty}_{1,2}$ and those of ΔH_m: low values of the interaction parameter correspond to less non-ideal solutions. Once again, alcohols depart from the general rule.

Values of the partial molar free energy of mixing show a good correlation with the corre-

TABLE III

PARTIAL MOLAR ENTHALPY AND FREE ENERGY OF MIXING

Solutes	ΔH_m (kcal mol^{-1})	ΔG_m (kcal mol^{-1})			
		353 K	373 K	393 K	413 K
n-Hexane	2.52	2.07	2.03	2.02	1.99
n-Heptane	2.48	2.17	2.13	2.13	2.11
n-Octane	2.56	2.26	2.23	2.23	2.20
n-Nonane	2.61	2.35	2.31	2.33	2.29
n-Decane	2.74	2.43	2.39	2.41	2.37
n-Undecane	2.92	2.53	2.48	2.48	2.45
n-Dodecane	3.12	2.62	2.57	2.56	2.53
Benzene	0.31	0.78	0.79	0.84	0.85
Toluene	0.41	0.90	0.92	0.97	0.98
Ethylbenzene	0.37	1.03	1.05	1.11	1.13
n-Propylbenzene	0.55	1.14	1.15	1.21	1.23
n-Pentylbenzene	1.23	1.39	1.37	1.39	1.41
Methyl formate	−0.09	0.86	0.89	1.03	0.99
Methyl acetate	0.50	0.85	0.85	0.90	0.90
Methyl butyrate	0.35	0.99	1.02	1.08	1.09
Methyl hexanoate	−0.04	1.16	1.22	1.30	1.36
Methyl heptanoate	0.71	1.21	1.21	1.26	1.29
Methyl octanoate	1.08	1.29	1.27	1.30	1.32
2-Butanone	0.67	1.05	1.07	1.10	1.11
2-Pentanone	0.77	1.10	1.11	1.15	1.15
2-Heptanone	0.73	1.20	1.22	1.26	1.27
2-Octanone	2.11	1.51	1.46	1.45	1.41
Methanol	1.87	1.30	1.27	1.24	1.20
Ethanol	1.58	1.26	1.24	1.25	1.19
n-Propanol	1.51	1.15	1.12	1.11	1.08
n-Butanol	1.38	1.11	1.08	1.09	1.05
n-Pentanol	0.87	1.05	1.04	1.07	1.08
n-Hexanol	1.15	1.09	1.06	1.09	1.07

sponding values of $\chi^{\infty}_{1,2}$, at all temperatures. The straight lines (not shown) obtained by plotting $\chi^{\infty}_{1,2}$ *versus* ΔG_m, at any temperature, including all 28 solutes, have correlation coefficients of 0.99 or better, and the four lines corresponding to 80, 100, 120 and 140°C, are almost indistinguishable when plotted on the same graph. There is, however, a small relative increase in the values of ΔG_m with increase in temperature (the four lines have slopes which increase slightly with temperature) owing to the contribution of the entropic term to the value of the partial molar free energy of mixing. Nevertheless, if all 112 values are included in one plot (28 solutes, four temperatures), a straight line with a correlation coefficient of 0.975 may be drawn, indicating how small the effect of temperature on ΔG_m is. The contribution of the entropic term to ΔG_m produces the following effect: if we take any solute and compare the plot of $\chi^{\infty}_{1,2}$ *versus* T with the corresponding plot of ΔG_m *versus* T (using the units of Tables II and III), we find that at any given temperature, the slope of the curve of the interaction parameter is lower than that of the curve of ΔG_m *versus* T at the same temperature. For this reason, Tables II and III show examples of solute–polymer systems where both magnitudes decrease from 80 to 140°C (*n*-alkanes, alcohols, 2-octanone) and others, with smaller changes in the value of $\chi^{\infty}_{1,2}$, in which the partial molar free energy of mixing does not change or increases by about 0.1 kcal/mol (1 cal. = 4.14 J) or less. The former instances correspond to systems with a partial molar enthalpy of mixing of, say, 1.5 kcal/mol or higher, whereas the latter present smaller values.

Thermodynamic parameters of solution

The values of ΔH_s and ΔG_s deduced for the different solute–Superox 20M pairs are given in Table IV. The fact that the values now do not follow too closely the tendencies found earlier is because the process of solution implies the transfer of molecules from the gas to the liquid phase, so both processes of condensation and mixing take place and, therefore, the thermodynamic parameters of vaporization must be taken into account (see Appendix). Fig. 3 shows the dependence of ΔH_s and ΔG_s on the number of carbon atoms of the molecule for each homologous series at 100°C. The plots are similar at other temperatures. Plots of $T\Delta S_s$ (not shown) obtained by difference (see Appendix) are equally straight.

The values of the slopes of the lines are presented in Table V. The correlation coefficients were 0.997 or better for ΔH_s and ΔG_s and 0.98 or better for $T\Delta S_s$. The slopes represent, in each instance, the contribution of the methylene group of that homologous series to the corresponding thermodynamic parameter. Accepting the additivity principle, we could consider that the value obtained for *n*-alkanes is the "genuine"

TABLE IV

THERMODYNAMIC PARAMETERS OF SOLUTION

Solute	ΔH_s (kcal mol^{-1})	ΔG_s (kcal mol^{-1})			
		353 K	373 K	393 K	413 K
n-Hexane	−4.86	−0.27	−0.02	0.25	0.51
n-Heptane	−5.77	−0.83	−0.56	−0.26	0.01
n-Octane	−6.56	−1.37	−1.08	−0.77	−0.49
n-Nonane	−7.45	−1.90	−1.60	−1.25	−0.97
n-Decane	−8.29	−2.43	−2.11	−1.75	−1.45
n-Undecane	−9.10	−2.95	−2.60	−2.23	−1.91
n-Dodecane	−9.95	−3.46	−3.08	−2.70	−2.36
Benzene	−7.38	−1.81	−1.51	−1.18	−0.88
Toluene	−8.13	−2.37	−2.05	−1.70	−1.40
Ethylbenzene	−8.80	−2.84	−2.52	−2.16	−1.84
n-Propylbenzene	−9.42	−3.28	−2.95	−2.57	−2.25
n-Pentylbenzene	−10.68	−4.25	−3.89	−3.51	−3.16
Methyl formate	−6.37	−0.73	−0.44	−0.03	0.19
Methyl acetate	−7.02	−1.20	−0.88	−0.52	−0.22
Methyl butyrate	−8.13	−2.15	−1.81	−1.44	−1.14
Methyl hexanoate	−9.70	−3.22	−2.85	−2.46	−2.12
Methyl heptanoate	−10.37	−3.71	−3.34	−2.95	−2.59
Methyl octanoate	−11.22	−4.23	−3.84	−3.43	−3.04
2-Butanone	−7.23	−1.52	−1.20	−0.86	−0.55
2-Pentanone	−7.79	−1.99	−1.67	−1.32	−1.02
2-Heptanone	−9.39	−3.09	−2.74	−2.36	−2.03
2-Octanone	−10.08	−3.60	−3.25	−2.86	−2.51
Methanol	−7.23	−0.87	−0.51	−0.14	0.21
Ethanol	−8.12	−1.28	−0.89	−0.47	−0.13
n-Propanol	−8.92	−1.94	−1.54	−1.13	−0.76
n-Butanol	−9.76	−2.57	−2.16	−1.73	−1.36
n-Pentanol	−10.60	−3.18	−2.75	−2.31	−1.93
n-Hexanol	−11.54	−3.76	−3.32	−2.85	−2.45

contribution of the methylene group to the parameter, as only methylene groups are present in the molecule. In all other instances, we must admit that the "polar" group at the end of the hydrocarbon chain (phenyl, methyl ester, acetyl or hydroxyl) has an effect on the nearby methylene groups, modifying their contribution to the thermodynamic parameters. This effect is "measured" in a way by the difference between the slopes of the lines corresponding to that homologous series and the *n*-alkanes. It may be observed that the effect diminishes in the order aromatics > esters > ketones > alcohols.

A study of the relationship between the chromatographic behaviour of the solutes and the thermodynamic parameters is summarized in Table VI for five substances of similar boiling point. The number of carbon atoms of the hypothetical *n*-alkane (6.35 carbon atoms) was deduced from a plot of the boiling points of *n*-alkanes *versus* the number of carbon atoms. The other figures in Table VI for that hydrocarbon were deduced by interpolation, using values from Tables II, III and IV.

The hydrocarbon has a retention index that is considerably lower than those of the other substances in Table VI. It may also be observed that the thermodynamic parameters of solution and

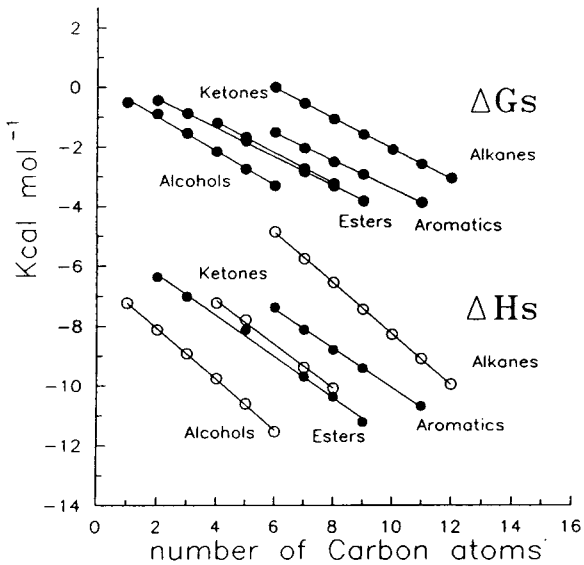

Fig. 3. Dependence of the values of ΔH_s and ΔG_s on the number of carbon atoms in the molecule at 100°C.

mixing and the solute–polymer interaction parameter ($\chi^{\infty}_{1,2}$) are also higher (or less negative) than in any of the other instances. Benzene, 2-butanone and methyl acetate have retention indices that follow the opposite tendency of the thermodynamic parameters and the values of $\chi^{\infty}_{1,2}$ (the lower the values, the higher is the retention index). Ethanol, however, seems to be an exception. The low value of the enthalpy of solution (the lowest in Table VI) would make us expect a higher retention index for this substance. However, the enthalpy of mixing, the partial molar free energy of solution and the interaction parameter $\chi^{\infty}_{1,2}$ show that ethanol does not mix with Superox 20M as easily as the other three compounds, probably owing to the high degree of autosolvation that alcohols present (observe also the higher enthalpy of vaporization of ethanol), and therefore its retention volume (and hence the retention index) are

TABLE V

SLOPES OF THE PLOTS OF THE THERMODYNAMIC PARAMETERS OF SOLUTION *VERSUS* THE NUMBER OF CARBON ATOMS OF THE ALKYL CHAIN [$s(X)$], AT 100°C, AND DIFFERENCE FROM THE SLOPE OF THE PLOT CORRESPONDING TO *n*-ALKANES [$\Delta s(X)$] (kcal mol^{-1})

Compounds	s (ΔH_s)	Δs (ΔH_s)	s (ΔG_s)	Δs (ΔG_s)	s ($T\Delta S_s$)	Δs ($T\Delta S_s$)
n-Alkanes	−0.85	–	−0.55	–	−0.33	–
Aromatics	−0.65	0.20	−0.47	0.08	−0.18	0.15
Esters	−0.69	0.16	−0.49	0.06	−0.20	0.14
Ketones	−0.73	0.12	−0.52	0.03	−0.21	0.12
n-Alkanols	−0.85	−0.01	−0.58	−0.03	−0.27	0.06

TABLE VI

DATA FOR FIVE SELECTED SOLUTES AT 373 K

Parameter	*n*-$C_{6.35}$	Benzene	2-Butanone	Methyl acetate	Ethanol
Boiling point (°C)	79.6	80.0	79.6	77.1	78.5
Retention index	635	966	907	828	912
ΔH_s (kcal mol^{-1})	−5.18	−7.38	−7.23	−7.02	−8.12
ΔH_m (kcal mol^{-1})	2.50	0.31	0.67	0.50	1.58
ΔH_v (kcal mol^{-1})	7.68	7.69	7.90	7.52	9.70
ΔG_s (kcal mol^{-1})	−0.21	−1.51	−1.20	−0.88	−0.89
$\chi^{\infty}_{1,2}$	1.16	−0.28	0.00	−0.16	0.23

lower than expected. Plots of retention index (from Table VI) versus ΔH_s, ΔH_m, ΔG_s or $\chi^{\infty}_{1,2}$ show that the best fit is obtained with retention index *vs.* ΔG_s plots. However, all the thermodynamic parameters listed in Table VI have some effect on the value of the retention index.

Solubility parameters of Superox 20M

The results obtained allow the calculation of the solubility parameter of Superox 20M at the experimental temperatures, as explained in the Appendix. The values are presented in Table VII. There seems to be a linear dependence of δ_2 on the absolute temperature, according to the equation

$$\delta_2 = 11.025 - 0.003T \ (\text{cal}^{1/2}\ \text{cm}^{-3/2})$$

with a correlation coefficient of 0.993. The linear dependence of the solubility parameter of polymers (δ_2) on temperature has been observed in the past [20–22]. If linearity holds for lower temperatures, we may deduce that the value of the solubility parameter of Superox 20M at 64°C (the minimum allowed operating temperature (MAOT) of non-immobilized Superox 20M [3]) should be 10.02 $\text{cal}^{1/2}\ \text{cm}^{-3/2}$, and the value at 50°C (the MAOT for immobilized Superox 20M) should be 10.06 $\text{cal}^{1/2}\ \text{cm}^{-3/2}$. Extrapolation to room temperature is not allowed owing to the existence of a transition temperature, below which the stationary phase solidifies. If extrapolation is carried out to higher temperatures, the value corresponding to 280°C (the maximum operating temperature for Superox 20M) will be 9.37 $\text{cal}^{1/2}\ \text{cm}^{-3/2}$. Solubility parameters of both the stationary phase and the solutes to be separated will probably play an important role in the prediction of the chromatographic performance of the system considered, and also in the prediction of the behaviour of mixed stationary phases (prepared by mixing two or more standard stationary phases).

TABLE VII

SOLUBILITY PARAMETERS OF SUPEROX 20M

Temperature (K)	δ_2 [$(\text{cal cm}^{-3})^{1/2}$]
353	9.956
373	9.900
393	9.820
413	9.780

CONCLUSIONS

It has been shown that both the thermodynamic and the interaction parameters measured by IGC for a number of solutes with respect to a particular stationary phase are indicative of the chromatographic behaviour that may be expected from the solute–stationary phase system.

SYMBOLS

a_1	activity of the solute in the stationary phase
B_{11}	second virial coefficient of the solute at the column temperature T
F_0	carrier gas flow-rate, as measured at the column outlet, at ambient temperature (T_0) and atmospheric pressure (p_0)
j	James and Martin's correction factor
M_1	molecular mass of the solute
p_0	pressure of the carrier gas in the flow meter, normally atmospheric pressure
P_1^0	saturated vapour pressure of the solute at the column temperature T
p_w	vapour pressure of the water at the flow meter temperature (T_0)
R	gas constant
T_0	absolute temperature of the carrier gas in the flow meter
T	absolute temperature of the column
t'_R	adjusted retention time of the solute
V_1^0, V_2^0	molar volumes of the solute and the stationary phase at the column temperature. The ratio V_1^0/V_2^0 has been taken as 0
V_g	the specific retention volume of the solute
w_1	mass fraction of the solute in the polymer
w_2	mass of the stationary phase in the column

Greek letters

δ_1, δ_2 solubility parameters of the solute (δ_1) and the stationary phase (δ_2)

ρ_1, ρ_2 densities of the solute and the polymer

$\chi^{\infty}_{1,2}$ Flory–Huggins solute–polymer interaction parameter

χ^{∞}_{s} entropic component of the Flory–Huggins solute–polymer interaction parameter

Ω^{∞}_{1} activity coefficient of the solute at infinite dilution, based on mass fraction.

Subscripts

Subscript 1 refers to the solute and 2 to the stationary phase.

ACKNOWLEDGEMENTS

This work was carried out under Project No. PB87-0393 of the Dirección General de Investigación Científica y Técnica (DGICYT) of the Ministry of Education of Spain. E.L. de B. is grateful to the Consejo Superior de Investigaciones Científicas for a scholarship.

APPENDIX

Specific retention volumes:

$$V_g = \frac{F_0 j}{w_2} \cdot t'_R \cdot \frac{273.15}{T_0} \cdot \frac{(p_0 - p_w)}{p_0} \quad \text{(A1)}$$

Activity coefficients at infinite dilution:

$$\ln\ \Omega^{\infty}_1 \equiv \ln\left(\frac{a_1}{w_1}\right) = \ln\left[\frac{273.15R}{P^0_1 V_g M_1} - \frac{P^0_1}{RT}(B_{11} - V^0_1)\right] \quad \text{(A2)}$$

Partial molar enthalpy of solution:

$$\Delta H_s = -R \cdot \frac{\partial(\ln V_g)}{\partial(1/T)} \quad \text{(A3)}$$

Partial molar enthalpy of mixing of the solute at infinite dilution:

$$\Delta H^{\infty}_m = R \cdot \frac{\partial(\ln \Omega^{\infty}_1)}{\partial(1/T)} \quad \text{(A4)}$$

Molar enthalpy of vaporization of the solutes:

$$\Delta H_v = \Delta H_m - \Delta H_s \quad \text{(A5)}$$

Partial molar free energy of sorption:

$$\Delta G_s = -RT \ln (M_1 V_g / 273.15R) \quad \text{(A6)}$$

Relationship between activity coefficients at infinite dilution and partial molar free energy of mixing:

$$\Delta G_m = RT \ln \Omega^{\infty}_1 \quad \text{(A7)}$$

Solubility parameters of the solutes (δ_1):

$$\delta_1 = [(\Delta H_v - RT)/V^0_1]^{1/2} \quad \text{(A8)}$$

Flory–Huggins interaction parameter:

$$\chi^{\infty}_{1,2} = \ln \Omega^{\infty}_1 + \ln\left(\frac{\rho_1}{\rho_2}\right) - \left(1 - \frac{V^0_1}{V^0_2}\right) \quad \text{(A9)}$$

Solubility parameters of the polymer (δ_2): deduced from a plot of the right-hand side of eqn. A10 *versus* δ_1:

$$\frac{\delta^2_1}{RT} - \frac{\chi^{\infty}_{1,2}}{V^0_1} = \frac{2\delta_2}{RT} \cdot \delta_1 - \left(\frac{\delta^2_2}{RT} + \frac{\chi^{\infty}_s}{V^0_1}\right) \quad \text{(A10)}$$

REFERENCES

1 T.J. Stark, P.A. Larson and R. Dandeneau, *J. Chromatogr.*, 279 (1983) 31.
2 P. Sandra, F. David, M. Proot, G. Diricks, M. Verstape and M. Verzele, *J. High Resolut. Chromatogr. Chromatogr. Commun.*, 8 (1985) 782.
3 E. Fernández-Sánchez, A. Fernández-Torres, J.A. García-Domínguez and M.D. Salvador-Moya, *J. Chromatogr.*, 556 (1991) 485.
4 A.V. Kiselev, *Adv. Chromatogr.*, 4 (1967) 113.
5 O. Smidsrod and J.E. Guillet, *Macromolecules*, 2 (1976) 272.
6 E. Fernández-Sánchez, A. Fernández-Torres, J.A. García-Domínguez, J. García-Muñoz, V. Menéndez, M.J. Molera and J.M. Santiuste, *J. Chromatogr.*, 410 (1987) 13.
7 D. Patterson, Y.B. Tewari, H.P. Schreiber and J.E. Guillet, *Macromolecules*, 4 (1971) 356.
8 G.J. Price, J.E. Guillet and J.H. Purnell, *J. Chromatogr.*, 369 (1986) 273.
9 R.C. Wilhoit and B.J. Zwolinski, *Handbook of Vapor Pressures and Heats of Vaporization of Hydrocarbons and Related Compounds*, Thermodynamics Research Centre, Texas A&M University, College Station, TX, 1971.
10 T. Boublík, V. Fried and E. Hàla, *The Vapour Pressures of Pure Substances*, Elsevier, Amsterdam, 1975.
11 J.P. O'Connell and J.M. Pruasnitz, *Ind. Eng. Chem., Process Des. Dev.*, 6 (1976) 245.

12 J.H. Dymond and E.B. Smith, *The Viral Coefficients of Pure Gases and Mixtures. A Critical Compilation*, Clarendon Press. Oxford, 1980.
13 National Research Council of the USA, *International Critical Tables of Numerical Data. Physics, Chemistry and Technology*, Vol. III, McGraw-Hill, New York, 1928.
14 *TRC Thermodynamic Tables*, Thermodynamics Research Centre, Texas Engineering Experiment Station, Texas A & M University, College Station, TX.
15 G. DiPaola-Baranyi and J.G. Guillet, *Macromolecules*, 11 (1978) 228.
16 M.R. Becerra, E. Fernández-Sánchez, A. Fernández-Torres, J.A. García-Domínguez and J.M. Santiuste, *J. Chromatogr.*, 547 (1991) 269.
17 P.I. Freeman and J.S. Rowlinson, *Polymer*, 1 (1960) 20.
18 T. Bohossian, G. Charlet and G. Delmas, *Polymer*, 30 (1989) 1695.
19 J.I. Iribarren, M. Iriarte, C. Uriarte and J.J. Iruin, *J. Appl. Polym. Sci.*, 37 (1989) 3459.
20 M.J. Fernández-Berridi, G. Martín Guzmán, J.J. Iruin and M.E. Elorza, *Polymer*, 24 (1983) 417.
21 O. Humpa, J. Uhdeová and M. Roth, *Macromolecules*, 24 (1991) 2514.
22 M.R. Becerra, E. Fernández-Sánchez, A. Fernández-Torres, J.A. García-Domínguez and J.M. Santiuste, *Macromolecules*, 25 (1992) 4665.

Journal of Chromatography A, 655 (1993) 21–29
Elsevier Science Publishers B.V., Amsterdam

CHROM. 25 087

Separation of acidic proteins by capillary zone electrophoresis and size-exclusion high-performance liquid chromatography: a comparison

Maria Estrella Legaz* and Mercedes M. Pedrosa

Laboratory of Plant Physiology, The Lichen Team, Faculty of Biology, Complutense University, 28040 Madrid (Spain)

ABSTRACT

Successful separations of alcohol dehydrogenase (pI = 5.4), β-amylase (pI = 5.2) and albumin (pI = 4.7) by capillary electrophoresis in uncoated fused-silica capillaries are reported. Different electrophoretic conditions, consisting in variation of temperature, applied voltage and ionic strength of the buffer used as electrolyte, were tested in order to compare the separation efficiency, resolution and selectivity of the acidic proteins. The results were compared with those obtained by size-exclusion chromatography. Rinsing of the capillary between runs, in order to eliminate adsorbed proteins, can shorten its useful lifetime.

INTRODUCTION

Electrophoresis is the separation of charged molecules based on differential migration in an applied potential field. In capillary zone electrophoresis (CZE), compounds are resolved according to their ability to migrate in an electric field gradient inside a fused-silica capillary of 200 μm I.D. or less. These separations are facilitated by the use of high voltages, which may generate electroosmotic and electrophoretic flows of buffer solutions and ionic species, respectively, within the capillary.

Zone electrophoresis in open capillaries is uniquely simple in the number of factors affecting solute band broadening. Electroosmosis resulting in a flat flow profile and the lack of a stationary phase virtually eliminate any band broadening due to resistance to mass transfer. However, adsorption is a particularly serious problem for proteins because of the multiplicity of polar, charged and hydrophobic sites on the molecular surface [1]. Protein adsorption can change the capillary surface characteristics, affecting results in subsequent runs and consequently the magnitude of electroendosmosis can drift as the capillary surface is modified by adsorption. McCormick [2] reported that phosphate forms complexes with silanols on the silica surface, reducing electroendosmosis and protein–silica interactions. Zhu *et al.* [3] suggested the use of acidic solutions to wash capillaries of 25 μm I.D. between runs. Rinsing with a solution of 0.1 *M* NaOH between protein runs resulted in restoration of the initial conditions of analysis [4]. However, all these procedures can cause capillary damage when using open tubes and examination of the capillary under a light microscope before and between several runs is strongly recommended.

In comparison with HPLC, CE is more limited with respect to the maximum mass load (*i.e.*, the maximum amount of sample that can be loaded on to the capillary without causing intolerable band broadening). In pure CZE, band broadening occurs only due to a single effect: longitudinal diffusion. Therefore, in CZE, the dispersion characteristics are more favourable compared with HPLC.

* Corresponding author.

0021-9673/93/$06.00

The objective of this work was to establish the potential utility of CE with particular emphasis on using open-tube, untreated fused-silica capillary columns for the separation of acidic proteins. Analyses of these proteins by CE were compared with those obtained by size-exclusion HPLC using a conventional TSK G5000 PW XL column.

EXPERIMENTAL

Chemicals

All chemicals used for the preparation of the buffers were of analytical-reagent grade (Merck, Darmstadt, Germany) and were used as received. Deionized water was doubly distilled and filtered through Millipore GS filters (0.22 μm pore diameter).

Albumin from egg (M_r 45 000), β-amylase from sweet potato (M_r 200 000) and alcohol dehydrogenase from yeast (M_r 150 000) were purchased from Sigma (St. Louis, MO, USA), kit No MW MWGF-1000. The neutral marker, benzene, was purchased from Merck (Darmstadt, Germany).

Instrumentation

Zone electrophoresis was performed using a Spectraphoresis 500 system from Spectra-Physics (Fremont, CA, USA). Microbore fused-silica tubing coated with polyimide (Scientific Glass Engineering, Milton Keynes, UK) of 50 and 75 μm I.D. and 190–360 μm O.D. with a total length of 70 cm and a separation length of 63 cm were used. The capillary was enclosed in a cassette for easy handling. On line-detection was performed with a variable-wavelength UV–Vis detector of band width 6 nm (Spectra-Physics). Detection of proteins was monitored at 200 nm and electropherograms were recorded using an SP 4290 integrator (Spectra-Physics).

HPLC separation was performed using a system consisting of an SP 8800 gradient pump module, an SP 8490 UV–Vis detector (both from Spectra-Physics) and a Model 7125 injector (Rheodyne, Cotati, CA, USA). Retention times and peak areas of proteins were measured by using the same SP 4290 integrator after detection at 200 nm.

Capillary photographs were taken with a light Nikon Labophot microscope system (Nippon Kogaku, Tokyo, Japan) by using a 20× acromatic objective, numerical aperture 0.4 (Ref. 160/0.17, Nikon). Prints were made using Kodak PlusX Pan film (125 ASA).

Electrophoresis

A capillary just purchased was first conditioned with 0.5 *M* NaOH for 5 min at 60°C, 0.05 *M* NaOH for 5 min at 60°C and doubly distilled, deionized, filtered water for 5 min at 60°C. Equilibration of the capillary was then performed by washing it with different concentrations (15, 25 and 75 m*M*) of sodium borate–phosphoric acid buffer (pH 7.2) for 10 min at 25°C. After this, the capillary was washed again with the same buffer for 10 min at 25°C under an applied voltage of 20 kV. This buffer system was chosen in order to produce a pH value higher than the isoelectric point (p*I*) of the proteins to be separated. This renders the proteins negatively charged, resulting in repulsion from the charged fused-silica capillary walls and thereby minimizing adsorption. Regeneration of the capillary surface between runs was performed by rinsing it in the following sequence: 0.05 *M* NaOH for 3 min, doubly distilled, deionized water for 5 min and the corresponding conditioning buffer for 3 min. The buffer used as electrolyte was 15, 25 or 75 m*M* sodium borate–phosphoric acid (pH 7.2).

Protein solutions of 29.5 μM albumin (pI = 4.7) + 6.6 μM β-amylase (pI = 5.2) + 8.4 μM alcohol dehydrogenase (pI = 5.4), prepared in the electrophoresis buffer diluted threefold, were injected into the capillary by siphoning for a fixed time of 8 s. Benzene at a concentration of 4% (v/v) in the same diluted buffer was used as a neutral marker. Two different voltages, 17 and 22 kV, were applied using positive-to-negative polarity. During electrophoresis, temperature control was employed as indicated.

HPLC separation

Protein solutions of 35 μM albumin + 2.5 μM β-amylase + 5.3 μM alcohol dehydrogenase, prepared in the mobile phase buffer, were injected on to a TSK G5000 PW XL column (30

cm × 7.8 cm I.D.) from Supelco (Progel, Saint Germain-en-Laye, France). The flow-rate of the mobile phase, 75 m*M* Tris–HCl buffer (pH 8.0), was 0.3 ml min^{-1} and the injection volume was 10 μl.

RESULTS AND DISCUSSION

Some aspects of the capillary

The fused-silica capillaries coated with polyimide of 50–75 μm I.D. (Fig. 1) used for free zone electrophoresis received no surface treatment in order to maintain electroosmotic flow. This electroosmotic flow is dependent on the concentration and pH value of the buffer electrolyte, corresponding to the degree of dissociation of the silanol groups. Especially with proteins, interactions with the untreated wall can lead to poor reproducibility of migration times because of changes in the electroosmotic flow. On the other hand, the separation efficiency decreases owing to adsorption of proteins on the wall [4,5]. In that event, in order to achieve a good optimization of the separation parameters, regeneration of the surface by rinsing the capillary with NaOH between runs is recommended [3,6]. However, such rinsing steps, which were done automatically after every run in our analysis and are essential, can shorten the useful lifetime of capillaries. Other phenomenas that can damage the inner wall of the capillary are temperature gradients across it or temperature changes with time due to heat dissipation between runs. Both events are the inevitable result of the application

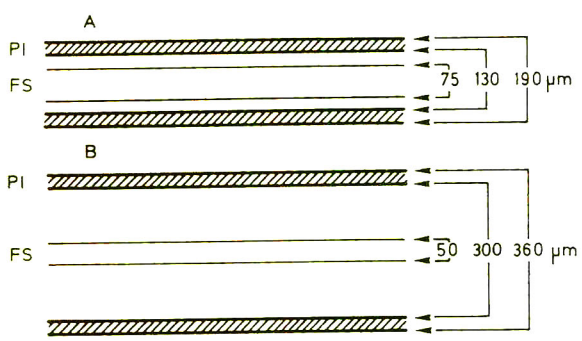

Fig. 1. Schematic representation of (a) 75 μm I.D. and (b) 50 μm I.D. untreated fused-silica capillaries. PI = Polyimide; FS = fused silica.

of high field strengths in capillary electrophoresis. Narrow-diameter capillaries help dissipation but are also more prone to clogging. Mechanical manipulation of the capillary should also be avoided and, once enclosed in the cassette, it should not be removed.

The effect of this damage can be detected by successive current decreases at the same applied voltage between runs. Fig. 2 illustrates some alterations produced in the capillary as a consequence of its utilization, analysed under a light microscope. A defective cutting (c) can lead to a flow interruption (d) by penetration of polyimide inside the capillary. Therefore, when a long capillary is purchased, the user must take care to ensure efficient cutting (b) in order to avoid the production of bubbles. A flow decrease or even interruption can be produced by irregularities in the inner wall (e–k). Damage to this wall caused by irreversible adsorption of proteins, silica cracks, pore formation (l), etc., causes a cavitation phenomenon that impedes the migration of solutes under constant electroosmotic flow. For all these reasons, the routine use of a light microscope is strongly recommended, to obtain good reproducibility of the results, especially in the analysis of proteins, when untreated fused-silica capillaries are used. As damage to the capillary inner wall seems to be an inverse function of the inner diameter, capillaries of 75 μm I.D. were used throughout this work.

Factors affecting mobility of acidic proteins in CZE

Efficiency is a function of the electroosmotic mobility [7], hence controlling the flow will be beneficial in maximizing efficiency and resolution, which could lead to superior separations. Without considering electroosmosis, the migration velocity, ν, in electrophoresis is given by

$$\nu = \mu_e E = \frac{\mu_e V}{L} \quad (1)$$

in cm s^{-1}, where μ_e is the electrophoretic mobility, E is the potential field strength (V/L), V is the voltage applied across the capillary and L is the capillary length [8]. Thus, higher voltages and shorter capillary lengths provide faster elution times. However, in the presence of electro-

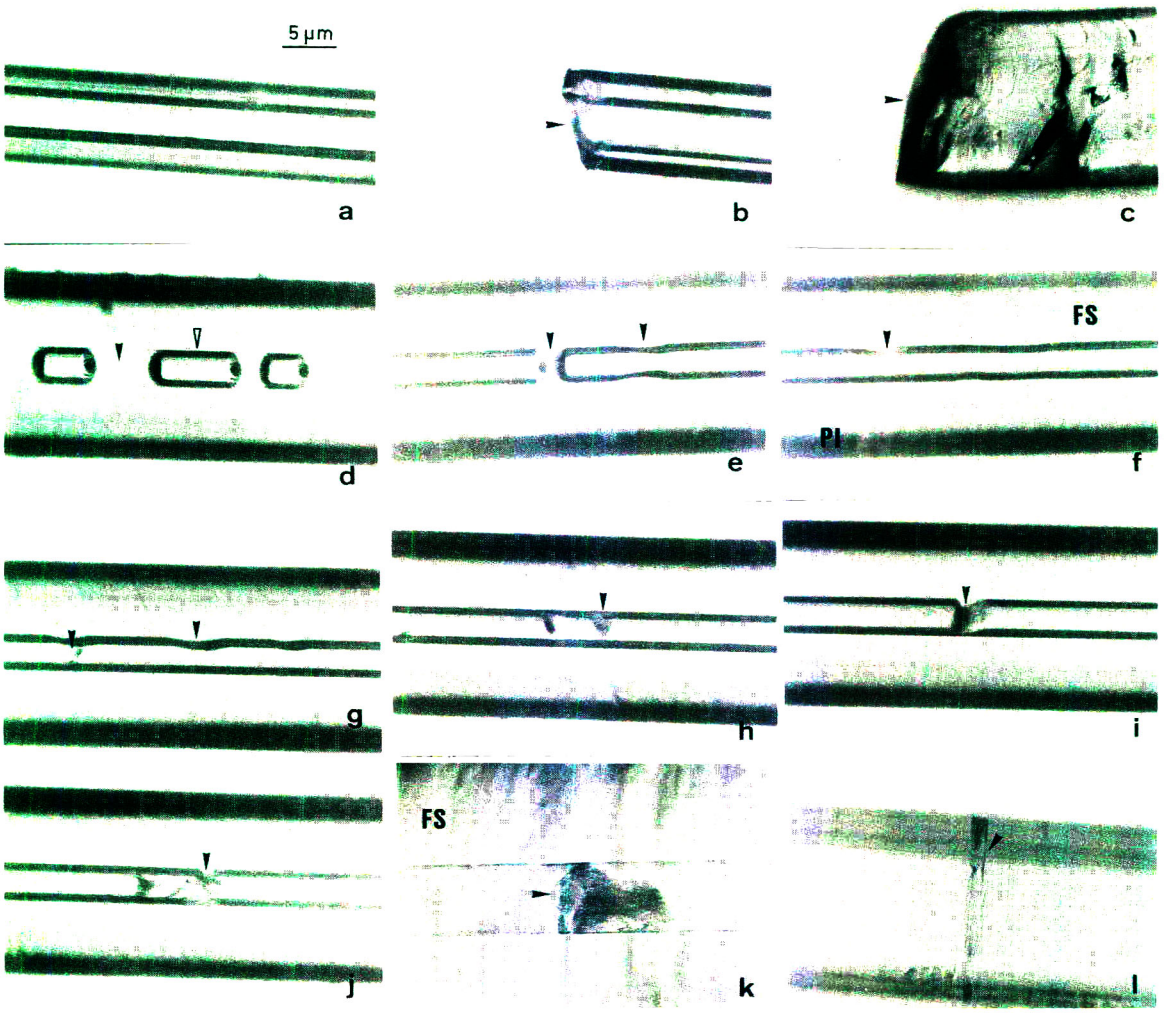

Fig. 2. Internal structure of the capillaries under a light microscope. (a, b) 75 μm I.D. capillary; (c–l) 50 μm I.D. capillary. Magnification procedure is described in the text. (a) Intact empty capillary; (b) good end cutting; (c) defective cutting with disrupted polyimide layer; (d), aspect of empty (open arrow) and full (full arrow) capillary; (e–k), different irregularities in the inner wall of the capillary; (l), pore formation through the wall of the capillary. PI = Polyimide; FS = fused silica.

osmotic flow, the migration velocity can be rewritten as

$$\nu = \frac{(\mu_e + \mu_{eo})V}{L} \qquad (2)$$

in cm s^{-1}, where μ_{eo} is the coefficient of electroosmotic flow [9]. This is because electroosmotic flow affects the amount of time a solute resides in the capillary and, in this sense, both separation efficiency and resolution are related to the flow-rate. The total velocity was higher for cations and lower for anions (as are the cited proteins at pH 7.2) than their electrophoretic velocity. Neutral molecules (benzene) moved with the same velocity as the electroosmotic flow. The migration sequence was thus cations (if present), benzene (neutral), alcohol dehydrogenase, β-amylase and albumin. The electroosmotic flow was dependent on the concentration and pH of the buffer electrolyte, corresponding to the

degree of dissociation of the silanol groups. We then attempted to use 4% (v/v) benzene as a neutral marker in the corresponding buffer system for each analysis.

Migration velocities calculated for alcohol dehydrogenase ranged from 0.089 to 0.226 cm s^{-1}, β-amylase from 0.082 to 0.213 cm s^{-1} and albumin from 0.073 to 0.193 cm s^{-1} (Table I). It is known that the mobility increases by 2% when the temperature is raised by 1°C [4]. Although temperature differences inside capillaries are small (less than 1°C under realistic conditions), they can be as high as several tens of degrees between the wall of the capillary and the surrounding air [10]. Therefore, an effective thermostating device is important in order to obtain sufficiently reproducible migration times over a long period of use. In our system, control of temperature with a precision of ±0.01°C was achieved with an oven Peltier high-speed fan and resistive thermal device (RTD).

The electrophoretic mobility for anions ($\mu_e + \mu_{eo}$) can be calculated from eqn. (2) and expressed as

$$\mu_e + \mu_{eo} = \frac{\nu L}{V} \quad (3)$$

in $cm^2\ V^{-1}\ s^{-1}$.

It can be seen from the results in Fig. 3 that the electrophoretic mobilities varied as a consequence of the current applied inside the capillary, although this is not a direct relationship. The current is proportional to the resistance, which, in turn, is a function of the temperature, the applied voltage and the ionic strength of the electrolyte. Using the same buffer molarity, 15 m*M* borate–phosphoric acid (Fig. 3A), the electrophoretic mobility of alcohol dehydrogenase, β-amylase and albumin increased as the current increased from 40 to 56 μA, and the differences between each pair were maintained. At 25 m*M* borate–phosphoric acid buffer (Fig. 3B), an increase in the current form 63 to 69 μA produced higher electrophoretic mobilities, but the differences of these mobilities between each pair of proteins were greater than those observed with a 15 m*M* buffer electrolyte. Moreover, the electrophoretic mobilities of alcohol dehydrogenase and β-amylase were similar to those obtained at 63 μA when the current was 99 μA, but the mobility of albumin was much lower than that observed at 63 or 69 μA. This implies a better resolution of the last peak. The resistance of the capillary to the flow current at 75 m*M* borate–phosphoric acid buffer (Fig. 3C) was the highest and the electrophoretic mobility differences between alcohol dehydrogenase and β-amylase and between β-amylase and albumin decreased as the current increased. In this instance, a higher electrolyte concentration resulted in a higher

TABLE I

MIGRATION VELOCITIES OF ALCOHOL DEHYDROGENASE, β-AMYLASE, ALBUMIN AND BENZENE (NEUTRAL MARKER) IN CZE DEPENDING ON TEMPERATURE, VOLTAGE AND IONIC STRENGTH OF THE BUFFER USED AS ELECTROLYTE

Capillary, 70 cm × 75 μm I.D. (63 cm to the detector); separation solutions, (A) 15, (B) 25 and (C) 75 m*M* borate–phosphoric acid (pH 7.2).

Protein	Migration velocity, ν (cm s^{-1})						
	A		B			C	
	30°C, 17 kV	30°C, 22 kV	17°C, 17 kV	25°C, 17 kV	25°C, 22 kV	17°C, 22 kV	25°C, 17 kV
Benzene	0.206	0.278	0.141	0.166	0.237	0.182	0.142
Alcohol dehydrogenase	0.158	0.226	0.089	0.096	0.119	0.128	0.105
β-Amylase	0.149	0.213	0.082	0.088	0.106	0.122	0.096
Albumin	0.134	0.193	0.073	0.076	0.080	0.116	0.088

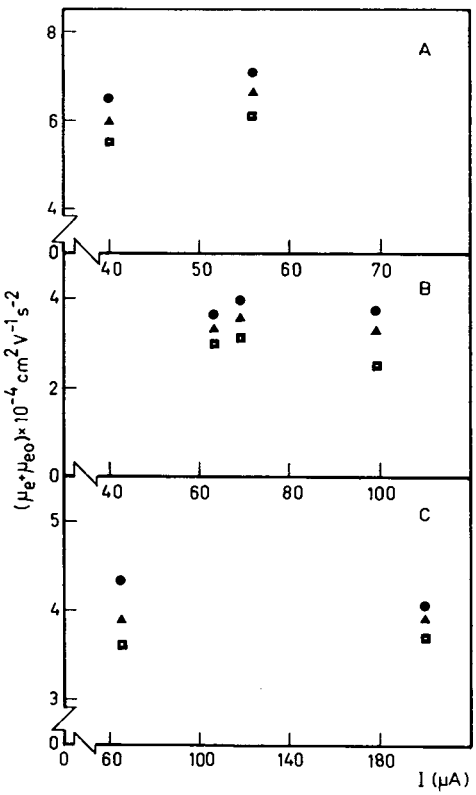

Fig. 3. Plot of electrophoretic mobility ($\mu_e + \mu_{eo}$) as a function of current (I) for (●) alcohol dehydrogenase, (▲) β-amylase and (□) albumin using as buffering electrolyte borate–phosphoric acid (pH 7.2) at (A) 15, (B) 25 and (C) 75 mM concentration. Electrophoresis was performed in a 70 cm × 75 μm I.D. (63 cm to the detector) capillary. Detection was achieved at 200 nm.

current being passed (199 μA) and therefore more heat to be dissipated. However, the electrolyte concentration of a solute in a zone or the change in solution conductivity in that zone will produce a change in the local potential gradient [8].

Factors affecting efficiency, resolution and selectivity of acidic proteins in CZE

Electroosmosis should not, in principle, affect the broadening of solute zones on the capillary for a given period of time, assuming longitudinal diffusion to be the main source of zone broadening [1,11]. However, electroosmotic flow can modify the time a solute resides in the capillary and then the efficiency and resolution are related to the flow-rate.

Fig. 4A–G illustrates this effect, where it can be observed how the band broadening of alcohol dehydrogenase, β-amylase and albumin differed according to the electroosmotic flow, which, in turn, is dependent on temperature, applied voltage and ionic strength of the electrolyte. Calculation of separation efficiency, including electroosmosis, as

$$N = \frac{(\mu_e + \mu_{eo})V}{2D} \quad (4)$$

where D is the diffusion coefficient of the solute, gave similar results for the three proteins, as can be seen from the results in Table II. The lowest separation efficiency was achieved by using 25 mM borate buffer at 25°C and 22 kV applied voltage. Under these electrophoretic conditions, the current was 99 μA and electrophoretic mobility decreased (Fig. 3B) with respect to that obtained at 63 and 69 μA using the same molarity of electrolyte. The highest efficiency was obtained at 199 μA with a temperature of 17°C and 22 kV applied voltage.

It has been demonstrated that high salt buffers reduce protein adsorption. Lysozyme (pI = 10.8) migrated as a sharp peak faster than the electroosmotic flow in a pH 9.0 high-salt buffer, even though the pH of the buffer was 2 units below the pI value of lysozyme [12]. Jorgenson [13] suggested that the protein adsorption may be due to the ion-exchange interaction between cationic sites in the protein and silica moities on the fused-silica surface.

The maximum differences in the number of theoretical plates between electrophoretic conditions that provide the highest (Fig. 4F) and the lowest (Fig. 4E) efficiency are 1409 for alcohol dehydrogenase, 1410 for β-amylase and 1623 for albumin. It is important to note that the separation efficiency, calculated from eqn. 4, is based on applied voltage but not on capillary length for similar diffusion coefficients. Under our experimental conditions, the diffusion coefficient of alcohol dehydrogenase ranged from $1.28 \cdot 10^{-5}$ to $3.22 \cdot 10^{-5}$ cm^2 s^{-1}, that of β-amylase from $1.17 \cdot 10^{-5}$ to $3.04 \cdot 10^{-5}$ cm^2 s^{-1} and that of albumin from $1.04 \cdot 10^{-5}$ to $2.76 \cdot 10^{-5}$ cm^{-2} s^{-1}

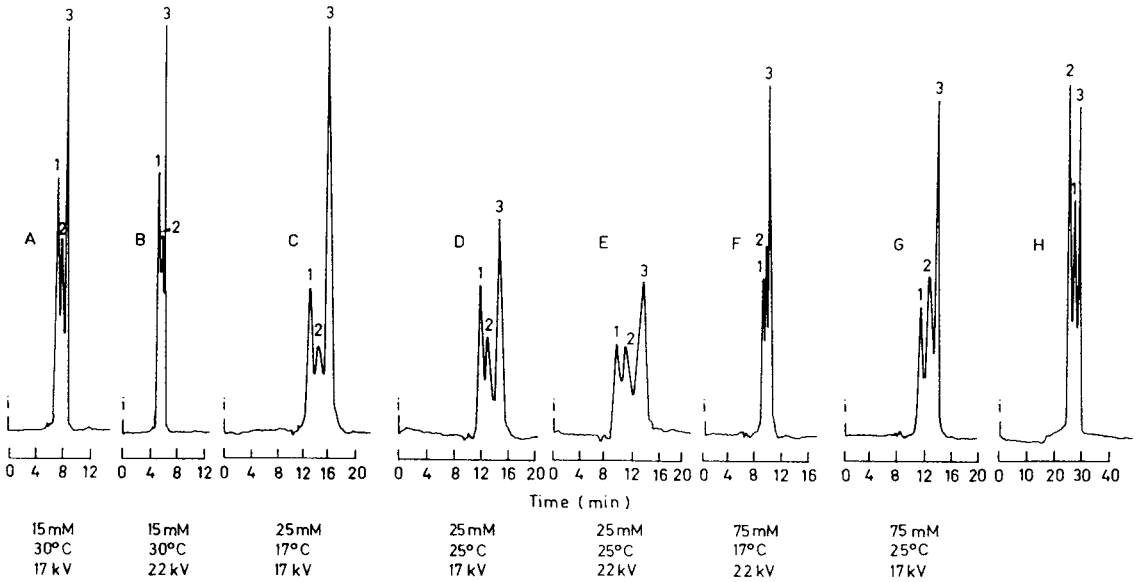

Fig. 4. (A–G) Electropherograms and (H) chromatogram of a mixture of (1) alcohol dehydrogenase, (2) β-amylase and (3) albumin. Proteins were prepared in a 1:5 dilution of the electrophoresis buffer. Electrophoresis was performed in a 70 cm × 70 μm I.D. (63 cm to the detector) capillary under the conditions specified in Table II. Detection was achieved at 200 nm. HPLC separation was performed in a 30 cm × 7.8 mm I.D. column packed with TSK G5000 PW XL. Mobile phase, 75 m*M* Tris–HCl buffer (pH 8.0) at a flow-rate of 0.3 ml min^{-1}. Detection was achieved at 200 nm. i = Injection.

(data not shown). The values of this coefficient were calculated from Fick's first law:

$$J = -D \cdot \frac{\delta c}{\delta x} \quad (5)$$

where J is the flux density in mol cm^{-2} s^{-1} and $\delta c/\delta x$ is the gradient concentration in mol cm^{-4}. Given the limitation of efficient heat dissipation, maximum separation efficiency will be obtained at high voltages and low diffusion coefficients with the highest value of the sum of the coefficients for electrophoretic mobility (μ_e) and electroosmosis flow (μ_{eo}).

The resolution (R) was also influenced by the buffer electrolyte molarity, temperature and applied voltage (Table II). The resolution between alcohol dehydrogenase and β-amylase and between β-amylase and albumin was improved with an increase in the buffer concentration at the same applied voltage. At an applied voltage of 17 kV, the resolution between alcohol dehydrogenase and β-amylase ranged from 0.39 at 15 m*M* buffer to 0.56 at 25 m*M* buffer and to 0.71 at 75 m*M* buffer. However, the resolution between β-amylase and albumin was not so linear at either 17 or 22 kV.

The best resolution is observed when $\mu_{eo} = \mu_e$; however, the trade-off is an increased analysis time. Electroosmosis towards the cathode resulted in a better resolution of anions, as were the cited proteins at pH 7.2, which migrated against the electroosmotic flow and were carried back toward the cathode [8]. Isaaq *et al.* [14] also observed a higher resolution of dansylamino acids with 200 m*M* than with 100 m*M* phosphate buffer. Resolution can be improved by increasing the size of the buffer cation [15]. A limited means of improving resolution is to increase the voltage. To double the resolution, the voltage must be quadrupled. The key to high resolution is to increase $\Delta\nu$. The control of the migration velocity is best accomplished through selection of the proper mode of capillary electrophoresis coupled with selection of the appropriate buffer [16].

Differences in selectivity (α) between alcohol dehydrogenase and β-amylase and between β-amylase and albumin are listed in Table II. The

TABLE II

EFFICIENCY (THEORETICAL PLATES N), RESOLUTION (R) AND SELECTIVITY (α) OF ALCOHOL DEHYDROGENASE (AD), β-AMYLASE (βA) AND ALBUMIN (A) IN CZE DEPENDING ON TEMPERATURE, VOLTAGE AND IONIC STRENGTH OF THE BUFFER USED AS ELECTROLYTE

Capillary, 70 cm × 75 μm I.D. (63 cm to the detector).

Electropherogram[a]	Electrophoretic conditions				Protein	N^b (per cm)	R	α
	Temperature (°C)	Voltage (kV)	Buffer concentration (mM)	Current (μA)				
A	30	17	15	40	AD	245 221	0.39	1.06
					β-A	244 800	0.97	1.11
					A	243 932		
B	30	22	15	56	AD	244 899	0.31	1.06
					β-A	244 967	0.74	1.10
					A	244 267		
C	17	17	25	63	AD	244 375	0.56	1.09
					β-A	244 307	0.89	1.13
					A	244 749		
D	25	17	25	69	AD	244 873	0.59	1.09
					β-A	244 909	1.35	1.16
					A	244 372		
E	25	22	25	99	AD	243 924	0.47	1.13
					β-A	243 875	1.05	1.32
					A	243 126		
F	17	22	75	199	AD	245 333	0.42	1.05
					β-A	245 285	0.84	1.05
					A	244 340		
G	25	17	75	67	AD	244 896	0.71	1.09
					β-A	244 594	0.71	1.09
					A	244 207		

[a] Electropherograms in Fig. 4.
[b] Separation efficiency calculated as $N = (\mu_e + \mu_{eo})V/2D$.

results show that the optimum separation for each pair was obtained at 99 μA and 199 μA gave the worst α values. An increase in current was accompanied by higher selectivity with 15 and 25 mM borate buffer, whereas with 75 mM buffer this did not occur. This indicates that differences in selectivity exist, which means that the buffer anion concentration affects the selectivity under the experimental conditions used. Similar results were obtained by Atamna *et al.* [15] working with dansylated amino acids.

Separation of acidic proteins by size-exclusion HPLC

Fig. 4H illustrates the separation of alcohol dehydrogenase, β-amylase and albumin by size-exclusion chromatography with an isocratic mobile phase composition using 75 mM Tris–HCl buffer (pH 8.0). These proteins eluted at 27.3, 29.11 and 33.4 min, respectively. As separation in size-exclusion chromatography is based on a physical sieving process and not on chemical attraction and interactions [17], variation of

TABLE III

EFFICIENCY (THEORETICAL PLATES, N), RESOLUTION (R) AND SELECTIVITY (α) OF β-AMYLASE, ALCOHOL DEHYDROGENASE AND ALBUMIN IN SIZE-EXCLUSION HPLC

The isocratic conditions of the mobile phase and the column used are given in the text.

Protein	N^a (per cm)	R	α
β-Amylase	49 770		
		0.74	1.07
Alcohol dehydrogenase	57 300		
		0.80	1.06
Albumin	101 670		

[a] Efficiency calculated as $N = 16(t_r/W_b)$, where t_r is the retention time (min) and W_b is the peak width at half-height (cm).

either mobile phase ionic strength or flow-rate did not produce any improvement of selectivity. The chromatogram observed in Fig. 4H was the best obtained by using a TSK G5000 PW XL column.

Results for the efficiency, resolution and selectivity are given in Table III. The separation efficiencies for alcohol dehydrogenase (N = 49 770), β-amylase (N = 57 300) and albumin (N = 101 670) were lower than those obtained in CZE for the same proteins. The resolution and selectivity of each pair were similar to those achieved by capillary electrophoresis.

CONCLUSION

We have demonstrated the potential applicability of CZE where acidic proteins can be separated within 18 min or less by using unmodified fused-silica capillaries. The experimental conditions used in this work show advantages over surface-modified capillaries where the instability and limited tolerable pH range prevent their routine utilization. Size-exclusion HPLC is an alternative for the separation of proteins although the efficiency is much lower than in CZE. The other great disadvantage of size-exclusion HPLC is the high cost of HPLC columns compared with capillaries for electrophoresis.

ACKNOWLEDGEMENTS

The authors are grateful to Professor C. Vicente for his encouragement and helpful discussions and the Miss M.C. Molina for technical assistance. This work was supported by a grant from the Comunidad Autónoma de Madrid (Spain), C 243/91.

REFERENCES

1 J.W. Jorgenson and K.D. Lukas, *Science*, 222 (1983) 266.
2 R.M. McCormick, *Anal. Chem.*, 60 (1988) 2322.
3 M. Zhu, R. Rodriguez, D. Hansen and T. Wehr, *J. Chromatogr.*, 516 (1990) 123.
4 Ch. Schwer and E. Kenndler, *Chromatographia*, 30 (1990) 546.
5 J.K. Twons and F.E. Regnier, *J. Chromatogr.*, 516 (1990) 69.
6 H.H. Lauer and D. McManigill, *Anal. Chem.*, 58 (1986) 166.
7 D. McManigill and S.A. Swedberg, in T.E. Hugli (Editor), *Techniques in Protein Chemistry*, Academic Press, San Diego, 1989, pp. 468–478.
8 R.A. Wallingford and A.G. Ewing, *Adv. Chromatogr.*, 29 (1989) 1.
9 A.W. Adamson, *Physical Chemistry of Surfaces*, Interscience, New York, 2nd ed., 1967, pp. 122–147.
10 J.H. Knox and I.H. Grant, *Chromatographia*, 24 (1987) 135.
11 J.W. Jorgenson and K.D. Lukas, *J. Chromatogr.*, 218 (1981) 209.
12 F.T.A. Chen, Ch.M. Liu, Y.Z. Hsieh and J.C. Stenberg, *Clin. Chem.*, 37 (1991) 14.
13 J.W. Jorgenson, in J.W. Jorgenson and M. Phillips (Editors), *New Directions in Electrophoretic Methods* (*ACS Symposium Series*, No. 335) American Chemical Society, Washington, DC, 1987, pp. 182–189.
14 H.J. Isaaq, I.Z. Atamna, C.J. Metral and G.M. Muschik, *J. Liq. Chromatogr.*, 13 (1990) 1247.
15 I.Z. Atamna, C.J. Metral, G.M. Muschik and H.J. Isaaq, *J. Liq. Chromatogr.*, 13 (1990) 2517.
16 H.T. Rasmussen and H.M. McNair, *J. Chromatogr.*, 516 (1990) 223.
17 J.M. Miller, *Chromatography: Concepts and Contrasts*, Wiley, New York, 1988, pp. 154–192.

Journal of Chromatography A, 655 (1993) 31–38
Elsevier Science Publishers B.V., Amsterdam

CHROM. 24 998

Image analysis of photochemically derivatized and charge-coupled device-detected phenothiazines separated by thin-layer chromatography

F. García Sánchez*, A. Navas Díaz and M.R. Fernández Correa

Department of Analytical Chemistry, Faculty of Sciences, University of Málaga, 29071 Málaga (Spain)

ABSTRACT

Phenothiazines previously separated by thin-layer chromatography were detected on the plates by photochemical derivatization and gave different R_F values in six solvent systems. The methanol–acetic acid (95:5, v/v) system gave the best separation and greatest chromatic and fluorescence intensities. Qualitative and quantitative information about propiomazine, acetopromazine and chlorpromazine was obtained by image analysis. Images were obtained with a charge-coupled device camera (CCD) under different conditions using both pseudocolour red–green–blue (RGB) and grey-scale tones and then filtering the light emitted when the derivative spots were excited by UV light. Calibration graphs for acetopromazine were linear from 3.94 to 22.00 m*M*, for chlorpromazine from 2.69 to 13.00 m*M* and for propiomazine from 3.31 to 15.00 m*M*.

INTRODUCTION

In contrast to liquid chromatography, thin-layer chromatography (TLC) suffers from a lack of automation. Image analysis can be useful in attempts to automate the analysis of TLC plates because it minimizes human intervention. Image analysis facilitates the extraction of quantitative characteristics from images and objective interpretation. Several articles have recently appeared in the literature describing the capabilities of multichannel imaging devices such as charge-coupled devices as detectors in TLC [1–4]. These systems involve the capture of the image; this image can then be stored in digital form on a host computer and operated on at any future time [5,6].

Computer-controlled scanning densitometers are the state of the art in commercial instruments to obtain quantitative information from TLC plates. The performances of video densitometers and scanning densitometers have previously been compared [1]. The mechanical scanners tend to be slow and expensive, and the results can be user dependent, however better spatial resolution is achieved than with video densitometers.

In situ photoxidation is particularly suitable for obtaining labelled compounds because the derivative is formed without dipping or spraying of the plate. Post-chromatographic derivatization in TLC allows the reaction of all standards and samples simultaneously under the same conditions, and the separation properties of the solutes are not changed by the reaction.

The phenothiazines (Fig. 1) are a group of well-known psychopharmaceuticals. These compounds contain a reduced sulphur that can be photoxidized to a sulphoxide [7]. Both chemical and photochemical oxidations of phenothiazines to fluorescent sulphoxide derivatives have been applied and significantly improve the detectability of these analytes [8–10]. However, this method has not been exploited for detecting phenothiazines separated by TLC.

In this work we determined the optimal sepa-

* Corresponding author.

0021-9673/93/$06.00

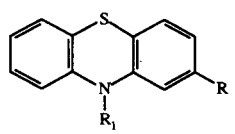

	R_1	R
Trimeprazine	CH_2-CH-CH_2-CH_2-N(CH_3)$_2$ (CH$_3$ on CH)	H
Promethazine	CH_2-CH-N(CH_3)$_2$ (CH$_3$ on CH)	H
Promazine	CH_2-CH_2-CH_2-N(CH_3)$_2$	H
Propiomazine	CH_2-CH-N(CH_3)$_2$ (CH$_3$ on CH)	CO-CH_3
Thioridazine	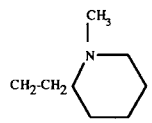	S-CH_3
Ethopropazine	CH_2-CH-N(C_2H_5)$_2$ (CH$_3$ on CH)	H
Chlorpromazine	CH_2-CH_2-CH_2-N(CH_3)$_2$	Cl
Acetopromazine	CH_2-CH_2-CH_2-N(CH_3)$_2$	CO-CH_3

Fig. 1. Structure of phenothiazines.

ration conditions for post-chromatographic photochemical detection on TLC plates. The plate images were acquired by using a charge-coupled device camera and then processed to extract the maximum information about the TLC plate.

EXPERIMENTAL

Thin-layer chromatography

The phenothiazine compounds were obtained from Sigma and the solvents used were purchased from Merck. All samples were prepared in ethanol and were sonicated for at least 10 min. The stock solutions of trimeprazine 8.13 m*M*, promethazine 4.58 m*M*, promazine 4.30 m*M*, propiomazine 18.51 m*M*, thioridazine 5.31 m*M*, ethopropazine 6.30 m*M*, chlorpromazine 15.14 m*M* and acetopromazine 25.23 m*M* were stored in the dark.

Phenothiazine mixtures were chromatographed on HPTLC silica gel 60 plates (Merck) following the procedure described previously [11] using methanol–acetic acid (95:5, v/v) as mobile phase.

Samples were applied by the spray-on technique using a Camag Linomat IV microprocessor-controlled device. Spots of 10-μl aliquots from the samples were placed on the plates at 10.0-mm intervals.

Phenothiazines were detected on the TLC plates by photolysis and analysing the images acquired by using a charge-coupled device camera and suitable software.

Photochemical–fluorimetric procedures

After chromatographic separation the plates were exposed for a fixed time to light from a photochemical reactor equipped with a 125-W mercury vapour lamp and water cooling [12].

For the photochemical–fluorimetric measurements in liquid solution, 100 ml of phenothiazine solution were placed in the photochemical reactor and irradiated for a fixed time. The fluorescence intensity of this solutions was then measured in a Perkin-Elmer LS-50 spectrofluorimeter.

Image acquisition

Images of the plate were captured with a Sony AVC-D7CE video camera with an 8-mm F/1.3 lens. Digitization of the video images was performed with an S-151 AT/VME digitizing tablet. The images were transferred in binary format to a host computer, which controls the working of the system through Visilog version 3.6 software.

To obtain absorbance measures, a light box with back illumination of the TLC plate was used. The geometrical arrangement of two tubular lamps (30 W each) in the light box ensured uniform lighting of the entire area of the plate. It should be noted that these are not true absorbance data since no logarithmic calculation was performed. To obtain fluorescence measures a 6-W Mineralight UV lamp Model, UVGL-58, in front the plate, at 45°, is used to excite the sample and a 365-nm filter was attached to the

camera lens to reduce extraneous excitation light.

The developed plates were placed on the light box surrounded by a non-transmitting background and the boundaries for the scanning area were set. To obtain complete information about the plate, two images were acquired with boundaries defined by the user. Orientation of the plate was fixed in such way that the "starting wells" were situated horizontally, and the direction of development was vertical, from the bottom to top of the image.

Images obtained were stored in a digital format in the computer, and they could be both displayed and manipulated. Digitization consisted of the transformation of the image into a matrix; each element of this matrix corresponds to a picture element or pixel. Each pixel can be considered as a miniature cuvette, and its intensity is a transmission, reflection or fluorescence value. From a monochrome image, each pixel is characterized by its grey-level value, coded by an integer number. Polychrome images are coded in the same way, but with three matrices corresponding to each colour channel: red, green and blue (RGB).

Monochrome and polychrome images were obtained in each mode —"absorbance" and fluorescence.

Image analysis

The digital image was used for quantitative as well as for qualitative work. A previous image processing is necessary to enhance and improve the image. Thus, the noise can be reduced. The noise results in pixels having abnormal grey levels that differ from those of their closest neighbours. To reduce noise, both random and systematic, we applied median filtering. In this case the neighbours of a given pixel were sorted according to their grey level. The pixel to be processed was replaced by the median grey level.

Once obtained, enhanced images were processed in order to extract a number of quantitative features. The steps result in the separation of objects from the background. Each separated spot can then be characterized by a number of numerical features. Thus, several morphological parameters were obtained which could be used to discriminate between the different detected spots according to shape or size or a combination thereof.

Also, the intensity values for each pixel were obtained for describing the distribution of light intensities. The graphic output can be considered a chromatogram, with intensity values on the y-axis and pixel on the x-axis. Because distortions of spots compromise resolution and introduce reading errors, readings were taken in four different positions of each spot. The fluorescence intensity was recorded as peaks of light intensity. In the absorbance mode the graphic output was blank subtracted because the intensity values are transmitted light.

The imaging detectors are wide-band, and filters or monochromators are necessary for extracting information in smaller bands. A cut-off 365-nm filter was used to filter excitation light in fluorescence mode. Additionally, absorbance mode images were also obtained with a 470-nm cut-off filter attached to the lens.

RESULTS AND DISCUSSION

Photolysis in ethanolic solutions

In order to obtain data about time of irradiation and chromogenic and fluorogenic behaviour subsequent to the photoexcitation of the reagents under study, the photolysis was studied in ethanolic solution, the medium used to solubilize the phenothiazine drugs. Table I shows the spectral characteristics before and 2 h after irradiation. Irradiation of phenothiazine drugs, which have weak native fluorescence, results in relevant changes in its fluorescence and colour characteristics. Up to a wavelength (λ) of 113 nm blue-shift in excitation (λ_{ex}) and up to 130 nm red-shift in emission (λ_{em}) maxima is observed. As an exception a 15-nm blue-shift emission maxima is observed for promethazine. A five-fold increase in relative fluorescence intensity at the emission maximum for promazine and ethopropazine was observed.

Photoxidation takes place immediately for all the compounds studied except for chlorpromazine, and is complete 2 h later. Propiomazine needs 6 h for complete photoxidation.

TABLE I

FLUORESCENCE OF PHENOTHIAZINES IN 100% ETHANOL

25°C; $slit_{ex} = 2.5$ nm; $slit_{em} = 5$ nm

Compound	Before irradiation			2 h after irradiation		
	λ_{ex}	λ_{em}	RFI[a]	λe_x	λ_{em}	RFI[a]
Trimeprazine, 1.02 m*M*	305	440	419	370	485	142
Promethazine, 0.60 m*M*	277, 330	440	227	390	455	150, 370
Promazine, 0.12 m*M*	300	440	211	320	365	1000
Propiomazine, 0.10 m*M*	300	530	114	360[b]	400[b]	143[b]
Thioridazine, 0.39 m*M*	300, 330	460	154	360	375	396
Ethopropazine, 0.11 m*M*	300	440	151	330	365	687
Chlorpromazine, 0.41 m*M*	300	440	145	370	455	180
Acetopromazine, 0.42 m*M* [c]	340, 395	560	70	390	485	190

[a] Relative fluorescence intensity.
[b] 6h after irradiation.
[c] $Slit_{ex} = 2.5$ nm; $slit_{em} = 10$ nm.

These data were used for the detection of the spots in the plates.

Chromatographic conditions

To optimize the mobile phase, a series of binary, ternary and quaternary solvent mixtures were prepared. In binary mixtures a fixed solvent was used and the other solvent was varied. Because the nature of photoproducts to be detected can be affected by the medium [1], the influence of acidity was considered by using as second solvent 25% ammonia, acetic acid and buffer of pH 9 and pH 3. Other solvent mixtures were also used. In Table II the different solvent compositions and the R_F values of each compound in the solvents studied are shown. The best separation was achieved by using the binary mixtures methanol–25% ammonia (95:5, v/v) and methanol–acetic acid (95:5, v/v) as mobile phases. In contrast, mobile phases methanol–buffer pH 9 (40:20, v/v) and methanol–buffer pH 3 (40:20, v/v) with similar acidity characteristics did not give good separation. The other systems gave intermediate results.

Before separation and irradiation all the spots were slightly coloured and fluorescent. After 5 min of plate irradiation the spots colour changes. The colour and fluorescence of spots changed with the mobile phase used. With methanol–25% ammonia (95:5, v/v) and methanol–acetic acid (95:5, v/v) all the compounds showed fluorescence and colour. With the methanol–acetic acid (95:5, v/v) system the values were greater.

Images of acetopromazine, chlorpromazine, propiomazine and mixtures at several concentrations were obtained. The results of the morphological measurements are given in Table III. The measured parameters are: area, perimeter and two form factors to account for specific shape characteristics. The first form factor (eccentricity) measures the elongation of the object in the chromatographic development direction. Its value is zero for round particles. The second form factor (compactness) is based on the ratio of perimeter squared to area and is minimal and equal to 1 for round particles. An elongated set has a high shape factor. It also measures an object's roughness, so a cranked disc has a high shape factor even though it is globally circular.

The results in Table III indicate that the area and perimeter spots increase with concentration of phenothiazine. From the near-zero eccentricity values it is deduced that the elongation of chlorpromazine and propiomazine spots is minimal, *i.e.* they are round spots. Greater elongation is observed for acetopromazine spots. The

TABLE II

R_F VALUES FOR PHENOTHIAZINES USING DIFFERENT MOBILE PHASES

Mobile phase composition (v/v)	Compound							
	Trimeprazine	Promethazine	Promazine	Propiomazine	Thioridazine	Ethopropazine	Chlorpromazine	Acetopromazine
Methanol–chloroform (1:9)	0.32	0.31	0.21	0.29	0.27	six spots	0.18	0.18
Methanol–25% ammonia (95:5)	0.66	0.61	0.53	0.65	0.56	three spots	0.59	0.56
Methanol–acetic acid (95:5)	0.42	three spots	0.34	0.50	0.46	–	0.40	0.31
Methanol–buffer borax hydrochloride pH 9 (40:20)	0.05	–	0.05	0.18	0.03	–	0.05	0.04
Methanol–buffer phthalate hydrochloride pH 3 (40:20)	0.31	–	0.28	0.31	0.24	–	0.28	0.23
Methanol–acetic acid–30% hydrogen peroxide (94:5:1)	0.58	–	0.57	0.60	0.54	–	0.60	0.57
Methanol–acetic acid–chloroform (45:15:30)	0.67	–	0.60	0.66	0.67	–	0.64	0.53
Acetone–isopropanol–25% ammonia (27:21:12)	0.73	0.72	0.78	0.73	0.73	–	0.92	0.71
Isopropanol–chloroform–water–25% ammonia (35:30:4:1)	0.64	0.55	0.44	0.63	0.53	four spots	0.53	0.47

TABLE III

MORPHOLOGICAL PARAMETERS OF PHENOTHIAZINE SPOTS SEPARATED BY TLC

	Quantity spotted (μg)	Area (mm^2)	Perimeter (mm)	Eccentricity	Compactness
Acetopromazine	17.4	5.00	15.50	2.72	3.82
	44.2	16.00	26.91	1.10	3.60
	97.3	33.00	40.26	0.31	3.91
Chlorpromazine	9.5	42.00	45.80	0.03	3.97
	25.3	63.00	52.37	0.02	3.46
	46.2	58.00	60.14	0.54	4.96
Propiomazine	15.1	41.00	43.02	0.00	3.59
	37.2	56.00	58.45	0.49	4.85
	68.5	83.00	75.41	0.84	5.45

second form factor values are high and similar for all spots. A combination of both form factors indicates that chlorpromazine and propiomazine spots are round with no elongation and roughness. Acetopromazine spots can be deduced to be highly elongated.

Quantitative analysis

Several phenothiazine mixtures were spotted and chromatographed. Figs. 2 and 3 represent graphic output of the blue component of the plates image in absorbance mode using a 470-nm filter. In the fluorescence mode the graphic

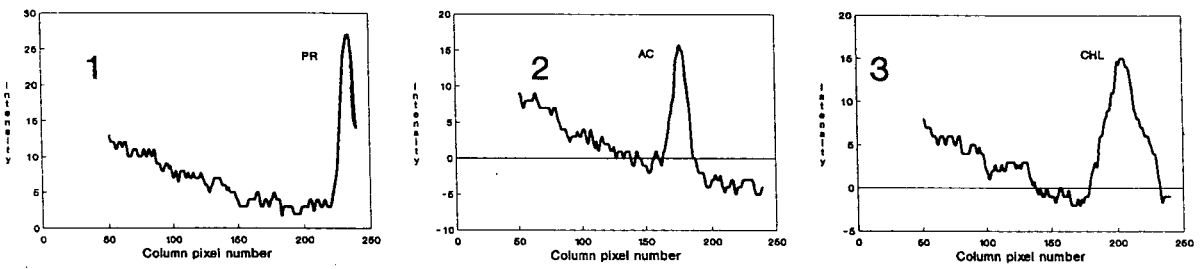

Fig. 2. Graphic output for the blue component in the absorbance mode and using a 470-nm filter. AC = Acetopromazine standard; CHI = chlorpromazine standard; PR = propiomazine standard.

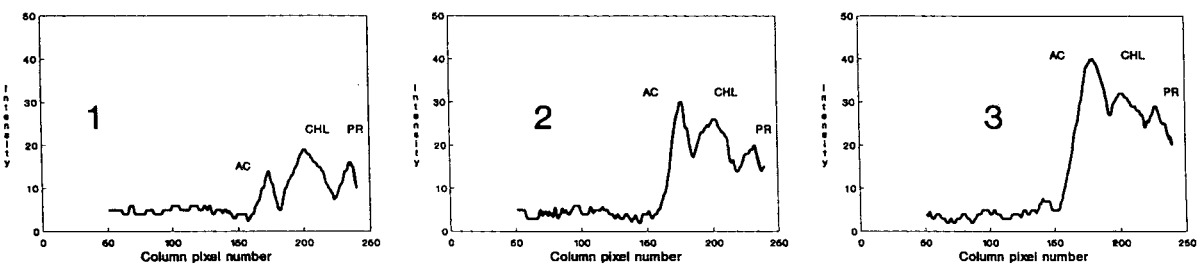

Fig. 3. Graphic output for the blue component in the absorbance mode and using a 470-nm filter. 1 = Mixture of 3.94 m*M* AC, 2.69 m*M* CHL and 3.31 m*M* PR; 2 = mixture of 10 m*M* AC, 7.14 m*M* CHL and 8.15 m*M* PR; 3 = 22 m*M* AC, 13 m*M* CHL and 15 m*M* PR. AC = Acepromazine; CHL = chlorpromazine; PR = propiomazine.

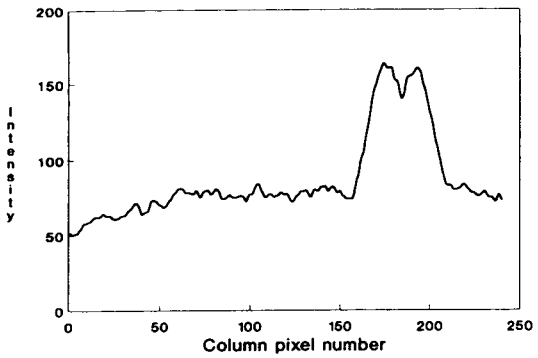

Fig. 4. Graphic output for the blue component in the fluorescence mode. Mixture of 10 m*M* acepromazine, 7.14 m*M* chlorpromazine and 8.15 m*M* propiomazine.

output shows wide peaks with low resolution (Fig. 4). The best-resolved peaks are obtained in the absorbance mode. The red colour gives greater noise than green and blue. Green gives data with lower noise but little signal intensity. Blue colour provides high intense signal and low noise. This illustrates the utility of pseudocolour selectivity.

Quantitative data were obtained using peak heights of standards, and calibration curves were constructed by plotting peak heights *versus* concentration. Table IV shows the standard curves for acetopromazine, chlorpromazine and propiomazine obtained in the absorbance mode. Propiomazine only showed a detectable signal in the fluorescence mode and by analysing the blue component in the absorbance mode. Calibration graphs were linear for acetopromazine in the range 3.94–22.00 m*M*, for chlorpromazine in the range 2.69–13.00 m*M* and for propiomazine in the range 3.31–15.00 m*M*.

CONCLUSIONS

The results obtained show that reliable man-independent techniques for qualitative and quantitative thin-layer chromatography can be achieved by computer-assisted image analysis.

Phenothiazines separated by TLC can be detected by photochemical derivatization and give rise to coloured or fluorescent spots. Images of the plates can be obtained by using a charge-coupled device, and subsequent analysis methods are easily performed given the right software.

The obtained morphological parameters of the spots gave quantitative information about their shape or size, and could be useful in future experiments as a measure of the separation quality. Image analysis under different conditions using both pseudocolour red–green–blue (RGB) and grey-scale tones, and then filtering

TABLE IV

STANDARD CURVES FOR ACETOPROMAZINE, CHLORPROMAZINE AND PROPIOMAZINE

y = concentration; x = intensity.

Compound	Image component analysed	Calibration curve ($n = 5$)	Correlation coefficient
Acetopromazine	Grey	$y = 1.1x - 24.7$	0.99
	Blue	$y = 0.3x - 15.1$	0.94
	Blue filter	$y = 0.7x - 6.6$	0.95
	Red	$y = 4.4x - 140.4$	0.99
	Red filter	$y = 1.4x - 48.2$	0.99
Chlorpromazine	Grey	$y = 0.4x - 11.7$	0.98
	Blue	$y = 0.3x - 14.6$	0.99
	Blue filter	$y = 0.8x - 12.5$	0.96
	Red	$y = 0.5x - 23.4$	0.98
	Red filter	$y = 0.4x - 19.0$	0.97
Propiomazine	Blue filter	$y = 0.8x - 10.2$	0.96

the light emitted when the derivative spots were excited by UV light, illustrates the utility of pseudocolour selectivity.

In future, the sensitivity and resolution of separation may be improved by better plate illumination and wavelength selection, respectively. Also, the acquisition of successive images during the chromatographic process could improve the separation in a similar manner to diode-array detection in liquid chromatography.

REFERENCES

1 P.B. Oldham, *Anal. Instrumentation*, 19 (1990) 49.
2 D.H. Burns, J.B. Callis and G.D. Christian, *Trends Anal. Chem.*, 5 (1986) 50.
3 P.K. Aldrigde, J.B. Callis and H. Burns, *J. Liq. Chromatogr.*, 13 (1990) 2829.
4 S.H. Wettlaufer, L.H. Weinstein, *J. Chromatogr.*, 441 (1988) 361.
5 D. Betrand, M.-F. Devaux and P. Robert, *Trends Anal. Chem.*, 10 (1991) 237.
6 P. Geladi, E. Bengtsson, K. Esbensen and H. Grahn, *Trends Anal. Chem.*, 11 (1992) 41.
7 J.W. Birks, *Chemiluminescence and Photochemical Reaction Detection in Chromatography*, VCH, New York, 1989, p. 151.
8 U. Breyer, *Biochem. Pharmacol.*, 18 (1969) 777.
9 A.H.M.T. Scholten, U.A.Th. Brinkman and R. Frei, *Anal. Chim. Acta*, 114 (1980) 137.
10 D. Chen, A. Ríos, M.D. Luque de Castro and M. Valcárcel, *Talanta*, 38 (1991) 1227.
11 A. Navas Díaz, *Anal. Chim. Acta*, 255 (1991) 297.
12 J.J. Aaron, J. Fidanza and M.D. Gaye, *Talanta*, 30 (1983) 649.

Journal of Chromatography A, 655 (1993) 39–43
Elsevier Science Publishers B.V., Amsterdam

CHROM. 25 155

Thin-layer chromatography and fibre-optic fluorimetric quantitation of thiamine, riboflavin and niacin

A. Navas Díaz*, A. Guirado Paniagua and F. García Sánchez

Departamento de Química Analítica, Facultad de Ciencias, Universidad de Málaga, Málaga (Spain)

ABSTRACT

Thiamine (vitamin B_1), riboflavin (vitamin B_2) and niacin (nicotinic acid) were separated by thin-layer chromatography and fluorimetrically determined by using a commercially available fibre-optic-based instrument. Under fluorimetric monitoring riboflavin shows native fluorescence, but nicotinic acid and thiamine had to be pre-chromatographically converted to fluorescent derivatives. A new fluorescent tracer, fluoresceinamine, isomer II, was used to label the nicotinic acid. Thiamine was converted to fluorescent thiochrome by oxidizing with potassium ferricyanide solution in aqueous sodium hydroxide. The analytes were separated on HPTLC silica gel plates using methanol–water (70:30, v/v) as mobile phase. In these conditions the R_F values for the thiamine, riboflavin and niacin derivatives were, respectively, 0.73, 0.86 and 0.91. The developed plate was scanned by a bifurcated fibre-optic that both transmits emission radiation to the plate and collects the emission signal to the fluorimeter. Calibration curves for the determination of thiamine 300–750 ng, riboflavin 48–320 ng and niacin 10–100 ng were established.

INTRODUCTION

Thiamine, riboflavin and niacin frequently occur together in foods. High-performance liquid chromatography (HPLC) can separate and determine these vitamins [1,2]. Thin-layer chromatography can be used to determine simultaneously thiamine, riboflavin and pyridoxine [3].

High-performance thin-layer chromatography (HPTLC) permits comparable separations to HPLC [4]. The high resolution obtained by HPTLC might remain unexploited without reliable instrumentation for *in situ* quantitation of planar separations [5]. Although measurements are possible by using mechanical densitometers, recent advances in fibre-optics have made it possible to couple these devices to commercial fluorescence spectrometers that permit spectroscopic measurements remote from the detector head. Consequently, absorption [6] or fluorescence [7] measurements are now possible in places where it is difficult or impossible to bring the sample to the spectrometer, such as a TLC plate.

Thiamine, riboflavin and niacin absorb in the UV range, but not strongly enough to be detected with sufficient sensitivity. Measurement of fluorescence is generally more sensitive than measurement of absorption. However, whereas riboflavin exhibits a high fluorescence quantum yield, thiamine and niacin do not fluoresce, so these compounds must be converted into fluorescent derivatives, either before or after chromatographic separation.

In pre-column derivatization of thiamine to fluorescent thiochrome [1,8–14] sample extracts are injected at high pH and in the presence of an excess of potassium ferricyanide. Both high pH and ferricyanide damage liquid chromatography columns. They must be removed before chromatographic analysis.

Moreover, when post-column derivatization [15–18] is used, the presence of an excess of oxidizing reagent in the mobile phase gives rise to fluorescent impurities that generate noise and

* Corresponding author.

0021-9673/93/$06.00

reduce the sensitivity of the detection method. These phenomena complement the existing disadvantages of post-column derivatization: they lengthen retention times, widen peaks and require a second pump system.

Derivatization of niacin with N,N′-dicyclohexyl-O-(7-methoxycoumarin - 4 - yl) -methylisourea for the vitamin determination by HPLC with fluorescent detection has been reported [19].

The simultaneous determination of water-soluble vitamins by HPLC has been demonstrated using photometric detection [2], but if sensitive fluorescence detection is required two detectors must be used [1,9,11,15–18]. The recoveries and reproducibility are good but the approaches are rather complex. Moreover, recently simultaneous determination of thiamine, riboflavin and pyridoxine by TLC with fluorimetric detection has been described [3].

In this work thiamine, riboflavin and niacin were separated by TLC before fluorescence analysis. Thiamine was pre-chromatographically converted to fluorescent thiochrome. Riboflavin revealed natural fluorescence, and fluoresceinamine, isomer II, was used to label niacin before chromatography [20].

EXPERIMENTAL

Materials

Thiamine hydrochloride, riboflavin, nicotinic acid, fluoresceinamine isomer II and N,N-dicyclohexylcarbodiimide (DCC), were obtained from Aldrich (Milwaukee, WI, USA) or Sigma (St. Louis, MO, USA). Potassium ferricyanide, sodium hydroxide and the solvents were purchased from Merck (Darmstadt, Germany). All samples were prepared in distilled–deionized water or in ethanol and were sonicated for at least 10 min.

Emission measurements were made with a Perkin-Elmer LS-50 luminescence spectrometer (Perkin-Elmer, Beaconsfield, UK) equipped with a plate-reader accessory. A 1-m glass fibre-optic bifurcated bundle (Oriel, Stratford, CT, USA) with a light transmission range of 390–1500 nm was used to transfer the excitation and emission energies between the plate and the spectrometer. Information was sent via the RS232C interface of the fluorescence instrument to an external computer. Instrumental parameters were controlled by Fluorescence Data Manager (FLDM) software (Perkin-Elmer). Three-dimensional and contour plots were made using SURFER software (Golden Software, Golden, CO, USA). Graphical print-out was from a NEC Silentwriter 2 laser printer (NEC, Tokyo, Japan).

Thin-layer chromatography

Samples were applied by the spray-on technique using a Linomat IV microprocessor-controlled device (Camag, Muttenz, Switzerland). Sample aliquots of 15 μl were applied to the plates in narrow 5-mm-long bands separated by 10 mm. The compounds were chromatographed on HPTLC Silicagel 60 plates without fluorescent indicator (Merck, No. 5631). The plates were developed in a Camag horizontal developing chamber for some 15 min over a distance of about 50 mm from the origin using methanol–water (70:30, v/v) as mobile phase. *In situ* measurements of thiamine, riboflavin and niacin were made at $\lambda_{ex} = 390$ nm, $\lambda_{em} = 440$ nm; $\lambda_{ex} = 464$ nm, $\lambda_{em} = 520$ nm, and $\lambda_{ex} = 501$ nm, $\lambda_{em} = 523$ nm, respectively. Blanks without analyte were measured in the same way as the analyte. Quantitative data were obtained using fluorescence intensity at the centre of the spots (peak heights). The calibration curves were constructed by plotting peak heights against concentration of standards.

Derivatization procedure

To samples containing thiamine, riboflavin and niacin were added 3 ml of 0.03 *M* potassium ferricyanide solution of 3.75 *M* aqueous sodium hydroxide; pH was adjusted to 7. To the neutralized solution were added fluoresceinamine and DCC in a molar ratio twice that of nicotinic acid. The reaction was carried out at room temperature for 24 h, and the precipitated cyclohexylurea was filtered through 0.2-μm nylon filter. The final solution was made up to 50 ml with ethanol before being subjected to thin-layer chromatography.

RESULTS AND DISCUSSION

Only riboflavin exhibits natural fluorescence. Nicotinic acid and thiamine were pre-chromatographically converted to fluorescent derivatives. A post-chromatographic derivatization of thiamine to fluorescent thiochrome on silica gel plate can be readily done, but for niacin this is difficult. Conversion of thiamine to the fluorescent derivative, thiochrome, is extensively used to detect this analyte by HPLC [1,8–18], and potassium ferricyanide in sodium hydroxide is used as the reagent. The same reagent concentration was found to be optimal to derivatize thiamine on the silica gel plate.

Fluorescent amines can be used to label the carboxylic groups. Because fluorescein derivatives offer high quantum efficiency, fluoresceinamine (isomer II) was selected to label the nicotinic acid. However, the carboxylic acid group had to be activated before coupling with the amines [21–23]. Carbodiimide derivatives such as N,N-dicyclohexylcarbodiimide (DCC) can be used for this.

$$RN=C=NR + R'\text{-}COOH \rightarrow RNH\text{–}\underset{\displaystyle OCOR'}{\underset{|}{C}}=NR$$

$$RNH\text{–}\underset{\displaystyle OCOR'}{\underset{|}{C}}=NR + R''NH_2 \rightarrow R'CONHR'' + RHNCONHR \text{ (cyclohexylurea)}$$

where R is the substituent of carbodiimide, R′ is the structure containing the carboxylic group and R″ is the structure that contains the amino group. The insoluble cyclohexylurea reaction product was filtered through a nylon filter. The reaction yield, as determined by preparative TLC, extrusion of the derivative band and subsequent fluorescent readings, appeared to be about 60–80%. An increase in the reaction temperature might improve this procedure, but this could lead to sample degradation.

The fluorescence spectra of thiamine, riboflavin and niacin and their derivatives were obtained. The excitation and emission maxima of riboflavin, thiochrome and niacin derivatized in ethanolic solutions and adsorbed on silica gel are shown in Table I. Only thiochrome modified their maxima with adsorption on silica gel.

To separate the vitamins on silica gel two mobile phases were analysed; methanol–water (70:30, v/v) and aqueous ammonia–chloroform–ethanol–acetone (2:2:2:1, v/v). Because similar separations were achieved with both these solvents, we choose the binary mixture methanol–water (70:30, v/v). With this mobile phase the R_F values for thiamine derivative, riboflavin, niacin derivative and fluoresceinamine were 0.73, 0.86, 0.91 and 1 respectively. The three-dimensional chromatogram and contour maps of the plate containing the separated vitamins, scanned at three different pairs of wavelengths are shown in Figs. 1 and 2. The fluorescence selectivity over that of HPTLC is well demonstrated because only the fluorescent vitamin gives a peak at each pair of wavelengths. The advantage of choosing

TABLE I

EXCITATION AND EMISSION MAXIMA OF THE INVESTIGATED VITAMINS IN ETHANOLIC SOLUTIONS AND ADSORBED ON SILICA GEL

	Ethanol		Silica gel	
	λ_{ex} (nm)	λ_{em} (nm)	λ_{ex} (nm)	λ_{em} (nm)
Thiamine derivative, $7.11 \cdot 10^{-6}$ M slit$_{ex}$ = 5 nm, slit$_{em}$ = 5 nm	369	415	390	440
Riboflavin, $4.25 \cdot 10^{-5}$ M slit$_{ex}$ = 2.5 nm, slit$_{em}$ = 2.5 nm	464	520	464	520
Nicotinic acid derivative, $4.8 \cdot 10^{-4}$ M slit$_{ex}$ = 2.5 nm, slit$_{em}$ = 5 nm	501	523	501	523

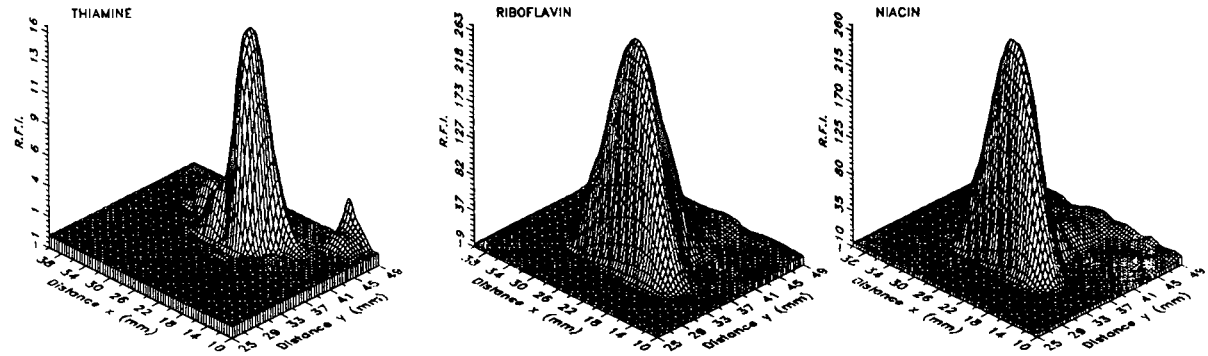

Fig. 1. Three-dimensional chromatogram with blank subtracted scanned at $\lambda_{ex} = 390$ nm and $\lambda_{em} = 440$ nm (thiamine, 200 ng spotted); $\lambda_{ex} = 464$ nm and $\lambda_{em} = 520$ nm (riboflavin, 96 ng spotted); $\lambda_{ex} = 501$ nm and $\lambda_{em} = 523$ nm (niacin, 169 ng spotted). R.F.I = Relative fluorescence intensity.

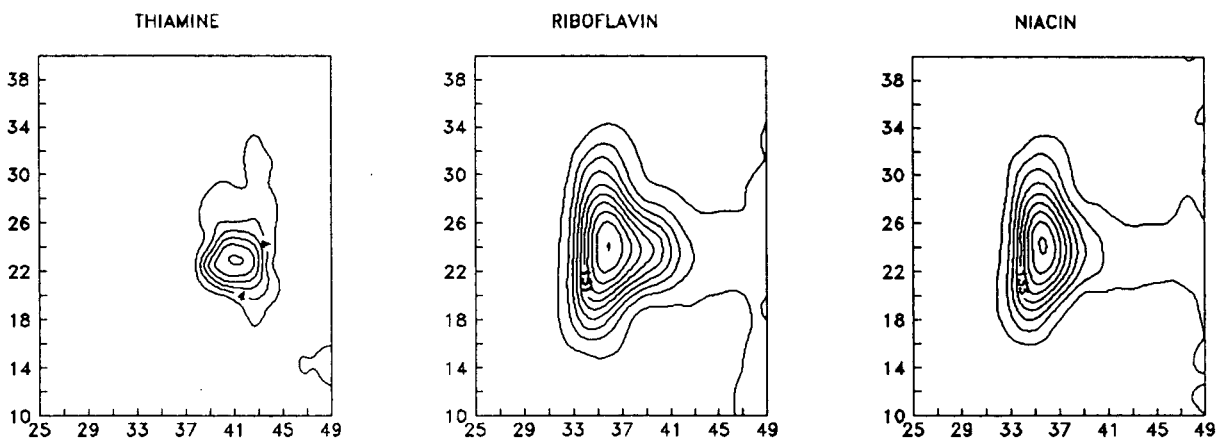

Fig. 2. Contour plots of the plate using the same parameters and concentrations as in Fig. 1.

the optimal detection wavelength for TLC by photodiode array spectrometry is described in ref. 6.

Quantitative analysis

Figs. 1 and 2 show that the peak widths of the different compound were very different. Because the sample substance was applied as a thin line at the origin, the concentration profiles of spots of separated substances exhibit a roughly Gaussian profile (cylinder character) [24]. The integral of the concentration density over the spot area was equal to the volume of the cylinder, which in turn is proportional to peak concentration value. In this way we can substitute integration by

TABLE II

STANDARD DEVIATION AND RELATIVE STANDARD DEVIATION

Compound	Concentration spotted (ng)	Mean peak height	S.D. ($n = 5$)	R.S.D. (%)
Thiamine	300	159	1.9	1.2
	450	245	5.9	2.4
	750	482	9.0	1.8
Riboflavin	48	35	4.6	13.1
	80	83	6.5	7.8
	160	210	11.0	5.2
Niacin	50	170	2.2	1.3
	70	212	1.8	0.8
	100	280	7.0	2.5

measuring the maximum fluorescence intensity (or peak height) at the centre of the spot.

The scanned relative fluorescence intensities (peak heights) as a function of spot concentration were found to be linear and ranged from 300 to 750 ng for thiamine, from 48 to 320 ng for riboflavin and from 10 to 100 ng for niacin. The respective regression coefficients were 0.9973 ($n = 5$), 0.9991 ($n = 5$) and 0.9992 ($n = 5$). Table II gives the mean peak heights, standard deviations (S.D.) and relative standard deviations (R.S.D.) for three different determinations at three concentration levels.

The repeatability of the derivatization procedure was checked by applying three loadings (15 μl each) of six solutions each with the same vitamin concentrations (thiamine $1.32 \cdot 10^{-4}$ M, riboflavin $1.78 \cdot 10^{-5}$ M and niacin $4.76 \cdot 10^{-5}$ M) and then subjecting them to the derivatization procedure. Repeatability [expressed as relative standard deviation (S.D.) ($n = 6$)] was 5.1% for thiamine, 6.0% for riboflavin and 4.2% for niacin.

Although the yield of the derivatization reaction is not high (60–80%), repetitive between-batch experiments showed good standard deviations of the measurements, consequently the method appears to be a reliable approach for determining the assayed compound. A calibration graph should be made before each assay.

The detection limit (DL) is defined as that concentration which gives an analytical signal equal to three times the blank noise and is calculated using the expression $DL = 3s_{bk}/m$, where s_{bk} is the standard deviation of the blank signals ($s_{bk} = 1.8$) and m is the slope of the calibration curve. Values for thiamine, riboflavine and niacin were 0.73, 1.71, and 2.08, respectively. The values of the detection limits were 7.4 ng, 3.1 ng and 2.6 ng for thiamine, riboflavin and niacin, respectively.

CONCLUSIONS

This method has several advantages over those mentioned in the literature. It is not necessary to eliminate the oxidation reagent excess and this permits simultaneous determinations of vitamins with only one detector. The separation time is 15 min. The sensitivities and selectivities of fluorescence detection allow these vitamins to be quantified with low detection limits and also to discriminate between several compounds whose chromatographic resolution is poor by spectral resolution.

REFERENCES

1 G.R. Skurray, *Food Chem.*, 7 (1981) 77.
2 G.W. Chase and A.M. Soliman, *J. Micronutr. Anal.*, 7 (1990) 15.
3 Y. Zang and Z. Ma, *Sepu*, 7 (1989) 243.
4 J. Sherma and B. Fried (Editors), *Handbook of Thin Layer Chromatography*, Marcel Dekker, New York, 1991.
5 C.F. Poole and S.K. Poole, *J. Chromatogr.*, 492 (1989) 539.
6 S. Bayerbach and G. Gauglitz, *Fresenius' Z Anal. Chem.*, 335 (1989) 370.
7 A. Navas Díaz, *Anal. Chim. Acta*, 255 (1991) 297.
8 C.Y.W. Ang and F.A. Moseley, *J. Agric. Food Chem.*, 28 (1980) 483.
9 J.K. Fellman, W.E. Artz, P.D. Tassinari, C.L. Cole and J. Augustin, *J. Food Sci.*, 47 (1982) 2048.
10 J. Augustin, *J. Assoc. Off. Anal. Chem.*, 70 (1984) 1012.
11 P.M. Finglas and R.M. Fulks, *Food Chem.*, 15 (1984) 37.
12 C. Hasselmann, D. Franck, P. Grimm, P.A. Diop and C. Soules, *J. Micronutr. Anal.*, 5 (1989) 269.
13 E.S.P. Reyes and L. Subryan, *J. Food Composition Anal.*, 2 (1989) 41.
14 G.W. Chase, Jr., W.O. Landen, Jr., R.R. Eitenmiller and A.-G.M. Soliman, *J. Assoc. Off. Anal. Chem.*, 75 (1992) 561.
15 D.J. Mauro and D.L. Wetzel, *J. Chromatogr.*, 299 (1984) 281.
16 R.L. Wehling and D.L. Wetzel, *J. Agric. Food Chem.*, 32 (1984) 1326.
17 P. Wimalarisi and R.B.H. Wills, *J. Chromatogr.*, 318 (1985) 412.
18 R.B.H. Wills, P. Wimalasiri and H. Greenfield, *J. Micronutr. Anal.*, 1 (1985) 23.
19 Y. Tsuruta, K. Kohashi, S. Ishida and Y. Ohkura, *J. Chromatogr.*, 309 (1984) 309.
20 F. García Sánchez, A. Navas, F. Alonso and J. Lovillo, *J. Agric. Food Chem.*, submitted for publication.
21 J. Goto, N. Goto and T. Nambara, *J. Chromatogr.*, 239 (1982) 559.
22 H. Lingeman, A. Hulshoff, W.J.M. Underberg and F.B.J.M. Offermann, *J. Chromatogr.*, 290 (1984) 215.
23 T. Chard, *An Introduction to Radioimmunoassay and Related Techniques*, Elsevier, Amsterdam, 3rd ed., 1989.
24 V.A. Pollak, *J. Chromatogr.*, 77 (1973) 245.

Journal of Chromatography A, 655 (1993) 45–49
Elsevier Science Publishers B.V., Amsterdam

CHROM. 24 973

Thin-layer chromatography of N,N-disubstituted dithiocarbamates of nickel(II) and cobalt(II)

B. Martinez and J.C. Orte*

Department of Physical Chemistry, Faculty of Pharmacy, University of Granada, Campus Universitario de Cartuja, 18071 Granada (Spain)

M. Miró

Department of Pharmacology, Faculty of Pharmacy, University of Granada, Granada (Spain)

G. Crovetto and J. Thomas

Department of Physical Chemistry, Faculty of Pharmacy, University of Granada, Campus Universitario de Cartuja, 18071 Granada (Spain)

ABSTRACT

The separation and chromatographic behaviour with different mobile phases of dithiocarbamates of Co(II) and Ni(II) is reported. The effects of the solvent strength and the amine from which the chelate is derived were studied. Slopes of the straight-line plot of R_M *vs.* log X_s (X_s = molar fraction of the more polar component in the mobile phase) showed the differences in the adsorption of the metal chelates.

INTRODUCTION

Separations of neutral dithiocarbamates (DTCs) using different chromatographic techniques have been reported [1,2]. However, there has not been much work on the TLC behaviour of dithiocarbamates.

In 1973, Galík [3] made a theoretical study of the chromatographic behaviour of metal chelates because practical studies had not been possible. Soundararajan and Subbaiyan reported the TLC of some DTCs of Zn, Cd and Hg [4] and the separation of Tl(I) and Tl(III) DTCs by TLC [5].

In this work, we studied the TLC behaviour of the DmetDTC (dimethyldithiocarbamate), DetDTC (diethyldithiocarbamate), BmetDTC (N-benzyl-N-methyl dithiocarbamate), BetDTC (N-benzyl-N-ethyldithiocarbamate), DbenDTC (N,N-dibenzyldithiocarbamate), (+)EpDTC [(+)-ephedrinedithiocarbamate], (−)EpDTC [(−)-ephedrinedithiocarbamate), (+)ΨEpDTC [(+)-Ψ-ephedrinedithiocarbamate], (−)ΨEpDTC [(−)-Ψ-ephedrinedithiocarbamate) and BetOHDTC (N-benzyl-N-ethanoldithiocarbamate) of Co(II) and Ni(II) with different mobile phases: hexane, toluene, benzene, diethyl ether and their binary mixtures.

The adsorption process of the chelates with binary mobile phase may be studied following Galík's equation [3]:

$$R_M = (-m/n) \log X_s + C$$

where C is a constant that includes the influence of the active component in the mobile phase (S),

* Corresponding author.

0021-9673/93/$06.00

the humidity and the temperature, X_s is the molar fraction of the active component S and m and n are the number of bonds with which the chelate and active solvent molecules, respectively, are adsorbed. Hence the slope $(-m/n)$ of the straight-line plot of R_M *vs.* log X_s is a measure of the degree of adsorption of chelate molecules.

EXPERIMENTAL

The sodium salts of dithiocarbamates were synthesized following the method suggested by Crovetto [6], Gómez [7] and Montes [8].

Thin layers (thickness 0.26 mm) were prepared by spreading a slurry of a mixture of 50 g of silica gel 60G (Merck, Darmstadt, Germany) and 120 ml of water with a Shandon multi-thickness applicator on clean glass plates (20 × 20 cm). In order to activate the layer for adsorption chromatography they were kept at 110°C for at least 90 min.

The samples were prepared by reaction of each ligand (sodium salts) with $CoSO_4 \cdot 7H_2O$ and $NiCl_2$ in aqueous medium up to saturation. The complex was extracted using ethyl acetate. The structure of the chelates studied is shown in Fig. 1.

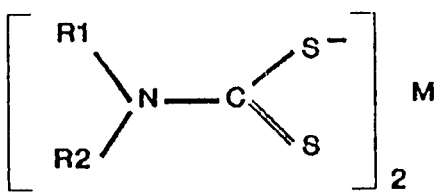

Dithiocarbamate derivative of	R_1	R_2
N,N-Dimethylamine (Dmet)	CH_3	CH_3
N,N-Diethylamine (Det)	CH_2–CH_3	CH_2–CH_3
N-Benzyl-N-methylamine (Bmet)	CH_2–C_6H_5	CH_3
N-Benzyl-N-ethylamine (Bet)	CH_2–C_6H_5	CH_2–CH_3
N,N-Dibenzylamine (Dben)	CH_2–C_6H_5	CH_2–C_6H_5
N-Benzyl-N-ethanolamine (BetOH)	CH_2–C_6H_5	CH_2–CH_2OH
(+)-Ephedrine [(+)Ep]	CH_3	$C_9H_{11}O$
(−)-Ephedrine [(−)Ep]	CH_3	$C_9H_{11}O$
(+)-Ψ-Ephedrine [(+)ΨEp]	CH_3	$C_9H_{11}O$
(−)-Ψ-Ephedrine [(−)ΨEp]	CH_3	$C_9H_{11}O$

Fig. 1. Structure of metal(II) N,N-disubstituted dithiocarbamates. M = Metal.

The mobile phases (toluene–diethyl ether, benzene–diethyl ether and hexane–benzene of various compositions) were prepared just before use. The polarity of the solvents increases in order hexane < toluene < benzene < diethyl ether.

The plates were kept at 20°C and laboratory humidity until they were cold in order to obtain reproducible R_F measurements. The solution of metal chelate and ethyl acetate was spotted 2 cm from the lower end of the plates, which were then placed in saturated tanks (Shandon). The solvent front was allowed to move 15 cm from the spotted regions. The chelates were made visible with iodine vapour.

RESULTS AND DISCUSSION

The hR_F values (average of at least three experiments) are listed in Table I. These data and Figs. 2–4 [R_F values of Co(II) and Ni(II) DmetDTC *vs.* percentage of the more polar component in the mobile phase] demonstrate the metals can be separated under conditions used.

DmetDTC, DetDTC, BmetDTC and BetDTC show similar behaviour with respect to the metals. The resolution increases with increasing polarity up to toluene, then it decreases.

The behaviour of (+)EpDTC is the same as that of (−)EpDTC. In this instance the separa-

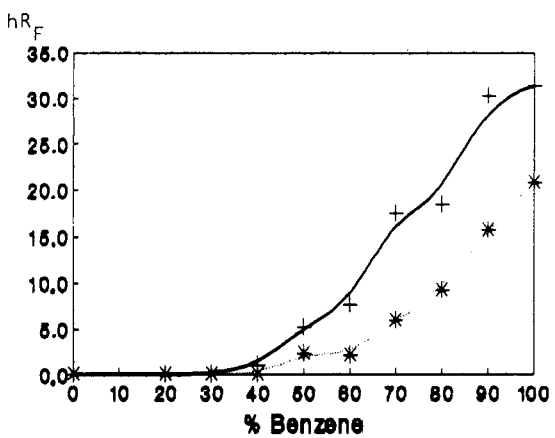

Fig. 2. Plots of hR_F *versus* percentage of benzene in the hexane–benzene binary mobile phase for (*) Co(II) and (+) Ni(II) DmetDTC.

TABLE I

R_F VALUES OF N,N-DISUBSTITUTED DITHIOCARBAMATES WITH BINARY MOBILE PHASES

Mobile phase	Composition	Metal	DTC									
			Dmet	Det	Bmet	Bet	Dben	(+)Ep	(−)Ep	(+)ΨEp	(−)ΨEp	BetOH
Benzene–diethyl ether	100:0	Ni	31.3	41.7	56.1	60.5	72.0	2.3	2.9	0.0	0.0	0.0
	90:10		63.7	72.1	75.3	77.1	79.2	27.8	30.1	6.9	7.5	2.5
	80:20		65.2	74.3	80.9	81.4	80.8	47.7	48.3	18.9	19.8	7.8
	50:50		70.7	77.2	82.2	83.0	84.0	65.8	71.7	52.9	51.0	23.6
	0:100							82.6	84.4	75.4	74.7	40.8
	100:0	Co	20.8	31.5	50.0	55.3	72.4	0.0	0.0	0.0	0.0	0.0
	90:10		62.2	75.1	78.2	79.7	80.7	9.1	9.1	1.0	1.6	0.0
	80:20		69.4	79.3	84.3	84.4	84.0	26.0	26.7	5.1	6.0	2.1
	50:50		72.4	82.3	84.6	85.2	86.1	61.7	71.0	31.3	28.7	10.4
	0:100							84.8	84.8	61.7	58.6	19.9
Toluene–diethyl ether	100:0	Ni	33.2	43.5	49.4	52.0	68.3	2.6	1.4	0.0	0.0	0.0
	90:10		43.3	64.7	70.3	77.0	83.2	22.1	24.0	4.1	4.9	1.1
	70:30		64.1	76.4	77.1	80.8	86.2	48.4	52.7	23.9	24.6	11.3
	50:50		66.7	74.4	83.8	83.9	87.4	62.8	68.5	43.2	44.3	21.8
	0:100		69.1					82.6	84.4	75.4	74.7	40.8
	100:0	Co	15.7	30.0	41.3	46.5	66.4	0.0	0.0	0.0	0.0	0.0
	90:10		43.9	63.7	72.0	78.9	85.4	4.7	4.9	0.0	0.0	0.0
	70:30		63.9	81.3	80.8	83.1	88.4	44.3	37.1	6.7	6.3	2.7
	50:50		65.1	79.7	84.9	85.1	90.5	56.3	60.3	20.6	21.3	8.4
	30:70		64.3					73.1	70.8	38.4	40.8	13.4
	0:100							84.8	84.8	61.7	58.6	19.9
Hexane–benzene[a]	80:20	Ni	0.0	1.7	0.6	3.0	6.3					
	60:40		1.0	7.5	6.7	14.4	19.9					
	40:60		7.8	21.5	20.8	29.8	40.5					
	20:80		18.5	33.3	43.1	48.5	63.7	0.0	0.0			
	0:100		31.3	41.7	56.1	60.5	72.0	2.3	2.9			
	70:30	Co	0.0	0.0	0.3	3.0	3.5					
	60:40		0.0	1.6	2.8	6.0	15.4					
	40:60		2.2	10.1	18.9	23.9	34.5					
	20:80		9.3	23.1	31.5	41.4	61.3	0.0	0.0			
	0:100		20.8	31.5	50.0	55.3	72.4	0.0	0.0			

[a] There is no mobility for (+)ΨEp, (−)ΨEp and BetOH with hexane–benzene as mobile phase.

tion occurs with higher solvent polarity, *i.e.*, with toluene–diethyl ether and benzene–diethyl ether binary mobile phases containing 10–50% of diethyl ether.

(+)ΨEpDTC, (−)ΨEpDTC and BetOHDTC have similar behaviour patterns. The resolution increases with increasing solvent strength from 20% of diethyl ether. There is no mobility with the mobile phase hexane–benzene.

N,N-Dibenzylamine derivatives show many differences from the other compounds studied. Low-polarity mobile phases such as hexane and high-polarity mobile phases such as diethyl ether allow their separation.

With reference to N,N-substituents, the mobilities increase in the order DbenDTC > BetDTC > BmetDTC > DetDTC > DmetDTC > (+)EpDTC ≥ (−)EpDTC > (+)ΨEpDTC ≥ (−)ΨEpDTC > BetOHDTC.

The slopes of the R_M *vs.* log X_s plots are given in the Table II. The greater slopes of the Co(II) chelates with all types of mobile phase indicate their strong adsorption.

DTC molecules are adsorbed on the silica gel

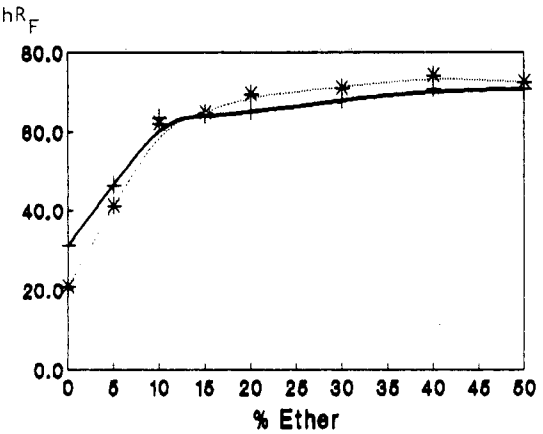

Fig. 3. Plots of hR_F *versus* percentage of diethyl ether in the benzene–diethyl ether binary mobile phase for (*) Co(II) and (+) Ni(II) DmetDTC.

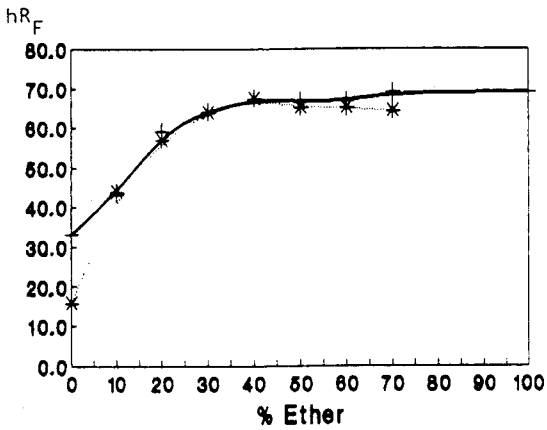

Fig. 4. Plots of hR_F *versus* percentage of diethyl ether in the toluene–diethyl ether binary mobile phase for (*) Co(II) and (+) Ni(II) DmetDTC.

TABLE III

BEST MOBILE PHASES SUGGESTED FOR THE SEPARATION OF N,N-DISUBSTITUTED DITHIOCARBAMATES OF Ni(II) AND Co(II)

Dimethyl-DTC	Toluene
Diethyl-DTC	Toluene
N-Benzyl-N-methyl-DTC	Hexane–benzene (20:80)
N-Benzyl-N-ethyl-DTC	Hexane–benzene (50:50 to 0:100)
N,N-Dibenzyl-DTC	Hexane–benzene (70:30)
(+)-Ephedrine-DTC	Benzene–diethyl ether (70:30)
(−)-Ephedrine-DTC	Benzene–diethyl ether (80:20)
(+)-Ψ-Ephedrine-DTC	Benzene–diethyl ether (60:40)
(−)-Ψ-Ephedrine-DTC	Benzene–diethyl ether (60:40)
	Toluene–diethyl ether (50:50)
N-Benzyl-N-ethanol-DTC	Diethyl ether

surface via the OH of the silica gel and the electron of the N atom of the thioureide. Also, the molecular area contributes to the adsorption of the chelate; if it increases, the adsorption of the molecule will decrease. However, (+)EpDTC, (−)EpDTC, (+)ΨEpDTC, (−)ΨEpDTC and BetOHDTC have an additional adsorbing site, namely the heteroatoms in their ligands, and thereby show lower R_F values in spite of their high molecular area. However, their mobilities increase with increasing polarity

TABLE II

SLOPES OF R_M *VERSUS* LOG X_s PLOTS FOR BINARY MOBILE PHASES WITH ACTIVE COMPONENTS DIETHYL ETHER AND BENZENE

Mobile phase	Metal	DTC									
		Dmet	Det	Bmet	Bet	Dben	(+)Ep	(−)Ep	(+)ΨEp	(−)ΨEp	BetOH
Benzene–diethyl ether	Ni	0.58	0.99	0.51	0.55	0.19	1.15	1.12	1.69	1.60	1.67
	Co	1.20	1.43	0.75	0.77	0.29	1.12	2.12	2.35	1.99	1.84
Toluene–diethyl ether	Ni	0.82	0.61	0.64	0.91	0.68	1.14	1.11	1.83	1.76	2.08
	Co	0.79	0.93	0.82	0.12	0.92	2.64	2.10	2.55	2.36	2.59
Hexane–benzene ether	Ni	4.57	3.71	3.88	3.14	5.08	1.38	1.65	−[a]	−[a]	−[a]
	Co	6.25	4.81	4.88	4.01	6.02	−[a]	−[a]	−[a]	−[a]	−[a]

[a] These R_M values are ∞.

of the mobile phase. This variation is due to the mobile phase competing with the chelate molecules for the adsorption sites on the silica gel surface.

On the other hand, the R_F values of DmetDTC, DetDTC, BmetDTC, BetDTC and DbenDTC increase with increasing molecular area, but the polarity of the solvents only affects them up to one particular value and above this polarity the R_F values remains constant. Moreover, Ni(II) chelates, usually faster moving than Co(II) chelates, are found to be slower moving above this particular polarity. This variation in mobility shows the predominance of solubilizing properties over the adsorption characteristics of this chelates [5].

In conclusion, the conditions suggested are suitable for the separation of the Co(II) and Ni(II) chelates. The best separations can be achieved with the mobile phases indicated in Table III.

ACKNOWLEDGEMENT

The authors thank M.M. Martínez for her help with translation.

REFERENCES

1 G.K.C. Low, P.R. Haddad and A.M. Duffield, *J. Liq. Chromatogr.*, 6 (1983) 311–323.
2 J. Lehotay, O. Liska and E. Brandsteterová, *J. Chromatogr.*, 172 (1979) 379–383.
3 A. Galík, *Anal. Chim. Acta*, 67 (1973) 357–376.
4 G. Soundararajan and M. Subbaiyan, *Indian J. Chem.*, 22A (1983) 402–406.
5 G. Soundararajan and M. Subbaiyan, *Sep. Sci. Technol.*, 18 (1983) 645–655.
6 G. Crovetto, *Doctoral Thesis*, Faculty of Pharmacy, University of Granada, Granada, 1980.
7 M.I. Gómez, *Doctoral Thesis*, Faculty of Pharmacy, University of Granada, Granada, 1988.
8 M.I. Montes, *Minor Thesis*, Faculty of Pharmacy, University of Granada, Granada, 1989.

Journal of Chromatography A, 655 (1993) 51–56
Elsevier Science Publishers B.V., Amsterdam

CHROM. 25 043

Supercritical fluid extraction of tributyltin and its degradation products from seawater via liquid–solid phase extraction

R. Alzaga and J.M. Bayona*

Environmental Chemistry Department, C.I.D.-C.S.I.C., Jordi Girona Salgado 18–26, 08034-Barcelona (Spain)

ABSTRACT

Quantitative extraction of di- and tributyltin compounds from aqueous matrices using C_{18} liquid–solid extraction (LSE) discs, followed by *in situ* Grignard ethylation and supercritical fluid extraction of derivatized LSE discs, is demonstrated for the first time. The optimum extraction efficiency of dibutyltin and tributyltin from synthetic seawater at pH 2 was achieved by using a combination of static and dynamic extraction procedures with supercritical carbon dioxide (10 MPa, 40°C). The extraction efficiency for dibutyltin and tributyltin ranged from 92 to 102%, and the R.S.D.s ($n = 5$) were 6.6 and 8.2%, respectively. The limit of detection of tributyltin (1 l of seawater) using a capillary gas chromatograph coupled to a single-flame tin-selective flame photometric detector was 6 ng/l, while the limit of quantitation of harbour seawater was 9 ng/l. Furthermore, analysis time and solvent usage are reduced by 50 and 90%, respectively, in comparison with classical methods involving liquid–liquid extraction in the presence of complexing agents.

INTRODUCTION

Of organometallic compounds, organotins have the highest industrial output, and this has increased over the last decade as a result of the use of organotins in a large variety of applications (*i.e.* catalysts, polymer additives, agricultural biocides, antifouling paints) [1]. Because of their pattern of usage, a significant portion of organotins are released directly into the marine environment or transported from continental areas. The strong toxicity of some organotin compounds is a cause of primary concern in coastal environments owing to their deleterious effects on biota at very low concentration levels. Indeed, some of them are included in the EC list of pollutants.

Analytical procedures for the determination of organotins in environmental samples should therefore be able to differentiate the toxic parent compounds from the less toxic degradation products. Furthermore, analytical procedures should be able to reach a limit of detection (LOD) below the environmental quality target (EQT) (0.2–20 ng/l) [2].

Several analytical procedures have been developed for organotin speciation in seawater [3–5], but most of these techniques rely on multiple extraction and derivatization steps and, consequently, they are not well suited for application to monitoring programmes involving a large number of samples. Although hydride generation (HG) coupled to cryogenic trapping GC and atomic absorption spectrometry (AAS) has been widely used during the last decade [6], recent interest has been focused on the alkylation reactions owing to the higher stability of alkylated derivatives and lower matrix depen-

* Corresponding author.

0021-9673/93/$06.00

dency of these reactions [7–10]. At present, the absolute LOD of HG–GC–AAS is higher than that of other analytical techniques such as capillary GC (cGC) coupled to flame photometric detection (FPD) [11], atomic emission detection (AED) [12] or MS in the single-ion monitoring (SIM) mode [13].

In this paper, an analytical procedure using liquid–solid extraction (LSE) with C_{18} extraction discs, *in situ* ethyl-Grignard derivatization and supercritical fluid extraction (SFE) with carbon dioxide and off-line cGC–FPD determination is presented. This procedure is clearly better than sequential liquid–liquid extraction (LLE) and derivatization procedures in terms of analysis time, extraction efficiency and waste reduction due to solvent minimization during the extraction step.

The application of LSE using extraction cartridges (Carbopack, silica-C_8 and -C_{18}) for the butyltin compounds has been previously evaluated [14,15]. However, several drawbacks are associated with this method: (1) the eluting solvent may extract potentially interfering compounds from the polypropylene housing and polyethylene frit; (2) batch-to-batch sorbent variability; (3) channelling, which prevents the interaction between components of interest and the sorbent; (4) low flow-rate (<10 ml/min) and (5) suspended matter can clog the limited number of flow paths.

Some of these disadvantages are avoided by the introduction of extraction discs (silica-C_{18}) [16], which have in fact been successfully applied to the recovery of tributyltin from seawater [17]. However, no attempts have been made to perform *in situ* derivatization and SFE, which has been a very successful approach for the extraction of polar compounds from solid matrices [18,19]. In fact, the derivatization reaction was also evaluated as carried out *in situ* on the Empore extraction disc for several reasons. Firstly, it is faster in comparison with conventional procedures involving an extended sample treatment. Secondly, derivatized organotin compounds are presumably easier to extract from the extraction disc. Finally, SFE can be coupled to other chromatographic techniques.

EXPERIMENTAL

Materials and reagents

Pesticide-grade diethylacetate, analytical-grade hydrochloric acid (32% v/v) and ethylmagnesium chloride in tetrahydrofuran (THF) were obtained from Merck (Darmstadt, Germany). Discs of 4.7 mm, Empore 3M (PTFE membrane enmeshed with 8-μm silica-C_{18}), were used for LSE. Instant Ocean was used to prepare synthetic seawater from Milli-Q-grade water (33 g/l). Natural seawater was sampled at the subsurface and bottom using a home-built system in a marina located in the N.W. Mediterranean Sea containing more than 400 moored vessels.

Standards

Monobutyltin chloride (MBT) was obtained from Aldrich (Stenheim an Albuch, Germany). Dibutyl- (DBT), tripropyl- (TPrT) and tributyltin (TBT) chlorides were provided by Fluka (Buchs, Switzerland). Stock solutions, used for cGC–FPD calibration, were prepared with *n*-hexane, while they were dissolved in acetone for water-spiking purposes at concentrations ranging from 2.3 to 4.8 μg/l.

Extraction and derivatization procedures

Samples were acidified to pH 2 with hydrochloric acid and spiked with MBT, DBT and TBT chlorides for method development purposes and with TPrT chloride as internal standard for natural seawater. Samples were kept at 4°C in the dark until analysis (less than 10 days).

Extraction discs were preconditioned in the extraction assembly using a sequential solvent elution programme with the following solvents: (a) 10 ml of ethyl acetate, (b) 5 ml of methanol and (c) 10 ml of Milli-Q water. A vacuum source was applied for 5 min during each solvent treatment until the first drops came out. The acidified sample (0.5–1 l) containing methanol (5–10 ml) was immediately transferred into the extraction assembly to avoid drying of the extraction disc. The vacuum was adjusted to keep the extraction flow-rate at 200 ml/min. Filters were dried for 1 h at room temperature, cut into small pieces and

introduced into a home-made cylindrical aluminium foil reaction cell built inside the extraction vessel. The derivatization reaction was performed with ethylmagnesium chloride (1.5 ml), keeping the extraction vessel at room temperature for 2 min. THF of Grignard reagent was removed before performing SFE, keeping the extraction vessel open at room temperature for 15 min after the derivatization step.

Instrumental analysis

SFE was carried out in an SFC 3000 series (Fisons Instruments, Milan, Italy) using 99.995% carbon dioxide (Carburos Metálicos, Barcelona, Spain). Extraction cells of 5 ml were obtained from Suprex (Pittsburgh, PA, USA). The flow-rate through the extraction vessel was adjusted with linear restrictors of different length (fused silica, 30 μm I.D. × 12–18 cm) (MicroQuartz, Munich, Germany). Derivatized organotins were collected in a vial containing 1 ml of *n*-hexane.

SFE extracts were analysed by cGC apparatus (Fisons Instruments) equipped with cold on-column injection and an FPD containing a 610-nm bandpass filter. The detector temperature was set to 225°C. A 2.5 m × 0.32 mm I.D. deactivated fused-silica tubing was coupled via a press-fitted back-connector to the analytical columns, which were a DB-5 (30 m × 0.25 mm I.D., film thickness = 0.1 μm) and a OV-1 (10 m × 0.25 mm I.D., film thickness = 0.15 μm). Column temperature was programmed from 60 to 225°C at 8°C/min, after an isothermal period of 2 min. Hydrogen was used as carrier gas at 50 cm/s. Data were acquired by a Nelson-PE interphase with a sampling frequency of 100 Hz and handled with a PS computer.

RESULTS AND DISCUSSION

Development of SFE of butyltins from extraction discs

Previous studies have shown that SFE of organotin chlorides requires significant amounts of modifiers for their quantitative recovery from solid matrices [20]. Furthermore, the restricted volatility of those compounds makes it necessary to perform a derivatization step prior to GC determination [9]. Therefore, in this paper we have explored the introduction of derivatization step prior to extract desorption (Fig. 1), aiming to obtain quantitative recoveries of organotin compounds by SFE with neat carbon dioxide and to proceed with the GC analysis of the recovered extract.

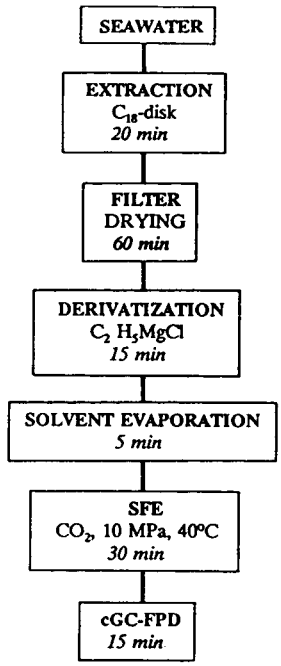

Fig. 1. Analytical scheme, showing the time consumed at each analytical step.

Therefore, the SFE of derivatized organotins was optimized using a standard mixture containing MBT, DBT and TBT, as the ethylated derivatives. The standard solution was spiked directly onto the Empore silica-C_{18} extraction disc and extracted by the dynamic method or by a combination of static and dynamic methods, using different extraction volumes of supercritical carbon dioxide. The extraction temperature was kept constant at low values (40°C) to minimize analyte degradation during the extraction period. At the same time, pressure was also kept relatively low (10 MPa) in order to enhance the extraction selectivity of organotin compounds from other sample components. Furthermore, higher pressures lead to higher flow-rates, which

could favour losses of the more volatile butyltin components, already extracted, from the collecting vial.

In order to evaluate whether, under the extraction conditions used (40°C, 10 MPa), losses of butyltins occur from the collection vial, we exposed a solution of ethylated butyltins to a stream of carbon dioxide, simulating the extract collection during the extraction process. Under these conditions, no losses of butyltins were observed in the range of extraction volumes evaluated. Consequently, extract collection vials were kept at room temperature.

The extraction efficiency of butyltins from spiked extraction discs was evaluated first in the dynamic mode according to the volume of carbon dioxide passed through the vessel. Extraction rates were dependent on the compound and on the extraction volume of carbon dioxide (Fig. 2). Thus, while MBT reached its highest extraction rate at the beginning of the extraction period, DBT presented a recovery maximum at higher extraction volumes. Conversely, TBT recovery steadily increased with extraction volume, but no maximum was apparent in the range of extraction volumes evaluated.

Therefore, the kinetics of desorption of each butyltin from the extraction disc are completely different and may depend on the hydrophobicity of the compound, since the contribution of compound vapour pressure is negligible at the low temperatures and moderate densities used during the extraction. Thus, the less hydrophobic components (*i.e.* MBT and DBT) are desorbed from the extraction disc faster than the more hydrophobic components (*i.e.* TBT).

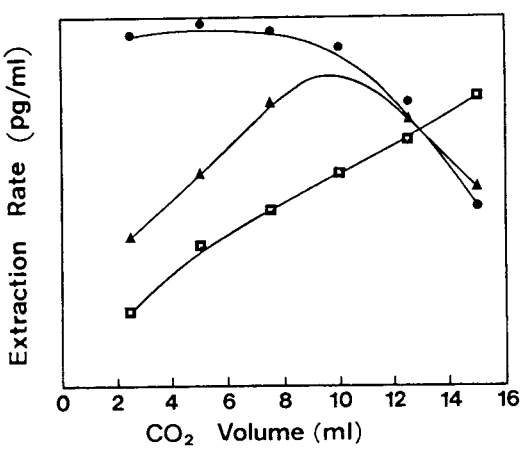

Fig. 2. Extraction rates of ethylated organotin derivatives from spiked extraction discs by dynamic SFE (10 MPa, 40°C) according to the volume of carbon dioxide used during the extraction. □ = TBT; ▲ = DBT; ○ = MBT.

Consequently, the dynamic extraction mode evaluated was not considered to be feasible for the quantitative extraction of all of the compounds of interest because the extraction volumes of carbon dioxide required are too large. Thus, a combination of static and dynamic extraction modes was tried. In this operational mode, quantitative extraction of all of compounds of interest was achieved by combining 1 ml of dynamic, 10 ml of static and 10 min of dynamic. Consequently, this extraction procedure was used further for the desorption of butyltins from the LSE discs.

Development of in situ organotin ethylation on the extraction disc and LSE of butyltins in seawater

Derivatization reaction on the Empore extraction disc was also evaluated so that thereafter SFE of the extraction disc could be performed without any kind of extract transfer. Taking into account the low solubility of the Grignard reagent (ethylmagnesium chloride) in the supercritical carbon dioxide, the derivatization reaction was previous performed at atmospheric pressure before the SFE. This derivatization reaction was performed within the extraction vessel, keeping the extraction disc covered with the derivatization reagent. The derivatization reaction was quantitative after 15 min of reaction time, and no cross-alkylation reactions were detected under these conditions.

In order to evaluate the extraction efficiency of Empore extraction discs, synthetic seawater was spiked with organotin chlorides at the ppb level. Fig. 3 shows a typical cGC–FPD chromatogram of an SFE extraction corresponding to a standard mixture used in the development of the method. Remarkably, satisfactory results were achieved in the cases of DBT and TBT (Table I). However, MBT exhibited poorer extraction efficiency and reproducibility, which

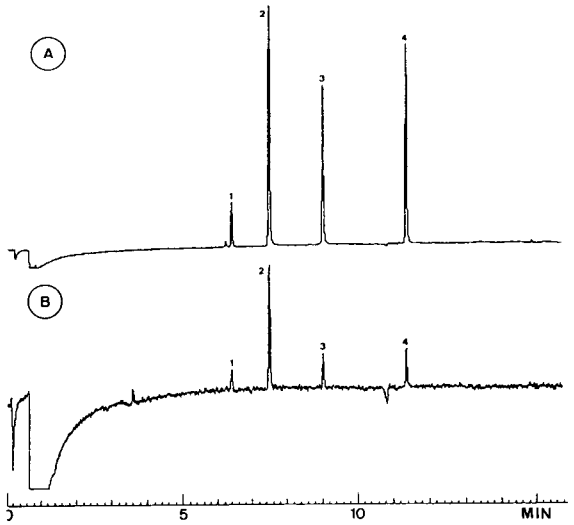

Fig. 3. cGC–FPD of SFE extracts isolated from (A) spiked synthetic seawater and (B) a real harbour water sample. Peaks: 1 = monobutyltin; 2 = tripropyltin; 3 = dibutyltin; 4 = tributyltin (analysed as ethyl derivatives).

could be attributed to its lower retention on the Empore extraction disc, or stronger adsorption on it. In preliminary work carried out using acetyl acetate as extraction solvent of the Empore disc, as described previously [17], MBT and DBT chlorides were not eluted from the disc. However, application of *in situ* derivatization reaction in the disc with the Grignard reagent coupled to SFE enables a quantitative recovery of DBT and to a lesser extent MBT. Following the derivatization reaction, they are easily desorbed because the polarized Sn–Cl bond is replaced by the less polar Sn–C, enhancing the solubility in the supercritical CO_2. Consequently, the poorer extraction recovery for MBT (Table I) may be attributable to a lower derivatization yield in the extraction membrane. Similar results have been found in an on-column or *in situ* derivatization ethylation using sodium tetraethylborate [21].

The LOD of the whole analytical procedure for TBT by extracting 1 l of water was estimated to be as low as 6 ng/l (Table II), which is satisfactory in terms of environmental quality target issued by most of national environmental protection agencies [2].

In order to evaluate breakthrough volumes in a realistic manner, different volumes of harbour seawater (surface and bottom) containing high levels of dissolved organic carbon were extracted. Fig. 4 shows a typical cGC–FPD chromatogram of a harbour water extract obtained with the OV-1 column, which enables resolution between TBT and the interference eluting as a negative peak. This compound was identified as di-*tert.*-butylmethylphenol by GC–MS and co-eluted in the 5% phenyl-substituted methypolysiloxane column.

On the other hand, no significant concentration differences between DBT and TBT were obtained from the extraction of 500–1000 ml of seawater, since the variation in the results fell within the S.D. of the analytical procedure (Fig. 4). Conversely, MBT exhibited larger variability according to the extracted volume, which could be attributed to the lower extraction recoveries for this compound (Table I). Higher water extraction volumes were not evaluated because the extraction period required was too long and

TABLE I

EXTRACTION EFFICIENCY AND REPRODUCIBILITY OF BUTYLTIN COMPOUNDS EXTRACTED BY LSE-DERIVATIZATION-SFE FROM SPIKED SYNTHETIC SEAWATER

	MBT	DBT	TBT
Recovery (%)[a]	69.9	91.8	102.0
S.D.[b]	12.2	6.1	8.4
R.S.D. (%)	17.4	6.6	8.2

[a] Spiking was performed at the low μg/l level.
[b] $n = 5$.

TABLE II

LIMIT OF DETECTION (LOD) OF THE WHOLE ANALYTICAL PROCEDURE[a]

	MBT	DBT	TBT
LOD	16	7	6

[a] It corresponds to 1000 ml of harbour water, concentrating the extract to 0.5 ml.

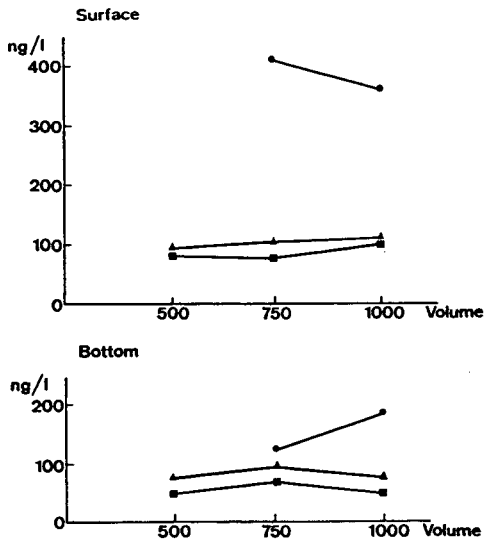

Fig. 4. Concentrations of butyltin compounds relative to the volume of extracted natural harbour water. ○ = MBT; ▲ = DBT; □ = TBT.

because the LOD of this technique meets with the most widely accepted EQT (20 ng/l).

CONCLUSIONS

LSE or butyltin compounds using C_{18} extraction discs has general advantages over LLE methods, *i.e.* solvent reduction, on-board extraction during sampling and extract storage. Also, LSE with extraction discs has advantages over LSE with cartridges: higher breakthrough volumes, less artifact formation and faster extraction rates. In the case of LSE extraction discs, artifacts are not apparent with tin-selective FPD if the proper conditioning is carried out. Another advantage of the use of extraction discs is the feasibility of "*in situ*" derivatization reaction, enabling the SFE of organotin compounds under mild conditions (CO_2, 40°C, 10 MPa) and, consequently, giving clean extracts that can be analysed directly without any further treatment. Finally, the procedural minimization of sample handling and intermediate steps leads to an enhancement of sensitivity and reproducibility and analysis time reduction. Further research is in progress in order to improve the MBT extraction from seawater.

ACKNOWLEDGEMENTS

Funding was provided by the CICYT from the Spanish National Plan for Research and Development (Grant AMB92-0218). One of us (R.A.) kindly acknowledges a predoctoral fellowship from CONACYT (México).

REFERENCES

1 S.J. Blunden, L.A. Hobbs and P.J. Smith, in H.J.M. Bowen (Editor), *Environmental Chemistry*, Royal Society of Chemistry, London, pp. 50–77.
2 M.J. Waldock, J.E. Thain and M.E. Waite, *Appl. Organomet. Chem.*, 1 (1987) 287.
3 C.L. Matthias, J.M. Bellama, G.J. Olson and F.E. Brinckman, *Environ. Sci. Technol.*, 20 (1986) 609.
4 L. Randall, O.F.X. Donard and J.H. Weber, *Anal. Chim. Acta*, 184 (1986) 197.
5 R.J. Maguire and H. Huneault, *J. Chromatogr.*, 209 (1981) 458.
6 O.F.X. Donard, S. Rapsomanikis and J.H. Weber, *Anal. Chem.*, 58 (1986) 772.
7 Y. Cai, S. Rapsomanikis and M.O. Andreae, *Anal. Chim. Acta*, 274 (1993) 243.
8 M.D. Müller, *Anal. Chem.*, 59 (1987) 617.
9 I. Tolosa, J.M. Bayona, J. Albaigés, L.F. Alencastro and J. Tarradellas, *Fresenius' Z. Anal. Chem.*, 339 (1991) 646.
10 K. Fent and J. Hunn, *Environ. Sci. Technol.*, 25 (1991) 956.
11 G.B. Jiang, P.S. Maxwell, K.W.M. Siu, V.T. Luong and S.S. Berman, *Anal. Chem.*, 63 (1991) 1506.
12 R. Lobinski, W.M.R. Dirkx, M. Ceulemans and F.C. Adams, *Anal. Chem.*, 64 (1992) 159.
13 J. Greaves and M.A. Unger, *Biomed. Environ. Mass Spectrom.*, 15 (1988) 565.
14 G.A. Junk and J.J. Richard, *Chemosphere*, 16 (1987) 61.
15 S. Chiavarini, C. Cremiscini, T. Ferri, R. Morabito and C. Ubaldi, *Appl. Organomet. Chem.*, 6 (1992) 147.
16 A. Krasut-vass and J. Thoma, *J. Chromatogr.*, 538 (1991) 233.
17 O. Evans, B.J. Jacobs and L. Cohen, *Analyst*, 116 (1991) 15–19.
18 S.B. Hawthorne, D.J. Miller, D.E. Nivens and D.C. White, *Anal. Chem.*, 64 (1992) 405.
19 J.W. Hills, H.H. Hill Jr and T. Maeda, *Anal. Chem.*, 63 (1991) 2152.
20 J.M. Bayona, J. Dachs and R. Alzaga, in *Final Report of BCR Contract 5367*, Bureau Community of Reference, Brussels, 1992.
21 J. Szpunar-Lobinska, M. Ceulemans, R. Lobinski and F.C. Adams, *Anal. Chim. Acta*, in press.

Journal of Chromatography A, 655 (1993) 57–62
Elsevier Science Publishers B.V., Amsterdam

CHROM. 25 150

Determination of organochlorine compounds in anion-exchange resins by UV irradiation and ion chromatography

L. Comellas*, J.Ll. Lliberia, A. Roca and R. Vallhonrat

Secció de Cromatografia, CETS Institut Químic de Sarrià (Universitat Ramon Llull), Institut Químic de Sarrià s/n, 08017 Barcelona (Spain)

M. Boronat

Associació Nuclear Ascó, CN Ascó, 43791 Ascó-Tarragona (Spain)

ABSTRACT

Anion-exchange resins may release organochlorine compounds during the demineralization of water in make-up plants. These substances can be decomposed by exposure to UV irradiation into chloride salts which can subsequently be determined by ion chromatography. The experimental conditions in the above method were studied and optimized. In addition, the method was validated using some organochlorine compounds of known structure. Finally, the method was applied to the determination of leachable organochlorine compounds in samples of anion-exchange resins.

INTRODUCTION

In one of the stages of ultrapure water production, water flows through a resin bed in a demineralizer. The structure of an anion-exchange resin consists of an aminated macropolymer, most commonly of the styrene–divinylbenzene type or an acrylic polyester. Leachable compounds in these resins may contaminate the water with organic substances. The fact that these contaminants are non-ionic makes them undetectable by conductivity or ion chromatographic methods.

If this water is intended for steam generation, these organic contaminants may undergo thermal decomposition under the conditions of pressure and temperature existing in the steam cycle. As a result, chlorinated compounds release chloride ions into the water, which may lead to corrosion [1].

Three possible sources can be ascribed to these contaminants. During anion-exchange resin manufacture, chlorine-containing solvents are used, *e.g.*, ethylene dichloride. At a certain stage of its manufacture, the resin is a chlorinated macropolymer [2], this chlorine later being replaced with amine groups. However, residual solvents or chlorinated compounds from the manufacturing process may be retained within the resin structure. As they are non-ionic they will be released slowly into the water during demineralization and leak through the resin bed. In water chlorination during pretreatment, chlorinating reagents used as disinfectants may react with natural organic substances already present in water and result in volatile chlorinated compounds such as trihalomethanes ($CHCl_3$, $CHBrCl_2$, $CHBr_2Cl$, $CHBr_3$) [3]. Therefore, it is

* Corresponding author.

0021-9673/93/$06.00

possible these substances are already present in the water supplied to the resin train demineralizer. Some power plant records give evidence of increases in steam water conductivity after new resins had been introduced into the demineralizer. The analysis revealed an increase in chloride ion concentration. As this water met the necessary specifications when introduced to the condensate, decomposition of organochlorine compounds seems to be the direct source of this increase [1]. To avoid these problems, it is necessary to check for very low levels of leachable organochlorine compounds in water.

The aim of this work was to develop a method that would achieve complete decomposition of organochlorine compounds into inorganic chloride, a method suitable for use in the laboratory that would enable one to predict the maximum amount of chlorine that might be measured in water by any other procedure. Ion chromatography with automatic sample preconcentration and conductimetric detection is a suitable technique that provides rapid and reproducible measurements of anion concentrations at the μg/l level [4,5]. The chloride is leached into water matrices that may contain trace amounts of other inorganic ions such as sulphates, fluorides or carbonates and small amounts of organic matter. Such substances do not interfere in the determination of chloride by the proposed technique.

The test suggested in this paper [6] is basically carried out in two steps. First, the water sample (previously in contact with the resin) is exposed to UV irradiation, this causes decomposition of organochlorine compounds, releasing chloride ions. The second step is the determination of the increase in chloride ion concentration by ion chromatography. The difference in chloride concentration before and after irradiation is a measure of the amount of organochlorine contaminants present initially in the water sample. The best results were obtained when a helium atmosphere was maintained inside the lamp vessel during irradiation, which avoids atmospheric sample contamination. In addition, the method was validated for chlorinated compounds of known structure and several resin samples were analysed.

EXPERIMENTAL

Irradiation source

The UV lamp used was a Model TNN 15/32 Quartz Lampen 5631 (0.13A) low-pressure mercury lamp from Hanau Heraeus (Berlin, Germany) [7], with wavelength maxima at 254 and 170 nm with an intensity ratio of 6:1 (Fig. 1).

Chromatographic conditions

The analyses were performed with a Waters Model 590 ion chromatograph equipped with a Waters Model 430 conductivity detector. The background conductivity was 320 μS/cm. The column was a Waters IC-Pak A Anion (50 mm × 4.6 mm I.D., 10 μm particle size) (Millipore, Bedford, MA, USA). The mobile phase was borate–gluconate (1.3 m*M*) buffer prepared according to the manufacturer's manual [8] at a flow-rate of 1.2 ml/min. Sodium gluconate, sodium tetraborate decahydrate and boric acid were supplied by Merck (Darmstadt, Germany).

Injection volumes were 100 μl of samples with ion concentrations above 100 μg/l; levels under 100 μg/l required sample concentration. For trace enrichment a Waters IC-Pak A Anion concentrator (8 mm × 5 mm I.D., 2.16 μequiv.) was used. Other conditions of this concentration were as follows: after a 2-min rinse of the preconcentrator system, the sample flowed through the concentrator column at 3 ml/min for 4 min and was finally eluted in the last 0.5 min of the programme.

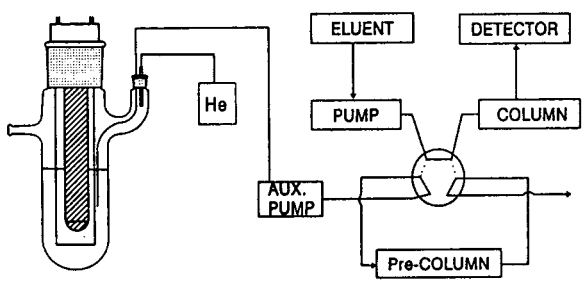

Fig. 1. Scheme of the overall assembly of the lamp and the chromatographic system.

Sample preparation

A 100-ml portion of resin was placed in a flask and 500 ml of ultrapure water obtained from a Milli-Q system (Millipore) were added. The mixture was stirred for 15 min and then filtered through an open column (50 cm × 3 cm I.D.). After placing 200 ml of the filtered liquid inside the lamp enclosure, the lamp vessel was closed and the air atmosphere was replaced with helium. An aliquot was analysed for anions by ion chromatography either by direct injection or using the preconcentrator. The water extract was irradiated for 60 min and chloride ions were determined a second time. The increase in chloride ions corresponds to the organochlorine content in the sample. All volumetric material used was prewashed several times with Milli-Q-purified water. Sodium chloride used in standards was obtained from Merck.

A sample of the same water used to prepare the resin extract was analysed as a blank. The chloride increase measured in the blank sample was subtracted from that obtained in the irradiated extract. At the same time this blank allowed the lamp container to be checked for possible contamination.

The initial chloride concentrations in the blanks were 3–5 μg/l and the corresponding increase usually ranged from 5 to 10 μg/l. Samples irradiated in an open atmosphere gave larger chloride increases and their blanks showed lower repeatibility, so in order to maintain the same inert conditions through the analysis, a helium atmosphere was used inside the lamp. Helium (quality 5.0) was supplied by Abelló (Barcelona, Spain).

Method validation

Owing to the origin of organochlorinate substances, no particular structure can be attributed to them and no specific analytical method can be applied. For this reason they were decomposed to inorganic chloride by UV irradiation and chloride ions were determined by ion chromatography. The purpose of this validation procedure was to monitor the decomposition and the subsequent increase in chloride ions after irradiation. It was also necessary to establish an irradiation period that ensures the complete decomposition for the organochlorine substances.

The method was applied to solutions of organochlorine compounds of known structure. The sample solution was irradiated and analysed following the same procedure as described for sample preparation.

There are differences in decomposition according to the nature of the carbon atom to which the chloride ion is linked to in the organic molecule. The behaviour of aliphatic chlorine compounds towards UV irradiation differs from that of aromatic chlorine compounds. An aqueous solution of chloroethanol (Merck) and a solution of 2,6-dichlorophenol (Merck) were selected to represent aliphatic and aromatic compounds, respectively. For these substances the test was carried out at two levels of concentration, mg/l and μg/l.

The increase in chloride ion concentration after irradiation is shown in Figs. 2 and 3. Decomposition during the UV irradiation proved to be faster for samples of aliphatic than aromatic chlorine compounds. The results indicate that for low concentrations of organochlorine compounds in water (μg/l level), decomposition was finished after 60 min of irradiation. This period was used for the resin tests. Although the organochlorine levels in resins may reach higher values they can be reduced after a resin treatment.

Application to anion-exchange resins

The concentration of chloride in anion-exchange resins produced by organochlorine compounds should not exceed 0.1 mg per litre of resin; this criterion is accepted as a resin specification [9].

After sample preparation, each extract was analysed for organochlorine content by ion chromatography. Owing to the high inorganic chloride levels in some resins, and knowing that in normal use the latter are regenerated and rinsed before use, the same treatments were applied to some resin samples. Subsequently the same method as described under *Sample preparation* was applied.

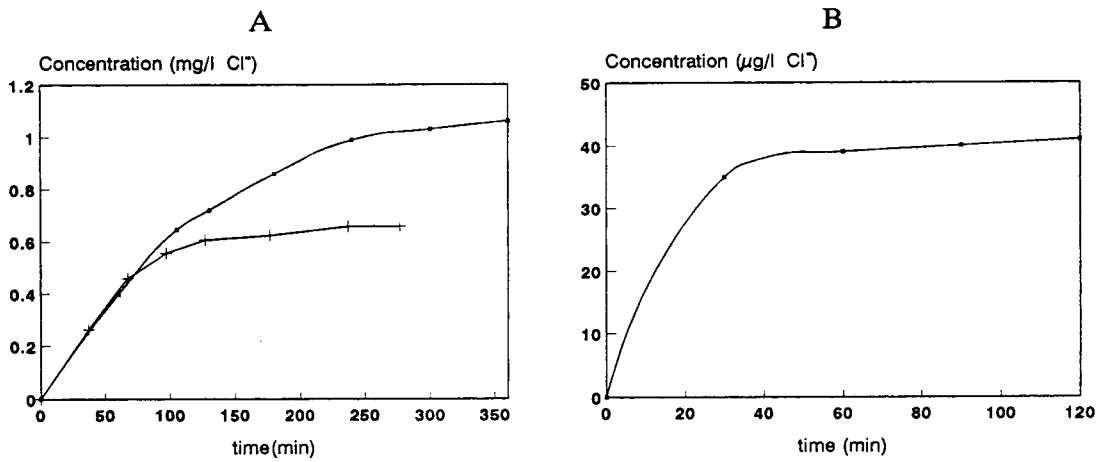

Fig. 2. Chloride concentration *versus* irradiation time of chloroethanol solutions at two concentration levels: (A) 2.4 mg/l (top curve) and 1.2 mg/l (bottom curve) of chloroethanol in Milli-Q-purified water; (B) 48 μg/l of chloroethanol in Milli-Q-purified water.

Regeneration method

This regeneration treatment was based on that used in power plants for resin regeneration, although modifications were made according to the resin volume employed. The method is as follows. A 100-ml portion of resin was placed in an open column and 500 ml of 2% NaOH (Merck) were poured through at a rate of 20 ml/min. After regeneration, the resin was rinsed with 5 l of Milli-Q-purified water at 40 ml/min. The final conductivity and pH were tested in the last 100 ml of water (conductivity values should be <25 μS/cm).

RESULTS AND DISCUSSION

Table I gives the data obtained in each resin analysis.

The chromatograms in Fig. 4 correspond to a

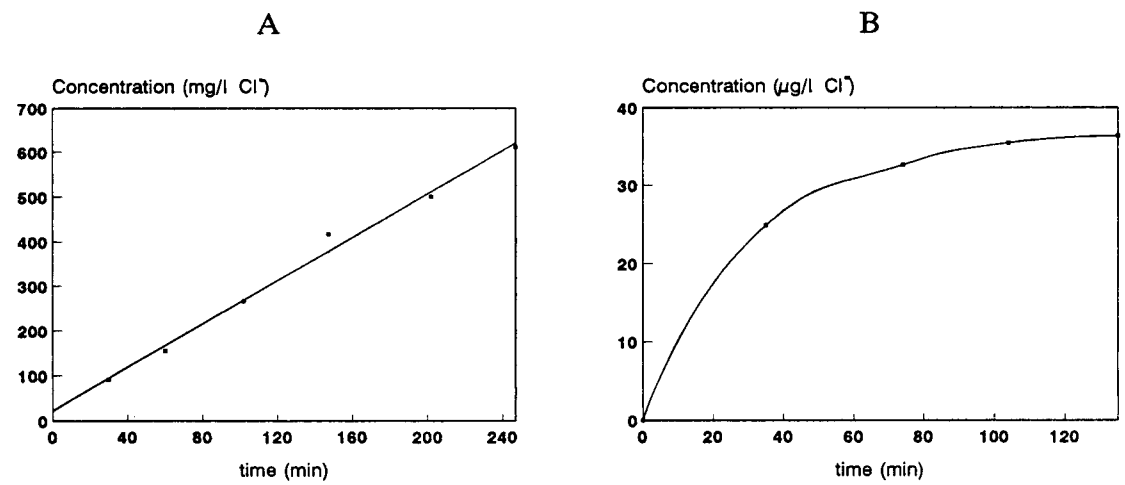

Fig. 3. Production of chloride with increasing irradiation time at different starting concentrations of 2,6-dichlorophenol. From a stock solution of 2,6-dichlorophenol (1050 mg/l in ethanol), dilutions were prepared using Milli-Q-purified water. (A) Solution of 2.3 mg/l of 2,6-dichlorophenol; (B) solution of 105 μg/l of 2,6-dichlorophenol.

TABLE I

RESIN ORGANOCHLORINE CONTENT EXPRESSED AS INCREASE IN ORGANIC CHLORIDE IN INDIVIDUAL SAMPLE EXTRACTS

Resin sample	Previous treatment	Cl^- in extract ($\mu g/l$)		
		Before irradiation	After irradiation	Increase
1	None	2	4	2
2	None	1	3	2
3	None	12	14	2
4	None	7400	7800	400
	Rinsed with 5 l of water[a]	270	290	20
	Rinsed with 10 l of water[a]	110	170	60
	Regenerated	10	22	12
5	None	2800	3000	200
	Regenerated	17	65	48
6	Regenerated	16	452	436
7	Regenerated	69	541	472
	Regenerated	102	228	126
8	None	2300	–	–
	Regenerated	47	94	33

[a] These samples were rinsed with the specified amounts of Milli-Q-purified water at a flow-rate of 20 ml/min with no previous regeneration.

water extract of one of the samples before and after irradiation.

Although detailed information on structure of the resin samples is not available, it is possible to summarize the available information as shown in Table II.

After rinsing with Milli-Q-purified water, the chloride concentration is decreased but regeneration proves to be more effective. The chloride levels both before and after irradiation in the water extract are more significantly reduced in the regenerated resin.

The chloride increase corresponds to the amount of organic chlorine in the resin. From the above results, it is possible to establish three different groups of resins according to their organic chloride content: (1) resins that do not need any treatment; the method can be applied directly to the supplied resin; these resins are described as nuclear grade and have undergone a more thorough treatment during manufacture; (2) resins that initially show a high organochlorine content but in the water extract after

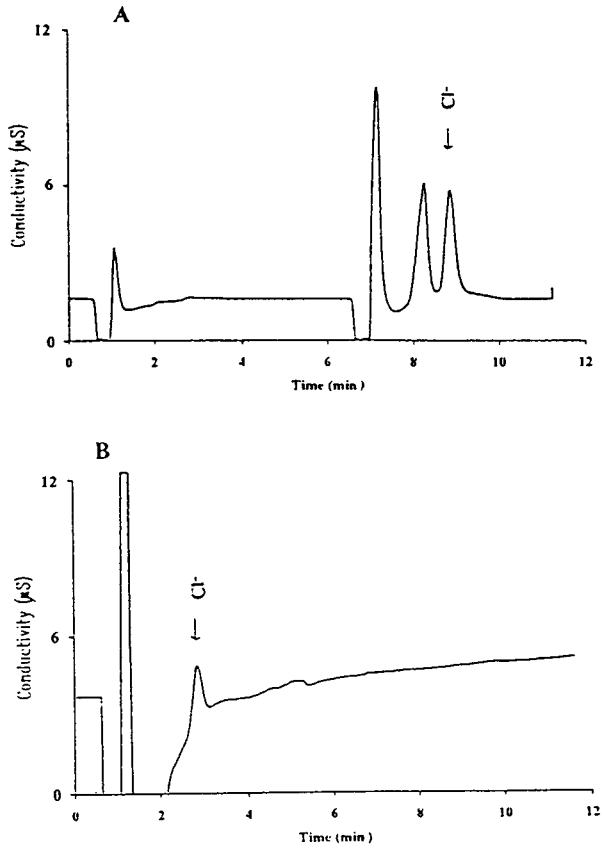

Fig. 4. Chromatograms of water extracts from resin (sample 7) after regeneration treatment and rinsing. (A) Analysis with sample preconcentration; (B) the same water extract after 60 min of irradiation. Direct injection.

TABLE II

RESIN CHARACTERISTICS

Resin	Characteristics
1	Nuclear grade, strong exchange OH^- resin
2	Nuclear grade, strong exchange OH^- resin
3	Not available
4	Weak exchange, chlorinated amine salt
5	Weak exchange
6	Weak exchange
7	Strong exchange chlorinated amine salt
8	Not available

TABLE III

ORGANOCHLORINE CONTENT OF SEVERAL SAMPLES FROM THE SAME RESIN (NO. 7, TABLE II) AFTER REGENERATION AND RINSING

Extract No.	Cl^- in extract (μg/l)		
	Before irradiation	After irradiation	Increase
1	102	228	126
2	112	411	291
3	67	367	273

regeneration this value decreases below 100 μg/l; and (3) resins that after regeneration show an increase exceeding 100 μg/l.

The whole process of regeneration, rinsing and irradiation of the water extract was carried out three times with samples of one of the resins (No. 7) and the results obtained are given in Table III. Each analysis was performed on a different day.

Specifications require chloride levels below 20 μg/l in the water extract. Considering this, we may conclude that resins 1–4 (after regeneration) were within the specifications.

ACKNOWLEDGEMENTS

We gratefully acknowledge the Spanish PWR nuclear power plants of C.N. Almaraz, C.N. Ascó, C.N. Cabrera, C.N. Trillo and C.N. Vandellós, which supplied the resin samples analysed.

REFERENCES

1 J. Irving, *Purolite Technical Service Report*, TS 2620. Bio-Tech, Bala Cynwyd, PA, 1992.
2 R. Kunin, *Elements of Ion Exchange*, Reinhold, New York, 1960, p. 36.
3 J.J. Rook, *Water Treat.*, 23 (1974) 234.
4 H. Small, *J. Chromatogr.*, 546 (1991) 3–15.
5 R.D. Rocklin, *J. Chromatogr.*, 546 (1991) 175–187.
6 F.M. Cutler, *Ultrapure Water*, 5, No. 6 (1988) 40.
7 F.M. Cutler, presented at the *EPRI Condensate Polishing Workshop, Little Rock, AR, 1989.*
8 *Waters Ion Chromatography*, Waters, Barcelona, 1987.
9 C. Cascante, personal communication, 1991.

Journal of Chromatography A, 655 (1993) 63–72
Elsevier Science Publishers B.V., Amsterdam

CHROM. 24 966

Separation of basic proteins by capillary electrophoresis using cross-linked polyacrylamide-coated capillaries and cationic buffer additives

A. Cifuentes, M. de Frutos, J.M. Santos and J.C. Diez-Masa*

Institute of Organic Chemistry (CSIC), Juan de la Cierva 3, 28006 Madrid (Spain)

ABSTRACT

A method for the preparation of fused-silica capillaries with a cross-linked polyacrylamide coating bonded to the internal wall is described. When these capillaries are used with acidic separation buffers containing 0.25 *M* morpholine as cationic additive to mask the residual effect of the negative charges on the silica surface, efficiencies between $3 \cdot 10^5$ and $5 \cdot 10^5$ plates/m can be obtained for basic proteins (p*I* 7–11). The reproducibility of migration times for these capillaries is better than 1% run-to-run and 2% capillary-to-capillary. The capillaries can be used for more than 90 h over the pH range 2–10 without any substantial alteration of the migration time or efficiency for the basic proteins assayed. It is also shown that the capillaries can be stored for more than 90 days in air with no appreciable variation in the migration time or the efficiency for several basic proteins.

INTRODUCTION

Capillary electrophoresis (CE) is an analytical and micropreparative technique with great potential, especially in the field of peptide and protein separations [1–3]. Using CE, almost all traditional modes of electrophoresis (free zone, sodium dodecyl sulphate polyacrylamide gel electrophoresis, isoelectric focusing, etc.) can be carried out. However, owing to the capillary format used in CE, shorter analysis times, higher efficiencies and fully automated operation can additionally be obtained with this technique.

Although theory predicts that efficiencies $>10^6$ theoretical plates could be obtained in the separation of proteins by CE, in practice a smaller plate number is obtained in the separation of such biopolymers. Among the several factors controlling band broadening in CE [4], protein adsorption on the internal wall of fused-silica capillaries seems to be the major cause of the low efficiency observed in some separations. Protein adsorption on the capillary can also cause poor migration time reproducibility and low recoveries. Protein adsorption is due to the electrostatic interaction between positively charged residues of the protein and negatively charged silanol groups which are intrinsic to the fused-silica surface. Many approaches have been devised to prevent this interaction. The first is pH manipulation. If the buffer pH is >11–12, most proteins do not have positively charged groups to interact with the capillary. Similarly, if the pH is <2, the capillary wall has no charge. Although working at the extremes of pH has been successful for some proteins [5,6], many of them are not stable or soluble under such conditions. In addition, working at very basic pH can dissolve the silica surface of the capillary, causing irreproducibility of analyte migration times.

The second approach consists in adding a positively charged ion (inorganic or organic) to the separation buffer. The added salt behaves as a competitor of the protein toward the silanol groups of the surface, therefore preventing pro-

* Corresponding author.

0021-9673/93/$06.00

tein adsorption on the wall. This idea was first introduced by Green and Jorgenson [7], who used K_2SO_4 as an additive to the buffer for the separation of some basic ($pI > 7$) proteins. Since then, other salts, such as KCl [8], cetyltrimethylammonium bromide [9,10], tetradecyltrimethylammonium bromide [11] and fluorosurfactant Fluoral FC-134 [12], have also been used. However, the high ionic strength necessary to avoid protein adsorption requires the use of capillaries of small inner diameter and low separation voltages because of the high conductivity of the buffer and the subsequent heat developed by the Joule effect. Zwitterionic additives, which have low electric conductivity, are a good alternative to cations in this approach [13,14]. However, the use of some zwitterions is limited by their low water solubility and the denaturing effect on some proteins.

In the third procedure, capillaries with their internal wall coated with an organic polymer such as the uncharged methylcellulose [15] or a positively charged synthetic polymer [16] are used. As the binding between the adsorbed polymer and the surface is fairly labile, these coatings are very unstable, giving rise to poor migration time reproducibility or requiring frequent capillary recoating.

Finally, a fourth approach has frequently been employed, utilizing capillaries with chemically bonded moieties on the fused-silica surface. Short organic functionalities such as glycero-glycidoxypropyl derivatives [17], arylpentafluoro moieties [18], diol coatings [19], maltose derivatives [19] or other silyl derivatives traditionally used in HPLC have been utilized. These coatings, although successful in certain instances, show poor hydrolytic stability at basic pH owing to the siloxane bond used for immobilization. The use of chemically bonded polymeric coatings has led to high efficiency and reproducible protein separations. Different polymers, including linear polyacrylamide [20,21], polyvinylpyrrolidone [17], poly(ethylene glycol) [22], polyethyleneimine [23], cross-linked polyacrylamide [24], hydroxylated polyethers [25], and even proteins [26], have been used in the preparation of these capillaries. Good separations of basic proteins have also been obtained using capillaries with C_{18} moieties chemically bonded to the capillary surface and surfactants or polymers adsorbed on them [27,28].

This paper describes a method for the preparation of fused-silica capillaries containing a bonded layer of cross-linked polyacrylamide. The associated effect of such a polymeric layer and some cationic additives in the buffer was evaluated as a means of improving the separation of basic proteins ($pI > 7$). Some model proteins such as lysozyme, cytochrome *c*, ribonuclease A and α-chymotrypsinogen were used to test the efficiency of the proposed method to prevent the interaction between basic proteins and the silica wall of the capillaries. These proteins represent a good model for those separations in which the analytes are stable only in a particular pH range (*i.e.*, antigen–antibody complexes, DNA fragment–antibody complexes, pH-sensitive proteins, etc.) and, therefore, CE procedures involving buffer pH control or buffers of high ionic strength cannot be used to prevent protein–capillary interactions.

EXPERIMENTAL

Instrumentation

Separations were carried out using a laboratory-made electrophoresis system. The apparatus included a Glassman (Whitehouse Station, NJ, USA) Model PS/EH50R2 power supply and a Linear Instruments (Reno, NV, USA) Model M-200 variable-wavelength UV–Vis detector with an in-house-modified flow cell operated at 230 nm. The cooling of the capillaries at room temperature was achieved with a fan. Electropherograms were recorded and analysed using an A/D converter (Flytech, Taiwan), an in-house-built amplifier, an Acer 500 PC computer (Multitech, Taiwan) and a Pascal program developed in this laboratory. During electrophoresis, the current through the capillary was measured using a Fluke (Everett, WA, USA) Model 83 multimeter. Fused-silica capillaries (Polymicro Technologies, Phoenix, AZ, USA) of 25 μm I.D., 360 μm O.D., 50 cm total length and 25 cm effective length (from the injection point to the detector) were used. Injection was carried out in the anode by electromigration.

The experiments on migration time reproducibility and optimization of morpholine concentration were accomplished in a Beckman (Fullerton, CA, USA) P/ACE 2000 HPCE electrophoresis apparatus controlled by an IBM PS/2 286 computer. The fused-silica capillaries used in this apparatus were similar to those used in the laboratory-made apparatus, but with 27 cm total length and 20 cm effective length. In this instance, the external temperature of the capillaries was maintained at 21°C. Injection was carried out in the anode using nitrogen pressure [0.5 p.s.i. (1 p.s.i. = 6894.76 Pa)]. Detection was effected at 214 nm. All the data were collected and analysed using System Gold software from Beckman running on the IBM PS/2 286 computer. In order to increase the migration time reproducibility, the capillaries were successively rinsed for 30 s each with water, air and buffer between injections.

Samples and chemicals

All the proteins (Table I) were purchased from Sigma (St. Louis, MO, USA) and used as received. The proteins were dissolved at the concentrations indicated in each case (ranging from 0.2 to 1 mg/ml) in water purified with a Milli-Q system (Millipore, Bedford, MA, USA), stored at 0°C and heated to room temperature before use. Phosphoric acid, sodium dihydrogenphosphate, tetramethylammonium bromide (TMAB), hexadecyltrimethylammonium bromide (HTMAB), potassium sulphate (all from Merck, Darmstadt, Germany), morpholine and triethylamine (both from Aldrich, Steinheim, Germany) were used in the different running buffers. Hydrochloric acid, sodium hydroxide (both from Merck), 3-methacryloxypropyl-3-trimethoxysilane (ABCR, Karlsruhe, Germany), acrylamide, N,N′-methylenebisacrylamide, ammonium peroxodisulphate and N,N,N′,N′-tetramethylethylenediamine (TEMED) (all from Schwarz, Cleveland, OH, USA) were used for the preparation of the cross-linked polyacrylamide-coated capillaries.

TABLE I

ISOELECTRIC POINTS OF THE PROTEINS USED

Protein	p*I*
Lysozyme, chicken egg white (Lys)	11.0
Cytochrome *c*, horse heart (Cyt *c*)	10.2
Ribonuclease A, bovine pancreas (Rib A)	9.3
α-Chymotrypsinogen, bovine pancreas (α-Chy)	9.2
Myoglobin, sperm whale skeletal muscle (Myo W)	8.1
Myoglobin, horse skeletal muscle (Myo H)	7.1

Buffers

A stock solution of 20 m*M* phosphate buffer (pH 5.5) was prepared by dissolving a weighed amount of sodium dihydrogenphosphate in Milli-Q-purified water and adding 1 *M* sodium hydroxide to adjust the pH to 5.5. Aliquots of this solution were used to prepare the buffers which contained the cationic additives. The additives (K_2SO_4, TMAB, HTMAB, triethylamine and morpholine) were dissolved in the phosphate buffer at the concentration indicated in each case. When necessary, the pH of these solutions was returned to 5.5 using concentrated phosphoric acid. The other buffers used were prepared by dissolving a weighed amount of sodium dihydrogenphosphate in Milli-Q-purified water and adjusting the pH with 1 *M* sodium hydroxide or 1 *M* hydrochloric acid. The buffers were stored at 4°C and heated to room temperature before use.

Preparation of cross-linked polyacrylamide-coated capillaries

The fused-silica capillaries were successively treated with 0.1 *M* hydrochloric acid for 1 h and 0.1 *M* sodium hydroxide solution for 2 h, then washed with 200 μl of Milli-Q-purified water and 200 μl of methanol. A length of 5 mm of the external polyimide coating was burned off in each capillary to make the detection window. The capillaries were flushed with 100 μl of a solution of 66% (v/v) of methacryloxypropyltrimethoxysilane in methanol and left for 3 h for reaction.

The polyacrylamide gel was prepared by dissolving a mixture acrylamide and bisacrylamide (4.2% C, 10% T) in thoroughly degassed 20 m*M* phosphate buffer (pH 5.5). To carry out polymerization, 3 μl of 10% (v/v) aqueous ammonium peroxodisulphate solution and the same amount

of 10% (w/v) TEMED solution in water were added per ml of buffer. Using such amounts of peroxodisulphate and TEMED, the polyacrylamide–bisacrylamide solution took about 45 min to reach a substantial degree of polymerization. This time interval was long enough to carry out the steps described below that are required for capillary preparation. After adding peroxodisulphate and TEMED, the polymerizing solution was homogenized using first a vortex mixer and then ultrasound for around 30 s each. Next, 50 μl of the polymerizing solution were injected into the capillaries prepared as indicated above. The solution was left for 1 min inside the capillaries before flushing them with nitrogen [0.8 atm (1 atm = 101 325 Pa)]. Immediately afterwards, the capillaries were heated at 140°C for 1 min in a gas chromatograph oven. The process of filling the capillary with polymerizing solution, flushing with nitrogen and heating was repeated three times in order to achieve a homogeneous coating of the inner capillary wall. Finally, in order to check that the gelling reaction had taken place within the capillaries, the unused portion of the polymerizing solution in its vial was heated in the oven for 1 min at 140°C.

RESULTS AND DISCUSSION

To ensure a strong interaction between proteins and silanol groups on the silica surface, which allow the evaluation of the masking efficiency of the different approaches investigated in this work, the buffer pH was fixed at 5.5. At this pH, a substantial proportion of the silanol groups on the silica surface are negatively charged and the proteins used (Table I) have a net positive charge, as can be deduced from their p*I* values.

Separation of basic proteins using uncoated and coated capillaries

The separation of three basic proteins (Cyt *c*, Rib A and α-Chy) using an uncoated fused-silica capillary and a 20 m*M* phosphate buffer (pH 5.5) gave rise to an electropherogram with a unique, tailing peak (result not shown). The poor peak shape is due to the strong electrostatic interactions that take place between the basic proteins and the silica surface at pH 5.5. When the same separation was carried out in the cross-linked polyacrylamide-coated capillaries using the same buffer, the separation of the three proteins was achieved. Reproducibility of the migration time for Cyt *c*, Rib A and α-Chy from run to run was 1.8, 2.8 and 3.4% (R.S.D., $n = 7$), respectively. This reproducibility is poor when compared with the value of less than 1% obtained using fused-silica capillaries with other coatings reported in literature [21,24,27]. The plate number achieved on the coated capillaries (around 10^5 plates/m for the three proteins tested) was almost one order of magnitude smaller than the values predicted by theory and about 3–5 times smaller than that obtained with other silanol-shielding techniques where the capillary–protein interactions have been reduced to a minimum [5,21,24]. This result indicates that some adsorption of the proteins on the capillary still occurs despite the polymeric layer covering the capillary wall. The low efficiency observed could be due to an inhomogeneous coating of the capillary, which could leave some areas of the fused silica uncovered, causing protein adsorption, and/or although the silica is completely covered by the polymeric coating, the small thickness of the layer could permit the electric charges on the silica surface to adsorb the proteins on the top of the polymeric layer; similar results have been observed previously with polyethyleneimine coatings [23].

Separation of basic proteins using uncoated and coated capillaries with cationic additives in the buffer

In order to mask the negative charges that still existed on the surface of the coated capillaries, we thought that an efficient method could be to use cationic additives in the separation buffer. Several additives, such as triethylamine, quaternary ammonium salts and morpholine, have traditionally been used in HPLC [29] to mask the effect of silanol groups. Others have been used for CE [30], particularly phosphate [17] and K^+ [7] ions. We compared the efficiency of an inorganic salt (K_2SO_4), two quaternary ammonium salts (TMAB and HTMAB), and two

amines (triethylamine and morpholine) as silanol maskers. To select the most appropriate additives to be tested with the coated columns, we first tried all of them in non-coated columns, expecting that in such demanding conditions the masking efficiency of each additive would be clearly demonstrated. In all instances, 20 m*M* phosphate buffers (pH 5.5) containing the additives studies at the concentrations indicated in each experiment were used.

When 0.25 *M* K_2SO_4 (a salt whose efficiency in preventing protein adsorption in CE has already been widely demonstrated [5,7,8,30]) was added to the buffer, good efficiency (around $4 \cdot 10^5$ plates/m) was observed for basic proteins. However, owing to the large electric current obtained with these buffers, a low voltage had to be used for the separation, causing a long analysis time (over 30 min). The two ammonium salts used led to electropherograms with broad peaks for the basic proteins, probably due to hydrophobic adsorption between the proteins and the alkylammonium moieties adsorbed on the capillary wall [31]. Finally, buffers containing 0.25 *M* morpholine or 0.25 *M* triethylamine were tried. Using both buffers, good efficiencies (between $1 \cdot 10^5$ and $5 \cdot 10^5$ plates/m) with a short analysis time (*ca.* 10 min) were obtained for the proteins tested. However, a poor reproducibility of the migration time of proteins (6–8.5% R.S.D.) was observed for both amines. It was concluded that morpholine and triethylamine presented some advantages over the other additives studied in terms of efficiency and seem to be better silanol maskers than the other additives. Consequently, we examined the effect of both buffers containing morpholine or triethylamine and coated columns in the separation of basic proteins.

The effect of buffers containing these two additives on the migration time reproducibility and efficiencies achieved on cross-linked polyacrylamide-coated columns is demonstrated in Table II. Better results were obtained in both respects with buffers containing morpholine. According to the pK_a value of these two additives (11.01 for triethylamine and 8.33 for morpholine), the percentage of protonated molecules is higher for triethylamine than for morpholine, and hence a higher shielding effect of the silanol groups would be expected for triethylamine at the working pH. The fact that a more efficient masking effect was observed for morpholine could be interpreted in terms of the stereochemistry of the two additives. Triethylamine, which has bulky ethylene groups surrounding the positively charged nitrogen atom, could have a higher steric hindrance than morpholine for the association with the negatively charged silanol groups on the surface.

In order to optimize the morpholine concen-

TABLE II

MIGRATION TIME REPRODUCIBILITY AND EFFICIENCY OBTAINED WITH CROSS-LINKED POLYACRYLAMIDE-COATED CAPILLARIES AND MORPHOLINE OR TRIETHYLAMINE AS ADDITIVE IN THE SEPARATION BUFFER

Buffer, 20 m*M* phosphate–0.25 *M* morpholine (pH 5.5) or 20 m*M* phosphate–0.25 *M* triethylamine (pH 5.5); capillary, coated 25 μm I.D., 360 μm O.D., 50 cm total length, 25 cm effective length; voltage, 25 kV; injection, 10 kV, 5 s; sample, 0.4 mg ml^{-1} Cyt *c*, 0.58 mg ml^{-1} Rib A and 0.51 mg ml^{-1} α-Chy; detection at 230 nm.

Protein	Morpholine			Triethylamine		
	t_m [a] (min)	R.S.D.$_t$ (%)	N [a] (plates/m)	t_m [a] (min)	R.S.D.$_t$ (%)	N [a] (plates/m)
Cyt *c*	9.6	1.3	322 000	6.8	1.8	256 000
Rib A	17.0	1.7	406 000	10.9	3.2	265 000
α-Chy	20.1	1.9	465 000	12.3	3.5	396 000

[a] t_m and N values are means value of five measurements.

tration, buffers containing 0.1, 0.25 and 0.5 *M* morpholine were compared in terms of the efficiency obtained for three basic proteins. In Table III it can be seen that for all the proteins assayed, the plate number reaches a maximum at 0.25 *M* morpholine. At lower concentrations of morpholine there are still some negative charges on the silica surface able to adsorb the proteins [32]. However, with buffers containing 0.5 *M* morpholine, the high current in the capillary (69 μA at 14 kV) could cause thermal overloading which leads to peak broadening.

In order to check the efficiency of the cross-linked polyacrylamide coating as a masker for the silanol groups of the silica surface, the electroosmotic flows and the electropherograms obtained on coated and uncoated capillaries with the same buffer [20 m*M* phosphate–0.25 *M* morpholine (pH 5.5)] were compared. Under these conditions, the electroosmotic coefficient for the coated capillary ($\mu_{eo} = 1.5 \cdot 10^{-5}$ cm^2 V^{-1} s^{-1}) was ten times smaller than that obtained for the uncoated capillaries ($\mu_{eo} = 1.7 \cdot 10^{-4}$ cm^2 V^{-1} s^{-1}). The separation of six basic proteins on uncoated and coated capillaries is shown in Fig. 1. As can be seen, peaks with low efficiency and poor resolution are obtained with uncoated capillaries owing to the adsorption of the proteins on the silica surface. The high electroosmotic flow observed for these capillaries also contributes to the low resolution obtained. Conversely, under the same separation conditions, the use of cross-linked polyacrylamide-coated capillaries gives a good separation of the basic proteins with efficiencies close to 500 000 plates (for Fig. 1B, lysozyme 310 000, cytochrome *c* 390 000, ribonuclease A 480 000, α-chymotryp-

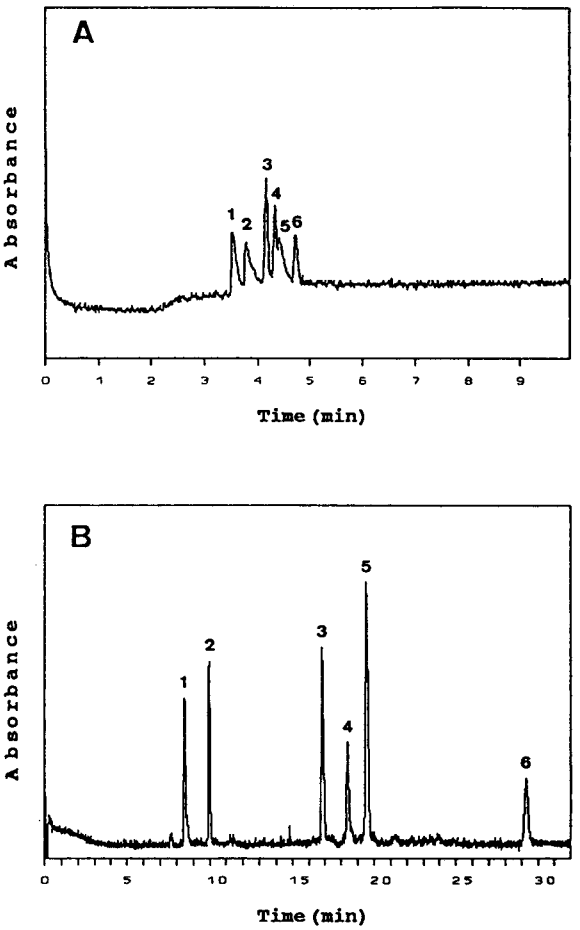

Fig. 1. Separation of basic proteins using (A) uncoated and (B) coated cross-linked polyacrylamide capillaries. Buffer, 20 m*M* phosphate–0.25 *M* morpholine (pH 5.5); capillary, 25 μm I.D., 360 μm O.D., 50 cm total length, 25 cm effective length; separation voltage, 20 kV (30 μA); injection at (A) 2.5 kV for 5s and (B) 4 kV for 5 s; detection at 230 nm. Peaks: 1 = 0.20 mg ml^{-1} lysozyme; 2 = 0.41 mg ml^{-1} cytochrome *c*; 3 = 1.07 mg ml^{-1} ribonuclease A; 4 = 0.21 mg ml^{-1} sperm whale myoglobin; 5 = 0.63 mg ml^{-1} α-chymotrypsinogen; 6 = 0.23 mg ml^{-1} horse myoglobin.

TABLE III

EFFECT OF MORPHOLINE CONCENTRATION ON THE EFFICIENCY FOR BASIC PROTEINS

Buffer, 20 m*M* phosphate–0.25 *M* morpholine (pH 5.5); capillary, coated with cross-linked polyacrylamide, 25 μm I.D., 360 μm O.D., 27 cm total length and 20 cm effective length; voltage, 14 kV; injection using nitrogen pressure (0.5 p.s.i.) for 2 s; sample, 0.25 mg ml^{-1} Cyt *c*, 0.31 mg ml^{-1} Rib A and 0.28 mg ml^{-1} α-Chy; detection at 214 nm.

Protein	Efficiency (plates/m)[a]		
	0.10 *M* morpholine	0.25 *M* morpholine	0.50 *M* morpholine
Cyt *c*	430 000	624 000	400 000
Rib A	300 000	422 000	280 000
α-Chy	300 000	323 000	200 000

[a] Reproducibility: 5% (R.S.D., $n = 5$).

sinogen 370 000, sperm whale myoglobin 430 000 and horse myoglobin 310 000 plates/m).

In order to gain some practical knowledge about the behaviour of the cross-linked polyacrylamide-coated capillaries working with buffers containing morpholine, the coating reproducibility, the stability of the coating at different buffer pHs and the column storage conditions were studied.

Coating reproducibility

The results of the study on the reproducibility of the coating are summarized in Table IV. The run-to-run reproducibility is excellent (R.S.D. 0.57–0.35%), as it would be expected from separations carried out on liquid thermostated (±0.1°C) capillaries. An acceptable day-to-day reproducibility is also obtained. More significant are the results obtained from three different capillaries prepared in the same batch (R.S.D. < 2%). This value is similar to those reported in the literature [21,27] for capillary-to-capillary reproducibility of coated tubes prepared by different methods. This means that a reasonable reproducibility could be expected between capillaries prepared in the same batch.

Coating stability

The stability of the polyacrylamide coatings during continued use with buffers in the pH range 2–12 was tested using a mixture of three basic proteins (Cyt *c*, Rib A and α-Chy) separated in a 20 m*M* phosphate–0.25 *M* morpholine buffer (pH 5.5). Several polyacrylamide-coated capillaries were prepared in the same batch. The test at each pH was run in a different capillary from the batch. Each test was performed in duplicate using different capillaries from the same batch. The capillary was filled with a very acidic (phosphoric acid for pH 2) or very basic (sodium hydroxide for pH 10–12) solution (henceforth called "pH test solution") and left for a certain amount of time. Then, the capillary was successively rinsed with 200 μl of water, air and 200 μl of the buffer used for the separation, electrolysed for 5 min at 20 kV and the migration time and efficiency for the basic proteins on the capillary were measured. The capillary was flushed with 500 μl of the pH test solution and left for a further period. The test lasted up to a total of 90 h. In order to verify if any appreciable modification took place on the polymeric coating by changing the capillary content from the buffer to the pH test solution and back to the buffer during the experiment, the separation of three basic proteins using a 20 m*M* phosphate–0.25 *M* morpholine (pH 5.5) buffer was carried out in a polyacrylamide-coated capillary. The capillary was then flushed with a new buffer consisting of 20 m*M* phosphate (pH 8), electrolysed for 5 min at 20 kV and the separation of acidic proteins (β-lactoglobulin A, β-lactoglobulin B and α-

TABLE IV

MIGRATION TIME REPRODUCIBILITY USING CROSS-LINKED POLYACRYLAMIDE-COATED CAPILLARIES AND MORPHOLINE IN THE SEPARATION BUFFER

Voltage, 12 kV; injection using nitrogen pressure (0.5 p.s.i.) for 4 s; sample: 0.6 mg ml^{-1} Cyt *c*, 0.7 mg ml^{-1} Rib A and 0.5 mg ml^{-1} α-Chy; other conditions as in Table III.

Protein	Run-to-run, ($n = 4$)[a]		Day-to-day, 3 days ($n = 12$)[a]		Capillary-to-capillary, 3 capillaries ($n = 12$)[a]	
	t_m (min)	R.S.D. (%)	t_m (min)	R.S.D. (%)	t_m (min)	R.S.D. (%)
Cyt *c*	9.33	0.35	9.36	0.94	9.31	1.27
Rib A	13.45	0.54	15.43	1.31	15.36	1.81
α-Chy	17.75	0.57	17.73	1.48	17.69	1.96

[a] *n* represents the total number of measurements carried out.

lactalbumin) was run several times. Next, the capillary was flushed with 200 μl of water, air and 200 μl of the initial buffer (morpholine buffer) and the separation of the basic proteins was run again under the above conditions. We observed that it was also necessary to electrolyse the capillary (20 kV for 5 min) before obtaining good reproducibility for the separation of the basic proteins. By using this cleaning routine, the reproducibility of the migration time before and after the replacement of buffer was within 1–1.5% R.S.D. ($n = 10$). This result indicates that it is possible to change from one buffer that contains morpholine to another one that does not and then back to the morpholine-containing buffer without modifying the migration time of the proteins in the capillaries.

A similar result, but with poor reproducibility [10–15% R.S.D. ($n = 10$)], was observed for the efficiency with basic proteins. This result also shows that with our polyacrylamide coating, a cleaning routine consisting in flushing the capillary with 200 μl of water, air and 200 μl of buffer and electrolysing it for 5 min at 20 kV seems to be very effective.

The results obtained for the pH stability test (Fig. 2) indicate that the stability of the polyacrylamide cross-linked capillaries is fairly good between pH 2 and 10. Within this pH range, the reproducibility of the migration time remains between 1 and 2.5% (R.S.D.) for a period of more than 90 h of continued use of the capillary. At pH 11–12, the stability of the column decreases in a short time, as shown by the continu-

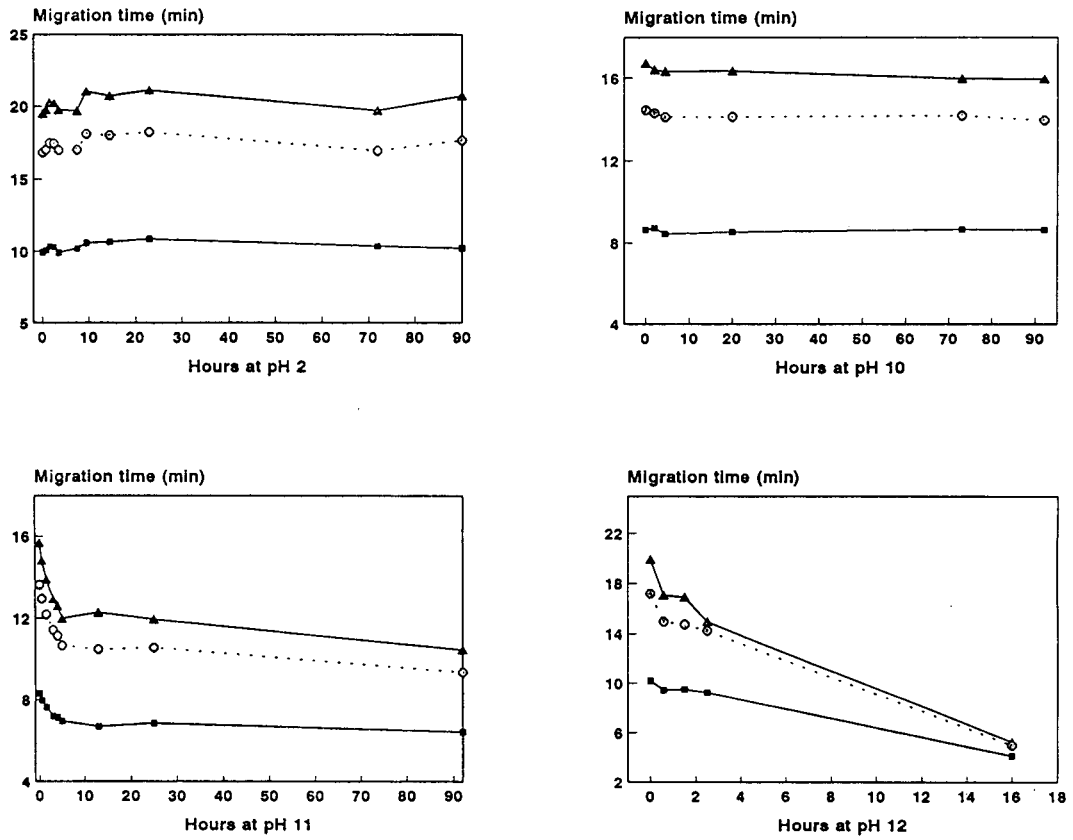

Fig. 2. Stability of the migration time for cross-linked polyacrylamide coatings in the pH range 2–12. Buffer, 20 mM phosphate–0.25 M morpholine (pH 5.5); capillary, 25 μm I.D., 360 μm O.D., 50 cm total length, 25 cm effective length; separation at 25 kV (40 μA); injection at 2.5 kV for 5 s. Sample: □ = 0.41 mg ml^{-1} cytochrome c; ○ = 1.07 mg ml^{-1} ribonuclease A; ▲ = 0.65 mg ml^{-1} α-chymotrypsinogen.

ous decrease of the protein migration time. This could be due to hydrolysis of the bonds that anchor the polymer to the silica [21], leaving an increasing number of free silanol groups uncovered. The increasing electroosmotic flow detected for the coated capillaries subjected to the test solution of pH 11–12 is responsible for the decrease in the migration time observed. On the other hand, a study of the stability of the cross-linked polyacrylamide coating in terms of the efficiency for basic proteins (Fig. 3) shows that the band broadening remains reasonably constant between pH 2 and 10 and quickly decreases at higher pH. As indicated before, degradation of the coating could leave an increasing number of silanol groups uncovered, which are able to adsorb the basic proteins, giving rise to this broadening of the protein peaks.

Column storage

The stability of the cross-linked polyacrylamide coating with respect to the storage time and the substance used to fill the capillary during storage was studied. In a similar fashion to that used for the coating stability test, a mixture of three basic proteins (Cyt *c*, Rib A and α-Chy) separated in a 20 m*M* phosphate–0.25 *M* morpholine buffer (pH 5.5) was used to check the variations of migration time and protein efficiency with the storage conditions. Three different capillaries containing either water, air or buffer [20 m*M* phosphate–0.25 *M* morpholine (pH 5.5)] were kept closed by pinning each end in a small piece of rubber. When the capillary was stored in water, the capillary was flushed with air, rinsed with 200 μl of the separation buffer and electrolysed for 5 min at 20 kV before

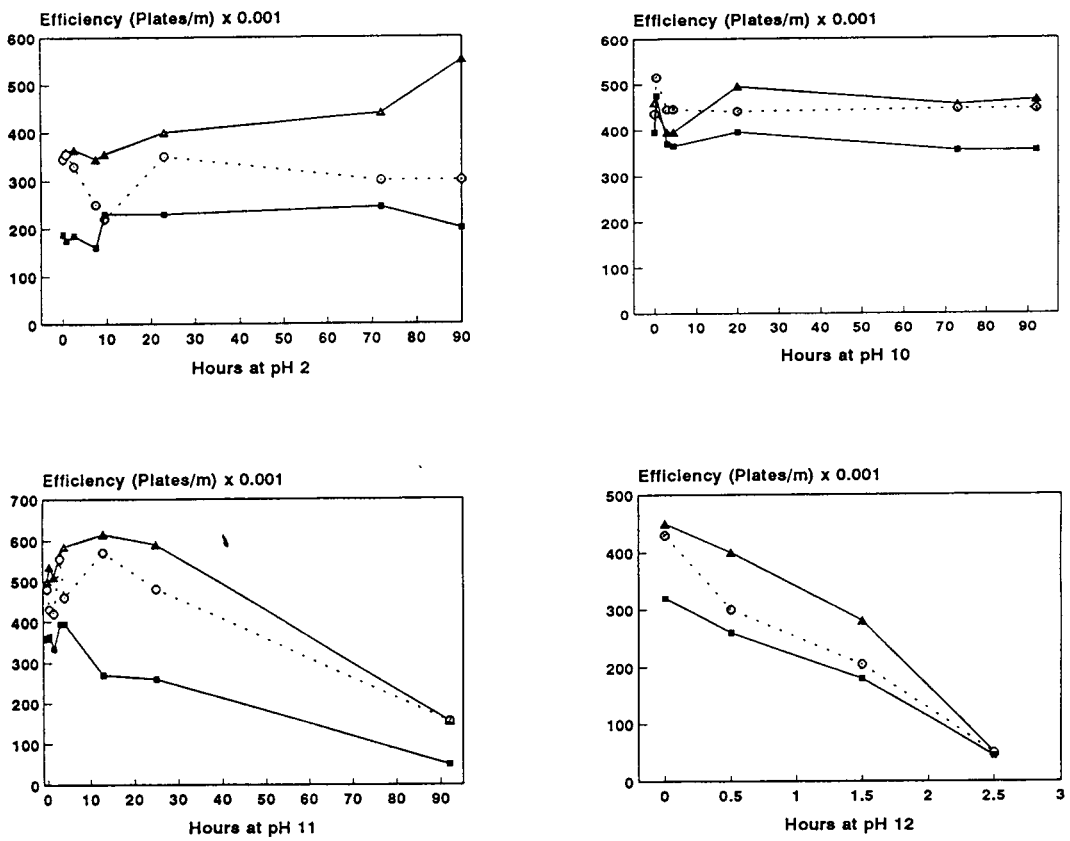

Fig. 3. Stability of the efficiency for cross-linked polyacrylamide coatings in the pH range 2–12. All other conditions and symbols as in Fig. 2.

the test was carried out. Likewise, when the capillary was stored in air, the buffer contained in the capillary was rinsed with 200 μl of water and air after the test.

The best results were obtained when capillaries were stored in air. After 90 days of storage, only a small decrease (*ca.* 1%) of the migration time was observed for the three proteins. However, the capillaries containing water or buffer showed a steady decrease in the migration time of the proteins with storage time (20% and 10%, respectively, in 90 days). Similar results were obtained for the protein efficiency on storage. While the capillaries containing air showed no decrease in efficiency for the three proteins tested, the capillaries kept in water or buffer showed a substantial decrease in efficiency after 12 days of storage. In conclusion, the cross-linked polyacrylamide coatings can be stored for a long period (at least 90 days) in air. After use of the capillaries and before storage, a thorough wash with water is advised in order to flush out the buffer used.

ACKNOWLEDGEMENTS

This work was supported by CICYT (Project ALI 91-0784). A. Cifuentes and M. de Frutos acknowledge M.E.C. for financial support. Special thanks are due to Beckman Instruments España for the loan of a P/ACE System 2000 to carry out part of the study. The authors also thank Dr. M.V. Dabrio for writing one of computer acquisition programs used in this work.

REFERENCES

1 W.G. Kuhr, *Anal. Chem.*, 62 (1990) 403R.
2 W.G. Kuhr and C.A. Monning, *Anal. Chem.*, 64 (1992) 389R.
3 M.V. Novotny, K.A. Cobb and J. Liu, *Electrophoresis*, 11 (1990) 735.
4 S. Hjertén, *Electrophoresis*, 11 (1990) 659.
5 H.H. Lauer and D. McManigill, *Anal. Chem.*, 58 (1986) 166.
6 J.W. Jorgenson and K.D. Lukacs, *Science*, 222 (1983) 266.
7 J.S. Green and J.W. Jorgenson, *J. Chromatogr.*, 478 (1989) 63.
8 Y. Walbrohel and J.W. Jorgenson, *J. Microcol. Sep.*, 1 (1989) 41.
9 K. Altria and C. Simpson, *Anal. Proc.*, 23 (1986) 453.
10 T. Tsuda, *J. High Resolut. Chromatogr. Chromatogr. Commun.*, 10 (1987) 622.
11 X. Huang, J.A. Luckey, M.J. Gordon and R.N. Zare, *Anal. Chem.*, 61 (1989) 766.
12 A. Emmer, M. Jasson and J. Roeraade, *J. High Resolut. Chromatogr.*, 14 (1991) 738.
13 M. Bushey and J.W. Jorgenson, *J. Chromatogr.*, 480 (1989) 301.
14 M. Merion, B. Bell-Alden, E. Grover, U. Neue and J. Peterson, presented at the *3rd International Symposium on High Performance Capillary Electrophoresis, San Diego, CA, February 1991*, poster 69.
15 S. Hjertén, *Chromatogr. Rev.*, 9 (1967) 122.
16 J.E. Wiktorowicz and J.C. Colburn, *Electrophoresis*, 11 (1990) 769.
17 R.M. McCormick, *Anal. Chem.*, 60 (1988) 2322.
18 S.A. Swedberg, *Anal. Biochem.*, 185 (1990) 51.
19 G.J.M. Bruin, R. Huisden, J.C. Kraak and H. Poppe, *J. Chromatogr.*, 480 (1989) 339.
20 S. Hjertén, *J. Chromatogr.*, 347 (1985) 191.
21 K.A. Cobb, V. Dolnik and M.V. Novotny, *Anal. Chem.*, 62 (1990) 2478.
22 G.J.M. Bruin, J.P. Chang, R.H. Kulman, K. Zegers, J.C. Kraak and H. Poppe, *J. Chromatogr.*, 471 (1989) 429.
23 J.K. Towns and F.E. Regnier, *J. Chromatogr.*, 516 (1990) 69.
24 M. Huang, W.P. Vorkink and M.L. Lee, *J. Microcol. Sep.*, 4 (1992) 233.
25 W. Nasabeh and Z. El Rassi, *J. Chromatogr.*, 559 (1991) 367.
26 Y.F. Maa, K.J. Hyver and S.A. Swedberg, *J. High Resolut. Chromatogr.*, 14 (1991) 65.
27 J.K. Towns and F.E. Regnier, *Anal. Chem.*, 63 (1991) 1126.
28 X.W. Yao and F.E. Regnier, presented at the *Sixteenth International Symposium on Column Liquid Chromatography, Baltimore, June 1992*, poster No. 412.
29 D.C. Leach, M.A. Stadalius, J.S. Berus and L.R. Snyder, *LC · GC Int.*, 1 (1988) 22.
30 J.A. Bullock and L.C. Yuan, *J. Microcol. Sep.*, 3 (1991) 241.
31 C. Tanford, *The Hydrophobic Effect: Formation of Micelles and Biological Membranes*, Wiley, New York, 2nd ed., 1980, pp. 146–164.
32 A. Cifuentes, M. de Frutos and J.C. Diez-Masa, in preparation.

Journal of Chromatography A, 655 (1993) 73–76
Elsevier Science Publishers B.V., Amsterdam

CHROM. 25 021

Determination of clenbuterol and salbutamol in urine by capillary gas chromatography with capillary columns of 100 μm

J.A. García Regueiro*, B. Pérez and G. Casademont

IRTA, Unitat Tecnologia Analítica, Centre de Tecnologia de la Carn, Granja Camps i Armet, 17121 Monells, Girona (Spain)

ABSTRACT

A method to determine clenbuterol and salbutamol in calf urine is described. Two independent extraction procedures using Extrelut (clenbuterol) and octadecylsilica (salbutamol) were used; the extracts obtained were mixed and purified over a cyanopropyl minicolumn. Trimethylsilyl derivatives were prepared and analysed by GC–MS in selected-ion monitoring mode using a fused-silica open tubular capillary column, 10 m × 100 μm coated with 5% phenylmethylsilicone. Splitless injection was optimized to achieve low percentage residual standard deviation of absolute areas. The best conditions were: injection volume 0.5 μl, column head pressure 22 p.s.i. (1 p.s.i. = 6894.76 Pa), inlet temperature 250°C and glass liner volume 250 μl. The recoveries of the complete procedure were in the range 50–60% for both compounds.

INTRODUCTION

β-Agonists can be used as growth promotors in animal production because they increase protein deposition and lipid degradation [1–3]. However β-agonist residues can affect the health of meat consumers, and their use in animal production is forbidden. Clenbuterol application in animal production has been intensively studied [3,4]. This compound is one of the most used illegal products and has been associated with toxic episodes in meat eaters [5].

Different analytical methods have been used to determine clenbuterol: high-performance thin-layer chromatography (HPTLC) [6,7], high-performance liquid chromatography (HPLC) [8–10] and gas chromatography–mass spectrometry (GC–MS) [11–14]. As other β-agonists can be used (*e.g.* salbutamol), methods for the simultaneous determination of β-agonists have been developed: clenbuterol and cimaterol are determined by HPTLC and HPLC [7], while a more general procedure described by Van Ginkel *et al.* [14] allows the analysis of four β-agonists by GC–MS using an immunoaffinity column to purify the extract. This procedure offers a high level of selectivity, but the purification step is slow. Capillary gas chromatography (cGC) coupled to mass spectrometry offers the most selective methodology, while HPTLC also allows a selective analysis but with lower sensitivity. Enzyme-linked immunosorbent assay is an alternative method of screening a large number of samples, but its lack of selectivity means that it is necessary to confirm positive results by other techniques (*e.g.* cGC–MS). The injection mode has a strong influence on the recovery of clenbuterol and salbutamol when cGC–MS is used, the best choice being on-column, with low residual standard deviation (R.S.D.) and highest recoveries [15]; splitless injection needs to be optimized and can be used taking care that inlet temperature is maintained below 250°C. The use

* Corresponding author.

0021-9673/93/$06.00

of capillary columns of 100 μm diameter in cGC–MS can improve the vacuum intensity and reduce the column bleed when a direct interface is used; but the injection in splitless mode becomes critical because it is difficult to transfer the solutes from the injector to a narrow column. In this work a method to determine clenbuterol and salbutamol by cGC–MS with columns of 100 μm diameter is presented, the injection conditions being optimized to allow the use of such capillary columns.

MATERIAL AND METHODS

Chemicals

Clenbuterol and salbutamol were from Promochem (Germany). Bis(trimethylsilyl)trifluoroacetamide (BSTFA) was from Supelco (USA). Triethylamine was from Fluka (Switzerland). β-Glucuronidase arylsulphatase (*Helix promatia*) and isooctane, acetonitrile and methanol of analytical grade were from Merck (Darmstadt, Germany). The fused-silica open tubular capillary column (10 m × 100 μm, 0.17 μm film thickness) was from Hewlett-Packard (USA).

Analytical procedure

Salbutamol solid phase extraction. The method was based on that described by Fürst *et al.* [12], but using an octadecylsilica column. A 20-ml volume of calf urine sample was enzymatically hydrolysed at pH 5.0 with 25 μl of β-glucuronidase arylsulphatase; the mixture was incubated overnight at 37°C. After the hydrolysis the pH was brought to 7.6 with 0.1 *M* sodium hydroxide and acetate buffer; the solution obtained was applied to an octadecylsilica minicolumn (500 mg, Waters–Millipore) previously activated with 6 ml of acetate buffer at pH 7.6. The column was rinsed with 4 ml of water and 2 ml of methanol–water (2:8); afterwards, salbutamol was recovered with 6 ml of methanol, this fraction was evaporated to dryness and redissolved in 0.5 ml of methanol.

Clenbuterol solid phase extraction. A 20-ml volume of calf urine sample was brought to pH 12 with 1 *M* sodium hydroxide and hydrolysed for 1 h at 45°C. The solution obtained was applied to an Extrelut column (Merck) and allowed to soak for 15 min; clenbuterol was recovered with 40 ml of dichloromethane, which was evaporated to dryness in a rotatory evaporator and redissolved in 0.5 ml of methanol.

Extract purification. This procedure was similar to that described by Brambilla *et al.* [9]. Salbutamol and clenbuterol extracts were mixed and applied to a cyanopropyl minicolumn (500 mg, Waters-Millipore) previously activated with 10 ml of methanol. The column was rinsed with 1 ml of methanol, and salbutamol and clenbuterol were eluted with 2 ml of 1% triethylamine in methanol. This solution was evaporated to dryness in a stream of nitrogen. The residue was redissolved with 200 μl of acetonitrile, and 50 μl of bis(trimethylsilyl)trifluoroacetamide (BSTFA) were added. The mixture was heated at 80°C for 1 h to obtain trimethylsilyl (TMS) derivatives; after this step the solution was evaporated to dryness in a stream of nitrogen and redissolved in 100 μl of isooctane. Blank samples of urine were spiked with clenbuterol and salbutamol to obtain 10, 5 and 2.0 ng/ml concentrations to study the recovery of the complete procedure.

Chromatographic analysis

The injection mode was splitless: the inlet temperature was 250°C, and the split valve was closed for 1 min using a deactivated glass liner of 250 μl volume. Carrier gas helium at a head column pressure of 22 p.s.i. (1 p.s.i. = 6894.76 Pa) was used. Column temperature was held at 80°C for 1 min, increased by 15°C/min to 150°C, then increased to 250°C at 5°C/min.

Samples and standards were analysed by cGC–MS using an HP 5890 gas chromatograph coupled to an HP 5970 mass-selective detector (Hewlett-Packard) by a direct interface at 280°C, under the following conditions: spectra were obtained in the electron-impact mode (70 eV), selected ions monitored were: *m/z* 86, dwell time 50 ms (salbutamol and clenbuterol); *m/z* 262, dwell time 100 ms (clenbuterol); and *m/z* 369, dwell time 50 ms (salbutamol). Methane positive chemical ionization was used to confirm clenbuterol identification by monitoring ions at *m/z* 349 and 333 and salbutamol at *m/z* 440 and

366, the dwell times being 100 ms; the instrument used was an HP 5971 A mass selective detector (Hewlett-Packard).

Standard solutions of clenbuterol and salbutamol (2.0, 1.6, 1.0 and 0.8 ng/μl) were prepared to evaluate the linear range and repeatability. A standard solution of clenbuterol and salbutamol (1.0 ng/μl) was used to evaluate splitless conditions: column head pressure (range 15–25 p.s.i.), glass liner volume (1000, 800 and 250 μl), temperature (240, 250, 260 and 280°C), sample volume (0.5–1.5 μl) and split valve closed time (45, 60 and 120 s). To establish the optimal conditions the peak width, resolution and analysis time were determined.

RESULTS AND DISCUSSION

Urine samples

The extraction of clenbuterol and salbutamol was carried out by two different procedures because it was not possible to recover both compounds with a single extraction. Extrelut columns were not able to recover salbutamol at basic or acid pH: the values obtained were lower than 20%. Solid phase extraction with octadecylsilica columns showed a low recovery for clenbuterol at pH 7.6, a value that was optimal for retaining salbutamol because at higher pH the phenolic group of this β-agonist remains ionized and it is impossible to retain it effectively. The purification step was performed in a single operation for both compounds. The recovery of this step was higher for clenbuterol (83%) than for salbutamol (70%). The recoveries of the complete procedure were 57.2% for clenbuterol (7% R.S.D.) and 47.8% for salbutamol (15.9% R.S.D.). These values agree with others reported previously [7].

GC–MS analysis

The use of a direct interface in GC–MS analysis requires the carrier gas flow to be as low as possible. One of the ways of achieving this is to use capillary columns of narrow diameter, for example 100 μm. A five-fold reduction in vacuum pressure compared with that obtained with capillary columns of 200 μm diameter was observed. The decrease of analysis time was not possible because high temperature ramps (>20°C/min) showed band broadening and lower resolution. Splitless injection is critical because it is difficult to transfer the solutes to a narrow column from the injector. It was observed that glass liners with volumes greater than 0.5 ml are not appropriate as they produce an increase in peak width; the optimal injection volume was 0.5 μl and long periods with the split valve closed did not improve the mass transfer. Column head pressures below 20 p.s.i. produced a slow introduction. An alternative procedure, increasing the inlet pressure only during the injection and reducing it afterwards during the separation, did not improve the resolution between clenbuterol and salbutamol peaks. Salbutamol showed a lower percentage R.S.D. (2.9%) than clenbuterol (7.8%), but in the case of spiked urine samples the repeatibility was poorer for both compounds amounting to 15% R.S.D. The calibration curve (areas *versus* concentration) of salbutamol was linear in the range 0.4–1.2 ng with $y = 148420 + 145343x$ ($r = 0.992$), and clenbuterol data in the same range of

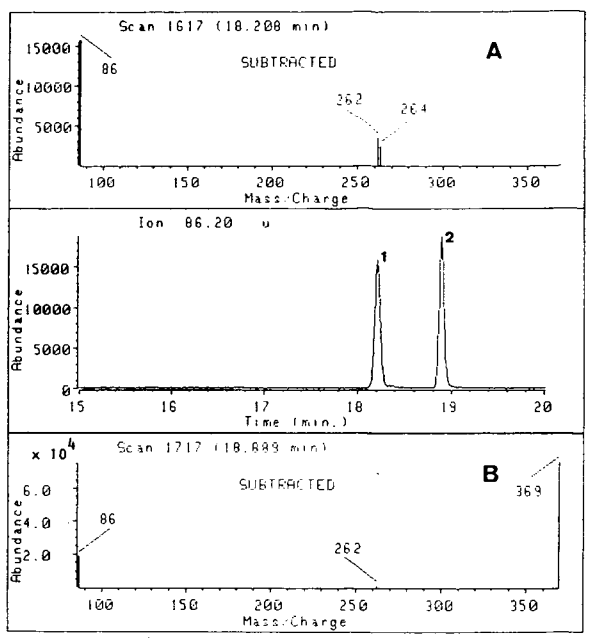

Fig. 1. GC–MS selected-ion monitoring chromatogram of clenbuterol (peak 1) and salbutamol (peak 2). Scan profile of the selected ions: (A) clenbuterol; (B) salbutamol.

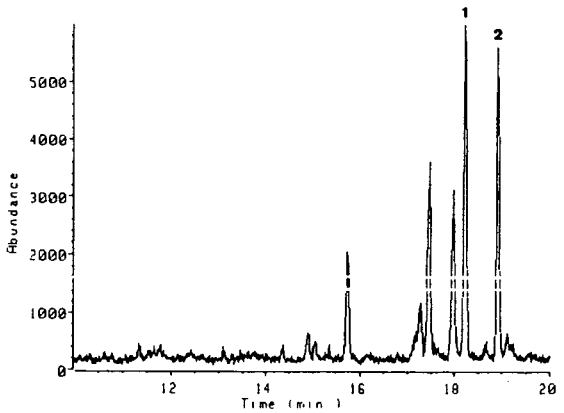

Fig. 2. GC–MS chromatogram of a urine sample spiked with 2 ng/ml clenbuterol (peak 1) and salbutamol (peak 2). For conditions, see text.

concentrations fitted the equation $y = 140631 + 130541x$ ($r = 0.994$). The sensitivity was 0.2 ng for both compounds (m/z 86 clenbuterol; m/z 369 salbutamol), allowing a limit of detection of urine samples of 1.5 ng/ml. Figs. 1 and 2 show chromatograms of standard and urine samples. Selected-ion monitoring in electron-impact mode presented problems for identifying the presence of clenbuterol because of the low mass of the ion with the highest abundance (m/z 86); however, urine blank samples did not show significant interference at the retention times of clenbuterol. In contrast, the identification of salbutamol was favoured in electron impact by the high abundance of the ion m/z at 369. Positive chemical ionization was used to ensure the identification of clenbuterol (Fig. 3), but the sensitivity was lower (0.4 ng, ions m/z 349 and m/z 333), allowing only a limit of detection of 3.0 ng/ml; but when ion at m/z 86 was used the sensitivity was similar to electron impact. Also, salbutamol can be identified by this technique using two m/z values at 440 and 366.

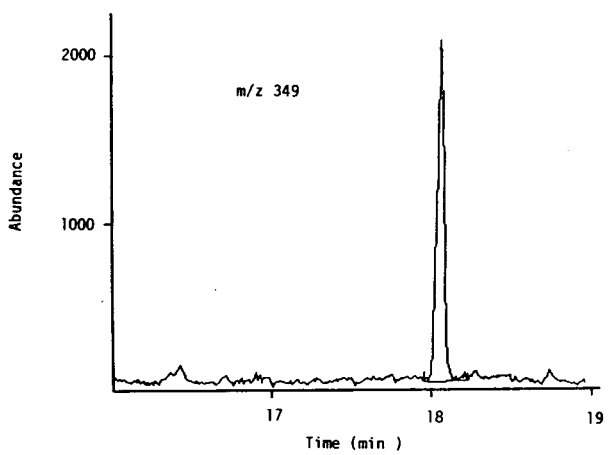

Fig. 3. GC–MS chromatogram of urine sample containing clenbuterol. Methane-positive chemical ionization at m/z 349. For conditions, see text.

ACKNOWLEDGEMENTS

This work was supported by the I.N.I.A. (Ministerio de Agricultura, Pesca y Alimentación, Spain) Project No. 8.580. B.P. thanks the I.N.I.A. for a predoctoral grant.

REFERENCES

1 C.A. Ricks, P.K. Baker, R.H. Dalrymle, M.E. Doscher, D.L. Ingle and J. Pankavish, *Fed. Proc.*, 43 (1984) 851.
2 R.H. Dalrymle, R.K. Baker, D.E. Gingher, D.L. Ingle, J.M. Pensack and C.A. Riks, *Poult. Sci.*, 63 (1984) 2376.
3 J.P. Hanrahan, *Beta-Agonists and their Effect on Animal Growth and Carcass Quality*, Elsevier Applied Science, London, 1987.
4 H.D. Meyer and L.M. Rinke, *J. Anim. Sci.*, 69 (1991) 4538.
5 J.F. Martínez-Navarro, *Lancet*, 336 (1990) 1311.
6 J.M. Degroodt, B.W. de Bukanski, H. Beernaert and D. Courtheyn, *Z. Lebensm.-Unters.-Forsch.*, 189 (1989) 128.
7 J.M. Degroodt, B.W. de Bukanski, J. de Groof and H. Beernaert, *Z. Lebensm.-Unters.-Forsch.*, 192 (1991) 430.
8 G. Ali Quershi and A. Erikssom, *J. Chromatogr.*, 441 (1988) 197.
9 G.F. Brambrilla, S. Castelli, A. Riberzni, M. Montana and F. Manca, *Ind. Aliment.*, 29 (1990) 674.
10 H. Hooigeringk, R. Schilt, W. Haasnot and D. Courteijn, *J. Pharm. Biomed. Anal.*, 9 (1991) 485.
11 P. Fürst, C. Fürst and W. Groebel, *Dtsch. Lebensm.-Rundsch.*, 85 (1989) 35.
12 P. Fürst, C. Fürst and W. Groebel, *Dtsch. Lebensm.-Rundsch.*, 85 (1989) 341.
13 F. David, P. Courselle, M. Schefault and P. Sandra, in P. Sandra (Editor), *Proceedings of the 10th International Symposium on Capillary Chromatography, Riva del Garda*, Huethig, Heidelberg, Vol. II, 1989, p. 1185.
14 L.A. van Ginkel, R.W. Stephany and H.J. van Rossum, *J. Assoc. Off. Anal. Chem.*, 75 (1992) 554.
15 P. Courselle, M. Schefault, P. Sandra and C. van Peteghem, in P. Sandra (Editor), *Proceedings of the 12th International Symposium on Capillary Chromatography, Riva del Garda*, Huethig, Heidelberg, Vol. I, 1991, p. 388.

Journal of Chromatography A, 655 (1993) 77–83
Elsevier Science Publishers B.V., Amsterdam

CHROM. 25 042

Separation and characterization of rat kidney isometallothioneins induced by exposure to inorganic mercury

M.A. Morcillo and J. Santamaría*

División de Isótopos, Centro de Investigaciones Energéticas, Medioambientales y Tecnológicas, 28040 Madrid (Spain)

ABSTRACT

High-performance liquid chromatography (HPLC) was applied to the separation of metallothionein (MT) isoforms from different tissues from a variety of eukaryotic species. Recently we reported an analytical method for ^{203}Hg–metallothionein, which detects the radioisotope bound to each iso-MT after separation by HPLC on a size-exclusion column coupled with on-line radioactivity flow detection. The MTs can be separated as distinct isoprotein peaks by elution with alkaline buffer solution owing to cation-exchange chromatographic action. In the present work, renal MT from rats exposed to inorganic mercury was separated into four peaks by UV and ^{203}Hg detection. Moreover, it was resolved into four components by non-denaturing polyacrylamide gel electrophoresis. The two major components correspond to MT-1 and MT-2, which were characterized by amino acid analysis. Finally, Hg induces and binds to both iso-MTs.

INTRODUCTION

Mercury is one of the non-essential elements that presents a high risk to human health. Following chronic exposure of animals to inorganic mercury the highest concentration of metal is found in the kidney [1] where it is mainly associated with metallothionein (MT) [2–4], a small protein rich in cysteinyl residues and heavy metals [5,6].

High-performance liquid chromatography (HPLC) has been applied to the separation of MT isoforms from different tissues and a variety of eukaryotic species. MT can be separated into different isoprotein peaks by HPLC on a size-exclusion column (HPSEC) by elution with an alkaline buffer solution due to a cation-exchange chromatographic action [7]. Thus, we have reported that the rat renal ^{203}Hg-MT induced by exposure to inorganic mercury can be resolved into at least three peaks by HPSEC connected on-line with a radioactivity detector, in order to obtain the simultaneous HPLC–UV and HPLC–radioactivity detection chromatograms [8].

In summary, the aim of this work was, first, to characterize by amino acid analysis the isometallothioneins (iso-MTs) induced in rat kidney by exposure to Hg(II) and, second, to determine whether the same number of components resolved by HPSEC can be obtained by polyacrylamide gel electrophoresis (PAGE). An attempt was made to correlate the change in the chromatographic elution profile after injection of rat renal Hg-MT on HPSEC and the mercury exposure dose.

EXPERIMENTAL

Reagents

Mercuric chloride, sucrose, hydrochloric acid,

* Corresponding author.

0021-9673/93/$06.00

β-mercaptoethanol and tris(hydroxymethyl)-aminomethane were obtained from Merck (Darmstadt, Germany), $^{203}HgCl_2$ from Amersham International (Amersham, UK), ammonium formate and ammonia solution 30% from Carlo Erba (Milan, Italy), rabbit liver metallothionein from Sigma (St. Louis, MO, USA), reagents for electrophoresis from LKB (Bromma, Sweden), Sephadex G-75 from Pharmacia (Uppsala, Sweden) and Atomflow from DuPont (Boston, MA, USA).

Preparation of rat kidney supernatant

Twenty-four male Sprague–Dawley rats (Cijisa, Madrid, Spain), weighing about 135 g, were randomly divided into four groups of six animals each. The groups were exposed to 1, 10 and 100 μg Hg as $HgCl_2$ per ml of drinking water for 8 weeks with food and water *ad libitum*. Following a single intraperitoneal dose of 23 μg of Hg per kg body mass (5–10 μCi of $^{203}HgCl_2$), the rats were sacrificed 3 h after dosing by exsanguination under light ether anaesthesia.

The kidneys were removed and homogenized in two volumes of 10 m*M* Tris–HCl buffer (pH 8.6)–0.25 *M* sucrose–5 m*M* 2-mercaptoethanol (bubbled with nitrogen before use) and the homogenate was centrifuged at 105 000 *g* for 90 min in a Centrikon T-1055 ultracentrifuge with a TFT 65.13 rotor (Kontron Instruments, Milan, Italy) at 4°C.

Separation of metallothionein on a Sephadex G-75 column

The renal supernatant was applied to a column (70 × 2.6 cm; Pharmacia, Uppsala, Sweden) of Sephadex G-75 that had been pre-equilibrated with 20 m*M* ammonium formate buffer, pH 7.65 (adjusted with ammonia solution), and the column was eluted with the same buffer (bubbled with nitrogen before use). Fractions (4.2 ml) were collected and the radioactivity in each fraction was measured in an LKB 1275 Minigamma solid scintillation spectrometer.

HPSEC

An aliquot of 100 μl of MT peak central fraction eluted from the Sephadex G-75 column was applied to a Protein-Pack 125 column (300 × 7.8 mm; Waters, Milford, MA, USA), which was eluted with 20 m*M* ammonium formate buffer (pH 7.65 at 25°C) at a flow-rate of 1 ml/min. Molecular absorbance at 254 nm was continuously monitored with a Model 484 ultraviolet detector (Waters) and the signal was registered by a Model 730 data module (Waters).

For simultaneous determination of the MT-associated radioactivity, the column outlet tube was connected on-line with a LKB Model 1208 Betacord radioactivity monitor. An aliquot of 1 ml of the MT peak eluted from the Sephadex G-75 column was dried on a Model SVC 100H SpeedVac concentrator (Savant, Farmingdale, NY, USA) and redissolved in 100 μl of 20 m*M* ammonium formate buffer (pH 7.65). The sample was subjected to HPLC analysis with a Protein-Pack 125 column and the same buffer at a flow-rate of 0.6 ml/min. A liquid scintillation cocktail, Atomflow, was added to the HPLC eluent at a flow-rate of 1.8 ml/min before the eluent passed through the flow cell of the radioactivity detector, and the presence of ^{203}Hg was simultaneously monitored.

Amino acid analysis

Samples of isometallothioneins were hydrolysed for 24 h at 116°C and subjected to amino acid analysis by the Pico.Tag method (Waters). For determination of cysteine, samples were oxidized with performic acid [9] before acid hydrolysis.

PAGE

For native PAGE the method described by Davis [10] was performed on an LKB 2001 vertical slab gel apparatus. The stacking gel contained 4.5% acrylamide, and the separation gel a gradient of 5–15% acrylamide. The gel was stained with Coomassie Blue R-250 and was scanned by an MIP-Interdens System densitometer (Microm, Barcelona, Spain).

RESULTS AND DISCUSSION

Fig. 1 shows typical elution profiles of the radioactivity associated to proteins in mercury-exposed rat kidney supernatant on a Sephadex

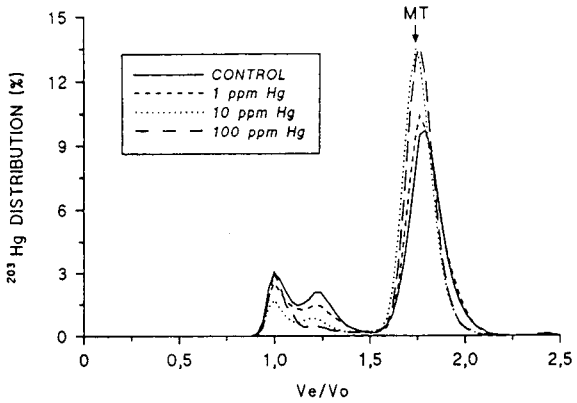

Fig. 1. Rat kidney supernatants were applied to a Sephadex G-75 column (70 × 2.6 cm) and eluted with 0.02 *M* ammonium formate buffer (pH 7.65). Fractions of 4.2 ml were collected and the radioactivity content in each fraction was determined.

G-75 column. The chromatographic profiles were different for each Hg dose studied. Thus, in the control group, 72% of the eluted cytosolic ^{203}Hg was associated with a broad band showing a peak with a ratio elution volume (V_e)/void volume (V_0) 1.6–2.1. Since metallothionein was shown to elute in this region, this peak was assumed to represent a ^{203}Hg–MT complex. The dietary mercury stimulated significantly the uptake of ^{203}Hg in renal MT, since around 85–90% is bound to MT from rats exposed to 10 and 100 ppm Hg(II).

A two-step, low-pressure, column chromatographic procedure generally involving a combination of size-exclusion and anion-exchange modes has been widely used to isolate MT from tissue extracts and continues to be the method of choice for the purification of MT on a preparative scale [11]. Whanger and Deagen [12] purified rat renal ^{203}Hg–MT by SEC (Sephadex G-75) and isolated three mercury–MT species from a DEAE-cellulose column. However, this approach is time consuming and requires relatively large amounts of sample. Recently, we reported that rat kidney ^{203}Hg–MT can be separated as distinct isoprotein peaks by HPSEC [8]; the separation of Hg–MT species on a HPSEC column revealed that they can be purified and characterized with a small sample size in a short time. Although in our above-mentioned study ^{203}Hg–MT was separated into three major peaks, in the present work an aliquot of MT (from the group exposed to 100 ppm) isolated on a Sephadex G-75 column and subjected to HPLC analysis on an SEC yielded four peaks (Fig. 2). These peaks were resolved by both UV (Fig. 2A) and ^{203}Hg detection (Fig. 2B). The radioactivity of the central fraction (number 60) was predominantly associated with the major peaks (2 and 3). Reversed-phase (RP) HPLC is a powerful technique for effectively separating peptides that differ in their composition by a single amino acid [13]. We have reported that rat renal ^{203}Hg–MT is separated into four peaks by RP-HPLC [8], therefore rat kidney mercury-induced MT is resolved into four peaks by both HPSEC and RP-HPLC.

The MT isoforms found in rat tissues can also be successfully separated by non-denaturing PAGE [14]. However, no success was achieved in isolating MTs containing variable amounts of copper (rat renal mercury-induced MT is a protein rich in copper [3,4]). The presence of copper appears to consistently affect the mobility of MT such that the lane of gel is generally a

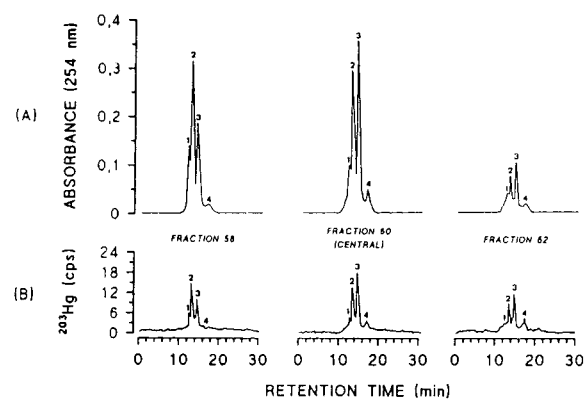

Fig. 2. An aliquot (1 ml) of mercury-exposed renal MT (100 ppm Hg group) isolated on a Sephadex G-75 column was concentrated and redissolved in 100 μl of 0.02 *M* ammonium formate buffer (pH 7.65). This sample was subjected to HPLC on a Protein-Pack 125 column (300 × 7.8 mm) and eluted with a 0.02 *M* ammonium formate buffer (pH 7.65) at a flow-rate of 0.6 ml/min. A liquid scintillation cocktail was added to the HPLC eluent at a flow-rate of 1.8 ml/min and the presence of radioactivity was continuously monitored. (A) UV chromatogram at 254 nm and (B) radioactivity detection chromatogram.

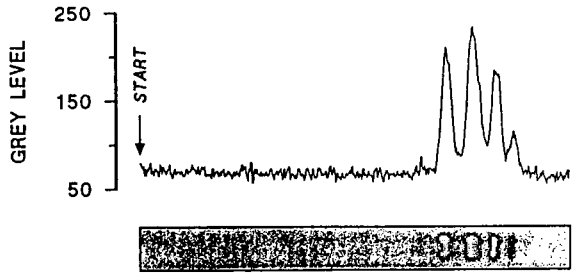

Fig. 3. A sample of mercury-exposed renal MT (100 ppm Hg group) was subjected to non-denaturing polyacrylamide gel electrophoresis. The stacking gel contained 4.5% acrylamide and the separation gel a gradient of 5–15% acrylamide. The gel was stained with Coomassie Blue R-250 and was scanned by a densitometer.

smear. Nevertheless, in the present work, Hg–MT was resolved into four components by non-denaturing PAGE (Fig. 3), which corroborates the results obtained by HPLC.

Suzuki *et al.* [15] have reported that SW and Sephadex columns are similar with respect to separation mechanisms; molecules of different molecular masses are separated by different elution rates through microspheres of hydrophilic polymer gels, and molecules of different isoelectric points are separated in a cation-exchange mode by ionized hydroxyl groups in alkaline solution. As the MT-1 and MT-2 isoforms possess two and three negative charges, respectively, between pH 7.5 and 9.5, a faster eluting metallothionein fraction on a Sephadex G-75 column is rich in iso-MT-2 and a slower eluting MT fraction is rich in iso-MT-1. Therefore, the former fraction gives lower, and the latter fraction higher, ratios of MT-1 to MT-2. In order to characterize the different peaks resolved by HPLC, the fractions of the rat kidney Hg–MT peak isolated on a Sephadex G-75 were analysed by HPSEC. Peak heights of iso-MTs were plotted against number fraction, as shown in Fig. 4. Peak 2 predominates in the faster eluting MT fractions, which indicates that peaks 2 and 3 presumably correspond to MT-2 and MT-1, respectively.

The absorption spectrum of MT in the range 240–300 nm results primarily from metal–ligand charge-transfer transitions. The shape of the absorption spectrum and the extinction coeffi-

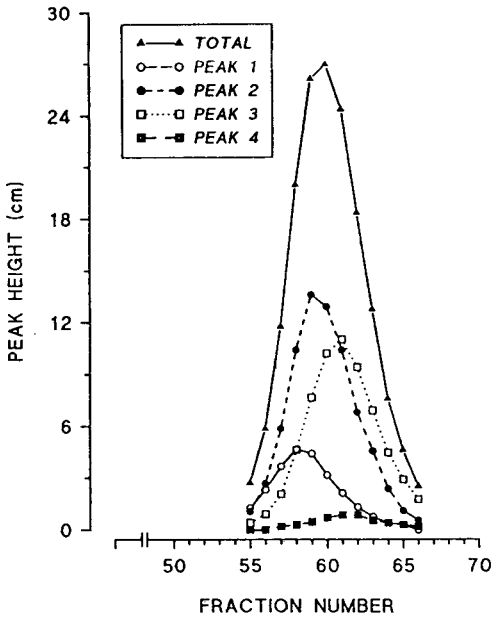

Fig. 4. Rat kidney supernatant (100 ppm Hg group) was applied to a Sephadex G-75 column (70 × 2.6 cm) and eluted with 0.02 *M* ammonium formate buffer solution, pH 7.65. Metallothionein was eluted at around tube 60. An aliquot (100 μl) of tubes 55–66 eluted from the Sephadex G-75 column was subjected to HPLC on a Protein-Pack 125 column (300 × 7.8 mm) and eluted with 0.02 *M* ammonium formate buffer solution (pH 7.65) at a flow-rate of 1 ml/min. Peak heights of the four components resolved by HPLC were plotted against fraction number. Peak 2 = MT-2; peak 3 = MT-1.

cients at various wavelengths are characteristic of metals bound to the thionein [16]. Thus, Hg–MT has a maximum absorption around 265 nm [17]. As shown in Fig. 5, peaks 2 and 3 have a maximum absorption at this wavelength.

In addition, rat kidney MT exhibits a third peak which eluted at the slowest rate on the SW column [15] owing to the presence of copper and intramolecular oxidation [18]. Oxidation of SH groups results in a denser and more globular monomer. This causes a decrease in the size of the protein molecule and the Stokes radius, and, as a consequence, an apparent loss in mass, determined by gel chromatography [19]. We have previously reported that replacement *in vitro* of metals in rabbit liver Cd,Zn–thionein with Cu^{2+} and Hg^{2+} produces additional peaks on HPSEC, which elute with longer retention time than the

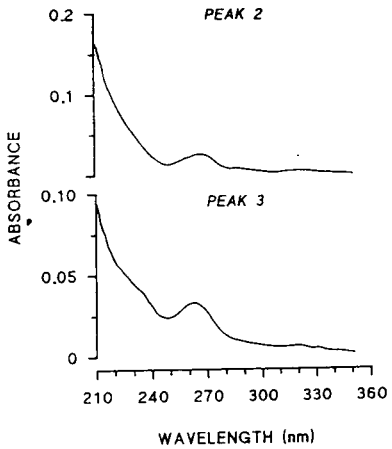

Fig. 5. A sample of mercury-exposed renal MT (100 ppm Hg group) isolated on a Sephadex G-75 column was subjected to HPLC on a Protein-Pack 125 column (300 × 7.8 mm) and eluted with 0.02 *M* ammonium formate buffer (pH 7.65) at a flow-rate of 1 ml/min. Peaks 2 and 3 were collected and an absorption spectrum was obtained by a UV–Vis 8450A spectrophotometer (Hewlett-Packard).

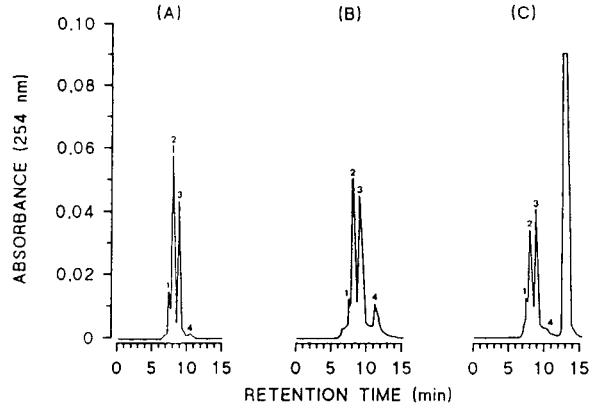

Fig. 6. A sample of mercury-exposed renal MT (100 ppm Hg group) isolated on a Sephadex G-75 column was maintained at room temperature in order to help its oxidation. Immediately, the sample was incubated in presence of 10 m*M* 2-mercaptoethanol and subjected to HPLC on a Protein-Pack 125 column (300 × 7.8 mm) and eluted with 0.02 *M* ammonium formate buffer (pH 7.65) at a flow-rate of 1 ml/min. (A) Original MT; (B) oxidized MT and (C) MT + 2-mercaptoethanol.

native molecule [4]. In order to determine whether peak resolved by HPSEC correspond to oxidized MT, an aliquot of the MT peak isolated on a Sephadex column was kept at room temperature for 1 week in order to help its oxidation. Afterwards, the sample was incubated in the presence of 10 m*M* 2-mercaptoethanol for 30 min at 37°C and subjected to HPSEC. The original Hg–MT gives the elution profile shown in Fig. 6A. The oxidized MT is characterized by a remarkable increment in peak 4 (Fig. 6B), which almost disappeared when the sample was incubated in the presence of 2-mercaptoethanol (Fig. 6C). Therefore, peak 4 may correspond to oxidized MT molecules resulting from the presence of copper/mercury and intramolecular oxidation.

A typical characteristic of MTs is their extremely high content of cysteine (about 33%); in addition to cysteine, most MTs also contain a relatively large proportion of serine (approximately 14%) and basic amino acids, especially lysine and, occasionally, arginine (lysine and arginine being around 13%) [20]. The amino acid composition of the different isoprotein peaks of rat kidney Hg–MT is shown in Table I. The results indicate that peaks 2 and 3 are

TABLE I

AMINO ACID COMPOSITION OF ISOMETALLOTHIONEINS

The values are expressed as percentages of the total number of residues in the molecule. Values were obtained from duplicate 24-h hydrolysates.

Amino acid	Rat kidney mercury-exposed MT				Rabbit liver MT	
	Peak 1	Peak 2	Peak 3	Peak 4	MT-1	MT-2
Asp	9.9	10.9	7.4	5.2	7.3	7.0
Glu	10.5	8.0	4.8	6.6	4.4	4.9
Ser	4.7	9.6	13.3	10.8	11.5	10.1
Gly	9.7	10.2	11.2	15.6	7.3	9.4
His	1.4	0.8	0.3	0.1	–	0.4
Arg	5.7	3.2	1.6	3.9	1.3	0.9
Thr	6.6	5.9	6.2	5.5	5.5	–
Ala	6.4	3.6	6.7	8.6	12.6	15.6
Pro	2.2	2.9	3.4	8.3	4.2	6.1
Tyr	–	0.5	–	–	–	–
Val	6.5	0.9	3.7	4.5	0.3	1.6
Cys	6.0	20.6	26.7	14.5	28.9	22.6
Ile	7.1	3.5	1.0	3.4	2.0	2.6
Leu	8.7	4.3	1.4	3.9	0.8	1.4
Phe	5.5	2.7	0.8	1.4	–	0.5
Lys	9.2	12.4	11.4	7.7	14.1	11.1

metallothionein-type proteins, with a characteristic cysteine content of around 21–27%, which is similar to the cysteine content of rabbit liver iso-MTs (Sigma). However, this cysteine content was lower than the cysteine content determined from DNA sequence data reported by Winge *et al.* [21]. The very confusing fact which has made impossible the unequivocal identification of several copper-proteins as MTs has been their low content of cysteine [22]. This low cysteine content has been explained by some authors [23] as a probable artefact on the basis that, in the presence of significant amounts of copper, cysteine contents are much lower. This is especially true when the method used for the determination of cysteine is based on its oxidation to cysteic acid. Therefore, the discrepancy observed between the cysteine content determined from amino acid analysis (Table I) and from DNA sequence analysis [21] could be explained by oxidative changes catalysed by Cu^{2+}. Peak 4 shows a lower content of cysteine (about 15%) than the others, and this phenomenon could be also caused by the circumstances mentioned above. Another characteristic of MTs is that they are lacking in aromatic amino acids. However, peak 2 isolated from HPSEC contained a small amount of phenylalanine. This indicates that the peak 2 sample might have been contaminated with a small amount of peak 1 (the Phe content of peak 1 is about 6%) and that the phenylalanine derived from this peak.

Winge *et al.* [22] initially reported the characterization of a distinct, non-metallothionein copper-rich protein from the livers of copper-injected rats. This putative species, called copper–chelatin, which is now generally considered to be artifactual, appeared to have a lower Cys content and to elute later than MT-2 on DEAE ion-exchange chromatography. Provided peak 1 elutes earlier than peak 2 (MT-2) on HPSEC (with this technique the iso-MTs are eluted in reverse order from an anion-exchange column) and its Cys content is 6%, it can be an artefact produced in the rat renal mercury-induced metallothionein purification.

On the other hand, we have applied HPSEC to determine whether some isoform of rat kidney Hg–MT is preferentially expressed in response to induction by different doses of mercury. Fig. 7 shows the chromatograms obtained after subjecting to HPSEC an aliquot of rat kidney MT induced by different doses of mercury. In response to mercury, both isoforms increased in a

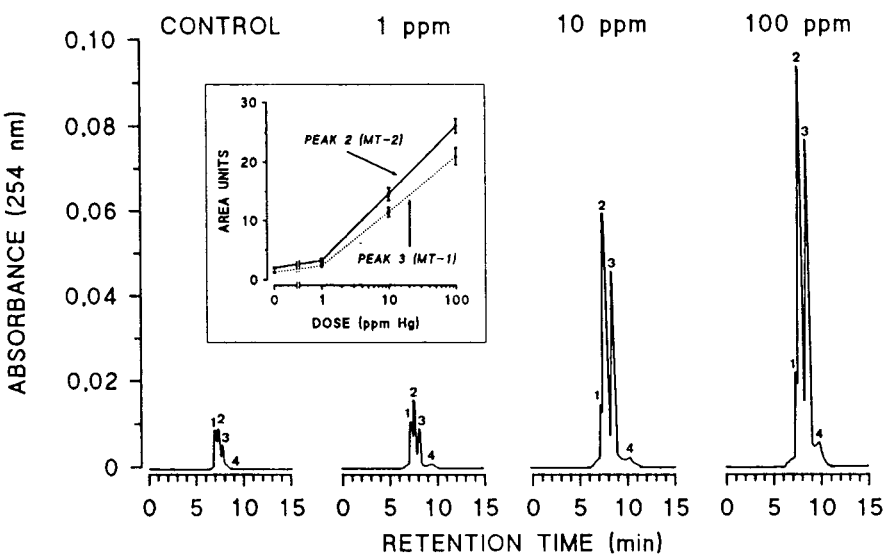

Fig. 7. An aliquot (100 μl) of mercury-exposed renal MT isolated on a Sephadex G-75 column was subjected to HPLC on a Protein-Pack 125 column (300 × 7.8 mm) and eluted with 0.02 *M* ammonium formate buffer solution (pH 7.65) at a flow-rate of 1 ml/min. Insert: Area units of MT-1 and MT-2 plotted against mercury dose.

similar way, since MT-1 and MT-2 increased thirteen- and sixteen-fold, respectively, compared with a control group (insert of Fig. 7).

In summary, rat kidney Hg–thionein yields four peaks on HPSEC and PAGE. Two of these, peaks 2 and 3, correspond to MT-2 and MT-1, respectively; the other two, peaks 1 and 4, correspond to an artifact and oxidized MT molecules, respectively. This corroborates previous evidence that there are only two functional MT isotypes in the rat, the MT-1 and MT-2 proteins [24]. Finally, Hg induces and binds to both isoforms.

REFERENCES

1 J.K. Piotrowski, B. Trojanowska, J.M. Wisniewska-Knypl and W. Bolanowska, *Toxicol. Appl. Pharmacol.*, 27 (1974) 11.
2 M. Jakubowski, J.K. Piotrowski and B. Trojanowska, *Toxicol. Appl. Pharmacol.*, 16 (1970) 743.
3 C.V. Nolan and Z.A. Shaikh, *Biol. Trace Elem. Res.*, 1 (1987) 419.
4 M.A. Morcillo, J. Santamaría, F. Sánchez, B. Ribas and I. Bando, in E. Merian and W. Haerdi (Editors), *Met. Compd. Environ. Life, 4, Sel. Pap. IAEAC Workshop Toxic Met. Compd. 4th 1991*, Science and Technology Letters, Northwood, 1992, p. 373.
5 J.H.R. Kägi and M. Nordberg (Editors), *Metallothionein*, Birkhaüser, Basle, 1979.
6 J.H.R. Kägi and Y. Kojima (Editors), *Metallothionein II*, Birkhaüser, Basle, 1987.
7 K.T. Suzuki, H. Sunaga, Y. Aoki and M. Yamamura, *J. Chromatogr.*, 281 (1983) 159.
8 M.A. Morcillo, J. Santamaría, B. Ribas and I. Bando, *Rev. Esp. Fisiol.*, 47 (1991) 57.
9 C.H.W. Hirs, *J. Biol. Chem.*, 219 (1956) 611.
10 B.J. Davis, *Ann. N.Y. Acad. Sci.*, 121 (1964) 404.
11 M. Vašák, *Methods Enzymol.*, 205 (1991) 41.
12 P.D. Whanger and J.T. Deagen, *Environ. Res.*, 30 (1983) 372.
13 M.P. Richards, *Methods Enzymol.*, 205 (1991) 217.
14 C.C. McCormick and L.Y. Liu, *Methods Enzymol.*, 205 (1991) 71.
15 K.T. Suzuki, T. Motomura, Y. Tsuchiya and M. Yamamura, *Anal. Biochem.*, 107 (1980) 75.
16 M. Webb (Editor), *The Chemistry, Biochemistry and Biology of Cadmium*, Elsevier, Amsterdam, 1979, p. 195.
17 G. Sokolowski, W. Pilz and U. Weser, *FEBS Lett.*, 48 (1974) 222.
18 K.T. Suzuki, H. Sunago, Y. Aoki and M. Yamamura, *J. Chromatogr.*, 281 (1983) 159.
19 A.K.M. Kabzinski and T. Paryjczack, *Chromatographia*, 27 (1989) 247.
20 Y. Koyima and P.E. Hunziker, *Methods Enzymol.*, 205 (1991) 419.
21 D.R. Winge, K.B. Nielson, R.D. Zeikus and W.R. Gray, *J. Biol. Chem.*, 259 (1984) 11419.
22 D.R. Winge, R. Premakumar, R.D. Wiley and K.V. Rajagopalan, *Arch. Biochem. Biophys.*, 170 (1975) 253.
23 H.J. Hartman and U. Weser, *Biochim. Biophys. Acta*, 491 (1977) 211.
24 R.D. Andersen, S.J. Taplitz, B.W. Binen, G. Bristol and H.R. Herschman, in J.H.R. Kägi and Y. Kojima (Editors), *Metallothionein II*, Birkhaüser, Basle, 1987, p. 373.

Journal of Chromatography A, 655 (1993) 85–88
Elsevier Science Publishers B.V., Amsterdam

CHROM. 24 981

Short Communication

Liquid chromatography and radioimmunoassay method for the determination of prostaglandins E_1 and E_2 in rat embryo incubates

G. Hotter, J. Roselló-Catafau*, D. Closa, G. Bioque and E. Gelpí

Molecular Pathology Unit, Centro de Investigación y Desarrollo, CSIC, Jordi Girona 18–26, 08034-Barcelona (Spain)

A. Javerbaum, E. González and M.A.F. Gimeno

CEFYBO-CONICET, Serrano 665, Buenos Aires (Argentina)

ABSTRACT

This paper describes the application of a combined high-performance liquid chromatography and radioimmunological assay method for the measurement of prostaglandins E_1(PGE_1) and E_2(PGE_2). Samples were acidified to pH 3.15, extracted twice with ethyl acetate and further processed through C_{18} solid-phase extraction cartridges. After HPLC purification, PGE_1 and PGE_2 were measured by radioimmunological techniques. The limit of detection for PGE_1 was 3.9 pg/ml and the intra-assay relative standard deviation was 7.8% for $n = 5$. The accuracy of the assay procedure was also verified. The method has been applied to the determination of PGE_1 and PGE_2 in embryo incubates from 10-day pregnant rats.

INTRODUCTION

Prostaglandin E_1(PGE_1) is a physiologically important metabolite of dihomo-γ-linolenic acid whose concentrations in human tissues are approximately one quarter of those of arachidonic acid (AA) [1]. PGE_1 has been virtually ignored in the HPLC–radioimmunoassay (RIA) profiling studies reported to date. The reason for such an omission could be that, in practice, PGE_1 is a minor metabolite compared with other AA cyclooxygenase metabolites such as prostaglandin E_2(PGE_2), although relatively elevated concentrations of up to 16 μg/ml PGE_1 have been determined in human seminal plasma [2–3].

In general, papers dealing with the HPLC separation of PGE_1 from other prostanoids are scarce [4], especially when these HPLC methods have to be combined with RIA. Taking this into account, we have evaluated an HPLC–RIA method for concurrent determination of PGE_1 and PGE_2. This method has been applied to a study of the release of both prostaglandins by 10-day old rat embryos.

EXPERIMENTAL

Rat embryo incubations

Pools of three embryos obtained from rats

* Corresponding author.

0021-9673/93/$06.00

after 10 days of pregnancy plus the covering membranes and free of maternal decidua were incubated in Krebs–Ringer–hydrogencarbonate (KBR) solution containing 11.0 m*M* glucose, in a metabolic shaking bath under an atmosphere of 5% carbon dioxide in 95% oxygen [5]. After 60 min of incubation, the incubating medium was recovered and acidified to pH 3.15 with 1 *M* hydrochloric acid. Finally, the prostaglandins were extracted three times with 2 ml of ethyl acetate and subsequently evaporated to dryness under a helium stream. Samples were stored at −80°C until assay.

Analyses of prostanoids

C_{18} Solid phase extraction. Dried ethyl acetate residues were resuspended in saline and acidified to pH 3.15 with 1 *M* hydrochloric acid. Following this, the samples were processed through C_{18} solid-phase extraction cartridges, as previously described [6]. Briefly, the cartridges were washed with 10 ml of acidified water (pH 3.15) and 20 ml of light petroleum ether. The prostaglandins were finally eluted with 4.5 ml of methyl formate, which was evaporated to dryness. Dried residues were resuspended in a formic acid/0.04 *M* triethylamine buffer–acetonitrile mixture (65:35) at pH 3.15 and 200-μl aliquots of this solution were analysed by HPLC.

High-performance liquid chromatography. Reversed phase-HPLC separation was performed using two Kontron 414 pumps connected to a Rheodyne 7125 injector and an ODS-2 column (300 × 3.9 mm I.D.), which was isocratically eluted with formic acid/0.04 *M* triethylamine–acetonitrile (65:35 at pH 3.15), as previously described [7]. Samples were collected at the retention times previously established for authentic standards of tritiated PGE_1(53.7 Ci/mmol) and PGE_2(184 Ci/mmol) by a Ray Test Ramona (Issomess, Strabenhardt, Germany) radioactivity detector coupled to the HPLC column. Collected eluates were lyophilized and redissolved in 100 m*M* Tris–HCl buffer pH 7.4 for subsequent radioimmunological assay.

Radioimmunological assay. PGE_1 and PGE_2 were measured in duplicate using specific rabbit antisera from the Pasteur Institute (Marnes La Coquete, Paris, France). Cross-reactivities of PGE_1 antiserum with other prostaglandins were as follows: 6-keto-$PGF_{1\alpha}$, 0.010%; thromboxane B_2, 0.010%; PGE_2, 15%; and PGD_2, 0.10%. Immunoassays for PGE_1 were peformed with tritiated PGE_1 as radioligand (24 pg, 40.7 Ci/mmol) and the above-mentioned antiserum at a final dilution of 1:44. A standard curve was prepared with authentic PGE_1 from 1.9 to 500 pg (nine points) diluted in 100 m*M* Tris–HCl buffer pH 7.4. HPLC eluates were taken up in 250 μl of buffer and the assays were carried out with 100-μl aliquots. In all cases, the samples and standards were incubated with a mixture of antisera and known tritiated standard at 4°C for 24 h. After incubation, prostaglandins were adsorbed in dextran-coated charcoal and the tritium remaining in supernatants was counted on an LKB1217 Racbeta (LKB, Turku, Finland). The unknowns were compared with a standard curve in which the logarithm of the concentration was plotted against the logit of B/B_0 values [the proportion of tracer bound (B) expressed as a percentage of tracer in the zero standard (B_0)]. Cross-reactivities of PGE_2 antiserum were 15% for PGE_1 and lesser than 0.01% for TXB_2, 6-keto $PGF_{1\alpha}$ and PGD_2. The radioimmunoassay for PGE_2 was performed as previously described [5,6].

RESULTS AND DISCUSSION

Fig. 1 shows the complete separation of tritiated 6-keto prostaglandin $F_{1\alpha}$, thromboxane B_2, prostaglandin E_2 and prostaglandin E_1 accomplished within 16 min. Under these experimental conditions prostaglandin D_2 practically co-elutes with PGE_1 (data not shown) [8]. The high volatility of the mixture of formic acid/0.04 *M* triethylamine–acetonitrile (65:35 at pH 3.15) facilitates the lyophilization and subsequent radioimmunological assay of both prostaglandins in the same HPLC fraction [8]. This is made possible by the high specificity of the PGE_1 antiserum as its cross-reactivity with PGD_2 is less than 0.10%. This HPLC separation has been routinely employed in our laboratory for simultaneous HPLC–RIA determination of series 2 prostanoids in human urine [9]. The method herein described could also be very useful for the

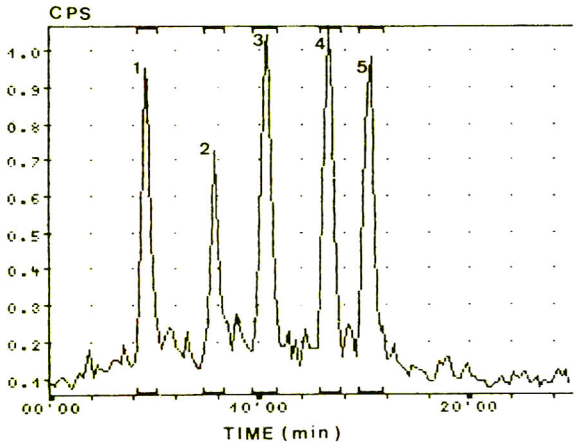

Fig. 1. Typical radiochromatography profile obtained with standards of tritiated 6-keto prostaglandin $F_{1\alpha}$ (1), thromboxane B_2 (2), prostaglandin $F_{2\alpha}$ (3), prostaglandin E_2 (4) and prostaglandin E_1 (5). The HPLC column was an ODS-2, 30 cm × 3.9 mm I.D. column eluted isocratically with formic acid/0.04 *M* triethylamine buffer–acetonitrile (65:35) pH 3.15. Flow-rate was 1 ml/min. Heavy bars in the abcissa define the collection time window set for this study.

concurrent analysis of urinary PGE_1 and PGE_2, especially in biomedical studies in which seminal contamination must be discounted [10]. It is known that PGE_1 and PGE_2 are major components of seminal plasma [11].

Overall recoveries obtained for tritiated PGE_1 and PGE_2 after ethyl acetate, C_{18} solid phase extractions and HPLC purification were higher than 65% for each prostaglandin.

The limit of detection of the assay for PGE_1 was *ca.* 3.9 pg/ml, as determined by the amount of standard displacing 10% of the bound radioactivity and by the mean plus two standard deviations of the ten zero-standards. The intra-assay variation coefficient established for five consecutive measurements was 7.8%. Biological samples in this study were assayed within the same analysis.

To test the accuracy of the procedure, HPLC aliquots of PGE_1 eluates collected from extracted incubates were enriched with known amounts of PGE_1 (3.9–125 pg). As shown in Fig. 2, a close linear correlation was established between the added and measured amounts of PGE_1 ($r = 0.9974$, slope = 0.978). Also, as indicated in Table I, the parallelism test using

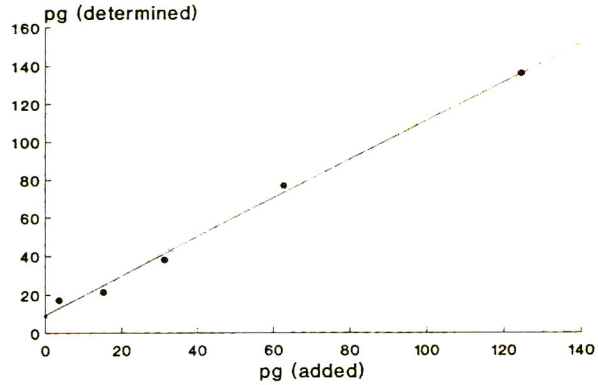

Fig. 2. Correlation plots of RIA PGE_1 values obtained from HPLC aliquots of extracted and supplemented incubate pools.

serially diluted aliquots of biological samples subjected to the whole procedure (liquid–liquid extraction, C_{18} solid-phase extraction, HPLC and RIA) gave good correlations for both series of samples ($r = 0.9953$, slope = 0.973).

The method has been applied to the determination of PGE_2 and PGE_1 levels in rat incubates, as shown in Fig. 3. These data reveal that the PGE_2 production in rat embryos is about four times higher than that of PGE_1, and also confirm the suitability of the assay when both prostaglandins must be measured by liquid chromatography combined with radioimmunoassay.

In conclusion, the HPLC–RIA techniques described herein; provide a specific, sensitive

TABLE I

SERIAL DILUTION OF A POOL OF EMBRYO INCUBATES SUBJECTED TO RIA. RESULTS FOR PGE_1 VALUES EXPRESSED AS pg/ml

Regression line: $n = 5$, $r = 0.9953$, slope = 0.973.

Dilution	Blank incubates	
	Measured	Expected
1:1	291.3	–
1:2	147.1	145.6
1:4	85.9	72.8
1:8	42.4	36.4
1:16	18.8	18.2
1:32	8.6	9.1

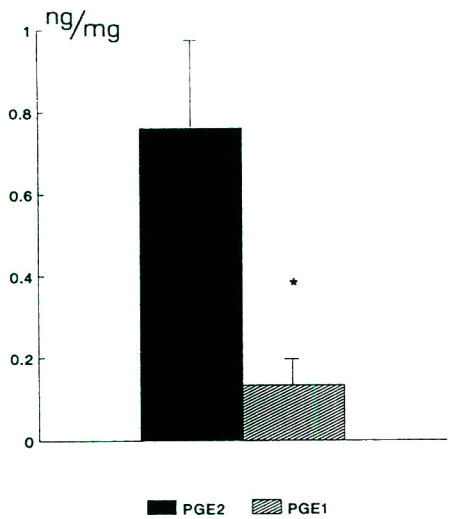

Fig. 3. PGE_1 and PGE_2 levels (ng per mg of protein) in rate embryo incubates ($n = 5$). $^*P < 0.05$ (Student's t-test).

and accurate method for PGE_1 assay in biological samples. The method could be useful for studying the relevance of PGE_2 and PGE_1 in relation to alterations of glucose metabolism in embryo and uterus from diabetic rats.

ACKNOWLEDGEMENTS

This work was supported by the Fondo de Investigaciones Sanitarias through Grant No. 92/281. We are grateful to Mrs. G. Gomez and C. Sarmiento for their technical assistance. (C. Sarmiento is a fellow of CIRIT.)

REFERENCES

1 R.B. Zurier, in B. Samuelsson, P.W. Ramwell, R. Paoletti, G. Folco and E. Granström (Editors), *Advances in Prostaglandin, Thromboxane and Leukotriene Research*, Vol. 21, Raven Press, New York, 1990, pp. 947–953.
2 M. Bygdeman and B. Samuelsson, *Clin. Chim. Acta*, 10 (1964) 566–568.
3 H.T. Jonsson, B.S. Middleditch and D.M. Desiderio, *Science*, 187 (1975) 1093–1095.
4 W.H. Hesse, H. Schweer, W. Seyberth and B.A. Peskar, *J. Chromatogr.*, 533 (1990) 159–165.
5 A.M. Franchi, M. Chaud, E.T. González, M.A.F. Gimeno and A.L. Gimeno, *Prostaglandins*, 38 (1989) 145–154.
6 I. Ramis, J. Serra, J. Roselló, C. Picado, E. Gelpí and A. Agustí-Vidal, *Prost. Leuk. Essent. Fatty Acids*, 34 (1988) 109–112.
7 I. Ramis, J. Roselló-Catafau, G. Gómez, J.M. Zabay, E. Fernández-Cruz and E. Gelpí, *J. Chromatogr.*, 557 (1991) 503–507.
8 E. Gelpí, I. Ramis, G. Hotter, G. Bioque, O. Bulbena and J. Roselló, *J. Chromatogr.*, 492 (1989) 223–250.
9 A. Muti, R. Alinovi, E. Bergamaschi, C. Biagni, S. Cavazzini, I. Franchini, R.R. Lauwerys, A.M. Bernard, H. Roels, E. Gelpí, J. Rosello, I. Ramis, R.G. Price, S.A. Taylor, M. De Broe, G.D. Nuyts, H. Stolte, L.M. Fels and C. Herbort, *Lancet*, 340 (1992) 189–193.
10 A. Ferretti and J.T. Judd, *Prost. Leuk. Essent. Fatty Acids*, 44 (1991) 47–50.
11 M.T. Johnsson, B.S. Middleditch and D.M. Desiderio, *Science*, 187 (1975) 1093–1095.

Journal of Chromatography A, 655 (1993) 89–94
Elsevier Science Publishers B.V., Amsterdam

CHROM. 25 080

High-performance liquid chromatographic determination of plasma triglyceride type composition in a normal population of Barcelona

Relationship with age, sex and other plasma lipid parameters

Matilde Parreño, Ana I. Castellote and Rafael Codony*

Unitat de Nutrició i Bromatologia, Departament de Ciències Fisiològiques Humanes i de la Nutrició, Facultat de Farmacia, Universitat de Barcelona, 08028 Barcelona (Spain)

ABSTRACT

A coupled TLC–HPLC procedure is proposed for the separation and determination of plasma triglycerides. The method was tested by application to plasma samples corresponding to a normal population of Barcelona (Spain). Eighteen different triglyceride types were identified and their relative proportions were established, in order to give a "normal profile" for men and women. Sex-related differences ($p < 0.05$) were only found for dioleostearin and palmitodilinolein + linoleooleopalmitolein (LLP + LOPa). A correlation study showed that palmitodiolein and total cholesterol levels increase with age, whereas LLP–LOPa decreases in men and palmitolinoleoolein + palmitooleopalmitolein in women.

INTRODUCTION

Plasma lipid fractions are currently receiving a great deal of attention owing to their involvement in the development of several atherogenic diseases with a wide incidence. Some of the parameters studied, such as total plasma cholesterol levels and lipoprotein distribution, have been shown to be risk factors for coronary heart disease [1–5]. However, the involvement of plasma triglycerides (TGs) in these diseases seem to be less clear [6–8], although it would be interesting to determine the relationship between total plasma TG levels and other factors. Other studies have attempted to establish a relationship between total plasma TG levels and/or plasma fatty acid composition and some metabolic upsets [9–11] and diet [12–21]. The increasing popularity of the Mediterranean diet, which is associated with lower morbidity and mortality caused by these diseases, has also led to further studies [22–26]. Although there have been numerous studies dealing with the chromatographic (GC and HPLC) separation, identification and determination of triglycerides in food and biological lipids [27–30], hardly any detailed research has been carried out into the proportion of each individual TG type in plasma [31]. For this reason, the purpose of this study was to determine the profile of plasma TG type composition in normal subjects who live in Barcelona and who follow the Mediterranean dietary patterns. We also propose a chromato-

* Corresponding author.

0021-9673/93/$06.00

graphic procedure for the separation and determination of individual plasma TG types suitable for routine analytical application.

EXPERIMENTAL

Samples

The study subjects were 27 adult men and 32 adult women from Barcelona with the following characteristics: (a) aged 18–61 years, mean (±S.D.) age 34 ± 10 years; (b) not overweight, with mean (±S.D.) mass and height 73 ± 5 kg and 175 ± 5 cm in men and 59 ± 8 kg and 162 ± 6 cm in women; (c) no subject was taking known medication (such as diuretics for hypertension, drug treatment for hyperlipaemia or insulin); (d) total plasma TG levels ranged from 40 to 170 mg/dl and cholesterol levels from 150 to 258 mg/dl; total plasma TGs and cholesterol were determined with an AutoAnalyzer (Technicon, Tarrytown, NY, USA); (e) other biochemical measurements (such as GOT, GPT and uric acid) were also normal.

Blood samples were obtained in 0.1 ml of EDTA (15%) from subjects in a fasting state (12 h overnight fast) by clean venipuncture, and plasma was separated at 4°C by centrifugation. The plasma was stored at −20°C until analysis.

Lipid extraction

A 1-ml volume of plasma was added to 9.5 ml of chloroform–methanol (2:1, v/v) following a modification of the method of Folch *et al.* [32]. The mixture was shaken for 30 min and centrifuged at 2000 *g* for 5 min. The organic phase was washed with 5 ml of distilled water and separated by centrifugation under the same conditions. It was then washed with 8 ml of saturated NaCl solution and centrifuged again. After filtration through anhydrous sodium sulphate, the lipid extract (clean chloroform fraction) was evaporated to dryness under nitrogen and the residue was dissolved in 100 μl of chloroform.

TLC isolation of triglyceride fraction

TGs were separated from other lipids by TLC on silica gel G60 (Merck, Darmstadt, Germany) with a hexane–diethyl ether–acetic acid (85:15:1, v/v/v) as solvent [33] and detected by spraying the plate with 2,7-dichlorofluorescein (0.2% solution in ethanol). The band corresponding to TGs was scraped from the plate, eluted with 10 ml of chloroform and stored at −20°C (in a conical tube) after drying under nitrogen. All chemicals used for sample preparation were of analytical-reagent grade (Merck).

HPLC determination of TG types

The TG analysis was performed on a Perkin-Elmer Series-10 high-performance liquid chromatograph coupled to a Perkin-Elmer (Norwalk, CT, USA) Model LC 25 refractive index (RI) detector and a Hewlett-Packard (Avondale, PA, USA) Model 3390A integrator. The HPLC column was 5-μm Spherisob ODS-2 (250 × 4 mm I.D.) (Tracer, Barcelona, Spain). The analysis was carried out at room temperature, using acetone–acetonitrile (64:36, v/v) as the mobile phase at a flow-rate of 1 ml/min [34]. Prior to analysis, the samples were dissolved in 50 μl of acetone and 10 μl of this solution were injected into the HPLC system. Acetone and acetonitrile were of HPLC grade (SDS, Peypin, France).

RESULTS AND DISCUSSION

Characteristics of the method

For identification of TG peaks we used a standard mixture of simple saturated TGs and vegetable oils whose TGs were well known, according to Goiffon and co-workers [35,36].

The fatty acid composition was determined in a pooled plasma in order to evaluate the average composition of plasma lipids from the subjects studied.

Quantification was carried out by normalization assuming that the detector response for all TG types was the same [37–39]. TGs were further quantified by grouping them by their equivalent carbon number (ECN).

A TG type is defined as a TG in which the three fatty acids are known, but not their position. The following code is used for fatty acids: L = linoleic (18:2), Ln = linolenic (18:3), O = oleic (18:1), P = palmitic (16:0), Pa = palmitoleic (16:1), M = myristic (14:0), S = stearic (18:0), La = lauric (12:0), where the number before the

colon indicates the acyl carbon number and that after the colon the number of double bonds.

The identification of the plasma TG types is shown in Table I, together with their respective experimental log α values. Some peaks could not be identified (NI), although they may correspond to one of the following groups of triglycerides: peak NI + NI with log $\alpha = -0.273 \pm 0.007$ might be MPaL–LaOL (48:3), MLM–LaPL (46:2), MOLa (44:1), MMM–LaMP (42:0); all included in the ECN-42. Other unidentified peaks in ECN-44 were log $\alpha = -0.173 \pm 0.002$, -0.156 ± 0.002 and -0.143 ± 0.002, which might be MOL–PLPa (50:2), MPL–MPaO–LaOO (48:2), MMO–LaPO (46:1) and MMP–LaPM (44:0) respectively.

TABLE I

IDENTIFICATION OF PLASMA TG TYPES IN THE SUBJECTS ANALYSED

Equivalent carbon number (ECN)	CN:n[a]	TG type	Log α[b]
42	54:6	LLL	−0.360 ± 0.004
42	54:6	LnLO	−0.337 ± 0.008
42	52:5	LnLP	−0.320 ± 0.015
42	–	NI + NI[c]	−0.273 ± 0.007
44	54:5	LLO	−0.241 ± 0.003
44	52:4	LLP	−0.208 ± 0.002
44	52:4	LOPa	−0.195 ± 0.002
44	–	NI[c]	−0.173 ± 0.002
44	–	NI[c]	−0.159 ± 0.002
44	–	NI[c]	−0.143 ± 0.002
46	54:4	LOO	−0.121 ± 0.002
46	54:3/50:2	PLO + POPa	−0.089 ± 0.002
46	50:2	PLP	−0.049 ± 0.002
46	50:2	MOO	−0.038 ± 0.002
46	–	NI[c]	−0.019 ± 0.002
48	54:3	OOO	0.000
48	52:2	POO	0.032 ± 0.002
48	50:1	POP	0.075 ± 0.003
48	48:0	PPP	0.121 ± 0.003
50	–	NI[c]	0.136 ± 0.003
50	54:2	SOO	0.146 ± 0.003
50	52:1	SOP	0.186 ± 0.004

[a] CN:n = Acyl carbon number : double bond number.
[b] α = Reduced retention time of triglycerides relatives to triolein. Values of log α are means ±S.D. ($n = 59$).
[c] NI = not identified.

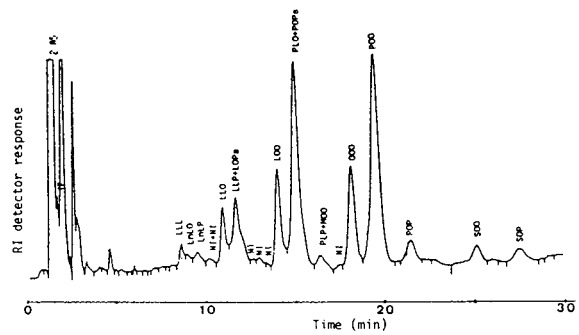

Fig. 1. HPLC of plasma triglycerides in a normal man.

Finally, the chromatographic peak with log $\alpha = -0.019$ may be assigned to MOS (50:1), MOP–PPPa (48:1) or MPP (46:0). Fig. 1 shows an HPLC profile of plasma triglycerides in a normal man.

In order to establish the sensitivity of the method, the detection limits were calculated by using a signal-to-noise ratio of 3:1 for the detection limit (DL) and of 10:1 for the quantification limit (QL). Results for triolein were DL = 0.82 μg and QL = 1.31 μg.

TG type composition of plasma

Details analysis of the TG type composition of plasma corresponding to this normolipaemic population is given in Fig. 2. Among the eighteen TG types identified, POO shows the highest proportion (26.5%). Other relevant groups were PLO + POPa with 24%, OOO with 11% and LLP + LOPa with 9.5%. This composition reveals a clear influence of the diet followed by the

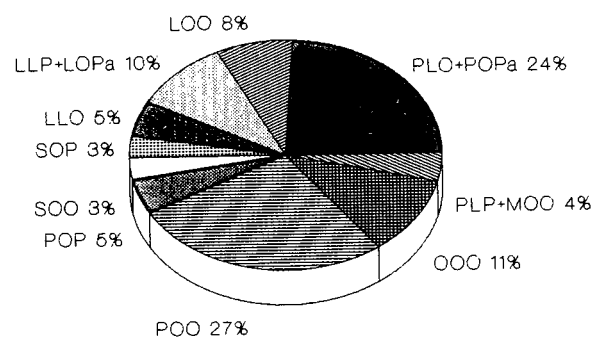

Fig. 2. Plasma TG type composition in the studied population ($n = 59$). Data given as relative percentage (mean ±S.D.).

population studied, which is characterized by high monounsaturated fatty acid levels (olive oil) and a lower intake of animal fats.

Influence of sex in plasma TG types, total TGs and cholesterol levels

The differences in the TG type proportions, ECN proportions and total triglyceride and cholesterol levels between men and women are shown in Table II. Applying Student's *t*-test we found statistically significant differences for ECN-50 ($p < 0.05$) and SOO ($p < 0.05$), which is included in this ECN. Moreover, the differences between men and women were statistically significant for the critical pair LLP + LOPa ($p < 0.05$). In both instances the values are higher for men. However, despite the tendency for OOO and PLO + POPa to show differences between men and women, these were not statistically significant ($p = 0.050$ and 0.057, respectively). It should be noted that the women had a significantly lower mean total TG level than the men ($p < 0.001$), which agrees with data reported by others [9].

We also studied the correlations between the different TG types in each sex group (Tables III and IV). In these instances, we only consider correlations for which $p < 0.001$.

Correlations with age and total cholesterol

We also studied correlations between total cholesterol, total TGs, TG types and ECN

TABLE II

COMPARATIVE STUDY OF THE TG TYPE PROPORTIONS, ECN PROPORTIONS AND TOTAL TGs AND CHOLESTEROL LEVELS BETWEEN MEN AND WOMEN

Data given as a percentage of total TG types. Values are means ±S.D.

Variable	Men ($n = 27$)	Women ($n = 32$)
ECN-42	5.74 ± 2.13	5.12 ± 1.81
ECN-44	15.69 ± 4.58	14.64 ± 4.07
ECN-46	33.95 ± 3.45	33.15 ± 4.02
ECN-48	38.91 ± 7.39	40.42 ± 6.22
ECN-50	5.65 ± 1.78	6.64 ± 2.43[a]
LLO	4.53 ± 1.87	4.70 ± 1.85
LLP + LOPa	10.32 ± 3.11	8.95 ± 2.63[a]
LOO	8.16 ± 2.30	8.63 ± 2.11
PLO + POPa	24.72 ± 3.01	23.34 ± 3.47
PLP + MOO	4.07 ± 2.00	4.15 ± 1.86
OOO	10.00 ± 3.86	11.74 ± 4.09
POO	27.04 ± 5.19	26.15 ± 4.25
POP	5.14 ± 2.14	5.32 ± 1.91
SOO	3.13 ± 1.06	3.78 ± 1.19[a]
SOP	2.84 ± 1.19	3.16 ± 2.05
Total TGs (mg/dl)	95.22 ± 33.62	65.87 ± 21.02[b]
Total cholesterol (mg/dl)	199.29 ± 26.01	190.06 ± 29.54

[a] Significantly different between men and women, $p < 0.05$ by Student's *t*-test.
[b] Significantly different between men and women, $p < 0.001$ by Student's *t*-test.

TABLE III

CORRELATIONS BETWEEN TG TYPES IN MEN ($n = 27$)

Variable	r^a, $p < 0.001$ (d.f. = 25 $r_t = 0.5974$)[b]
LLO/LLP + LOPa	0.62121
LLO/POO	−0.63628
LLP + LOPa/PLO + POPa	0.62286
LLP + LOPa/POO	−0.88157
LLP + LOPa/SOO	−0.71763
PLO + POPa/OOO	−0.80107
PLP + MOO/OOO	−0.69767
PLP + MOO/POP	0.63858
POO/SOO	0.63292

[a] r = Experimental correlation coefficient.
[b] d.f. = Degrees of freedom, r_t = theoretical correlation coefficient.

TABLE IV

CORRELATIONS BETWEEN TG TYPES IN WOMEN ($n = 32$)

Variable	r^a, $p < 0.001$ (d.f. = 30 $r_t = 0.5541$)[b]
LLO/LLP + LOPa	0.68683
LLO/POO	−0.56684
LLP + LOPa/POO	−0.58328
LOO/POP	−0.55438
PLO + POPa/OOO	−0.79697
PLP + MOO/POP	0.68875

[a,b] See Table III.

TABLE V

CORRELATIONS WITH AGE IN MEN

Variable	r (d.f. = 25)[a]
ECN-44	−0.52508[b]
LLP + LOPa	−0.58892[b]
ECN-48	0.59268[b]
POO	0.6022[c]
Total cholesterol	0.40479[d]

[a] See Table III.
[b] Statistical significance: $p < 0.01$, theoretical correlation coefficient $r_t = 0.4868$.
[c] Statistical significance: $p < 0.001$, $r_t = 0.5974$.
[d] Statistical significance: $p < 0.05$, $r_t = 0.3809$.

fractions with age for men and women separately, for those that showed statistical significance.

In men (Table V), there is a increase in POO percentage with age ($p < 0.001$), and also ECN-48 ($p < 0.01$), which includes POO, and a decrease in LLP + LOPa ($p < 0.01$) and ECN-44 ($p < 0.01$), which includes LLP + LOPa. The results also show an increase in total plasma cholesterol level with age ($p < 0.05$).

In women (Table VI) there is an increase in POO and ECN-48 with age ($p < 0.05$), which is less significant than in men. A decrease is also observed in PLO + POPa ($p < 0.05$), which is not observed in men. The total cholesterol level also increases with age ($p < 0.05$) in women. It seems that levels of more unsaturated TG types fall slightly with age, while the total plasma cholesterol increases.

TABLE VI

CORRELATIONS WITH AGE IN WOMEN

Variable	r (d.f. = 30)[a]
PLO + POPa	−0.37083[b]
ECN-48	0.35058[b]
POO	0.43363[b]
Total cholesterol	0.48288[c]

[a] See Table III.
[b] Statistical significance: $p < 0.05$, theoretical correlation coefficient $r_t = 0.3493$.
[c] Statistical significance: $p < 0.01$, $r_t = 0.4487$.

TABLE VII

CORRELATIONS OF TG TYPES AND TOTAL TGs WITH TOTAL CHOLESTEROL IN PLASMA

Variable	r[a]
Men (d.f. = 25)[a]	
ECN-44	−0.43879[b]
LLO	0.46311[b]
LLP + LOPa	0.42124[b]
Total TGs	0.40350[b]
Women (d.f. = 30)[a]	
POO	0.37719[c]
Total TGs	0.49610[d]

[a] See Table III.
[b] Statistical significance for men: $p < 0.05$, theoretical correlation coefficient $r_t = 0.3809$.
[c] Statistical significance for women: $p < 0.05$, $r_t = 0.3493$.
[d] Statistical significance for women: $p < 0.01$, $r_t = 0.4487$.

Table VII shows the correlations found for ECN fractions, TG types and total TGs with cholesterol levels for both sexes. This shows that the percentage of POO increases in women, as does total plasma TG in both men and women, and LLO and LLP + LOPa decrease in men with increase in the total cholesterol level. All this suggests that in plasma there is a replacement of unsaturated TGs by more saturated TGs with increase in cholesterol.

REFERENCES

1 Report of Inter-Society Commission for Heart Disease Resources, *Circulation*, 70 (1984) 155A.
2 Report of Nutrition Committee, *Circulation*, 65 (1982) 839A.
3 A. Keys, C. Aravanis, H. Blackburn, R. Buzina, B.S. Djordjevic, A.S. Dontas, F. Fidanza, M.J. Karvonen, N. Kimura, A. Menotti, I. Mohacek, S. Nedeljkovic, V. Puddu, S. Punsar, M.L. Taylor and F.S. Van Bunchen, *Seven Countries, A Multivariate Analysis of Death and Coronary Heart Disease*, Harvard University Press, Cambridge, MA, 1980.
4 A. Keys, C. Aravanis, F.S.P. Van Buchen, H. Blackburn, R. Buzina, B.S. Djordjevic, F. Fidanza, M.J. Karvonen, N. Kimura, A. Menotti, S. Nedeljkovic, V. Puddu and M.L. Taylor, *Lancet*, ii (1981) 58.
5 Pooling Project Research Group, *J. Chron. Dis.*, 31 (1978) 201.
6 L.A. Carlson, L.E. Böttiger and P.E. Ahfeldt, *Acta Med. Scand.*, 206 (1979) 351.

7 L.A. Carlson and L.E. Böttinger, *Lancet*, i (1972) 865.
8 D.F. Brown, *Am. J. Med.*, 46 (1969) 691.
9 W.B. Kannel, *Am Heart J.*, 114 (1987) 413.
10 W.S. Harris, W.E. Connor, S.B. Inkeles and D.R. Illingworth, *Metabolism*, 33 (1984) 1016.
11 J.D. Brunzell and E.L. Bierman, *Med. Clin. North Am.*, 66 (1982) 455.
12 D. Kromhout, E.B. Bosschieter and C. de Lezenne Coulander, *N. Engl. J. Med.*, 312 (1985) 1205.
13 F.M. Mattson and S.M. Grundy, *J. Lipid Res.*, 26 (1985) 194.
14 B.E. Phillipson, D.W. Rothrock, W.E. Connor, W.S. Harris and D.R. Illingworth, *N. Engl. J. Med.*, 312 (1985) 1210.
15 T.A. Sanders, D.R. Sullivan, J. Reeve and G.R. Thompson, *Arteriosclerosis*, 5 (1985) 459.
16 P.J. Nestel, S. Connor, S. Wong and R. Boston, *J. Clin. Invest.*, 74 (1984) 82.
17 W.S. Harris, W.E. Connor and M.P. McMurry, *Metabolism*, 32 (1983) 179.
18 W.E. Connor and S.L. Connor, *Med. Clin. North Am.*, 66 (1982) 485.
19 S.H.jr. Goodnight, W.S. Harris, W.E. Connor and D.R. Illingworth, *Arteriosclerosis*, 2 (1982) 87.
20 A. Kuksis, J.J. Myher, K. Geher, G.J.L. Jones, C.J. Packard, J.D. Morrisett, O.D. Tauton and A.M. Gotto, *Atherosclerosis*, 41 (1982) 221.
21 E.J. Schaefer, R.I. Levy, N.D. Ernst, F. Van Sant and H.B. Brewer, *Am. J. Clin. Nutr.*, 34 (1981) 1758.
22 C.R. Sirtori, E. Tremoli, E. Gatti, G. Montanari, M. Sirtori, S. Colli, G. Gianfranceschi, P. Maderna, C.Z. Dentone and G. Testolin, *Am. J. Clin. Nutr.*, 44 (1986) 635.
23 A. Ferro-Luzzi, P. Strazzullo, C. Scaccini, A. Siani, S. Sette, M.A. Mariani, P. Mastranzo, R.M. Dougherty, J.M. Iacono and M. Mancini, *Am. J. Clin. Nutr.*, 40 (1984) 1927.
24 W.B. Kannel, J.T. Doyle, A.M. Ostfeld, C.D. Jenkins, L. Kuller, R.D. Podell and J. Stamler, *Circulation*, 70 (1984) 157A.
25 R. Salvadori, *La Dieta Mediterranea*, Idee Libro, Rome, 1984.
26 V.K. Ovacov and V.A. Bystrova, *World Health Stat. Q.*, 31 (1978) 208.
27 J. Skorepa, V. Kahudová, E. Kotrlíková, P. Mares and H. Todorovicová, *J. Chromatogr.*, 273 (1983) 180.
28 P. Mares, J. Skorepa, E. Sindelková and E. Tvrzická, *J. Chromatogr.*, 273 (1983) 179.
29 J.V. Hinshaw, Jr. and W. Seferovic, *J. High Resolut. Chromatogr. Chromatogr. Commun.*, 9 (1986) 731.
30 J.D. Baty and N.W. Rawle, *J. Chromatogr.*, 395 (1987) 395.
31 E.G. Perkins, D.J. Hendren, N. Pelick and J.E. Bauer, *Lipids*, 17 (1982) 460.
32 J. Folch, M. Lees and G.H.S. Stanley, *J. Biol. Chem.*, 226 (1957) 497.
33 B. Kolarova, G. Dimitrov and M. Bojadzieva, *Grasas Aceites (Seville)*, 29 (1978) 329.
34 A.I. Castellote, *PhD Thesis*, Universidad de Barcelona, Barcelona, 1987, p. 95.
35 J.P. Goiffon, C. Reminiac and M. Olle, *Rev. Fr. Corps Gras*, 28 (1981) 167.
36 J.P. Goiffon, C. Reminiac and D. Furon, *Rev. Fr. Corps Gras*, 28 (1981) 199.
37 Y. Lozano, *Rev. Fr. Corps Gras*, 9 (1983) 333.
38 J.L. Perrin and M. Naudet, *Rev. Fr. Corps Gras*, 7 (1983) 279.
39 G. Sempore and J. Bezard, *J. Chromatogr.*, 366 (1986) 261.

Journal of Chromatography A, 655 (1993) 95–99
Elsevier Science Publishers B.V., Amsterdam

CHROM. 25 056

Supercritical fluid extraction of fluvalinate residues in honey. Determination by high-performance liquid chromatography

J. Atienza* and J.J. Jiménez

S.I.A. Laboratory, P.O. 172, 47080-Valladolid (Spain)

J.L. Bernal and M.T. Martín

Department of Analytical Chemistry, Faculty of Sciences, Valladolid (Spain)

ABSTRACT

A method for the analysis of fluvalinate residues in honey from beehives treated with this product to prevent varroatosis is described. The method involves supercritical fluid extraction with carbon dioxide and further analysis by high-performance liquid chromatography on a C_{18} reversed-phase column, acetonitrile–water (80:20) as mobile phase and detection at 254 nm. This method is simpler than the one in which extraction with organic solvents, thin-layer chromatography and gas chromatography is used.

INTRODUCTION

Varroatosis is an external form of parasitosis caused by the mite *Varroa jacobsoni* which affects bees at all stages of development. It is regarded as a severe disease since it results in massive losses in bee colonies that in turn results in occasional dramatic economic losses. Most chemical treatments used against this parasitic mite include bromopropilate, coumaphos, amitraz, chlordimeform or fluvalinate —the last being the most widely employed for the purpose because of its high effectiveness [1].

Spanish law sets no maximum allowable limit for fluvalinate concentration in honey. However, the law does specify maximum permitted concentrations for other products, such as corn forage (3 mg/kg), citric and stone fruits (1 mg/kg), tomato and pepper (0.5 mg/kg), corn grains (0.10 mg/kg) and cotton seed (0.05 mg/kg), as well as a generic concentration of 0.01 mg/kg for all other vegetable products.

The determination of fluvalinate in honey is usually performed by using methods that involve prior extraction of the compound with acetonitrile–hexane or benzene–isopropanol mixtures and subsequent cleaning by means of a Florisil or octadecylsilane column or, alternatively, isolation by thin-layer chromatography. The final extract obtained is typically analysed by gas chromatography with an electron-capture or nitrogen–phosphorus detector [2–10]. The use of gas chromatography poses the problem that fluvalinate decomposes readily by heating, so it has been quantified by applying GC–MS to its degradation products [11]. The degradation resulting from the thermal lability of the analyte can be overcome by using high-performance liquid chromatography (usually with UV detection), although the sensitivity achieved by HPLC

* Corresponding author.

0021-9673/93/$06.00

is somewhat lower than that provided by GC [3,12].

Supercritical fluids, particularly carbon dioxide, which is highly efficient for extractions from complex matrices [13–15], are gaining increasing popularity as replacements for standard solvent extraction techniques.

In this work we present the results of a comparison of the standard extraction–TLC–GC procedure and a supercritical fluid extraction (SFE)–HPLC–UV method developed in our laboratory. The applicability of the newly developed procedure for the analysis of honey from beehives treated with fluvalinate is also presented.

EXPERIMENTAL

Reagents

The following organic solvents, which were of residue analysis grade and supplied by Scharlau (Barcelona, Spain), were used: methanol, ethanol, isopropanol, chloroform, dioxane, toluene, carbon tetrachloride, benzene, acetone and dichloromethane.

HPLC-grade acetonitrile purchased from Panreac (Barcelona, Spain) was also used.

Ultrapure water obtained from a Milli-Q plus apparatus (Millipore, Milford, MA, USA) was employed throughout.

Fluvalinate, coumaphos, chlordimeform, amitraz and bromopropilate certified purity pesticide standards were purchased from Chemservice (West Chester, PA, USA).

Finally, C-60 grade carbon dioxide (purity = 99.9999%) was provided by Carburos Metálicos (Madrid, Spain).

Gas chromatographic system

The gas–liquid chromatographic set-up used consisted of a Hewlett-Packard (HP) 5890 chromatograph (Avondale, PA, USA) equipped with an HP 7673A sample autoinjector, an electron-capture and a nitrogen–phosphorus detector using argon–methane and helium, respectively, as auxiliary gas, and a 30 m × 0.25 mm × 0.25 μm DB5 capillary column from J&W Scientific (Folsom, CA, USA) employing helium at a flow-rate of 0.6 ml/min as carrier gas. The assembly was controlled by an HP 3396A integrator. The temperatures of the injection port and detector were 200 and 300°C, respectively, and the temperature programme used was as follows: initial temperature, 125°C for 5 min; temperature gradient, 2.5°C/min; final temperature, 270°C for 15 min. An injected volume of 5 μl was employed throughout.

HPLC system

The HPLC system used was composed of a ConstaMetric 4100 pump fitted with four eluent ways, an AutoMetric 4100 autosampler, a SpectroMonitor 3200 UV–visible detector and a membrane degasser, all of which were supplied by LDC Analytical (Riviera Beach, FL, USA). Data were obtained and processed by means of a computerized system developed in our laboratory that controlled the entire set-up. The operating conditions employed were as follows: 15 cm × 4.6 mm Novapak C_{18} chromatographic column from Waters–Millipore (Milford MA, USA); mobile phase, acetonitrile–water (80:20) containing 14 ml/l 0.01 *M* HAcO; flow-rate, 1.5 ml/min; injected volume, 20 μl; wavelength, 254 nm.

Extraction with organic solvents–TLC

Fluvalinate was extracted from a honey sample of 150 g that was treated with four 75-ml portions of benzene–isopropanol (7:3, v/v). Each mixture was stirred mechanically for 20 min. The extracts were joined and evaporated to dryness under a nitrogen atmosphere at 35°C. The residue obtained was dissolved in 0.5 ml of methanol.

The extract was cleaned by two-dimensional thin-layer chromatography using glass plates covered with a 0.5-mm layer of Kiesegel 60 (Merck, Darmstadt, Germany), onto which 200 μl of the extract in methanol were placed. The plates were developed with chloroform–ethanol (1:1 v/v) in one direction and with toluene–carbon tetrachloride (4:1, v/v) in the other. Once the plates were dried, the fluvalinate spot (detected by a 254-nm UV lamp) was scraped and brought into contact with 1 ml of methanol for 24 h in order to ensure complete dissolution. Then, the solution was filtered through PTFE

with 0.5 μm pore size (MFS, Dublin, CA, USA). The processed sample was ready for the determination of fluvalinate.

Extraction with supercritical carbon dioxide

The extraction was carried out with a Hewlett-Packard 7680A supercritical fluid extractor using CO_2 as extractant under the following optimal working conditions: fluid density, 0.45 g/ml; working pressure, 138 bar; extraction chamber temperature, 70°C; flow-rate, 0.8 ml/min; dynamic extraction time, 20 min; analyte collection over a trap packed with stainless-steel balls at a nozzle temperature of 75°C with 1 ml of methanol.

Before the extraction step the sample needs a pretreatment: 20 g of honey were mixed with an amount of water equivalent to about 20% of the resulting mixture. Then, cellulose powder (Aldrich, Steinheim, Germany) was added in a proportion equivalent to 10% of the original honey sample. The mixture was homogenized by stirring and the preparation was frozen at −40°C and lyophilized in Telstar equipment (Barcelona, Spain). A fraction of 2 g of lyophilizate was treated with 25 μl of benzene–isopropanol (7:3, v/v) as organic modifier for CO_2, thereby being made ready for extraction.

RESULTS AND DISCUSSION

Stability of fluvalinate

In order to check the stability of the analyte, several solutions taken from an available formulation, Mavrick (Sandoz, Basle, Switzerland), were prepared. After filtration, they were analysed by HPLC at different times after preparation.

As can be seen in Fig. 1, metabolite peaks started to appear soon after the elution began. Such peaks were virtually the only ones observed in chromatograms run after 12 days.

Consequently, taking into account the phytosanitary procedure used to apply fluvalinate and the acidity and diastatic activity of honey, the analyte will hardly be encountered as such in this natural product.

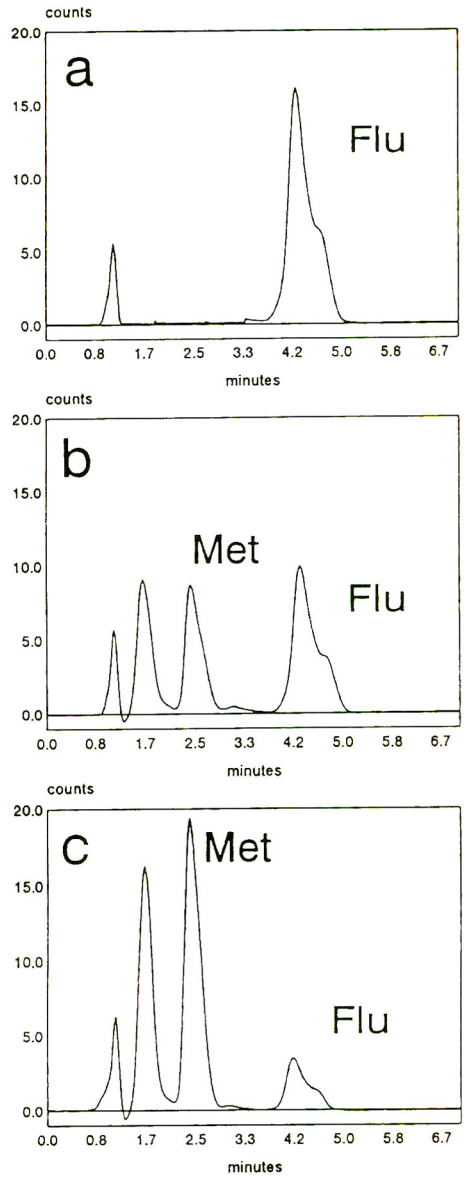

Fig. 1. Chromatograms obtained by HPLC–UV of a commercial preparation of fluvalinate (Mavrick) in methanol. The fluvalinate concentration in 10 mg/l. (a) One day after preparation. (b) Six days after preparation. (c) Ten days after preparation. Flu = Fluvalinate; Met = evaluated metabolite.

On the other hand, the chromatograms of fluvalinate samples attained by the use of GC show a greater number of compounds of decomposition than the HPLC ones.

Thin-layer chromatographic clean-up

The optimal operational conditions for the application of this procedure were established by assaying several kinds of plates: aluminium covered with alumina or cellulose and glass covered with cellulose or silica gel. The last one was finally chosen. Even more important was the choice of the eluent used to isolate fluvalinate from other acaricides, such as bromopropilate, amitraz, coumaphos, chlordimeform, etc., potentially present in honey. For this purpose we assayed methanol, acetonitrile, toluene, dichloromethane, benzene, isopropanol, dioxane, acetone, ethanol and chloroform, which were used on plates onto which 9 μg of standard in methanol had been previously placed.

Pure non-polar eluents failed to elute any of the products. On the other hand, polar eluents elute fluvalinate, bromopropilate and coumaphos in the front, whereas eluents of intermediate polarity (benzene, dichloromethane) resulted in an intermediate situation.

Based on the results provided by the pure eluents and the polarity of the compounds involved, a test set with binary mixtures of the solvents was carried out. None of the mixtures in question allowed complete separation by one-dimensional TLC. On the basis of the partial separations achieved, the use of the two-dimensional procedure was chosen, which allowed fluvalinate to be isolated from the other acaricides and chromatographic interferents present in honey (Fig. 2).

Extraction with supercritical CO_2

Table I lists the results obtained in the extraction of fluvalalinate from fortified honeys using the SFE–HPLC method. The recovery was less than the fortification level. Recovery from honey samples fortified at 0.5 mg/kg was 94% and at 10 mg/kg 53%; relative standard deviation was about 1.4–3.0%.

Table II shows the recoveries of fluvalinate obtained after the organic solvent extraction–TLC–GC procedure was applied to fortified honeys. The recovery was 88% at a fortification level of 0.5 mg/kg and 49% at 10 mg/kg, with relative standard deviations of 2.8 and 6.1%, respectively.

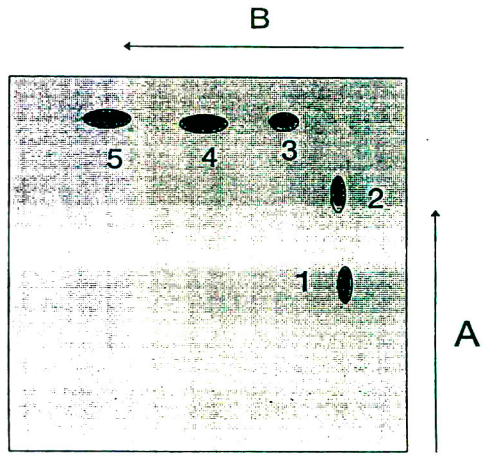

Fig. 2. Chromatogram obtained by two-dimensional thin-layer chromatography by the use of the elect eluents. 1 = Amitraz; 2 = chlordimeform; 3 = coumaphos; 4 = bromopropilate; 5 = fluvalinate. (A) First eluent, chloroform–ethanol (1:1). (B) Second eluent, toluene–carbon tetrachloride (4:1).

TABLE I

RECOVERIES (%) AND STANDARD DEVIATIONS (σ_{n-1}) OF FLUVALINATE OBTAINED AFTER SFE–HPLC OF FORTIFIED HONEYS ($n = 5$)

Fortified amount (mg/kg)	SFE–HPLC	
	Recovery (%)	σ_{n-1}
10	53	1.6
5	80	1.6
1	84	1.5
0.5	94	1.3

TABLE II

RECOVERIES (%) AND STANDARD DEVIATIONS (σ_{n-1}) OF FLUVALINATE OBTAINED AFTER STANDARD SOLVENT EXTRACTION–TLC–GC OF FORTIFIED HONEYS ($n = 5$)

Fortified amount (mg/kg)	TLC–GC	
	Recovery (%)	σ_{n-1}
10	49	3.0
5	71	2.7
1	77	2.5
0.5	88	2.5

The linear range for fluvalinate response of the HPLC–UV system was 0.1–5 mg/l. The detection limit of fluvalinate, calculated from successive dilutions of a standard, was about 0.06 mg/l. So, the detection limit for SFE–HPLC analytical procedure was 0.02 mg fluvalinate per kg of honey.

Application of the SFE–HPLC procedure

The analysis of sixteen honey samples collected from beehives in the provinces of Zamora, Valladolid and Salamanca, all of them treated with fluvalinate in different doses, and six commercial available honey samples shows that fluvalinate was not present in amounts above the detection limit, according to the high degradation observed on standard solutions.

On chromatograms of honey extract the metabolite peak labelled "Met" in Fig. 1 was detected. The amount of fluvalinate in honeys was determined on the assumption that the metabolite concentration is related to the initial certified fluvalinate concentration by using temporally degraded fluvalinate certified standards.

On the above basis, fluvalinate occurs in all honeys except two commercial samples. The fluvalinate concentration range was 0.029–0.750 mg/kg in beehive honeys and 0.055–0.215 mg/kg in commercial honeys.

CONCLUSIONS

SFE of fluvalinate residues from a complex polar matrix such as honey is better than extraction with organic solvents and avoids the need for a clean-up step. On the other hand, the HPLC technique gives simpler chromatograms than GC.

Two-dimensional TLC can be used for clean-up purposes as part of the standard extraction method since it allows the prior isolation of other acaricides that may accompany fluvalinate in the sample.

Fluvalinate as phytosanitary product has only been detected in properly preserved laboratory fortified honey samples. It has never been detected in beehive honey owing to its rapid degradation, which results in several chromatographic peaks that can be ascribed to some of its natural metabolites.

REFERENCES

1 M.C. Rodríguez, M. Hidalgo, A. Telleza and F. Capón, *Contamimantes en Alimentos y Toxicología*, 4 (1989) 23.
2 W.L. Fitch, C.C. Helisten, I.M. Visser and W.W. Miller, *Analytical Methods for Pesticides and Plant Growth Regulators*, XIII (1984) 79.
3 P.G. Baker and P. Bottomley, *Analyst*, 107 (1982) 206.
4 C. Avila, L. Ruiz and V. Balaguer, *Vida Apícola*, 44 (1990) 14.
5 R. Borneck and B. Merle, *Revue Française d'Apiculture*, 485 (1989) 228.
6 O. Stricker, K. Gierschmer and G. Vorwohl, *Dtsch. Lebensm. Rundsch.*, 85 (1989) 72.
7 R. Khazanchi and S.K. Handa, *J. Assoc. Off. Anal. Chem.*, 72 (1989) 512.
8 M.J. Sancho, S. Muniategui, J. F. Huidobro and J. Simal, *Rev. Agroquim. Tecnol. Aliment.*, 31 (1991) 417.
9 G.B. Quistad and L.E. Staiger, *J. Agric. Food Chem.*, 32 (1984) 1134.
10 J. Permayer, N. Gabalda and J.M. Grases, presented at the *10th International Symposium on Capillary Chromatography, Riva del Garda, May 1989.*
11 W.L. Fitch, A.C. Sjolander and W.W. Miller, *J. Agric. Food Chem.*, 36 (1988) 764.
12 M. Haovar, L. de Cormis and J. Rey. *Agronomie*, 2 (1990) 133.
13 D.J. Miller, D.E. Nivens and D. White, *Anal. Chem.*, 64 (1992) 405.
14 M.L. Hopper and J.W. King, *J. Assoc. Off Anal. Chem.*, 74 (1991) 234.
15 N. Alexandrou, M.J. Lawrence and J. Pawliszyn, *Anal. Chem.*, 64 (1992) 301.

Journal of Chromatography A, 655 (1993) 101–110
Elsevier Science Publishers B.V., Amsterdam

CHROM. 25 034

High-performance liquid chromatographic determination of ten heterocyclic aromatic amines with electrochemical detection

M.T. Galceran, P. Pais and L. Puignou*

Departament de Química Analítica, Universitat de Barcelona, Av. Diagonal 647, 08028 Barcelona (Spain)

ABSTRACT

Conditions for the HPLC–electrochemical detection determination of ten mutagenic heterocyclic amines that can be produced by heat processing of protein-rich food products were established. The use of reversed-phase chromatography and acetonitrile–ammonium acetate (10:90) at pH 4.0 for the separation of 2-amino-3-methylimidazo[4,5-*f*]quinoline, 2-amino-3,4-dimethylimidazo[4,5-*f*]quinoline (MeIQ), 2-amino-3,8-dimethylimidazo[4,5-*f*]quinoxaline (MeIQx), 2-amino-3,4,8-trimethylimidazo[4,5-*f*]-quinoxaline (4,8-DiMeIQx) and 2-amino-6-methyldipyrido[1,2-*a*:3′,2′-*d*]imidazole (Glu-P-1), and of acetonitrile–ammonium acetate (30:70) at pH 6.0 for the separation of 2-amino-1-methyl-6-phenylimidazo[4,5-*b*]pyridine, 3-amino-1-methyl-5H-pyrido[4,3-*b*]indole (Trp-P-2), 2-amino-3-methyl-9H-pyrido[2,3-*b*]indole, 1-methyl-9H-pyrido[4,3-*b*]indole (harman) and 9H-pyrido[4,3-*b*]indole (norharman) was proposed. The figures of merit were calculated; reproducibility gave a relative standard deviation of 1.6–4.6% when measured by peak area. Detection limits (signal-to-noise ratio 2:1) ranged from 0.2 ng for Trp-P-2 to 3.4 ng for 4,8-DiMeIQx. The method was applied to the determination of some of these compounds in a commercial beef extract. Levels of 5.1 ng g^{-1} MeIQx, 5.8 ng g^{-1} MeIQ and 15.5 ng g^{-1} of Glu-P-1 were found.

INTRODUCTION

Aromatic amines are one of the few classes of chemical compounds for which there is convincing evidence that some members induce cancer in humans [1]. This group of compounds includes several heterocyclic amines of two or generally three condensed aromatic cycles with one or more nitrogen atoms in the ring system; most of these heterocycles belong to two main classes of compounds: aminocarbolines and aminoimidazo azaarenes. These products, which can be found in cooked protein-containing food products in the low parts per billion (w/w) range, have shown mutagenic activity by means of the Ames test, and in some cases have also been found to be carcinogenic [2–6]. Humans are continually exposed to carcinogenic heterocyclic amines in heat-processed foods, and some heterocyclic amines have been detected in urine samples from healthy volunteers eating a normal diet [7].

These findings suggest the need to develop analytical techniques to determine these compounds in various heat-processed foods. To screen for mutagenic and carcinogenic compounds it is necessary to develop a simplified method that can analyse these compounds simultaneously using a fast, selective and sensitive analytical technique. The techniques presently available either require sophisticated and/or expensive equipment, such as enzyme-linked immunosorbent assay (ELISA) [8], HPLC–MS [9,10] or GC–MS [11,12], or are restricted to the determination of a selected group of compounds. HPLC with UV detection has been found appropriate to determine most of these compounds simultaneously [13]. However, HPLC with electrochemical detection (ED) is an option to be considered, since high selectivity and sensitivity

* Corresponding author.

0021-9673/93/$06.00

2-amino-3-methylimidazo[4,5-f]quinoline	IQ	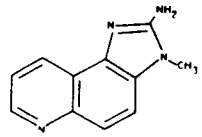
2-amino-3,4-dimethylimidazo[4,5-f]quinoline	MeIQ	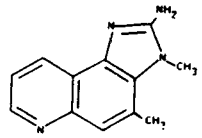
2-amino-3,8-dimethylimidazo[4,5-f]quinoxaline	MeIQx	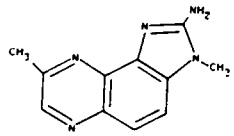
2-amino-3,4,8-trimethylimidazo[4,5-f]quinoxaline	4,8-DiMeIQx	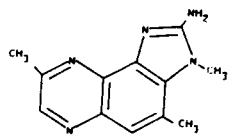
2-amino-1-methyl-6-phenylimidazo[4,5-b]pyridine	PhIP	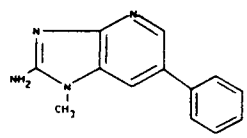
3-amino-1-methyl-5H-pyrido[4,3-b]indole	Trp-P-2	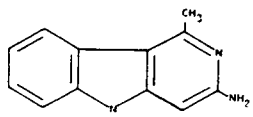
2-amino-6-methyldipyrido[1,2-a:3',2'-d]imidazole	Glu-P-1	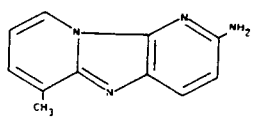
2-amino-3-methyl-9H-pyrido[2,3-b]indole	MeAαC	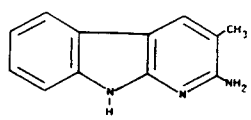
1-methyi-9H-pyrido[4,3-b]indole	Harman	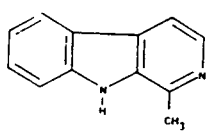
9H-pyrido[4,3-b]indole	Norharman	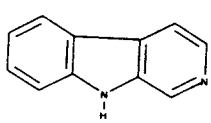

Fig. 1. Chemical structures of the mutagenic heterocyclic amines.

are achieved. Some aminoimidazo azaarenes have been detected using this technique [14–16], and recently both separation and ED of 2-amino-3-methylimidazo[4,5-*f*]quinoline (IQ), 2-amino-3,8-dimethylimidazo[4,5-*f*]quinoxaline (MeIQx), 2 - amino - 6 - methyldipyrido[1,2-*a*:3′,2′-*d*]imidazole (Glu-P-1), 3-amino-1,4-dimethyl-5H-pyrido[4,3-*b*]indole (Trp-P-1) and 3-amino-1-methyl-5H-pyrido[4,3-*b*]indole(Trp-P-2) have been described [17], although in all cases the procedures are restricted to the determination of a reduced number of compounds.

In this study conditions are established for the determination of ten heterocyclic amines, selected from those identified in beef extracts [IQ, 2 - amino - 3,4 - dimethylimidazo[4,5-*f*]quinoline (MeIQ), MeIQx and 2 - amino - 3, 4, 8 - trimethylimidazo[4, 5 - *f*]quinoxaline (4, 8 - DiMeIQx)] [13,18–20], and in cooked meat and fish [2-amino-1-methyl-6-phenylimidazo[4,5-*b*]pyridine (PhIP), Glu-P-1, Trp-P-2, 2-amino-3-methyl-9H-pyrido[2,3-*b*]indole (MeAαC), 1-methyl-9H-pyrido[4,3-*b*]indole (harman) and 9H-pyrido[4,3-*b*]indole(norharman)] [11,13,15,16,18–25], using HPLC–ED. The figures of merit have been calculated and the method has been applied to the determination of some of these compounds in a commercial beef extract.

EXPERIMENTAL

Chemicals

The compounds studied are listed in Fig. 1 and were purchased from Toronto Research Chemicals (Toronto, Canada), except harman and norharman, which were from Aldrich (Steinheim, Germany); stock standard solutions of 100 μg ml^{-1} in methanol were prepared and used for further dilutions. 2-amino-3,7,8-trimethylimidazo[4,5-*f*]quinoxaline (7,8-DiMeIQx) and 2-amino-3,4,7,8-tetramethylimidazo[4,5-*f*]-quinoxaline(4,7,8-TriMeIQx) were used as internal standards. Extrelut extraction cartridges (20 ml) were provided by Merck (Darmstadt, Germany). Bond-Elut propylsulphonyl silica gel (PRS; 500 mg) and C_{18} (100 mg) cartridges as well as coupling pieces and stopcocks were from Analytichem International (ICT, Basle, Switzerland). These cartridges were respectively preconditioned with dichloromethane and water–methanol (1 + 3 ml).

Other solvents and chemicals were HPLC or analytical grade, and the water was purified using a Culligan (Barcelona, Spain) system. All the solutions were passed through a 0.45-μm filter before injection into the HPLC system.

Instruments

HPLC was carried out with a Gilson Model 302 pump with an 802 monometric module (Gilson, Villier-le-Bel, France) and a Metrohm wall jet electrochemical detector, Model 656,

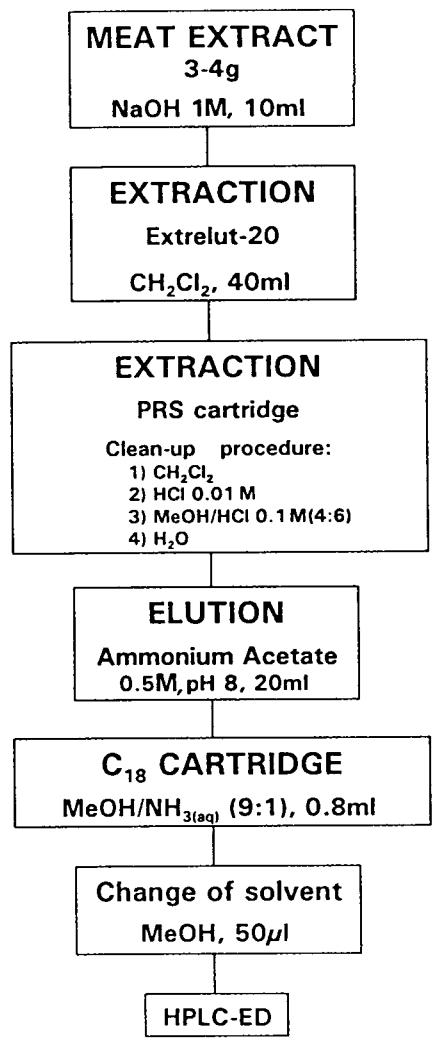

Fig. 2. Clean-up procedure.

TABLE I

CAPACITY FACTORS (k') OF HETEROCYCLIC AMINES AT DIFFERENT ACETONITRILE CONCENTRATIONS

– = Retention time > 50 min; + = not detected. Retention times > 50 min at 10% acetonitrile and pH 6.0 and 6.5.

	pH 3.5				pH 4.0				pH 4.5				pH 5.0				pH 5.5				pH 6.0			pH 6.5		
Acetonitrile (%) Analyte	10	20	25	30	10	20	25	30	10	20	25	30	10	20	25	30	10	20	25	30	20	25	30	20	25	30
IQ	3.17	0.69	0.00	0.00	4.16	0.83	0.00	0.00	5.92	0.94	0.00	0.00	8.59	1.36	0.67	0.00	9.50	1.50	0.82	0.00	1.97	0.89	0.79	1.98	1.04	0.00
Glu-P-1	3.80	0.96	0.00	0.00	5.06	1.44	1.01	0.90	9.20	1.96	1.45	1.01	13.50	3.05	1.87	1.43	–	3.75	2.27	1.45	4.78	1.38	1.64	4.53	2.43	1.53
MeIQx	5.20	0.96	0.00	0.00	6.03	0.97	0.00	0.00	7.54	1.03	0.00	0.00	9.90	1.45	0.76	0.00	10.58	1.42	0.86	0.00	2.06	0.91	0.71	1.89	0.98	0.00
MeIQ	5.02	0.96	0.00	0.00	7.19	1.10	0.00	0.00	10.35	1.45	0.82	0.00	–	2.04	0.97	0.00	–	2.29	1.27	0.87	3.20	1.91	1.00	3.47	1.70	0.99
4,8-DiMeIQx	21.21	1.70	0.97	0.00	13.97	1.75	1.03	0.00	–	1.87	1.09	0.00	–	2.72	1.27	0.86	–	2.75	1.49	0.94	3.63	1.49	1.07	3.47	1.68	0.88
7,8-DiMeIQx	11.21	1.43	0.00	0.00	11.93	1.51	0.84	0.00	–	2.97	0.91	0.00	–	3.73	1.60	0.00	–	2.17	1.94	0.80	2.76	2.18	0.86	4.96	1.38	0.81
TriMeIQx	–	2.18	1.30	0.75	–	2.39	1.39	0.90	–	2.72	1.57	0.87	–	3.65	1.69	1.00	–	4.08	1.85	1.09	4.77	1.94	1.29	4.79	2.15	1.17
Trp-P-2	–	4.14	2.44	1.25	–	4.53	2.61	1.48	–	5.29	2.56	1.52	–	6.68	2.76	1.64	–	6.08	2.90	1.73	7.57	3.08	1.93	7.60	4.10	1.78
PhIP	–	+	+	+	–	+	+	2.36	–	9.64	5.41	3.03	–	15.89	6.89	3.93	–	–	8.23	4.25	13.77	6.89	4.50	–	9.12	4.38
Harman	–	+	+	+	–	+	+	+	–	+	+	+	–	–	+	1.93	–	–	4.40	2.60	–	8.14	4.14	–	11.67	3.19
Norharman	–	+	+	+	–	+	+	+	–	+	+	+	–	–	+	2.50	–	–	6.05	3.60	–	8.78	5.46	–	12.82	5.21
MeAαC	–	10.76	7.52	4.24	–	–	11.29	6.59	–	–	13.91	7.35	–	–	14.23	7.93	–	–	14.27	7.99	–	3.33	8.00	–	14.60	8.17

equipped with a working electrode (Glassy Carbon Electrode, Model 6.0805.010), a reference electrode (Ag/AgCl/KCl 3 *M*) and an auxiliary electrode (Glassy Carbon Electrode, Model 6.0805.010) (Metrohm, Herisau, Switzerland). A data processor, Chromatopac C-R3A (Shimadzu, Kyoto, Japan), was used. The sample was introduced by a Rheodyne 7125 injector (Rheodyne, Cotati, USA) equipped with a loop of 50 μl. A TSK-Gel ODS 80T (5 μm) C_{18} column (25.0 cm × 4.6 mm) (Toso Haas, Stuttgart, Germany) and a Supelguard LC-8-DB precolumn (Supelco, Gland, Switzerland) were used at room temperature. Acetonitrile–50 m*M*

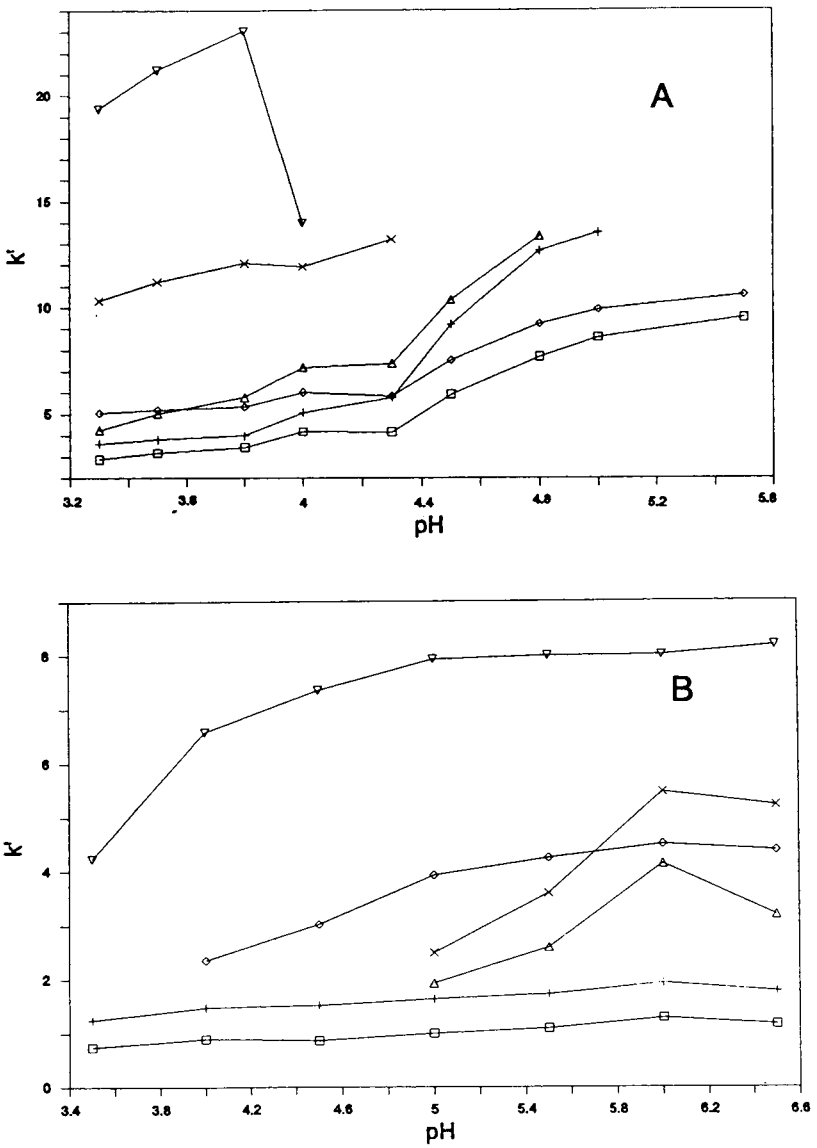

Fig. 3. Effect of mobile phase pH on the separation of heterocyclic amines. (A) Mobile phase: acetonitrile–50 m*M* ammonium acetate (10:90). + = Glu-P-1; □ = IQ; △ = MeIQ; ◇ = MeIQx; ▽ = 4,8-DiMeIQx; × = 7,8-DiMeIQx. (B) Mobile phase: acetonitrile–50 m*M* ammonium acetate (30:70). + = Trp-P-2; △ = PhIP; ▽ = MeAαC; × = harman; ◇ = norharman; □ = 4,7,8-TriMeIQx.

ammonium acetate at different pH values was used as mobile phase at a flow-rate of 1.0 ml/min. A Supelco Visiprep and Visidry SPE vacuum manifold (Supelco, Gland, Switzerland) were used for the clean-up procedure.

Analytical procedure

Sample preparation and clean-up were carried out according to the method proposed by Gross [13], which is summarized in Fig. 2. The method uses a diatomaceous earth cartridge (Extrelut-20) coupled to a propylsulphonic cartridge (PRS). The sample was eluted from the first cartridge and introduced into the second using dichloromethane. Elution was carried out with ammonium acetate pH 8.0, and clean-up using a C_{18} cartridge was carried out to give the final extract (methanol–ammonia). The solvent was evaporated with a stream of nitrogen and the analytes were dissolved with 50 μl of the internal standard (I.S.) in methanol. IQ, MeIQ, MeIQx, Glu-P-1 and 4,8-DiMeIQx were analysed by HPLC using 50 m*M* ammonium acetate (pH 4.0)–acetonitrile (90:10, v/v) as mobile phase, and 7,8-DiMeIQx as internal standard; otherwise Trp-P-2, PhIP, harman, norharman and MeAαC were analysed using 50 m*M* ammonium acetate (pH 6.0)–acetonitrile (70:30, v/v) as mobile phase; the internal standard used in this case was TriMeIQx. The working potential of the electrochemical detector was set at +1000 mV.

The compounds were quantified by the standard addition method. The spiked samples were prepared by addition of accurately measured amounts of each standard (125, 250 and 500 ng) at the beginning of the clean-up process. Recoveries were estimated from the slope of the regression line performed with the added amount *versus* the measured amount.

RESULTS AND DISCUSSION

Optimization of the chromatographic conditions

In order to establish the chromatographic conditions for the separation of the ten aromatic amines, variables such as pH and composition of the mobile phase were studied. Different binary phases of acetonitrile–50 m*M* ammonium acetate at different pH values were tested. The mixtures contained between 10 and 30% acetonitrile and the pH varied from 3.5 to 6.5. Values of capacity factor (k') obtained for the compounds in all the mobile phases are indicated in Table I. The increase in acetonitrile caused a reduction of k' values for the compounds at all the pH values. An increase in the pH produced an enhancement of k' due to a decrease in the amine ionization. In Table I it can be seen that PhIP, harman and

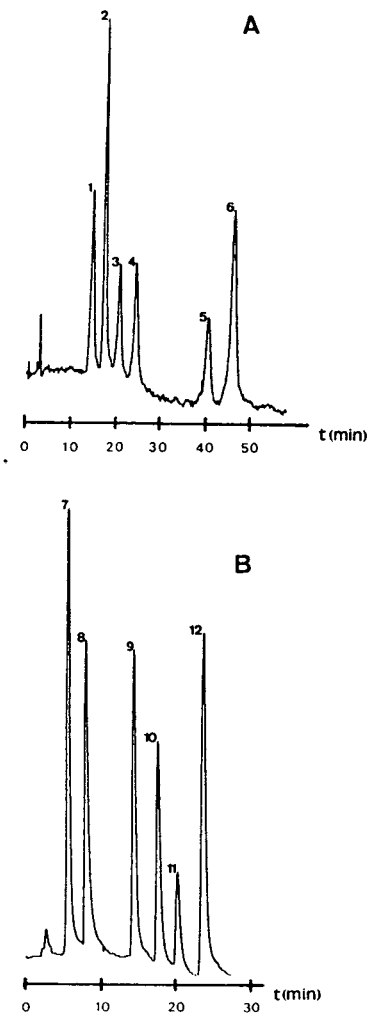

Fig. 4. Chromatogram of standard solution. (A) Mobile phase: acetonitrile–50 m*M* ammonium acetate (pH 4.0) (10:90). Peaks: 1 = IQ; 2 = Glu-P-1; 3 = MeIQx; 4 = MeIQ; 5 = 7,8-DiMeIQx; 6 = 4,8-DiMeIQx. (B) Mobile phase: acetonitrile–50 m*M* ammonium acetate (pH 6.0) (30:70). Peaks: 7 = 4,7,8-TriMeIQx; 8 = Trp-P-2; 9 = PhIP; 10 = harman; 11 = norharman; 12 = MeAαC.

norharman are not detected at pH less than 5, probably because of their low degree of oxidation at this pH, since the electrochemical oxidation of aromatic amines takes place with the loss of hydrogen ions [26].

From the values in Table I, it can be concluded that for the separation of the ten above-mentioned compounds using isocratic mode (gradient detection is difficult to perform with this detector) it is necessary to work at two different conditions. Thus the analysis of IQ, MeIQ, MeIQx, Glu-P-1, 4,8-DiMeIQx and 7,8-DiMeIQx can be performed using acetonitrile–50 m*M* ammonium acetate (10:90) (see Fig. 3A, which shows the plots of *k'* *vs.* pH). At pH 4.0 all the compounds can be separated, as can be

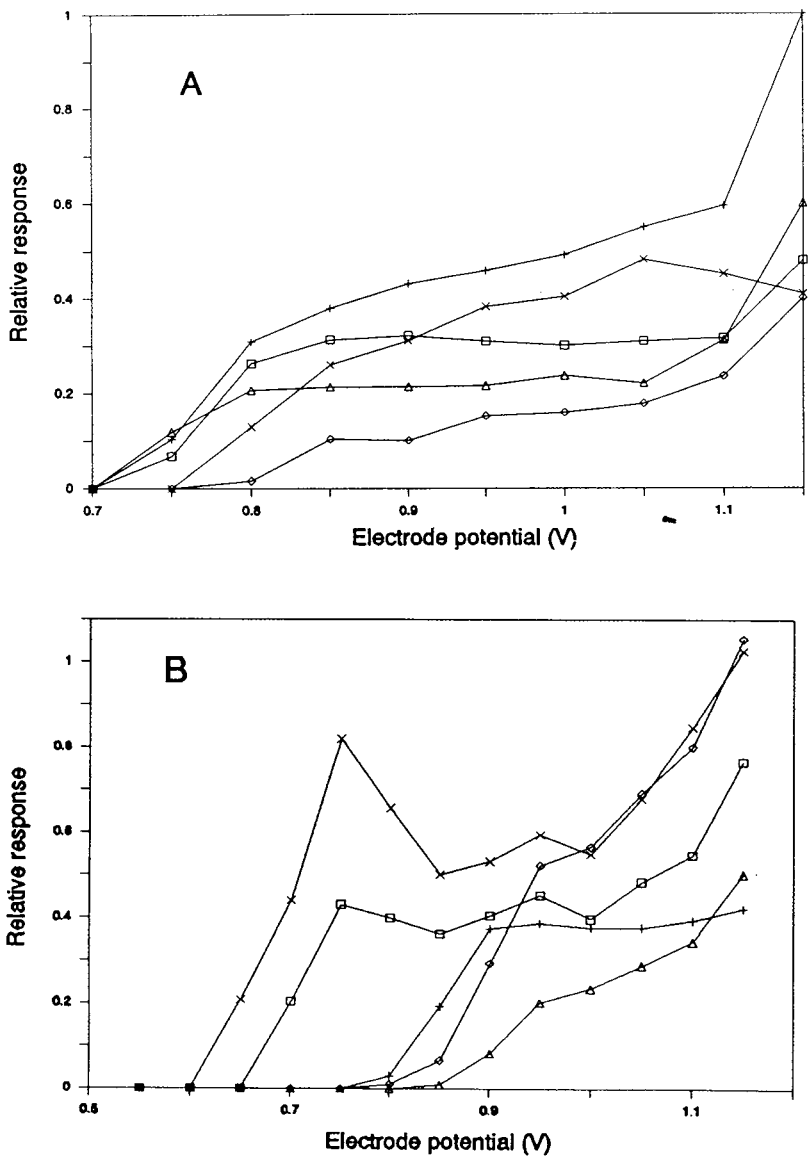

Fig. 5. Hydrodynamic voltammograms. Relative response to Glu-P-1 signal. (A) Mobile phase: acetonitrile–50 m*M* ammonium acetate (pH 4.0) (10:90). + = Glu-P-1; □ = IQ; △ = MeIQ; ◇ = MeIQx; × = 4,8-DiMeIQx. (B) Mobile phase: acetonitrile–50 m*M* ammonium acetate (pH 6.0) (30:70). □ = Trp-P-2; + = PhIP; × = MeAαC; △ = harman; ◇ = norharman.

seen in Fig. 4A, which shows the chromatogram of a standard solution of these compounds at this pH. Mobile phases with 30% acetonitrile are used for the separation of Trp-P-2, PhIP, harman, norharman, MeAαC and TriMeIQx. Their capacity factors at different pH values are given in Fig. 3B, and the separation obtained at pH 6.0 can be seen in Fig. 4B.

The optimum working potential was obtained from the hydrodynamic voltammograms of the compounds at the separation conditions previously established. Fig. 5A and B shows the hydrodynamic voltammograms obtained by raising the potential from +600 to +1150 mV. High responses were obtained for all compounds at +1150 mV; at higher potentials an increase occurred in both the background noise and the residual current, so the working potential chosen to give the best response for all the compounds and low background noise was +1000 mV.

From the voltammograms it can be observed that at electrode potentials lower than +750 mV no detectable response were obtained for any compound except for the aminoindol derivatives Trp-P-2 and MeAαC, which gave high responses at this potential; this behaviour can thus be used for the characterization of these compounds in complex samples.

Quality parameters

Calibrations for heterocyclic amines in methanol were carried out in the optimum separation conditions for each compound, with concentrations in the range 0.1–15 μg ml^{-1}. Peak area was used as the response. The correlation coefficients of calibration functions in the interval of linearity were better than 0.999 for all the heterocyclic amines.

Six replicate determinations of 30 ng (2 μg ml^{-1} solution) of each heterocyclic amine in methanol were carried out under the optimum conditions to determine the precision of the analysis. Relative standard deviations (R.S.D., %) in the range 1.6–4.6% based on peak area were obtained.

The detection limits for the quinoline and quinoxaline derivatives, based on a signal-to-noise ratio of 2:1 ranged from 0.7 to 3.5 ng, according to their retention times, as can be seen in Table II. The low detection limit for Glu-P-1 may be related to its higher relative response at the working potential. The other compounds analysed with mobile phase acetonitrile–50 m*M* ammonium acetate (30:70) pH 6.0 gave lower detection limits related to their higher responses at this pH. These values are higher than the ones indicated in the literature for IQ, MeIQx, 4,8-DiMeIQx by Takahashi and co-workers [15,16] and Billedeau *et al.* [17]. The differences can be attributed to the pH of the mobile phase; at higher pH values lower detection limits are obtained (about 0.1 ng) but the separation of the compounds is poorer, as can be seen in Table I. Thus, if good separation is needed the use of the mobile phase at pH 4.0 is compulsory, but in this case the detection limits are high. In order to

TABLE II

FIGURES OF MERIT

Analyte	Interval of linearity (ng)	Limits of detection (ng)	Precision (R.S.D., %)
IQ	3.14–156.8	0.74	2.91
Glu-P-1	3.42–171.2	0.51	3.50
MeIQx	4.35–222.4	1.34	3.01
MeIQ	3.36–163.2	1.72	2.58
4,8-DiMeIQx	6.46–161.6	3.37	3.78
Trp-P-2	1.62–161.6	0.19	2.33
PhIP	1.65–164.8	0.26	4.57
Harman	2.61–260.8	0.26	3.95
Norharman	1.60–160.0	0.26	1.68
MeAαC	1.55–155.2	0.74	1.61

improve the limit of detection, an increase in the pH is required, but under these conditions a worse separation is achieved. Values for Glu-P-1 obtained at pH 5.5 are in agreement with those obtained by Billedeau *et al.* [17] for this compound.

Application

The analytical method studied in this paper was mainly developed to determine heterocyclic amines and related compounds in processed-food samples. Estimates of the amounts of IQ, MeIQ, MeIQx and 4,8-DiMeIQx in beef extract have been reported previously [13,15,16,18–20], but procedures that allow the simultaneous analysis of a large number of heterocyclic amines by HPLC–ED have not been reported. So the method was applied to the determination of these compounds in a commercial beef extract. Purification of the sample was performed by the method proposed by Gross [13], as described in the Experimental section. The percentage recovery for each compound is indicated in Table III. These results are in agreement with the data published by Gross [13], and for some compounds our results are slightly higher. Amines such as Glu-P-1 gave low recovery factors, and PhIP, Trp-P-2, MeAαC, harman and norharman were not recovered by this method. The use of different clean-up methods for recovery of these compounds is currently being studied.

Glu-P-1, MeIQ and MeIQx were identified and quantified in the beef extract, and the results are given in Table III. Fig. 6 shows the chromatograms of the sample and the spiked sample

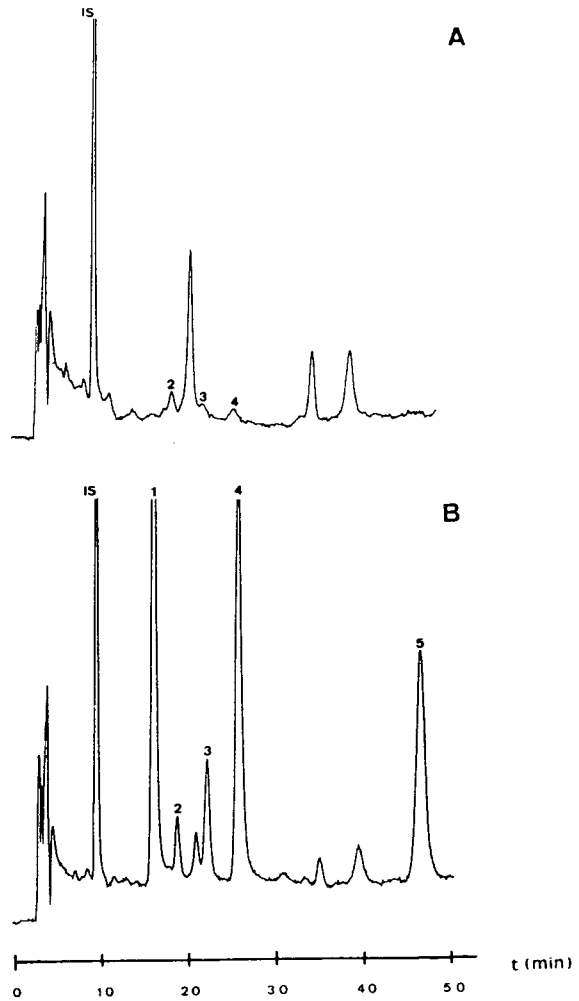

Fig. 6. Chromatograms of a beef extract. Mobile phase: acetonitrile–50 m*M* ammonium acetate (pH 4.0) (10:90). (A) Extract, (B) extract spiked before the clean-up (500 ng of each compound). Peaks: IS = aniline; 1 = IQ; 2 = Glu-P-1; 3 = MeIQx; 4 = MeIQ; 5 = 4,8-DiMeIQx.

TABLE III

ANALYSIS OF A BEEF EXTRACT

ND = Not detected.

Analyte	Recovery (%)	Results (ng/g)
IQ	68.28	ND
Glu-P-1	17.66	15.54
MeIQx	62.93	5.07
MeIQ	77.37	5.77
4,8-DiMeIQx	66.26	ND

and confirms the presence of Glu-P-1, MeIQ and MeIQx. Furthermore, it can be seen that the peak eluted at 21.1 min is not MeIQx, which appears at higher retention times (see spiked sample); likewise, the peaks at 35.0 and 39.0 min were identified. The internal standard used was aniline because of the interfering peak that appeared near to 7,8-DiMeIQx. IQ and 4,8-DiMeIQx, which have been detected in some beef extracts, could not be detected as clear peaks in the sample (Fig. 6). The limits of

detection of these compounds in our system are 0.74 and 3.4 ng, respectively. Thus, if they were present it would be at <0.8 and <3.5 ng g^{-1}, respectively.

CONCLUSIONS

Quantification of mutagenic and carcinogenic heterocyclic amines in cooked foods is essential for estimation of their risk to human beings. In this study conditions have been established for the separation and determination by HPLC–ED of ten heterocyclic amines. The applicability, selectivity, linearity and sensitivity of the method have been studied. The procedure has been applied to the determination of IQ, MeIQx, MeIQ, 4,8-DiMeIQx and Glu-P-1 in a beef extract. Research is currently in progress to optimize the extraction and clean-up methods for the determination, in cooked foods, of the other heterocyclic amines whose chromatographic characteristics and detection limits have been established in this study.

REFERENCES

1 R.C. Garner, C.N. Martin and D.B. Clayson, in C.E. Searle (Editor), *Chemical Carcinogens*, Vol. 1, American Chemical Society, Washington, DC, 2nd ed., 1984, pp. 175–275.
2 H. Ohgaki, H. Hasegawa, T. Kato, M. Suenaga, M. Ubukata, S. Sato, S. Takayama and T. Sugimura, *Environ. Health Perspect.*, 67 (1986) 129.
3 J.S. Felton, M. Knize, N. Shen, B. Andresen, L.B. Bjeldanes, F. Hatch and T. Fred, *Environ. Health Perspect.*, 67 (1986) 17.
4 S. Nishimura, *Environ. Health Perspect.*, 67 (1986) 11.
5 A. Abu-Shakra, C. Ioannides and R. Walker, *J. Sci. Food Agric.*, 42 (1988) 343.
6 T. Sugimura, *Trends Pharmacol. Sci.*, 9 (1988) 205.
7 H. Ushiyama, K. Wakabayashi, M. Hirose, H. Itoh, T. Sugimura and M. Nagao, *Carcinogenesis*, 12 (1991) 1417.
8 M. Vanderlaan, B.E. Watkins, M. Hwang, M. Knize and J.S. Felton, *Carcinogenesis*, 9 (1988) 153.
9 C.G. Edmonds, S.K. Sethi, Z. Yamaizumi, H. Kasai, S. Nishimura and J.A. McCloskey, *Environ. Health Perspect.*, 67 (1986) 35.
10 H. Milon, H. Bur and R. Turesky, *J. Chromatogr.*, 394 (1987) 201.
11 S. Murray, N.J. Gooderham, V.F. Barnes, A.R. Boobis and D.S. Davies, *Carcinogenesis*, 8 (1987) 937.
12 S. Murray, N.J. Gooderham, A.R. Boobis and D.S. Davies, *Carcinogenesis*, 9 (1988) 321.
13 G.A. Gross, *Carcinogenesis*, 11 (1990) 1597.
14 S. Grivas and T. Nyhammar, *Mutat. Res.*, 142 (1985) 5.
15 M. Takahashi, K. Wakabayashi, M. Nagao, M. Yamamoto, T. Masui, T. Goto, N. Kinae, I. Tomita and T. Sugimura, *Carcinogenesis*, 6 (1985) 1195.
16 M. Takahashi, K. Wakabayashi, M. Nagao, Z. Yamaizumi, S. Sato, N. Kinae, I. Tomita and T. Sugimura, *Carcinogenesis*, 6 (1985) 1537.
17 S.M. Billedeau, M.S. Bryant and C.L. Holder, *LC–GC Int.*, 4 (1991) 38.
18 W.A. Hargraves and M.W. Pariza, *Cancer Res.*, 43 (1983) 1467.
19 R.J. Turesky, J.S. Wishnok, S.R. Tannenbaum, R.A. Pfund and G.H. Buchi, *Carcinogenesis*, 4 (1983) 863.
20 G.A. Gross, G. Philippossian and H.U. Aeschbacher, *Carcinogenesis*, 10 (1989) 1175.
21 T. Matsumoto, D. Yoshida and H. Tomita, *Cancer Lett.*, 12 (1981) 105.
22 Z. Yamaizumi, H. Kasai, S. Nishimura, C.G. Edmonds and J.A. McCloskey, *Mutat. Res.*, 173 (1986) 1.
23 J.S. Felton, M.G. Knize, N.H. Shen, P.R. Lewis, B.D. Adreson, J. Happe and F.T. Hatch, *Carcinogenesis*, 7 (1986) 1081.
24 X.M. Zhang, K. Wakabayashi, Z.C. Liu, T. Sugimura and M. Nagao, *Mutat. Res.*, 201 (1988) 1081.
25 J.S. Felton, M.G. Knize, C. Wood, B.J. Wuebbles, S.K. Healy, D.H. Stuermer, L.F. Bjeldanes, B.J. Kimble and F.T. Hatch, *Carcinogenesis*, 5 (1984) 95.
26 J. Volke, in T.H. Ryan (Editor), *Electrochemical Detectors. Fundamentals Aspects and Analytical Applications*, Plenum Press, New York, 1984, p. 117.

Journal of Chromatography A, 655 (1993) 111–117
Elsevier Science Publishers B.V., Amsterdam

CHROM. 25 002

Determination of organic acids in grape musts, wines and vinegars by high-performance liquid chromatography

E. García Romero and G. Sánchez Muñoz*

Consejería de Agricultura de Castilla-La Mancha, Estación de Viticultura y Enología, Carretera de Torrenueva s/n, 13300 Valdepeñas, Ciudad Real (Spain)

P.J. Martín Alvarez and M.D. Cabezudo Ibáñez

Instituto de Fermentaciones Industriales, C.S.I.C., Juan de la Cierva 3, 28006 Madrid (Spain)

ABSTRACT

A method for the determination of tartaric, malic, shikimic, lactic, acetic, citric, succinic, citramalic and fumaric acid in musts, wines and vinegars is proposed, based on high-performance liquid chromatography using two 3-μm C_{18} columns (250 × 4.6 mm I.D.) in series, providing an efficiency between 50 000 and 80 000 theoretical plates/m. The mobile phase is phosphate buffer (pH 2.35) to which is added a small amount of methanol (3%) as polar modifier. The relative standard deviations were <6% and no effect of sample preparation (filtration and passage through Sep-Pak C_{18}) on the results was observed.

INTRODUCTION

Organic acids account for a significant fraction of musts, wines and vinegars. Their origins are diverse, the most important being biosynthesis by the vine, metabolic pathways related to sugar fermentation, malolactic fermentation and ethanol oxidation (in the case of acetic acid in vinegars). Organic acids affect stability, colour [1,2] and flavour of the final product.

Each acid may be determined enzymatically or spectrophotometrically after separating it from the other components [3], but there is no official method of analysis of this type for some of them, such as shikimic acid, fumaric acid and citramalic acid.

Proposals have been made for analysis by gas chromatography (GC) in the form of esters [4–6], by direct injection (acetic acid) [7] and by oxidation of lactic acid to acetaldehyde for headspace analysis [8]. For ion chromatographic analysis, it is necessary to separate sugars and polyalcohols previously in order to prevent them from interfering with the determination of some of the acids [9,10], or to limit the analysis to acids that separate well [3,11] or to adopt double detection of multiple peaks by means of UV and refractive index methods [12–14]. However, it would be very difficult to apply this technique to the determination of organic acids in musts or sweet wines because of the high concentration of sugars present.

Reversed-phase high-performance liquid chromatographic (RP-HPLC) analysis has also been described, but owing to the complexity of the oenological substrates, pretreatment of the sample is essential. With C_8 and C_{18} columns, polyphenols and anthocyanins must be separated previously, as they elute at the end of the

* Corresponding author.

0021-9673/93/$06.00

chromatogram and would interfere in subsequent analyses. Activated charcoal [15], ion-exchange resins [16], mixed procedures [17] and Sep-Pak C_{18} cartridges [3,18,19] have been recommended for this step.

In this paper, a method for the determination of tartaric, malic, shikimic, lactic, acetic, citric, succinic, citramalic and fumaric acid by RP-HPLC is described, applicable to musts, wines and vinegars, based on the passage of the initial sample through Sep-Pak C_{18} cartridges and the use of two 250 × 4.6 mm I.D. columns in series with a 3-μm C_{18} packing. The method permits the determination of all the acids mentioned in a single run because of the high efficiency achieved with this system of columns, and with no problems due to the sugars present or to the anthocyanins and polyphenols, which are eliminated in sample preparation.

EXPERIMENTAL

Reagents

All the chemicals used were of analytical-reagent grade. Tartaric, malic, lactic, acetic, citric, succinic, fumaric and phosphoric acid and diammonium hydrogenphosphate were supplied by Merck (Darmstadt, Germany), shikimic and citramalic acid by Fluka (Buchs, Switzerland) and methanol by Panreac (Barcelona, Spain). Water purified using a Milli-Q system (Millipore, Bedford, MA, USA) was used.

Sample preparation

The samples were filtered through 0.2-μm pore-size membranes (Dynagard, 0.8 cm^2; Microgon, Laguna Hills, CA, USA). They were then fractionated using Sep-Pak C_{18} Classic cartridges (Millipore) that had previously been conditioned by means of succesive washes with 3 ml of methanol and 10 ml of water, drying the cartridge with air after each wash. A 0.5-ml volume of the filtered sample was passed through the cartridge and the retained acids were eluted with aliquots of phosphoric acid (5%) up to a final volume of 2 ml; in this way the sample was diluted fourfold.

Chromatographic method

The equipment consisted of an SEC-4 solvent chamber (Perkin-Elmer, Norwalk, CT, USA), a Series 10 pump (Perkin-Elmer), a Model 7125 injection valve (Rheodyne, Cotati, CA, USA), an LC-90 variable-wavelength UV–Vis detector (Perkin-Elmer), a 450-MT2 data processing system (Kontron Instruments, Milan, Italy) and a MicropH 2001 pH meter (Crison Instruments, Barcelona, Spain).

Samples were injected through a 6-μl loop into a system consisting of two 250 × 4.6 mm I.D. columns in series (3-μm ODS-2; Symta, Madrid, Spain) and a 20 × 2 mm I.D. guard column (Pellicular C_{18}; Alltech, Deerfield, IL, USA). The mobile phase was 0.02 *M* diammonium hydrogenphosphate–methanol (97:3) (adjusted to pH 2.35 with phosphoric acid) at a flow-rate of 0.5 ml/min at room temperature and a working pressure of 3200–3500 p.s.i. (1 p.s.i. = 6894.76 Pa). Detection was by means of measurement of UV absorption at 210 nm.

Data treatment

Data were processed by means of the BMDP statistical package [20], using linear regression analysis (BMDP1R program) on a VAX 9200 computer.

RESULTS AND DISCUSSION

Preparation of samples

The volume of the initial sample and the volume of the elute collected from the Sep-Pak cartridges were calculated so as to elute the maximum amount of acids with minimum dilution of the original sample. Under these conditions, polyphenols and anthocyanins are retained in the cartridge.

Chromatographic separation

The variation of the capacity factor (k') of the different acids as a function of the mobile phase pH is shown in Fig. 1. It was considered desirable to give priority to the separation of tartaric acid, as this is the most significant acid among those deriving from grapes and because there is no enzymatic method for its measurement. At

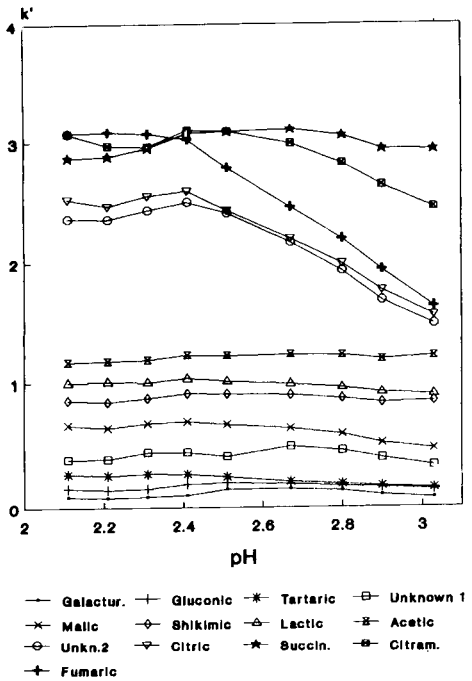

Fig. 1. Plots of capacity factors of organic acids *versus* eluent pH.

pH <2.4, tartaric acid separates well from gluconic and galacturonic acid and most other polar compounds of the sample, but it is not advisable to use much lower pH values so as not to shorten the life of the columns. Two unidentified compounds, unknown 1 and unknown 2, have been included in Fig. 1 in order to separate them and prevent them from being superimposed on the peaks of some of the remaining acids. Separation is good in all instances, with the exception of succinic, citramalic and fumaric acid, which elute very close together, although this can be improved by adding a polar modifier (3% methanol) to the mobile phase. As this is a difficult separation it is extremely important to adjust the mobile phase pH exactly.

The use of two columns in series (50 cm total length) with a packing of small particles (3 μm) ensures that the flow-rate does not exceed 0.5 ml/min so as not to subject the system to excessive pressure. Under these conditions, the efficiency achieved ranges from 50 000 to 80 000 theoretical plates/m for lactic and citric acid, respectively. In the literature efficiencies of 40 000 theoretical plates/m have been reported for succinic acid [15] and 17 000 theoretical plates/m for lactic acid [16]. Hence the use of the system of columns described makes it possible to double the reported efficiency and provides the necessary resolution to be able to determine all the acids of interest in a single run, with no interferences with each other or with other compounds in the sample. This makes it possible to achieve greater accuracy in quantitative analysis.

Fig. 2 shows the chromatogram of a standard mixture of all the acids in aqueous solution at concentrations close to those in which they are usually found in wines, and Figs. 3, 4 and 5 show the chromatograms obtained under the conditions described for a grape must, a wine and a wine vinegar, respectively.

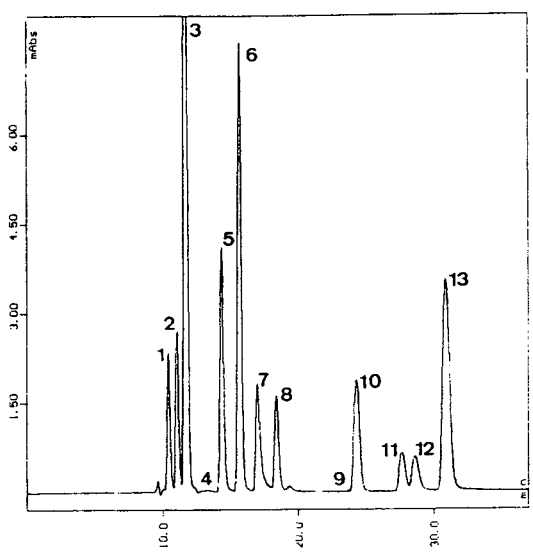

Fig. 2. Chromatogram of a synthetic solution of organic acids. Isocratic elution using two 3-μm ODS-2 columns (250 × 4.6 mm I.D.). Mobile phase, 0.02 *M* diammonium hydrogenphosphate–phosphoric acid (adjusted to pH 2.35) containing 3% of methanol as polar modifier; flow-rate, 0.5 ml/min. Peaks of acids: 1 = galacturonic (1.620 g/l); 2 = gluconic (0.801 g/l); 3 = tartaric (2.029 g/l); 4 = unknown 1; 5 = malic (1.002 g/l); 6 = shikimic (31.6 mg/l); 7 = lactic (1.016 g/l); 8 = acetic (0.710 g/l); 9 = unknown 2; 10 = citric (0.545 g/l); 11 = succinic (0.420 g/l); 12 = citramalic (0.437 g/l); 13 = fumaric (11.3 mg/l).

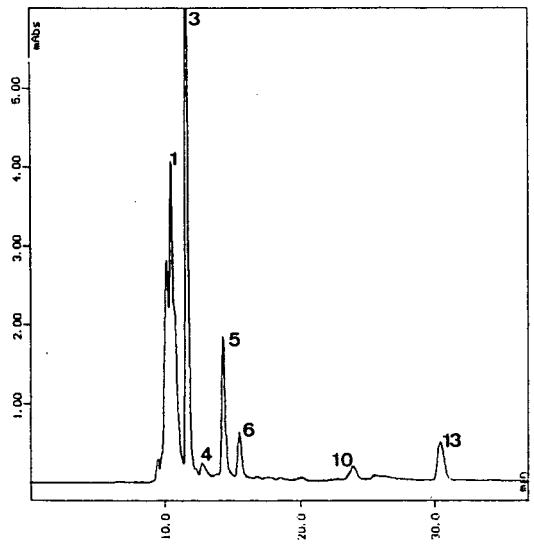

Fig. 3. Chromatogram of an Airén grape must. Chromatographic conditions and peak identification as in Fig. 2.

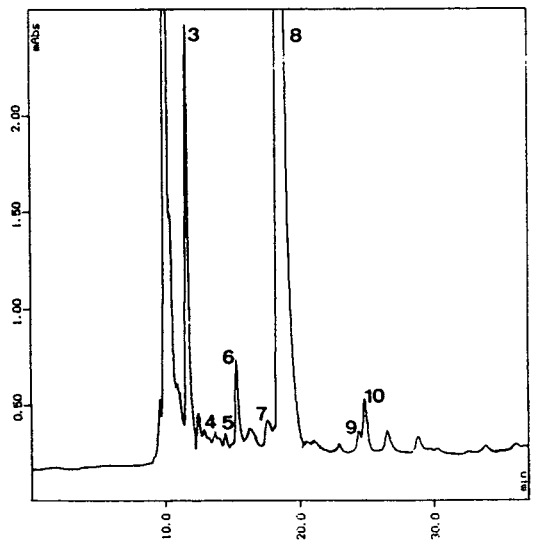

Fig. 5. Chromatogram of a commercial table wine vinegar. Chromatographic conditions and peak identification as in Fig. 2.

Quantitative analysis

In order to ascertain the precision of the method for quantitative analysis, all the acids in different concentrations were added to the same wine, each of the samples being injected in triplicate. The results are given in Table I. The relative standard deviations (R.S.D.s) are lower than 6% for all determinations within a relatively wide range of concentrations and the recoveries are satisfactory. These results suggest that, in order to achieve good quantitative accuracy, it is sufficient to inject a standard solution at the beginning and end of the working day.

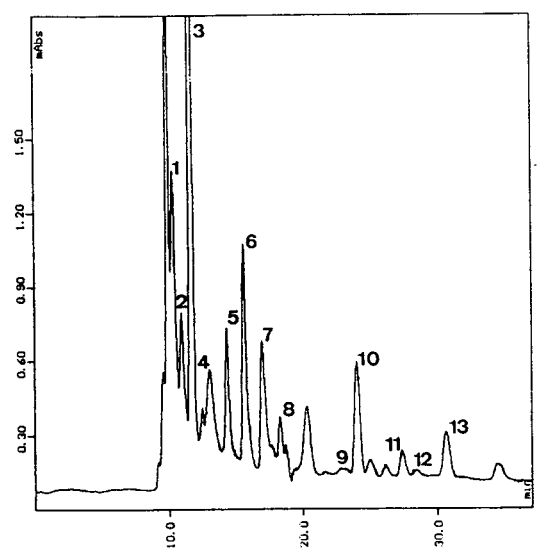

Fig. 4. Chromatogram of a red wine submitted to malolactic fermentation. Chromatographic conditions and peak identification as in Fig. 2.

Five different sample preparations of the same wine were also made up and analysed in triplicate on five different days. The R.S.D.s obtained for each acid on the same day (due to the chromatographic method) are *ca.* 3% and always lower than 6%, and those due to sample preparation (obtained on different days) are between 0.7% for shikimic acid and 5.7% for lactic acid, with a mean of 3.2%. These results, corresponding to fifteen determinations of each acid, demonstrate that there are no important differences due to the chromatographic method or to sample preparation.

Determination of organic acids in different substrates

The proposed method enabled data to be collected on the content of fixed acids in grape musts and wines from recent harvests in the Castilla-La Mancha (Spain) area and in commercial vinegars (Table II).

TABLE I

ANALYSIS OF THE SAME WINE BEFORE AND AFTER ADDITION OF ACIDS IN INCREASING AMOUNTS

Acid	Concentration added (g/l)	Peak area (mV min) (mean ± S.D., $n = 3$)[b]	Regression line		Initial acid concentration in the wine (g/l)	Recovery (%)
			Slope	r^2		
Tartaric	0.000	52.70 ± 2.52 (4.8)	16.646	0.997	3.192	–
	0.253	58.28 ± 0.70 (1.2)				96.1
	0.505	60.99 ± 0.56 (0.9)				95.2
	1.214	73.36 ± 0.14 (0.2)				97.2
Malic	0.000	22.43 ± 0.12 (0.5)	10.241	0.970	2.212	–
	0.249	26.00 ± 0.11 (0.4)				100.4
	0.564	27.55 ± 0.12 (0.4)				99.3
	0.972	32.91 ± 0.18 (0.6)				93.8
Shikimic	0.00[a]	22.44 ± 0.08 (0.4)	0.755	0.968	30.72[a]	–
	5.00[a]	28.45 ± 0.38 (1.3)				106.3
	11.00[a]	30.68 ± 0.76 (2.5)				94.0
	18.00[a]	36.87 ± 0.59 (1.6)				101.4
Lactic	0.000	3.72 ± 0.20 (5.4)	6.024	0.994	0.640	–
	0.259	5.68 ± 0.18 (3.2)				96.6
	0.477	6.60 ± 0.21 (3.2)				96.9
	0.924	9.41 ± 0.02 (0.3)				103.2
Acetic	0.000	2.82 ± 0.14 (5.0)	7.896	0.988	0.393	–
	0.212	5.08 ± 0.11 (2.2)				103.7
	0.389	6.32 ± 0.00 (0.0)				98.6
	0.750	8.87 ± 0.28 (3.2)				98.4
Citric	0.000	13.85 ± 0.17 (1.2)	14.424	0.984	0.993	–
	0.183	17.85 ± 0.26 (1.4)				98.4
	0.368	19.24 ± 0.04 (0.2)				98.2
	0.786	25.64 ± 0.34 (1.3)				98.5
Succinic	0.000	4.13 ± 0.09 (2.2)	7.446	0.997	0.574	–
	0.214	5.97 ± 0.14 (2.4)				96.4
	0.395	7.35 ± 0.23 (3.1)				95.0
	0.803	10.16 ± 0.38 (3.8)				95.7
Citramalic	0.000	4.86 ± 0.14 (2.9)	11.239	0.995	0.462	–
	0.170	7.00 ± 0.28 (4.0)				93.0
	0.241	7.95 ± 0.09 (1.2)				99.1
	0.531	10.87 ± 0.20 (1.9)				87.5
Fumaric	0.00[a]	7.41 ± 0.22 (3.0)	1.500	0.988	5.23[a]	–
	2.76[a]	11.96 ± 0.25 (2.1)				94.2
	6.26[a]	18.31 ± 0.28 (1.5)				94.7
	10.79[a]	23.41 ± 0.06 (0.3)				93.4

[a] Concentrations in mg/l.
[b] R.S.D. (%) in parentheses.

CONCLUSIONS

The HPLC method proposed for the determination of organic acids in oenological substrates consists of the use of two 3-μm C_{18} columns in series, which provide an efficiency of between 50 000 and 80 000 theoretical plates/m. The mobile phase is phosphate buffer (pH 2.35) to

TABLE II

RANGES OF CONCENTRATION OF ORGANIC ACIDS IN DIFFERENT OENOLOGICAL SUBSTRATES

Acid[a]		Grape must		Wine		Wine vinegar ($n = 24$)
		White ($n = 11$)	Red ($n = 12$)	White ($n = 22$)	Red ($n = 47$)	
Tartaric	Max.	6.47	7.65	3.94	5.74	4.01
	Min.	3.94	4.07	1.77	2.60	0.13
Malic	Max.	2.04	2.91	2.64	3.13	0.93
	Min.	1.34	1.99	0.11	0.06	0.10
Shikimic[b]	Max.	18.29	22.25	30.90	40.59	38.07
	Min.	12.39	5.09	15.94	16.12	2.01
Lactic	Max.	–	–	2.98	4.89	1.80
	Min.	–	–	0.13	0.07	0.10
Acetic	Max.	–	–	1.50	1.44	44.46
	Min.	–	–	0.20	0.30	26.28
Citric	Max.	0.30	0.35	0.54	0.40	2.84
	Min.	0.20	0.25	0.21	0.17	0.06
Succinic	Max.	–	–	1.19	1.22	0.58
	Min.	–	–	0.27	0.48	0.03
Citramalic	Max.	–	–	0.31	0.34	–
	Min.	–	–	0.09	0.17	–
Fumaric[b]	Max.	7.49	10.69	6.22	12.56	2.46
	Min.	6.00	5.11	1.45	1.30	0.23

[a] Concentrations in g/l except where indicated.
[b] Concentrations in mg/l.

which is added a small amount of methanol (3%) as polar modifier.

The efficiency achieved with this system is much superior to those described previously and, as interferences are avoided, permits greater accuracy of the results. The R.S.D.s are <6% and no differences are observed in the results depending on sample preparation (filtration and passage through Sep-Pak C_{18}).

ACKNOWLEDGEMENT

One of the authors (E.G.R.) is grateful to the Spanish Instituto de Investigación y Desarrollo Agrario y Alimentario del Ministerio de Agricultura, Pesca y Alimentación, for a grant.

REFERENCES

1 C.A. Sims and J.R. Morris, *Am. J. Enol. Vitic.*, 36 (1985) 181.
2 T.C. Sommers and M.E. Evans, *J. Sci. Food Agric.*, 28 (1977) 279.
3 *Recueil des Méthodes Internationales d'Analyse des Vins et des Moûts*, Office International de la Vigne et du Vin, Paris, 1990.
4 B.H. Gump, S. Saguandeekul, G. Murray and V. Teresita, *Am. J. Enol. Vitic.*, 36 (1985) 248.
5 D.L. Shooley, F.M. Kubiak and J.V. Evans, *J. Chromatogr. Sci.*, 23 (1982) 67.
6 J.E. Marcy and D.E. Carrol, *Am. J. Enol. Vitic.*, 33 (1982) 176.
7 S.A. Kupina, J.L. Kutschinski, R.D. Williams and R.T. DeSoto, *Am. J. Enol. Vitic.*, 33 (1982) 67.
8 A.J. Buglass and S.C. Garnham, *Am. J. Enol. Vitic.*, 42 (1991) 63.

9 A. Rapp and A. Ziegler, *Dtsch. Lebensm.-Rundsch.*, 75 (1979) 396.
10 P. Beaud, J. Marie and J.D. Aubort, *Trav. Chim. Aliment. Hyg.*, 80 (1989) 420.
11 S.A. Kupina, C.A. Pohl and J.L. Gannotti, *Am. J. Enol. Vitic.*, 42 (1991) 1.
12 R.F. Frayne, *Am. J. Enol. Vitic.*, 37 (1986) 281.
13 P. Pfeiffer and F. Radler, *Z. Lebensm.-Unters.-Forsch.*, 181 (1985) 24.
14 S. Testa, *Enotecnico*, 10 (1991) 81.
15 M.H. Auguste and A. Bertrand, Office International de la Vigne et du Vin, Paris, F.V. 721 (1980) 1.
16 J.P. Goiffon, A. Blachere and C. Reminiac, *Analusis*, 13 (1985) 218.
17 M.C. Polo, F. Barahona and I. Caceres, *Connaiss. Vigne Vin*, 20 (1986) 175.
18 D. Tusseau and C. Benoit, *J. Chromatogr.*, 395 (1987) 323.
19 V. Dell'Oro and R. di Stefano, *Vini Ital.*, 33 (1991) 53.
20 W.J. Dixon, *Biomedical Computer Programs*, University of California Press, Los Angeles, 1983.

Journal of Chromatography A, 655 (1993) 119–125
Elsevier Science Publishers B.V., Amsterdam

CHROM. 24 999

Photodiode array detection for elucidation of the structure of phenolic compounds

B. Bartolomé*, M.L. Bengoechea, M.C. Gálvez, F.J. Pérez-Ilzarbe, T. Hernández, I. Estrella and C. Gómez-Cordovés

Instituto de Fermentaciones Industriales, C.S.I.C., Juan de la Cierva 3, 28006 Madrid (Spain)

ABSTRACT

A photodiode array detector was employed to obtain spectral data and to study a set of derived parameters in order to assign some structural features (functional group conjugated with aromatic ring, degree of substitution, position of substituents, etc.) to unknown chromatographic peaks of low-molecular-mass phenolics.

INTRODUCTION

Phenolic compounds are characteristic of vegetable tissues and are of great interest in the study of food and beverages of that origin [1–3]. Identification of these compounds by chromatographic techniques requires the availability of commercial standards or the extraction and purification of the product from natural extracts, prior to the use of other analytical techniques (NMR, mass spectrometry, hydrolysis etc.) [4,5].

The photodiode array detector has led to considerable improvements in the HPLC analysis of phenolic compounds, as not only the retention time but also the UV spectrum can be used for identification purposes. Quantification also becomes more exact owing to the simultaneous recording of different wavelengths and the possibility of peak purity checking [6–8].

In only a few instances [9–12] has the UV spectrum obtained by diode array detection been used for the identification of unknown chromatographic peaks, by comparison with standards giving similar spectra. It was considered necessary, therefore, to make a detailed study of the possibilities and methodology for the use of this chromatographic detector in the elucidation of the structures of unknown phenolic compounds.

In this work we studied different parameters obtained from spectral data with the software of the equipment. The parameters studied were those useful in assigning structural features, *e.g.*, functional groups and number and position of substituents, to low-molecular-mass phenolics such as phenols, benzyl alcohols, benzoic acids, benzaldehydes, cinnamic acids, cinnamyl alcohols, phenylacetic acids, phenethyl alcohols, 3-phenyl-1-propionic acids, 3-phenyl-1-propanols and mandelic acids.

We chose a wide variety of commercial standards of phenolic compounds that are present in vegetable foods. Our aim was to obtain the information to infer rapidly the structure of unknown compounds present in food extracts and eluted under the same chromatographic

* Corresponding author.

0021-9673/93/$06.00

conditions. According to the literature [13], the UV spectra of these compounds are composed of two bands (called E and B) corresponding to the benzene ring, and a third band (called K) that appears when there is a substituent conjugated with the aromatic ring.

EXPERIMENTAL

Standards

Standards of phenolic compounds from Merck (Darmstadt, Germany), Fluka (Buchs, Switzerland), Sigma (Deisenhofen, Germany) and Aldrich (Steinheim/Albuch, Germany) of high purity were used: eight phenols, five benzyl alcohols, seventeen benzoic acids, twelve benzaldehydes, six cinnamic acids, one cinnamyl alcohol, seven phenylacetic acids, three phenethyl alcohols, two 3-phenyl-1-propionic acids, one 3-phenyl-1-propanol and four mandelic acids. The structures are shown in Fig. 1.

HPLC analysis

Solutions of 0.25 mg/ml in acetonitrile–water (4:1, v/v) were used. Variable amounts from 0.1 to 0.7 μg were injected into a Waters (Milford, MA, USA) chromatograph equipped with a Model 600E pump system controller, a U6K universal injector and a Model 991 photodiode-array detector.

The column was a reversed phase Nova-Pak C_{18} (300 × 3.9 mm I.D.). The gradient elution conditions are given in Table I; solvent A was water–acetic acid (98:2, v/v) and solvent B was water–methanol–acetic acid (68:30:2, v/v). Detection was performed by scanning from 210 to 400 nm with an acquisition speed of 1 s.

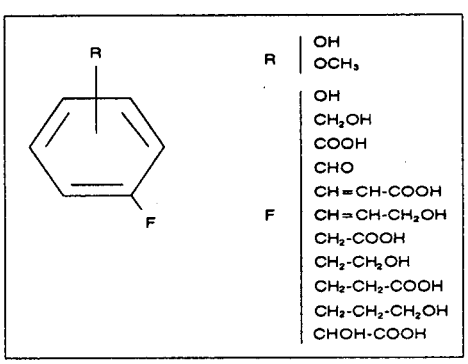

Fig. 1. Structure of the compounds studied.

TABLE I

MOBILE PHASE GRADIENT COMPOSITION AND FLOW-RATE

Time (min)	Flow-rate (ml/min)	A (%)	B (%)
0	0.8	100	0
59	0.8	20	80
70	0.8	20	80

RESULTS AND DISCUSSION

Assignment of spectral bands

The bands denoted E, K and B in the literature will be referred to as 1, 2 and 3, respectively (Fig. 2). Band 2, due to substituents conjugated with the aromatic ring, will be called 2_1 if it is a carboxyl group, 2_2 if it is a carbonyl group or 2_3 if there is a C=C double bond conjugated with the benzene ring.

The position and height of the maxima depend on the main functional group of the ring and also

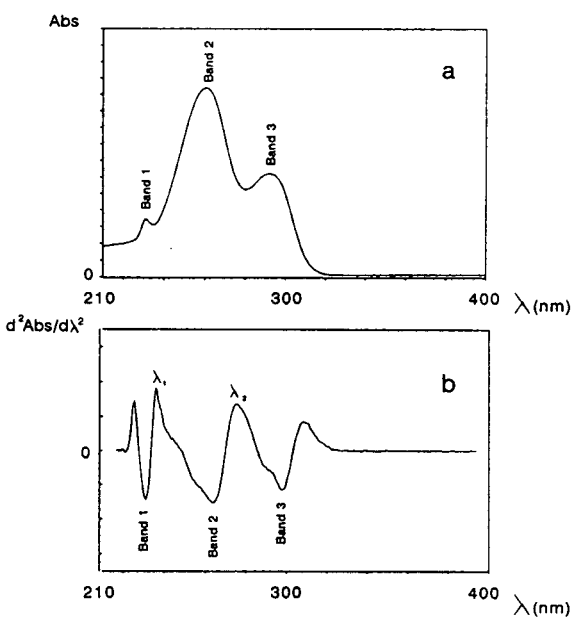

Fig. 2. Spectral bands: (a) Original spectrum; (b) second-derivative spectrum. Abs = Absorbance.

on the nature, number and positions of the remainder of the substituents. In all the compounds, the maxima vary in the ranges 219–235 nm for band 1, 236–298 nm for band 2 and 266–358 nm for band 3 (Table II). It has been demonstrated that changes in the composition of mobile phase during the gradient have no effect on the position and height of the maxima.

Simple phenols. The UV spectrum of phenols and benzyl alcohols is constituted by two bands, 1 and 3 (Fig. 3a and b). The same applies to phenylacetic acids, phenethyl alcohols, 3-phenyl-1-propionic acids, 3-phenyl-1-propanols and mandelic acids, as none of them has a double or triple bond conjugated with the aromatic ring (Fig. 3g, h, i, j and k, respectively).

Benzoic acids. The spectrum of benzoic acids (Fig. 3c) shows three bands. The position of band 2 (2_1) varies with the substituents on the ring, with the possibility of overlapping band 1 (with 3-hydroxy, 2-hydroxy and 2,5-dihydroxy substituents) or band 3 (as with 4-hydroxybenzoic, 3,4,5-trihydroxybenzoic and 3,5-dimethoxy-4-hydroxybenzoic acids) (Table II).

In the 3-hydroxybenzoic acid spectrum, the overlap is due to the hypsochromic effect of the *meta* substituents (deactivating position). The spectrum of 3,5-dihydroxybenzoic acid shows three distinct bands, as the effect of the substituents is offset by the bathochromic effect of the high symmetry of the molecule.

The hypsochromic shift of the carboxylic band in the 2-hydroxybenzoic acid spectrum may be due to the formation of hydrogen bonds between the carboxyl and the hydroxyl groups in *ortho* positions. The bands do not overlap in the 2,6-dihydroxybenzoic acid spectrum because the hypsochromic effect of the *ortho* position is counteracted by the bathochromic effect of the molecule symmetry.

The effects of *ortho* and *meta* positions are combined in the 2,5-dihydroxybenzoic acid spectrum, so the bands 1 and 2_1 overlap. However, the 2,3-dihydroxybenzoic acid spectrum has three bands because of the hydrogen bond between substituents, which compensates for their hypsochromic effect.

The shift in band 2_1 that causes overlap with band 3 (4-hydroxybenzoic, 3,4,5-trihydroxybenzoic and 3,5-dimethoxy-4-hydroxybenzoic acids) is due to the delocalizing effect of the *para* substitution and to the symmetry of the molecules.

Benzaldehydes. The UV spectrum of benzaldehydes (Fig. 3d) also shows three bands and, as happens to benzoic acids, bands 2_2 and 3 are overlapped when there are 4-hydroxy and 3,5-dimethoxy-4-hydroxy substituents.

Cinnamyl alcohols. The spectrum of cinnamyl alcohols (Fig. 3f) contains three bands, band 2_3 corresponding to the C=C double bond conjugated with the aromatic ring.

Cinnamic acids. The spectrum of cinnamic acids (Fig. 3e) contains a fourth band in addition to the three of the cinnamyl alcohols owing to the carboxyl group that is conjugated with the double bond and hence conjugated with the benzene ring. This band is also called 2_1 (it is due to a carboxyl group) and overlaps with band 1, except for 4-hydroxy-3-methoxycinnamic acid. Bands 2_3 and 3 are separated in every spectrum, except that of 3,5-dimethoxy-4-hydroxycinnamic acid, owing to the described effects of *para* substitution and the high symmetry that cause overlapping.

Study of parameters

The photodiode array detector permits of the different parameters in the UV spectra (Table II) to be measured to establish the relationship between structure and UV spectrum. These parameters are not dependent on the amount injected for the range of concentrations considered.

Retention time. The retention time depends on the main functional group and on the substituents of the benzene ring, so it is difficult to infer the structure of a compound solely from its retention time.

Position of maxima. For the same substitution pattern of the benzene ring, the maximum wavelength of band 2 decreases in the order cinnamic acids (2_3) > benzaldehydes (2_2) > benzoic acids (2_1). Cinnamyl alcohols are not included owing to insufficient data. In the same way, the maximum wavelength of band 3 decreases in the order cinnamic acids > benzaldehydes > benzoic acids > phenols > compounds with a saturated

TABLE II

VALUES OF PARAMETERS OBTAINED WITH THE PHOTODIODE ARRAY DETECTOR

t_R = Retention time (min); M1 = absorbance maximum (nm) of band 1; $M2_1$, $M2_2$, $M2_3$ = absorbance maxima (nm) of band 2 (see text); M3 = absorbance maximum (nm) of band 3; $C2_1$, $C2_2$, $C2_3$ = convexity intervals (nm) of band 2; C3 = convexity interval (nm) of band 3; 260/320, 270/300 = ratios between absorbances of different wavelengths (nm); λ_1, λ_2 = absorbance maxima (nm) of second-derivative spectra. Spectra were recorded after correcting for solvent absorption.

Compound	t_R	M1	$M2_1$	$M2_2$	$M2_3$	M3	$C2_1$	$C2_2$	$C2_3$	C3	260/320	270/300	λ_1	λ_2
Phenols														
Phenol	26.8	229.5				270.2				19.6	307	388	249.1	
4-Hydroxy-	7.0	231.2				288.1				23.9	1560	0.7	255.0	
3-Hydroxy-	9.5	231.2				273.8				19.3	1601	3437	251.7	
2-Hydroxy-	14.6	231.0				275.1				20.8	178	167	253.0	
2-Methoxy-	38.1	232.5				275.4				19.5	196	233	248.1	
2,6-Dimethoxy-	50.7	228.5				268.6				19.7	113	104	250.4	
2,3-Dihydroxy-	6.2	230.0				266.0				19.3	138	241	250.4	
3,5-Dihydroxy-	5.4	229.1				266.0				17.9	212	52	250.4	
Benzyl alcohols														
4-Hydroxy-	14.9	235.0				273.8				21.5	1120	356	253.2	
4-Methoxy-	43.0	232.5				272.8				21.3	298	254	246.8	
2-Hydroxy-	21.4	227.0				273.8				21.8	220	254	251.7	
4-Hydroxy-3-methoxy-	21.9	233.8				279.3				20.7	139	72	252.0	
3,4-Dimethoxy-	39.8	233.5				277.7				19.6	151	132	251.7	
Benzoic acids														
4-Hydroxy-	21.5	226.0	255.6			–[a]	37.4			–[a]	407	143	236.4	–
3-Hydroxy-	29.4	–[a]	237.7			295.9	–			27.9	1.4	0.3	–	256.9
2-Hydroxy-	57.3	–[a]	242.0			301.1	–			29.5	0.2	0.2	–	255.6
2,6-Dihydroxy-	17.8	230.0s[b]	246.5			306.3	16.7			29.7	0.9	0.1	–	266.3
2,6-Dimethoxy-	39.6	223.5s[b]	242.6			280.3	–			18.7	14	2.2	–	263.4
2,5-Dihydroxy-	20.6	–[a]	236.4			327.1	–			40.9	0.1	0.1	–	256.0
2,4-Dihydroxy-	26.1	226.0	255.6			294.6	18.2			20.9	32	1.1	236.4	273.8
2,4-Dimethoxy-	61.7	225.0	255.6			292.0	18.5			18.6	30	1.4	232.0	275.1
2,3-Dihydroxy-	29.2	228.0s	245.2			314.1	–			38.5	0.8	0.1	–	271.2
3,4-Dihydroxy-	10.1	228.6	258.2			294.6	20.4			18.5	38	1.5	241.3	277.7
4-Hydroxy-3-methoxy-	30.9	231.0	259.8			292.3	20.7			17.0	77	1.8	239.0	278.0
3,4-Dimethoxy-	56.3	235.0	259.5			292.3	20.8			16.9	94	1.9	242.6	277.7
3,5-Dihydroxy-	13.0	231.0	249.1			306.3	18.3			31.3	2.2	0.5	244.5	271.2
3,5-Dimethoxy-	<70	224.7	249.4			305.3	22.0			30.3	2.2	0.6	232.5	274.1
3,4,5-Trihydroxy-	6.5	231.0	271.2			–[a]	37.7			–[a]	27	2.8	246.5	–
3,5-Dimethoxy-4-hydroxy-	36.4	223.4	275.1			–[a]	42.3			–[a]	31	2.2	247.8	–
2,4,6-Trihydroxy-	10.2	231.2	255.6			293.3	17.9			17.8	41	2.1	241.6	275.1
Benzaldehydes														
4-Hydroxy-	27.8	228.0		284.2		–[a]		40.8		–[a]	11	1.5	242.9	–
3-Hydroxy-	31.2	228.6		254.3		315.4		19.6		35.3	3.6	1.7	237.7	276.4
2-Hydroxy-	49.8	229.0		255.6		324.5		18.1		43.8	3.3	1.6	237.0	273.8
2,5-Dihydroxy-	27.5	230.0		258.2		358.3		16.2		43.7	6.4	8.6	245.2	277.7
2-Hydroxy-5-methoxy-	62.3	229.0		258.2		357.0		16.8		42.8	5.9	7.9	245.2	277.2
2,3-Dihydroxy-	29.5	228.3		266.0		345.3		24.8		47.8	7.2	17	245.2	288.1
2-Hydroxy-3-methoxy-	50.3	228.0		264.7		344.0		23.8		47.1	5.9	14	245.2	286.2
3,4-Dihydroxy-	19.8	232.5		280.3		310.2		26.4		24.9	0.7	1.2	251.7	297.2
3-Hydroxy-4-methoxy-	36.6	231.0		279.0		311.5		25.8		25.3	0.7	1.2	250.4	295.9
4-Hydroxy-3-methoxy-	36.4	235.1		280.3		308.9		24.9		24.6	0.6	1.0	250.4	295.9
3,4-Dimethoxy-	60.7	233.0		277.7		308.9		21.4		23.4	0.7	1.1	247.8	294.6
4-Hydroxy-3,5-dimethoxy	44.5	229.5		307.6		–[a]		46.4		–[a]	0.1	0.3	250.4	–

TABLE II *(continued)*

Compound	t_R	M1	$M2_1$	$M2_2$	$M2_3$	M3	$C2_1$	$C2_2$	$C2_3$	C3	260/320	270/300	λ_1	λ_2
Cinnamic acids														
4-Hydroxy-	47.7	–[a]	232.5		298.0s	308.9	–		–	52.3	0.2	0.4	251.7	308.2s[b]
3-Hydroxy-	54.7	–[a]	235.1		279.0	325.0s[b]	–		29.8	16.1	2.5	2.0	251.7	303.7
2-Hydroxy-	65.4	–[a]	233.5		276.4	323.2	–		31.8	30.6	1.2	2.1	249.1	301.1
3,4-Dihydroxy-	27.5	–[a]	233.8		290.0s[b]	323.2	–		–	25.4	0.3	0.4	259.5	307.6
4-Hydroxy-3-methoxy-	55.0	219.0	236.0		292.0s[b]	323.5	–		–	31.7	0.2	0.4	260.8	306.3
3,5-Dimethoxy-4-hydroxy-	58.7	–[a]	237.5		323.2	–[a]	–		–[a]	51.1	0.1	0.2	258.2	–
Cinnamyl alcohol														
4-Hydroxy-3-methoxy-	44.0	231.2			262.4	304.0s[b]			23.2	19.8	22	2.5	242.9	281.9
Phenylacetic acids														
4-Hydroxy-	28.6	233.5				275.1				20.5	150	155	251.7	
4-Methoxy-	59.7	233.8				274.1				19.6	172	180	249.4	
3-Hydroxy-	30.9	231.2				272.8				21.0	172	222	246.8	
2,5-Dihydroxy-	9.9	232.5				291.0				23.5	10	0.4	249.4	
3,4-Dihydroxy-	17.9	233.8				280.6				19.6	75	27	252.0	
4-Hydroxy-3-methoxy-	35.6	233.8				280.6				19.5	68	29	251.0	
3,4-Dimethoxy-	55.2	235.1				278.0				19.3	159	99	250.0	
Phenethyl alcohols														
4-Hydroxy-	24.1	231.2				276.0				20.7	189	186	249.5	
4-Methoxy-	58.3	231.2				275.4				19.7	199	237	246.8	
4-Hydroxy-3-methoxy-	31.2	233.8				279.3				19.5	90	56	249.4	
3-Phenyl-1-propionic acids														
4-Hydroxyphenyl-	40.1	233.5				276.4				21.6	165	151	251.7	
3,4-Dihydroxyphenyl-	27.9	233.8				280.6				19.7	72	26	249.4	
3-Phenyl-1-propanol														
4-Hydroxyphenyl-	37.2	231.2				276.7				20.4	135	128	266.3	
Mandelic acids														
4-Hydroxy-	5.1	233.8				274.1				18.5	31	49	251.2	
4-Methoxy-	12.6	235.1				279.3				18.3	95	52	249.0	
4-Hydroxy-3-methoxy-	7.3	235.1				279.3				18.4	78	54	249.0	
3,4-Dihydroxy-	3.2	235.1				280.6				19.6	79	56	250.7	

[a] Overlapping with the nearest band.
[b] s: Considered as a shoulder.

side-chain (benzyl alcohols, phenylacetic acids, phenethyl alcohols, 3-phenyl-1-propionic acids, 3-phenyl-1-propanols and mandelic acids).

The effect of the substituents on the UV spectrum depends more on their position and interactions between them than on their nature. The *ortho* and *meta* positions give hypsochromic shifts of band 2 and bathochromic shifts of band 3. However, the effect of the substituents is not additive, owing to possible interactions between substituents. The 2,5- and 2,3-substituents correspond to the most separated wavelengths for band 2 (very low with respect to the other substitutions) and for band 3 (very high). The symmetry of the molecule (2,6- and 3,5-substituents) compensates for the effects of *ortho* and *meta* positions.

The effect of *para* substitution is opposite to that of *meta* and *ortho* substitution, *i.e.*, a bathochromic effect on band 2 and a hypsochromic effect on band 3.

Width of convexity interval. The convexity interval is defined for bands 2 and 3 as the distance (in nm) between the inflection points before and after the maximum. These inflection points are the maximum and minimum, respectively, of the first-derivative spectrum.

For the same substitution pattern of the aromatic ring, the convexity interval is larger in benzaldehydes than in benzoic acids for both

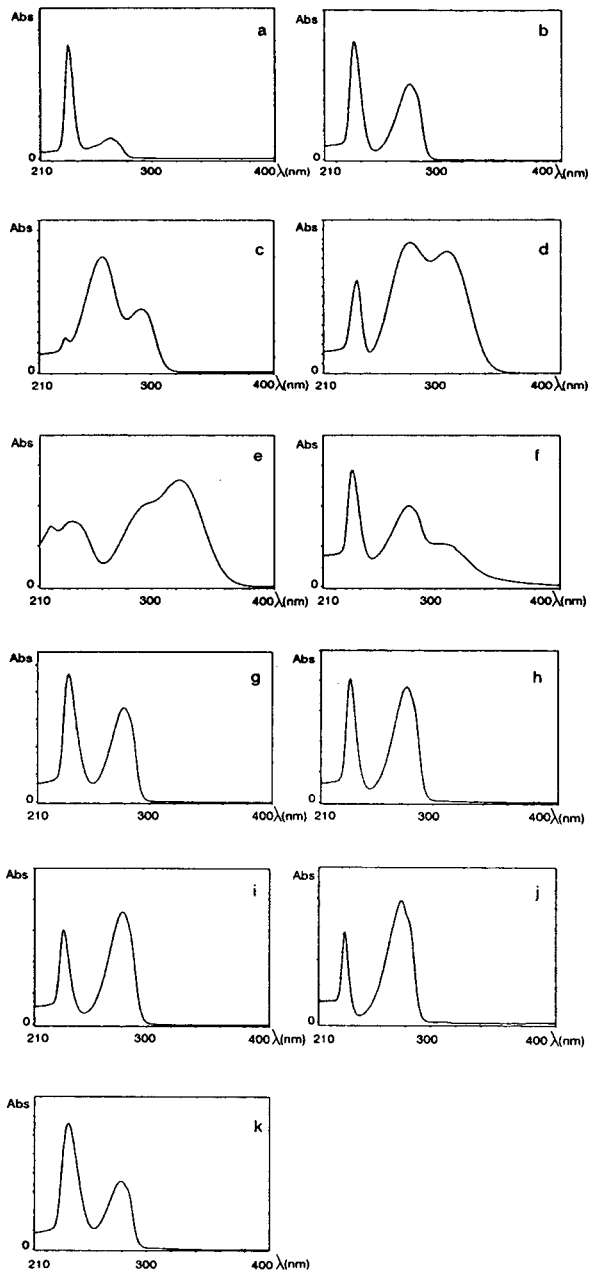

Fig. 3. Spectra of some of the compounds. (a) 3,5-Dihydroxyphenol; (b) 4-hydroxy-3-methoxybenzyl alcohol; (c) 4-hydroxy-3-methoxybenzoic acid; (d) 4-hydroxy-3-methoxybenzaldehyde; (e) 4-hydroxy-3-methoxycinnamic acid; (f) 4-hydroxy-3-methoxycinnamyl alcohol; (g) 4-hydroxy-3-methoxyphenylacetic acid; (h) 4-hydroxy-3-methoxyphenethyl alcohol; (i) 3-(3,4-dihydroxyphenyl)-1-propionic acid; (j) 3-(4-hydroxypheny)-1-propanol; (k) 4-hydroxy-3-methoxymandelic acid.

band 2 and band 3. There are no significant differences in the convexity interval of band 3 of the compounds with a saturated side-chain. Substituents in the 2,5- and 2,3-positions give the highest values of the convexity interval for band 3 with any type of functional group.

The position of the maximum and the convexity interval of the bands are related: a bathochromic shift of the maximum corresponds to an increase in the convexity interval. The study of these two parameters can be used to determine the presence, in an unknown compound, of a group conjugated with the aromatic ring (*i.e.*, if it is a benzoic acid, benzaldehyde, cinnamic acid or cinnamyl alcohol). In this instance, the spectrum will be composed of three distinct bands or two bands, that of highest wavelength having a convexity interval greater than 25 nm (because of overlapping of bands).

Absorbance ratios. The photodiode array detector permits the rapid calculation of absorbance ratios between different wavelengths. Several ratios were tested in order to classify the spectra by functional groups or by other criteria (number of substituents, relative position, etc.). Only the ratios A_{260}/A_{320} and A_{270}/A_{300} can partially differentiate the studied functional groups. In this way, a value of A_{270}/A_{300} of less than 17 indicates the presence of a double bond conjugated with the aromatic ring (benzoic acid, benzaldehyde, cinnamic acid or cinnamyl alcohol). The only exceptions are 4-hydroxyphenol, 4-hydroxybenzoic acid and 2,5-dihydroxyphenylacetic acid. The ratio A_{260}/A_{320} establishes very similar separation limits.

Position of maxima in the second-derivative spectrum. The maxima of the second-derivative spectrum (λ_1 and λ_2) correspond to the minima of the original spectrum (Fig. 2b). Thus, the maximum λ_1 corresponds to the minimum between bands 1 and 2 of the original spectrum. Maximum λ_2 corresponds to the minimum between bands 2 and 3 (if the latter exists), or between bands 2_1 and 2_3 of the cinnamic acids.

These parameters are related to the nature and position of the substituents on the ring. In compounds without a double bond conjugated with the aromatic ring (phenols, benzyl alcohols, phenylacetic acids, phenethyl alcohols, 3-phenyl-

1-propionic acids, 3-phenyl-1-propanols and mandelic acids), λ_1 takes higher values when there are hydroxyl groups far from the main functional group (3- and 3,4-positions). Methoxyl groups have a hypsochromic effect.

For compounds in which λ_2 is defined (benzoic acids, benzaldehydes, cinnamic acids and cinnamyl alcohols), the substituents that are far from the functional group (4- or 3,4-positions) have a very marked bathochromic effect, whereas the positions 2-, 2,5-, 2,6- and 3-positions lead to low values of λ_2. The 2,3-, 2,4- and 3,5-positions give intermediate values (see Table II).

The possibility of using all these parameters to develop an algorithm for establishing the possible structures of phenolic compounds is being studied.

ACKNOWLEDGEMENT

We acknowledge financial support from the "Comisión Interministerial de Ciencia y Tecnología" (project ALI91-0468).

REFERENCES

1 V.L. Singleton and P. Esau, *Phenolic Substances in Grapes and Wine and Their Significance*, Academic Press, New York, 1969.
2 B. Fernández de Simón, J. Pérez-Ilzarbe, T. Hernández, C. Gómez-Cordovés and I. Estrella, *J. Agric. Food Chem.*, 40 (1992) 1531.
3 F. Tomás-Lorente, C. García-Viguera, F. Ferreres and F.A. Tomás-Barberán, *J. Agric. Food Chem.*, 40 (1992) 1800.
4 K.R. Markham, *Techniques of Flavonoid Identification*, Academic Press, London, 1982.
5 J. Macheix, A. Fleuriet and J. Billot, *Fruit Phenolics*, CRC Press, Boca Raton, FL, 1990.
6 O.M. Andersen, *Bull. Liaison Groupe Polyphénols*, 15 (1990) 240.
7 Y.S. Velioglu and G. Mazza, *J. Agric. Food Chem.*, 39 (1991) 463.
8 M.L. Ramnaraine and M. Tuchman, *J. Chromatogr. Sci.*, 23 (1985) 549.
9 F. Siewek and R. Galensa, *J. Chromatogr.*, 294 (1984) 385.
10 V. Hong and R.E. Wrolstad, *J. Agric. Food Chem.*, 38 (1990) 708.
11 R.G. Bailey, J. McDowell and H.E. Nursten, *J. Sci. Food Agric.*, 52 (1990) 509.
12 J. Pérez-Ilzarbe, T. Hernández and I. Estrella, *Z. Lebensm.-Unters.-Forsch.*, 192 (1991) 551.
13 E. Pretsch, T. Clerc, J. Seibl and W. Simon, *Tablas para la Elucidación Estructural de Compuestos Orgánicos*, Alhambra, Madrid, 1985.

Journal of Chromatography A, 655 (1993) 127–132
Elsevier Science Publishers B.V., Amsterdam

CHROM. 25 044

Determination of organophosphorous and nitrogen-containing pesticides in water samples by solid phase extraction with gas chromatography and nitrogen–phosphorus detection

C. de la Colina, A. Peña Heras, G. Dios Cancela and F. Sánchez Rasero*

Estación Experimental del Zaidín (C.S.I.C.), Profesor Albareda 1, E-18008 Granada (Spain)

ABSTRACT

Organophosphorus and nitrogen-containing pesticides were extracted from water using solid-phase extraction (SPE) with Sep-Pak C_{18} cartridges and eluted with acetone and hexane. Different methods were evaluated to concentrate the eluates and, finally, pesticides were determined in the concentrated eluates by gas–liquid chromatography with nitrogen–phosphorus detection. Recoveries varied with the physico-chemical properties of the pesticides, being from 0% to 91%.

INTRODUCTION

The presence of pesticides in groundwaters in an agricultural area demands a suitable way of detecting large numbers of those chemicals at concentrations below the EEC regulations [1].

Extraction and concentration of pesticides from water has evolved in recent years. Liquid–liquid partition [2–4] produces good results but is time-consuming, polluting, unhealthy and expensive. Solid phase extraction (SPE) [5–9] is becoming increasingly popular as it does not have these disadvantages. Different supports have been used in the determination of pesticides from aqueous solutions [6–9], although octadecyl-bonded porous silica (C_{18}) is one of the most common ones [5,7,10–12].

The "Vega de Granada" (Grenada, South of Spain) is an area with a high agricultural production. Groundwater is in some places present less than 2 m below the surface. Therefore, contamination of groundwater with pesticides is likely to occur, depending on, among other factors, soil type, adsorption of the pesticides to the soil and the water solubility and chemical nature of the compounds applied.

A multiresidue method of analysis for pesticides present in the soils and groundwater of the "Vega de Granada" is being developed to assess their contamination levels. An SPE method, with a quantitative study of its different steps, for the determination of organophosphorous and nitrogen-containing pesticides in water is presented here. Later, this method might be used to monitor the groundwater contamination in this area.

EXPERIMENTAL

Reagents

Pesticides were selected according to their use in the studied area and all of them were reagent grade: fonofos, formothion, fenthion, chlorpyrifos, phosmet, azinphos-methyl, phosalone and amitraz were acquired from Labor Dr.

* Corresponding author.

0021-9673/93/$06.00

Ehrenstorfer (Augsburg, Germany). The following pesticides were gifts from the producers: dimethoate, diazinon, methidathion and simazine (Ciba-Geigy, Münchwilen, Switzerland), fenitrothion and malathion (Sumitomo, Osaka, Japan) and pirimicarb (ICI Agrochemicals, Yalding, UK). Propiconazole (Ciba-Geigy) was used as internal standard.

All solvents used were residue analysis grade. Water was purified with a Milli-Q water purification system (Millipore, Bedford, MA, USA).

Stock solutions of the pesticides and the internal standard were prepared in acetone (Probus, Badalona, Spain) at 1 g/l, except fenthion, which was prepared in isopropanol (Carlo Erba, Milan, Italy), and azinphos-methyl, which was prepared in toluene (Merck, Darmstadt, Germany). Simazine was prepared in acetone at 0.5 g/l. Dilutions were conveniently prepared in hexane (Probus, Badalona, Spain).

Standard mixtures. A concentrated standard mixture at 10 mg/l was prepared from the individual pesticide stock solutions, by a 1:100 dilution. The standard mixture at a concentration of 0.5 mg/l was a 1:20 dilution of the concentrated solution.

Glass wool and anhydrous sodium sulphate (Merck, Darmstadt, Germany) were extracted in a Soxhlet apparatus for 24 h with acetone. Anhydrous sodium sulphate was heated at 90°C for 1 h to remove the solvent and the glass wool left at room temperature until the solvent had evaporated [13].

Sep-Pak Classic short-body C_{18} cartridges with 360 mg of packing material/cartridge were used (Waters, Milford, MA, USA).

Apparatus

A Hewlett-Packard (Seville, Spain) 5880 gas chromatograph equipped with a split/splitless injector, a nitrogen–phosphorus detection (NPD) system and a Hewlett-Packard 5880A terminal to integrate peak areas, was employed. An HP-1 capillary column (cross-linked methyl silicone gum), 12 m × 0.2 mm I.D. (0.33 μm), with helium as the carrier gas at 1 ml/min was used. Injector and detector temperatures were 250 and 280°C, respectively. A 1-μl aliquot of the sample was injected in the splitless mode with the following temperature programme: 45°C (2 min), increase at 30°C/min to 160°C (2 min), increase at 4°C/min to 190°C (2 min) and increase at 20°C/min to 250°C (3 min).

The microcolumn was from Afora (Barcelona, Spain) and the rotary evaporator from Heidolph (Germany).

Procedure

Linearity. Linearity of the responses in the gas chromatograph was studied with mixtures of the pesticides at concentrations between 0.12 and 1.00 mg/l. Every sample was injected three times.

Repeatability. The standard mixture, at 0.5 mg/l, was injected eight times.

Concentration. Two different methods for concentration of the Sep-Pak eluates were investigated. A 10-μl volume of the concentrated standard mixture was added to 8 ml of acetone–hexane (1:1) and concentrated to about 0.3 ml using a microcolumn in a water bath at 75°C, or to about 2 ml in a rotary evaporator at 40°C under a 400 mbar vacuum. Further concentration of both solutions to a final volume of 0.2 μl was carried out under a gentle stream of helium. To an aliquot of 100 μl, carefully measured with a 100-μl Hamilton syringe, 5 μl of the internal standard at a concentration of 20 mg/l were added.

Sample extraction. A Sep-Pak cartridge was conditioned by consecutive passing 2 ml of hexane, 2 ml of acetone–hexane (1:1), 2 ml of acetone and 16 ml of Milli-Q water. Later, a volume of 1 l of water, spiked with 10 μl of the concentrated standard mixture, at pH 6.5, was passed through the cartridge at 30–40 ml/min under vacuum. Then, it was dried by sucking air for 30 min.

Compounds retained in the cartridge were eluted with 2 ml of acetone, 2 ml of acetone–hexane (1:1) and 2 ml of hexane. The eluate was dried on anhydrous sodium sulphate, which was washed with an additional 1-ml volume of each eluting solvent. The combined fractions were concentrated in a rotary evaporator and added with the internal standard, as indicated above.

RESULTS AND DISCUSSION

Fig. 1 shows the separation of the pesticides at 0.5 mg/l. All the pesticides are basically resolved at the baseline.

In a multiresidue method, the components of the sample under investigation and the standard sample may not always be at the same concentration. Therefore, to confirm that results can be extrapolated from one concentration to the other, linearity of the NPD responses for all the pesticides, including the internal standard, was studied in the range 0.12–1.00 mg/l (Table I). The results show that the response to the different chemicals is linear in the range studied, with correlation coefficients between 0.996 and 1.000.

A sample at a concentration of 0.5 mg/l, *i.e.* in the linear range, was injected eight times to determine the repeatability of the response. The results presented in Table II are expressed as areas relative to that of propiconazole. As can be seen, relative standard deviation (R.S.D.) is in all cases, except for fonofos, below 10%, and in general around 6–7%.

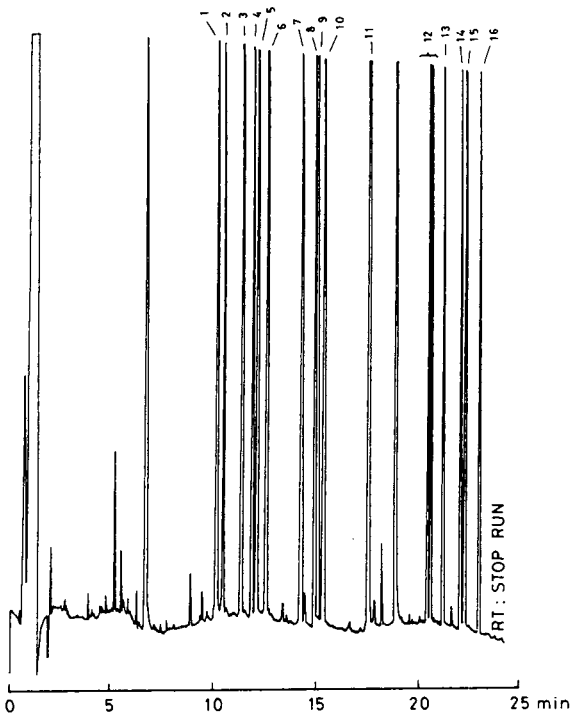

Fig. 1. Gas chromatogram showing the separation of organophosphorous and nitrogen-containing pesticides at about 0.5 mg/l. Volume injected: 1 μl. Chromatographic conditions as explained in the text. Peaks: 1 = dimethoate; 2 = simazine; 3 = fonofos; 4 = diazinon; 5 = formothion; 6 = pirimicarb; 7 = fenitrothion; 8 = malathion; 9 = fenthion; 10 = chlorpyrifos; 11 = methidathion; 12 = propiconazole (internal standard); 13 = phosmet; 14 = azinphos-methyl; 15 = phosalone; and 16 = amitraz.

Although high recovery levels have been reported for different pesticides using C_{18} silica cartridges [14,15], unexpectedly high deviations of the results were obtained in the first assays, so possible losses of the eluates during the concentration step were investigated.

Some preliminary assays were undertaken with three different concentration processes, with or without a keeper (toluene). These were: microcolumn (MC), rotary evaporator (RE) and a gentle steam of helium. The addition of toluene led in general to lower recoveries [16] and to an increase in concentration times. In the RE, the increase in time was slight, from 1 to 1.5 min, but in the MC time was increased from 5 to 20 min. Concentration of the whole eluate in a stream of helium yielded good results but was time-consuming, and finally rejected. Therefore, MC and RE without toluene were studied more in depth.

The different conditions studied showed that the residence time of the solution in the water bath for both the MC and the RE had an influence on the recovery of the different pesticides. Temperatures had to be chosen so that the evaporation time was as short as possible, without being so high as to decompose the compounds. The final temperature for the water bath in MC was therefore 75°C with a total residence time of above 5 min, and for the RE 40°C with a time of about 1 min. In the latter case, the vacuum produced by the pump also had an influence on the concentration process. The higher the vacuum, the shorter the concentration time, but a certain loss of the chemicals was observed. A vacuum of 400 mbar was a good compromise in our conditions.

Table III shows the recoveries in both cases, between 87 and 137% for RE (R.S.D. 1–6%) and between 82 and 131% for MC (R.S.D. 3–14%). Both systems gave similar results. The RE concentration process was finally chosen for

TABLE I

LINEARITY OF THE RESPONSE FOR STANDARD SOLUTIONS AT DIFFERENT CONCENTRATIONS

A = Average of peak areas for three injections; R^2 = correlation coefficient.

	1.00 mg/l		0.50 mg/l		0.25 mg/l		0.12 mg/l		R^2
	A	R.S.D. (%)	A	R.S.D. (%)	A	R.S.D. (%)	A	R.S.D. (%)	
Dimethoate	280.74	19.81	122.50	11.96	62.93	2.80	24.37	17.74	0.997
Simazine	188.30	13.99	85.01	7.68	43.81	8.38	22.40	20.83	0.997
Fonofos	347.30	11.25	156.80	8.89	82.46	8.83	44.67	16.15	0.996
Diazinon	178.44	10.76	80.35	11.23	40.63	5.88	22.80	14.69	0.996
Formothion	225.82	42.72	117.33	10.21	60.37	2.59	31.53	10.89	1.000
Pirimicarb	215.22	12.90	98.07	8.94	52.23	5.07	27.76	15.15	0.997
Fenitrothion	206.18	13.60	97.72	8.27	51.44	8.72	28.54	15.61	0.998
Malathion	175.79	12.06	84.33	8.48	43.76	6.34	24.13	15.12	0.999
Fenthion	165.56	12.55	78.21	8.16	40.02	7.93	22.45	14.11	0.998
Chlorpyriphos	194.07	12.46	90.87	8.44	48.30	7.14	27.24	14.01	0.998
Methidathion	255.00	13.93	122.63	8.46	63.64	5.72	34.86	13.39	0.999
Propiconazole	185.54	21.11	93.32	13.45	54.30	3.35	24.66	3.12	0.998
Phosmet	258.20	17.77	124.36	8.87	62.65	4.06	31.94	7.76	1.000
Azinfos-methyl	223.75	19.63	109.35	7.67	57.05	3.04	28.63	8.11	0.996
Phosalone	239.92	16.91	115.08	8.51	58.11	5.94	31.40	10.58	0.999
Amitraz	150.45	19.91	71.72	6.98	37.45	3.83	20.24	14.64	0.999

this method because of its rapidity, lower R.S.D. and slightly higher recovery levels.

A 1-l volume of water spiked with 0.1 μg of the different pesticides was extracted and determined according to the proposed method. The results (Table IV) show different levels of recovery for the different pesticides: low (0–6%) for dimethoate, formothion, fenthion and amitraz; intermediate (19–56%) for simazine, fonofos and chlorpyriphos; and high (66–91%) for the others, diazinon, pirimicarb, fenitrothion, malathion, methidathion, phosmet, azinphos-methyl and phosalone.

The low recovery levels for dimethoate and formothion may be explained by their high solubility in water (25 and 2.6 g/l, respectively [17]). This indicates that both pesticides were not retained in the cartridge [3,4] and were eluted with the passage of water. Besides, as is known, formothion in aqueous solutions quickly degrades to dimethoate [17]. Better results for both organophosphorous pesticides may be obtained either with more polar beds (*i.e.* active carbon [6]) or with different eluents [14]. Fenthion, although not very water soluble (2 ppm), is extremely soluble in dichloromethane or propan-2-ol (>1 kg/kg), so that other elution processes might yield better results for this pesticide.

TABLE II

REPEATABILITY FOR EIGHT INJECTIONS OF THE STANDARD MIXTURE AT 0.5 mg/l

	$CL^a = \bar{x} \pm \sigma t/n^{1/2}$	R.S.D. (%)
Dimethoate	0.48 ± 0.03	7.65
Simazine	0.69 ± 0.03	4.55
Fonofos	0.74 ± 0.06	10.11
Diazinon	0.46 ± 0.03	6.69
Formothion	0.43 ± 0.03	6.99
Pirimicarb	0.89 ± 0.03	4.55
Fenitrothion	0.49 ± 0.03	7.53
Malathion	0.41 ± 0.03	8.35
Fenthion	0.37 ± 0.02	7.56
Chlorpyriphos	0.49 ± 0.03	6.77
Methidathion	0.80 ± 0.04	6.38
Phosmet	0.43 ± 0.03	6.95
Azinphos-methyl	0.37 ± 0.02	7.02
Phosalone	0.39 ± 0.02	6.28
Amitraz	0.41 ± 0.01	3.41

[a] Confidence interval of the average. Peak areas relative to that of propiconazole. σ = Standard deviation; t = Student's t test for $\alpha = 0.05$.

TABLE III

RECOVERY LEVELS FROM THE CONCENTRATED ELUATE MIXTURE USING MC AND RE

	MC		RE	
	CL[a]	R.S.D. (%)	CL	R.S.D. (%)
Dimethoate	130.58 ± 59.13	14.48	136.95 ± 4.48	1.78
Simazine	94.18 ± 18.73	6.36	102.24 ± 2.37	1.26
Fonofos	86.21 ± 7.64	2.83	93.08 ± 2.32	1.36
Diazinon	86.95 ± 7.57	2.78	98.05 ± 1.87	1.04
Formothion	112.79 ± 34.70	9.83	124.85 ± 6.33	2.76
Pirimicarb	86.17 ± 11.08	4.11	94.55 ± 3.09	1.78
Fenitrothion	87.44 ± 8.13	2.97	97.94 ± 2.14	1.19
Malathion	86.42 ± 10.67	3.95	94.30 ± 2.55	1.47
Fenthion	81.56 ± 7.86	3.08	91.48 ± 6.23	3.71
Chlorpyriphos	85.45 ± 7.30	2.73	94.42 ± 1.35	0.78
Methidathion	87.84 ± 11.54	4.20	96.05 ± 1.74	0.99
Phosmet	91.45 ± 18.44	6.45	99.71 ± 3.15	1.72
Azinphos-methyl	92.54 ± 20.71	7.51	102.02 ± 3.68	1.97
Phosalone	90.20 ± 18.05	6.40	96.45 ± 2.42	1.36
Amitraz	85.15 ± 19.16	7.19	86.71 ± 9.30	5.84

[a] Confidence interval of the average, as in Table II; $n = 5$ for MC and $n = 4$ for RE. Each replicate was injected three times.
[b] Relative standard deviation ($\sigma/\bar{x} \cdot 100$).

Amitraz has been reported to be unstable at pH < 7 [17].

Other authors [18,19] have compared different methods of extraction and, although there is a general agreement about the slightly higher recovery of the liquid–liquid method, it is also generally accepted that it presents many disadvantages that may be avoided by using the SPE process, whose different steps are studied in this paper.

TABLE IV

RECOVERY LEVELS FROM 1 l OF WATER SPIKED WITH 0.1 μg OF EACH PESTICIDE

	CL[a]	R.S.D. (%)
Dimethoate	3.48 ± 7.67	182.77
Simazine	39.14 ± 15.14	32.90
Fonofos	18.75 ± 13.06	64.86
Diazinon	90.64 ± 15.81	27.50
Formothion	0.25 ± 0.65	387.30
Pirimicarb	85.67 ± 16.88	26.58
Fenitrothion	74.06 ± 11.69	22.76
Malathion	66.12 ± 14.76	25.22
Fenthion	0.80 ± 1.14	211.03
Chlorpyriphos	55.73 ± 9.02	26.49
Methidathion	69.77 ± 15.35	23.34
Phosmet	66.20 ± 7.41	17.67
Azinphos-methyl	82.00 ± 8.45	15.98
Phosalone	68.82 ± 16.65	36.29
Amitraz	6.16 ± 7.31	172.11

[a] Confidence interval of the average, as in Table II; $n = 5$ and each replicate was injected three times.

ACKNOWLEDGEMENTS

The authors thank the Dirección General de Investigación Científica y Técnica (DGICYT) for its financial support (Project No. NAT91-0407). Ms. Dolores Maroto is acknowledged for her technical assistance.

REFERENCES

1 *EC Drinking Water Directive (80/778/EEC)*, European Community, Brussels.
2 A.J. Cessna, R. Grover, L.A. Kerr and M.L. Aldred, *J. Agric. Food Chem.*, 33 (1985) 504.
3 *Standard Methods for the Examination of Water and Wastewater*, American Public Health Association, Baltimore, MD, 16th ed., 1985, p. 538.
4 *Test Method 608, Organochlorine Pesticides and PCBs*, Environmental Monitoring Systems Laboratory–US Environmental Protection Agency, Cincinnati, OH, 1984.

5 J. Sherma and W. Bretschneider, *J. Liq. Chromatogr.*, 13 (1990) 1983.
6 A. Di Corcia and M. Marchetti, *Anal. Chem.*, 63 (1991) 580.
7 L. Torreti, A. Simonella, A. Dossena and E. Torreti, *J. High Resolut. Chromatogr.*, 15 (1992) 99.
8 L.M. Davì, M. Baldi, L. Penazzi and M. Liboni, *Pestic. Sci.*, 35 (1992) 63.
9 B. Edelmann, W. Dedek, L. Weil and B. Niessner, *Fresenius' J. Anal. Chem.*, 343 (1992) 148.
10 J.C. Moltó, Y. Picó, G. Font and J. Mañes, *J. Chromatogr.*, 555 (1991) 137.
11 P.R. Loconto and A.K. Gaind, *J. Chromatogr. Sci.*, 27 (1989) 569.
12 W.E. Johnson, N.J. Fendinger and J.R. Plimmer, *Anal. Chem.*, 63 (1991) 1510.
13 *Analytical Methods for Pesticide Residues in Foods*, Ministry of National Health and Welfare, Ottawa, 2nd ed., 1986, pp. 12.25–12.26.
14 H.J. Borburgh and W.E. Hammers, *Toxicol. Environ. Chem.*, 35 (1992) 79.
15 G.A. Junk, M.J. Avery and J.J. Richard, *Anal. Chem.*, 60 (1988) 1347.
16 A.S.Y. Chau, B.K. Afghan and J.W. Robinson, *Analysis of Pesticides in Water*, Vol. 1, CRC Press, Boca Raton, FL, 1982, p. 63.
17 *The Pesticide Manual. A World Compendium*, British Crop Protection Council, Thornton Heath, 8th ed., 1987, 1081 pp.
18 G.H. Tan, *Analyst*, 117 (1992) 1129.
19 A. Geissler and H.F. Schöler, *Chemosphere*, 23 (1991) 1029.

Journal of Chromatography A, 655 (1993) 133–140
Elsevier Science Publishers B.V., Amsterdam

CHROM. 25 045

Gas chromatographic screening of organic compounds in urban aerosols

II. Changes in hydrocarbon composition during storage

Merce Aceves

Environmental Control Service, Entitat Metropolitana de Barcelona, Carrer 62, 420 Edifici A Zona Franca, 08004-Barcelona, Catalonia (Spain)

Joan O. Grimalt*

Department of Environmental Chemistry (C.I.D.-C.S.I.C.), Jordi Girona 18, 08034-Barcelona, Catalonia (Spain)

ABSTRACT

Gas chromatographic and gas chromatographic–mass spectrometric analyses of inadequately stored filters and hydrocarbon extracts of urban aerosols have shown the occurrence of microbially mediated transformation processes giving rise to hydrocarbon patterns different from the original composition of the samples. In all cases, a strong decrease in the concentration of the unresolved complex mixture of hydrocarbons is observed. The modifications also involve the formation of mixtures of C_{29}–C_{34} iso- and anteisoalkanes and modal distributions of C_{15}–C_{20} *n*-alkanes with no even/odd carbon number preference in vials and filters, respectively. These *n*-alkane distributions may even dominate the chromatographic profiles of the aliphatic hydrocarbon fractions corresponding to long-term stored filters. Decay of the polycyclic aromatic hydrocarbons of lower stability, *e.g.* 4(H)-cyclopenta[*cd*]pyrene and benzo[*a*]pyrene, is also observed in the filters. These *de novo*-produced *n*-alkane and iso- and anteisoalkane distributions occur at the initial stages of transformation, providing a useful tool for the detection of this type of post-sampling process.

INTRODUCTION

Very little attention has been paid to modifications of hydrocarbon composition in environmental samples after storage. In general, there is a wide consensus that the samples should be deep frozen (*ca.* −20°C) immediately after collection, taking stringent precautions to prevent external contamination. However, the information available on possible changes in composition under these storage conditions, or when they are not fulfilled, is very limited. Furthermore, the few studies described in the literature only concern sedimentary materials [1,2]. To the best of our knowledge post-sampling transformations of organic constituents in stored aerosol samples have not been reported.

These aspects are relevant in monitoring studies, in which samples may be regularly collected at distant places, and in some cases the filters may not be stored deep frozen immediately after collection. A correct evaluation of the analytical results corresponding to these cases requires the availability of safety criteria based on knowledge of the changes in composition that may be produced under these accidental circumstances. On the other hand, an additional activi-

* Corresponding author.

0021-9673/93/$06.00

ty of many of these monitoring studies is the storage of representative samples to keep a record of the temporal evolution of the environment of interest. These deep-frozen filters may provide information in subsequent additional studies. Examples of retrospective investigations based on the materials kept in these archives are available in the literature, *e.g.* asthma epidemics studies [3,4], but again reference data on possible storage-related modifications are needed for a correct interpretation of the results.

Since 1985 we have regularly monitored the composition of solvent-extractable compounds in the air from Barcelona (Catalonia, Spain) using methods based on gas chromatography (GC) and GC coupled to mass spectrometry (MS). As described in the previous study of the present series [5], this regular sampling and analysis affords a detailed knowledge of the distributions of the major lipids among the atmospheric particulates of the city. Aliquots of the filters analysed were stored at −20°C to provide a temporal record for subsequent investigations.

In the course of some retrospective studies, comparison of the hydrocarbon composition (aliphatics and aromatics) in filter aliquots analysed after sampling or after long storage times showed that major transformations occurred in cases of accidental storage at ambient temperature. In addition to these, changes were also observed in the vials in which the hydrocarbon fractions were stored, and in this case the transformation could occur even in deep-frozen conditions. Interestingly, the modifications produced in the filters or vials were rather uniform, leading to well-defined hydrocarbon patterns. These patterns were very different from the original distributions. However, they could easily be confused with real atmospheric mixtures.

The hydrocarbon patterns generated in these post-sampling transformations are described in the present study. They are compared with the original mixtures and the main features for their recognition are discussed. These results provide evidence of post-sampling transformation reactions as possible modifiers of the original molecular composition in aerosols.

EXPERIMENTAL

Materials

Pestipur-grade dichloromethane was purchased from Mallinckrodt (Paris, TX, USA). Chromatography-quality *n*-hexane, methanol, isooctane, neutral silica gel (Kieselgel 40, 70–230 mesh) and alumina (aluminium oxide 90 active, 70–230 mesh) were from Merck (Darmstadt, Germany). The Soxhlet cartridges were from Schleicher & Schürl (Dassel, Germany). The glass microfibre filters were purchased from Whatman (Maidstone, UK).

The silica gel, the alumina and the Soxhlet cartridges were extracted with dichloromethane–methanol (2:1, v/v) in a Soxhlet apparatus for 24 h. After solvent evaporation, the silica and the alumina were heated for 12 h at 120 and 350°C, respectively. A total of 5% (w/w) Milli-Q-grade water was then added to the chromatographic adsorbents for deactivation. The glass-fibre filters were kiln fired for 12 h at 400°C and weighed prior to sampling.

The purity of the solvents was checked by concentrating under vacuum 100 ml of solvent to 10 μl for GC analysis. Blank requirements were as follows: splitless injection of 2 μl should result in chromatograms with no unresolved GC envelope and only few peaks, representing up to 1 ng in terms of their flame ionization detector response. This threshold, under the above dilution factor, is equivalent to less than 0.02 pg/m^3 when referred to 100 ml of solvent used for the extraction of one-third of a filter that corresponds to 1000 m^3 of air sample.

Sampling, extraction and fractionation

The air samples (1200 m^3 and 50 m^3/h) were taken with a High-Vol pumping system (CAV-P; MCV, Collbato, Catalonia, Spain) equipped with 20.3 × 25.4 cm glass microfibre filters (catalogue No. 1820866 Whatman, Maidstone, UK). After sampling the filters were frozen at −20°C until analysis in the laboratory. One-third of each filter was Soxhlet extracted with 100 ml of dichloromethane for 24 h. The extract was vacuum and nitrogen evaporated until almost dry and diluted to 0.5 ml with *n*-hexane. Then, it was

fractionated by column chromatography according to previously established methods [6]. These methods were scaled down to suitable amounts of solvents and packings according to the small lipid content of the filters. A column filled with 1 g each of 5% water-deactivated alumina (top) and silica (bottom) was used. The aliphatic hydrocarbons were obtained in the first fraction (4 ml of *n*-hexane) and the aromatic hydrocarbons were collected in the second fraction (4 ml of 20% dichloromethane in *n*-hexane). These fractions were vacuum and nitrogen concentrated until almost dry and redissolved with isooctane.

Instrumental analysis

The samples were analysed by GC and GC–MS. These analyses were performed, respectively, with a Carlo-Erba 5300 system equipped with a flame ionization detector, and with a Hewlett-Packard 5970 system provided with an HP-5994A data aquisition system. A 30 m × 0.25 mm I.D. DB-5 (film thickness 0.2 μm) fused-silica capillary column (J&W Scientific, Folsom, CA, USA) was used in all cases. The GC analyses were performed with an oven temperature programme of 60–300°C at 6°C/min, injector and detector temperatures of 280 and 330°C, respectively, and hydrogen as carrier gas (50 cm/s). The oven temperature programme for the GC–MS analyses was from 60 to 280°C at 6°C/min, injector and transfer line temperatures were 280 and 300°C, respectively, and helium was the carrier gas (50 cm/s). Data were acquired in the electron impact (EI) mode (70 eV), scanning from 40 to 600 mass units at 1 s per decade. In both cases the injector was in the splitless mode (1 μl, hot needle technique), the split valve being closed for 35 s.

RESULTS AND DISCUSSION

Glass-fibre filters

As indicated above, the changes in composition observed in the filters stored at ambient temperature exhibit rather uniform trends leading to characteristic GC profiles. These profiles are illustrated in Fig. 1, in which the aliphatic

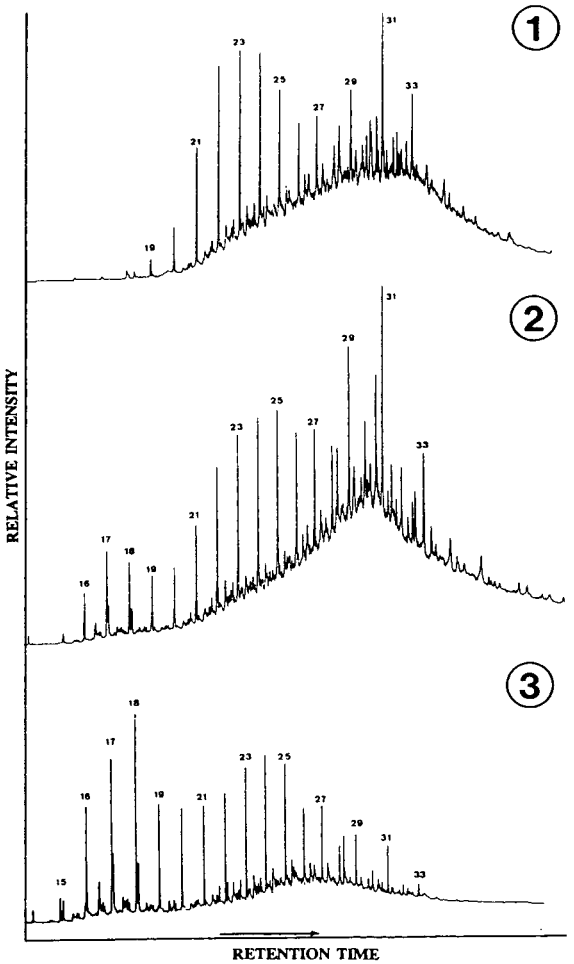

Fig. 1. GC profiles of the aliphatic hydrocarbon mixtures corresponding to three glass-fibre filter aliquots analysed (1) a few days after deep-frozen storage, (2) after 1 year and (3) after 2 years of ambient temperature storage. Peak numbers refer to *n*-alkane carbon number. Pr = Pristane; Ph = phytane.

hydrocarbon composition of filter aliquots analysed a few days after collection and after 1 and 2 years of storage at ambient temperature are compared.

The GC profile of the aliquot analysed after collection is dominated by a bimodal *n*-alkane distribution ranging between the C_{19} and C_{33} homologues with no even/odd carbon number predominance in the first mode (C_{19}–C_{27}) and with odd-to-even carbon number predominance in the second mode (C_{27}–C_{33}). These *n*-alkanes

overlie an important unresolved complex mixture (UCM) of hydrocarbons, which constitutes one of the most distinct features of this type of sample. Two types of sources are represented in this aliphatic hydrocarbon fraction, the first modal distribution of *n*-alkanes and the UCM correspond to petrogenic residues and vehicular exhausts [7,8], and the *n*-alkanes defining the second mode originate from higher plant waxes [9].

The filter aliquot stored at ambient temperature for 2 years exhibits a very distinct hydrocarbon composition (Fig. 1). An additional modal distribution of C_{15}–C_{20} *n*-alkanes is now present and dominates the whole GC profile. This distribution of shorter chain length homologues exhibits no even/odd carbon number preference and occurs together with pristane and phytane. The other major change concerns the practical disappearance of the UCM. The aliquot corresponding to 1 year of storage at ambient temperature represents an intermediate situation in which the C_{15}–C_{20} *n*-alkane mode is present but not dominant and a considerable UCM can still be observed. In quantitative terms, the *n*-alkanes in the aliquots corresponding to 1 and 2 years of storage represent about 70 and 50% of those present in the original mixture.

The modal *n*-alkane distribution eluting in the C_{15}–C_{20} range has not been observed in any of the aerosol samples collected in Barcelona and stored in deep-frozen conditions [5]. In fact, it may rarely be found in high proportion in aerosols because these lower-molecular-mass hydrocarbons are usually associated to the gas phase [10]. This type of distribution is characteristic of microbial inputs [11,12], and its occurrence may be indicative of microbially mediated post-sampling transformations. Microbial reworking of hydrocarbon mixtures during storage has also been observed in sediment samples although other *n*-alkane distributions were produced [1,2].

The other distinct feature of the filter samples stored at ambient temperature is the large decrease in UCM. This transformation contrasts with the biodegradation trends observed in many natural sedimentary environments where microbial activity is reflected in *n*-alkane removal and the preservation of the UCM [13–15].

The changes in aromatic hydrocarbon content of these filter aliquots are illustrated in Fig. 2 by comparison of the GC profiles corresponding to analyses performed after collection and after 1 year of ambient temperature storage. The hydrocarbon mixtures displayed in Fig. 2A are characteristic of those found in the atmosphere of Barcelona [5]; the abundance of catacondensed structures and the predominance of parent over alkylated homologues are indicative of pyrolytic

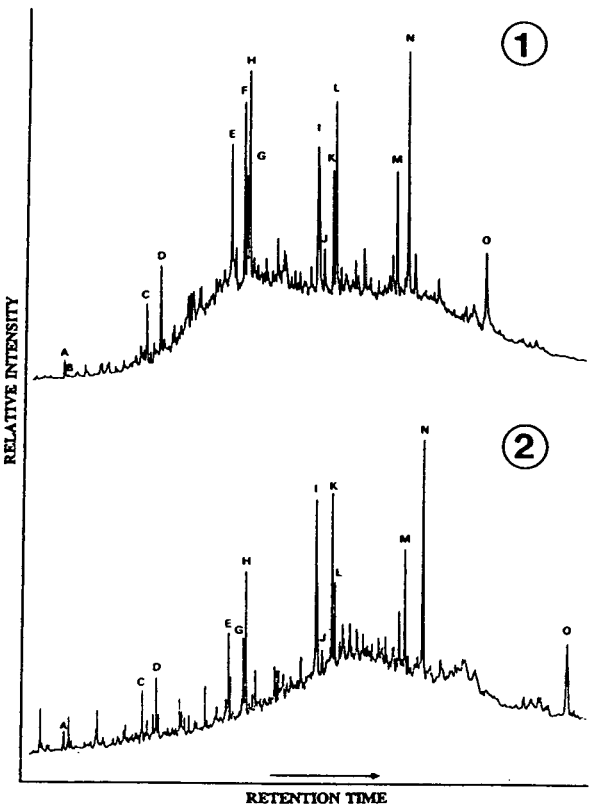

Fig. 2. GC profiles of the aromatic hydrocarbon mixtures corresponding to glass-fibre filter aliquots analysed (1) after a few days of deep-frozen storage and (2) after 1 year of ambient temperature storage. Lettered peaks are as follows: A = phenanthrene; B = anthracene; C = fluoranthene; D = pyrene; E = benzo[*ghi*]fluoranthene; F = 4(H)-cyclopenta-[*cd*]pyrene; G = benz[*a*]anthracene; H = chrysene/triphenylene; I = benzo[*b*/*j*]fluoranthene; J = benzo[*a*]fluoranthene; K = benzo[*e*]pyrene; L = benzo[*a*]pyrene; M = indeno[1,2,3-*cd*]pyrene; N = benzo[*ghi*]perylene; O = coronene.

origins [16,17]. The main differences between the two profiles (Fig. 2A and B) concern the disappearance of 4(H)-cyclopenta[*cd*]pyrene and the decrease in benzo[*a*]pyrene in the aliquot stored at ambient temperature. The lower concentration of these two compounds is likely to reflect their lower stability, especially in the case of 4(H)-cyclopenta[*cd*]pyrene [18,19]. In atmospheres with a high content of reactive gases such as O_3 or NO_x these compounds may even be degraded on the filter surface during collection [20,21]. However, extended degradation of aromatic hydrocarbons also involves the decay of benz[*a*]anthracene with respect to chrysene [18,22], which is not observed in the GC profiles of Fig. 2.

Vials

The post-sampling changes in composition of aliphatic hydrocarbons observed in the vials also lead to characteristic GC profiles which are different from those observed in the filters. These profiles are illustrated in Fig. 3, in which the aliphatic hydrocarbons from two Barcelona sampling stations, Molina and Poble Nou, are compared with the distributions found in the same vials after 1 year of storage at ambient temperature. The chromatograms corresponding to long-term stored vials exhibit the same pattern, irrespective of the differences in composition of the original mixture. As described for the filters, the UCM has disappeared but now no modal profile of low-carbon-number *n*-alkanes is generated. Conversely, the final mixture of this type of transformations contains a distribution of C_{23}–C_{37} *n*-alkanes with low odd-to-even carbon number predominance and a distribution of C_{29}–C_{34} iso- and anteisoalkanes. In quantitative terms, the total *n*-alkanes in the vials stored at ambient temperature represent between 60 and 80% of those in the original mixture.

The distributions of C_{29}–C_{34} iso- and anteisoalkanes also exhibit a uniform pattern that is shown in Fig. 4 by enhancement of the GC–MS

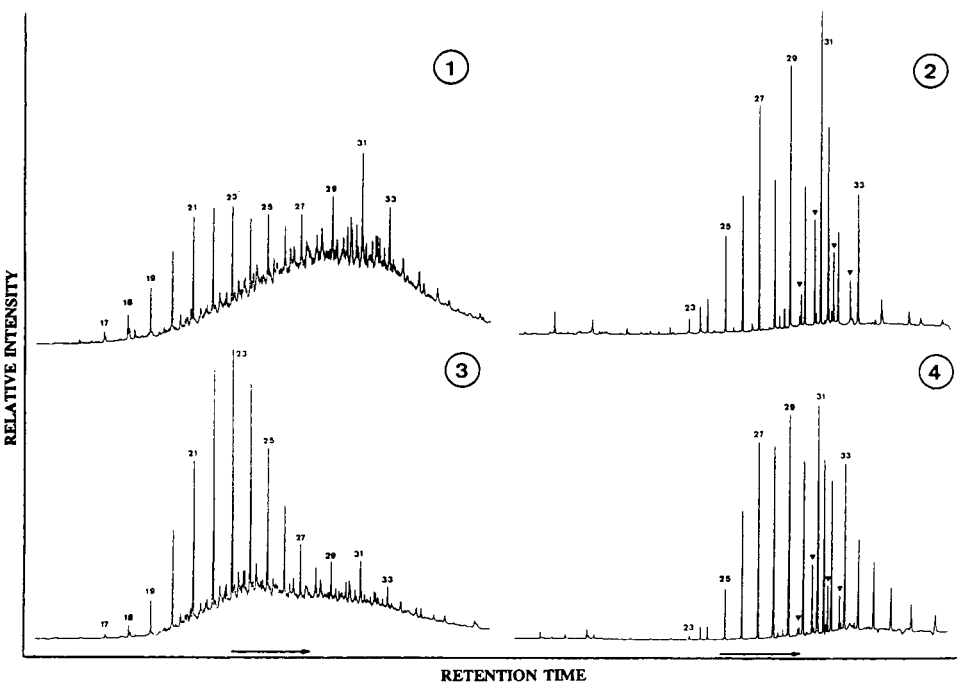

Fig. 3. GC profiles of the aliphatic hydrocarbon extracts from Molina (1 and 2) and Poble Nou (3 and 4) sampling stations stored in vials kept at −20°C (1 and 3) or ambient (2 and 4) temperature. Peak numbers refer to *n*-alkane carbon number. ▼ = Iso- and anteisoalkanes.

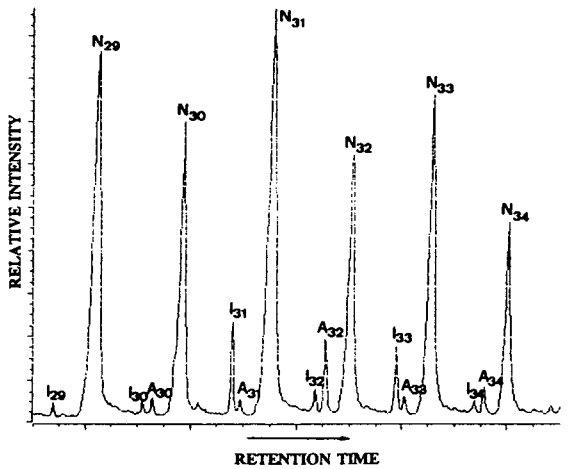

Fig. 4. Enhanced GC–MS total-ion current profile showing the composition of the C_{29}–C_{34} iso- and anteisoalkanes produced in the vials during storage. Peak numbers refer to carbon number.

total-ion trace. Representative mass spectra of iso and anteiso homologues are displayed in Fig. 5. The isoalkanes are recognized by their intense $M - C_3H_7$ mass fragment and their distinct $M - CH_3$ peak [23]. The anteisoalkanes exhibit an intense $M - C_2H_5$ fragment together with a characteristic $M - C_4H_9$ ion [24]. Not even traces of these compounds are observed when GC analysis is performed a few days after separation of the aliphatic hydrocarbon fractions by the column chromatography procedure described in the Experimental section.

All these modifications suggest that microbial reworking is again at the origin of the transformation process. In this respect, the occurrence in aquatic environments of distributions of iso- and anteisoalkane homologues with carbon number higher than C_{22} has been attributed to

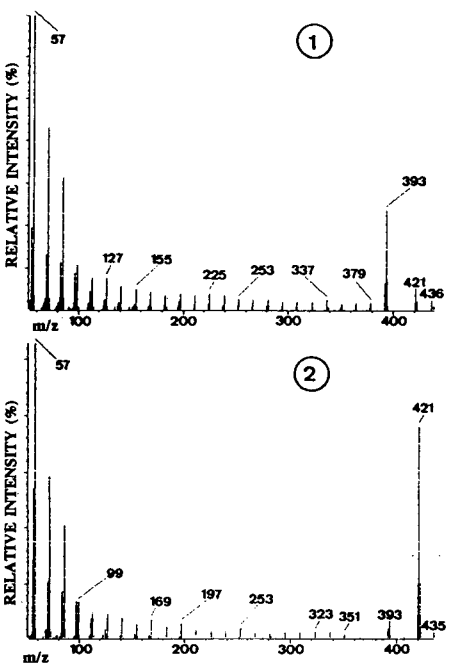

Fig. 5. Mass spectra of (1) isohentriacontane and (2) anteisodotriacontane.

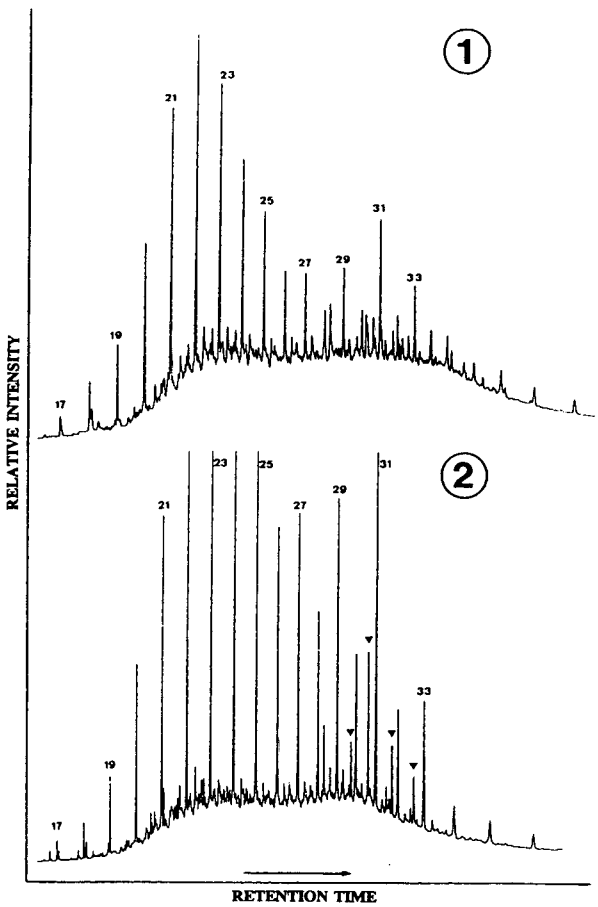

Fig. 6. GC profiles of aliphatic hydrocarbon fractions analysed (1) after separation by column chromatography and (2) after 1 year of storage at −20°C. Peak numbers refer to *n*-alkane carbon number. ▼ = Iso- and anteisoalkanes.

microbial reworking of petrogenic hydrocarbon mixtures [15,25].

These C_{29}–C_{34} iso- and anteisoalkanes are useful for the early identification of post-sampling changes because they may be detected at initial stages of the reworking process. This is illustrated in Fig. 6, in which the GC profiles corresponding to one aliphatic hydrocarbon fraction analysed after column chromatography isolation and after 1 year of storage at −20°C are shown. The general composition of *n*-alkanes has not been modified substantially, but these branched alkanes may already be identified. It is not the purpose of the present study to ascertain whether or not the differences between these two chromatographic traces correspond to processes effectively occurring at −20°C. It cannot be excluded that this sample was taken out of the freezer for very short periods. The aspect to be emphasized is the availability of two series of hydrocarbons indicative of changes in composition during storage that can be identified at early stages of transformation.

CONCLUSIONS

Major changes in the hydrocarbon composition of aerosol samples are observed in filter particulates and vial-contained extracts when the conditions of deep-frozen storage are not fulfilled. The modifications follow rather uniform trends, involving a strong depletion of the UCM and the generation of new distributions of straight-chain or branched alkanes, which suggests that the processes are mediated by the activity of microorganisms.

In the filters, a new distribution of C_{15}–C_{20} *n*-alkanes with no even/odd carbon number preference is produced. This distribution may dominate the GC profile of the hydrocarbon extract and is already observed at the initial stages of ambient temperature transformations. The polycyclic aromatic hydrocarbon mixtures of these filters exhibit a decrease of the less stable compounds such as the disappearance of 4(H)-cyclopenta[*cd*]pyrene and the decay of benzo-[*a*]pyrene.

In the vials, both the UCM and the lower carbon number *n*-alkanes are depleted, which results in distributions of C_{29}–C_{34} *n*-alkanes with low odd-to-even carbon number preference. These distributions occur together with a characteristic mixture of C_{29}–C_{34} iso- and anteisoalkanes which is not present in the original hydrocarbon fractions and can be detected at the initial stages of transformation.

Early stages of post-sampling modifications of atmospheric hydrocarbons due to inadequate storage may therefore be detected by the presence of C_{15}–C_{20} *n*-alkanes with no even/odd carbon number preference in the filters and C_{29}–C_{34} iso- and anteisoalkanes in the vial-contained extracts.

ACKNOWLEDGEMENT

We are thankful to P. Teixidor, LIFS, Faculty of Geology, University of Barcelona, for her help in some GC–MS analyses.

REFERENCES

1 Y. Debyser, *Geochim. Cosmochim. Acta*, 39 (1975) 531.
2 J.O. Grimalt, E. Torras and J. Albaiges, *Org. Geochem.*, 13 (1988) 741.
3 J.M. Anto, J. Sunyer, J.O. Grimalt, M. Aceves and Ch.E. Reed, *N. Engl. J. Med.*, 321 (1989) 1128.
4 M. Aceves, J.O. Grimalt, J. Sunyer, J.M. Anto and Ch.E. Reed, *J. Allergy Clin. Immunol.*, 88 (1991) 124.
5 M. Aceves and J.O. Grimalt, *J. Chromatogr.*, 607 (1992) 261.
6 M. Aceves, J.O. Grimalt, J. Albaiges, F. Broto, L. Comellas and M. Gassiot, *J. Chromatogr.*, 436 (1988) 503.
7 B.R.T. Simoneit, *Atmos. Environ.*, 18 (1984) 51.
8 C.V. Hampton, W.R. Pierson, D. Schuetzle and T.M. Harvey, *Environ. Sci. Technol.*, 17 (1983) 699.
9 G. Eglinton and R. Hamilton, *Science*, 156 (1967) 1322.
10 A. Rosell, J.O. Grimalt, M.G. Rosell, X. Guardino and J. Albaiges, *Fresenius' J. Anal. Chem.*, 339 (1991) 689.
11 J. Han and M. Calvin, *Proc. Natl. Acad. Sci. U.S.A.*, 64 (1969) 436.
12 C.W. Bird and J.M. Lynch, *Chem. Soc. Rev.*, 3 (1974) 309.
13 W. Giger, M. Reinhardt, C. Schaffner and W. Stumm, *Environ. Sci. Technol.*, 8 (1974) 454.
14 S.C. Wakeham, *Mar. Pollut. Bull.*, 7 (1976) 206.
15 I. Ramos, M. Fuentes, R. Mederos, J.O. Grimalt and J. Albaiges, *Mar. Pollut. Bull.*, 20 (1989) 262.
16 R.E. LaFlamme and R.A. Hites, *Geochim. Cosmochim. Acta*, 42 (1978) 289.
17 B.R.T. Simoneit, *Int. J. Environ. Anal. Chem.*, 29 (1985) 203.

18 R.M. Kamens, J.N. Fulcher and G. Zhishi, *Atmos. Environ.*, 20 (1986) 1579.
19 T. Nielsen, *Atmos. Environ.*, 22 (1988) 2249.
20 F.S.C. Lee, W.R. Pierson and J. Ezike, In A. Bjorseth and A.J. Dennis (Editors), *Polynuclear Aromatic Hydrocarbons: Chemical and Biological Effect*, Battelle Press, Columbus, OH, 1980, p. 543.
21 J. Peters and B. Seifert, *Atmos. Environ.*, 14 (1980) 117.
22 R.M. Kamens, Z. Guo, J.N. Fulcher and D.A. Bell, *Environ. Sci. Technol.*, 22 (1988) 103.
23 E.D. McCarthy and M. Calvin, *Tetrahedron*, 23 (1967) 2609.
24 R.B. Johns, T. Belsky, E.D. McCarthy, A.L. Burlingame, P. Haug, H.K. Schnoes, W. Richter and M. Calvin, *Geochim. Cosmochim. Acta*, 30 (1966) 1191.
25 G. Gassmann, *Mar. Pollut. Bull.*, 13 (1982) 309.

Journal of Chromatography A, 655 (1993) 141–149
Elsevier Science Publishers B.V., Amsterdam

CHROM. 25 035

Preconcentration of samples by steam distillation–solvent extraction at low temperature

Gracia P. Blanch, Marta Herraiz*, Guillermo Reglero and Javier Tabera

Instituto de Fermentaciones Industriales, C.S.I.C., Juan de la Cierva 3, Madrid 28006 (Spain)

ABSTRACT

Operation of a micro steam distillation–solvent extraction (SDE) device in two different modes, namely at reduced pressure and involving the concentration of the dynamic headspace resulting from purging the sample with an inert gas, was investigated. A notable advantage of the proposed micro SDE apparatus is that the use of extraction solvents denser or lighter than the sample solvent is feasible with only one configuration. The modified simplex method was used to improve the performance of the analytical procedure by optimization of several experimental conditions involved in the process.

INTRODUCTION

Sample preparation for the GC analysis of complex mixtures still remains a difficult step that can significantly alter the composition of the sample to be analysed. Obviously, the possibility of introducing qualitative or quantitative changes during sample preparation should be strongly avoided, as eventual losses of important compounds cannot be made up for in a later stage of the analytical procedure. Hence too severe treatments are in general unwise and even the use of extremely mild conditions may be required if thermolabile compounds are present in the sample or degradation products resulting from chemical reactions must be precluded.

The past few years have seen the development of different isolation and concentration techniques involving adsorption, absorption, distillation and extraction [1–4]. However, continuing interest in the investigation of preconcentration methods is engendered by the realization that there is not and probably never will be a single sample preparation procedure that is suitable for all samples under all conditions. Therefore, careful selection of the preliminary isolation process which best suits the nature of the sample and the requirements of the analysis to be carried out is necessary.

Likens and Nickerson [5,6] described an apparatus for continuous steam distillation with constant liquid–liquid extraction of the distillate (SDE). Several modifications of the original design have subsequently been proposed [7–9] and also a micro version that permits operation with small amounts of extraction solvents without requiring enrichment by evaporation has been reported [10,11]. This micro SDE version has already been employed for the preconcentration of different types of samples [12–17].

Recently we proposed a further modification of the micro SDE device [18] which allows the use of solvents denser or lighter than the sample solvent with only one configuration, since both the distillation solvent and distillation sample arms enter the mixing chamber at the same height. The enlarged volume of this chamber, placed at the top of the apparatus, contributes to effective mixing of the sample and the extraction solvent vapour.

A further interesting feature of the device is

* Corresponding author.

0021-9673/93/$06.00

the introduction of a water-jacket concentric with a cold finger, which significantly increases the condenser surface available in the former SDE micro version [10,11]. As a result, the cooling system allows losses of the most volatile compounds to be minimized. Operation at normal pressure was optimized and excellent recoveries were, in general, obtained for several compounds of different polarities, volatilities and water solubilities [18].

As far as optimization procedures for analytical techniques are concerned, the use of the sequential simplex method [19] has already proved its usefulness for adjusting the controlling variables affecting a particular process so that some results achieve the best possible level [18,20–24].

In this work, we investigated the scope of the new micro SDE for operation both at reduced pressure or involving the concentration of the dynamic headspace from the sample in the aeration mode of operation [3]. For this purpose, optimizations of the experimental conditions involved in both approaches were accomplished by using the modified simplex procedure [25].

EXPERIMENTAL

Steam distillation–solvent extraction

The SDE apparatus used in this study was constructed in our laboratory by modifying the design of Godefroot *et al.* [10]. A detailed description of the new version was presented in a previous paper [18].

The test mixture consisted of fourteen compounds covering a wide range of polarity and volatility (see Table III for composition). A stock solution containing about 7.14% of each pure component was stored at −30°C in the dark. Test solutions having concentrations of 1 mg/l of each compound were obtained by adding an appropriate volume of the stock solution to 100 ml of water purified in a Milli-Q system (Millipore).

All reagents were of GC grade and were purchased from Merck (Darmstadt, Germany) (isoamyl acetate, ethyl hexanoate, ethyl octanoate, benzaldehyde, diethyl succinate, ethyl dodecanoate, 2-phenylethanol), Aldrich Chemie (Steinheim, Germany) (1-hexanol, linalool, α-terpineol, γ-decalactone) and Sigma (St. Louis, MO, USA) (β-ionone, ethyl tetradecanoate).

In all instances, *ca.* 100 ml of test solution (containing 1 mg/l of each compound) were heated on a water-bath and 2 ml of freshly doubly distilled dichloromethane (Merck) distilled at the same time. Cleaned boiling chips were added to the sample and solvent flasks. Vapours of sample and solvent were condensed by the cold finger and the concentric water-jacket, as mentioned above. When enrichment was complete, all the steam distillable material present in 100 ml of the test solution was collected in *ca.* 2 ml of dichloromethane. Consequently, concentration by a factor of 50 was finally achieved.

Methyl octanoate (Fluka, Buchs, Switzerland) (0.1 μl) and methyl decanoate (Fluka) (0.1 μl) were added as internal standards to the extracted compounds.

After finishing the extraction time, a further concentration step was not necessary [10,11,18] and the GC analysis was subsequently performed by sampling a 2-μl volume of the obtained extract.

The SDE was rinsed with acetone (Merck, Darmstadt, Germany) and Milli-Q-purified water between consecutive runs.

Preparation of banana extracts

Ripe peeled bananas (Musa cavendishii var. enana) from the local market (about 50 g), the same amount of $(NH_4)_2SO_4$ (enzymic inhibition) (26) and 100-ml of water purified in a Milli-Q system were homogenized. The sample was placed in a 500-ml flask and a 2-ml volume of twice-distilled dichlorometane was used as extracting solvent.

After finishing the enrichment step a 0.2-μl volume of methyl octanoate (internal standard) was added to the extracted compounds and subsequently 0.5-μl of the banana extract was chromatographed.

The SDE operation was performed in experimental conditions selected after the optimization procedure described below.

Capillary gas chromatography–mass spectrometry

All samples were analysed by gas chromatography using a 50 m × 0.22 mm I.D. fused-silica capillary column (SGE, Ringwood, Australia) coated with a 0.25-μm layer of cross-linked BP-21 (FFAP). A Perkin-Elmer Model 8500 gas chromatograph provided with a Perkin-Elmer PTV injector and a flame ionization detector, operated at 250°C, were used. The equipment was coupled to a Model 2600 chromatography software system (Nelson Analytical). Helium at 40 p.s.i.g. (1 p.s.i. = 6894.76 Pa) served as the carrier gas.

The temperature of the chromatographic column was first kept at 70°C for 5 min, then raised at 5°C/min to 180°C. This final temperature was held for 15 min. In all instances, injections were carried out in the cold split (1:10) mode by maintaining the vaporizer at 30°C on injection. This temperature was increased at 14°C/s to 250°C.

To confirm peak identification, the gas chromatograph was linked to a Perkin-Elmer ITD-50 ion-trap detector (electron impact, 70 eV). The column and chromatographic conditions were the same as above.

Compounds were identified by comparison of spectra with those of the NBS (National Bureau of Standards) library. Moreover, most components were identified by matching the spectral data with those of authentic reference compounds analysed under identical conditions.

Simplex optimization

According to Spendley *et al.* [27], the initial experimental design (initial simplex) was established after fixing the initial values for each of the selected variables (termed factors). The experimental points defining the first simplex are thus located by establishing values for the factors such that the points lie at the vertices of a regular simplex of the required dimensionality.

Eqn. 1 was used to calculate physical values of the factors from their mathematical coordinates:

$$X_{phys} = X_0 + X_{mat}s \quad (1)$$

where X_{phys} is the physical value of variable X, X_{math} the corresponding mathematical coordinate, X_0 its base level (starting physical value) and s is the step size.

The selection of the factors to be optimized was based on a prior knowledge of the system or on preliminary experimentation. The step size was chosen arbitrarily but it was intended that the step should produce for each factor a comparable change in response.

After running the first simplex, the worst experimental value was eliminated and a new vertex was defined to form a new simplex with the retained vertices. This new vertex was obtained by modifying the simplex in the direction opposite to the undesirable result. If we define C as the centroid of the retained vertices in the movement and V_i as the rejected vertex, then the coordinates of the new vertex (V_i^*) can be calculated from the equation

$$V_i^* = C + \alpha(C - V_i) \quad (2)$$

where α is a factor by which the volume of the simplex is changed by the operations of reflection ($\alpha = 1$), contraction ($\alpha < 1$) or expansion ($\alpha > 1$).

Subsequently, the simplex design is applied in the direction given by the rules of movement of the modified simplex until the region of the optimum is located. In all instances, a minimum of two replicates of each analysis were performed.

RESULTS AND DISCUSSION

Table I shows the variables, base levels and step sizes considered in the optimization study of the micro SDE device operated at reduced pressure.

In order to evaluate how each modification of the selected variables affects the final results, the response value (R) defined in eqn. 3 was calculated after each experimental run.

$$R = \frac{\sum(C_i - C_i^0)^2}{n} + 800T \quad (3)$$

where C_i is the concentration of the considered compound, C_i^0 is the expected concentration of the same compound, n is double the number of replicates performed for each experimental point and T is the sample heating bath temperature. It

TABLE I

VARIABLES, BASE LEVELS AND STEP SIZES CONSIDERED IN THE OPTIMIZATION STUDY OF THE SDE PROCEDURE AT REDUCED PRESSURE

Variable	Base level	Step size
Sample heating bath temperature, T (°C)	75	10
Solvent heating bath temperature, T_s (°C)	7	10
Coolant temperature, T_c (°C)	−7	5
Extraction time, t (min)	90	15
Pressure, P (mmHg; 1 mm Hg = 133.322 Pa)	206	50

should be noted that differences between the concentration of a compound and its corresponding expected value were squared to magnify errors affecting quantification. On the other hand, it was intended that the simplex should progress towards low sample heating bath temperatures since our objective was to develop a procedure suitable for the preconcentration of thermolabile compounds. For this purpose, the temperature was weighted with a factor of 800, which was established from previous experimentation. Obviously, the simplex optimization refers here to the minimization of the response function. In all cases, two different internal standards (methyl octanoate and methyl decanoate) were used to quantify each compound in each replicate.

Data obtained through the simplex optimization procedure are given in Table II. Previous considerations concerning the constraints for the system (*i.e.*, the boundaries on the variables which cannot or should not be crossed) suggested that we should not accept values higher than 90°C for the sample heating bath temperature in order to avoid artefact formation. Coolant temperatures lower than −10°C were also considered to be outside the experimental region owing to the temperature limitation of the equipment. According to the rules of the modified simplex method, any step that represents a boundary violation should be rejected without experimentation and the response at this point is considered to be the worst in the corresponding simplex.

With regard to the data in Table II, several observations can be made. After performing the initial simplex (defined by the first six experiments in Table II), vertex 4 was rejected as it provided the worst (highest) value of the response function. The new simplex was then formed by using the retained vertices besides that resulting from reflecting the rejected vertex. As can be seen in Table II, at vertex 7 the response is the best in the simplex, so it is expanded using $\alpha = 2$, thus resulting in vertex 8 [24,25]. Further expansions with different values of α give rise to vertices 18 and 19. In contrast, vertices 11, 14, 16, 21 and 24 resulted from different contractions. At vertices 10, 15, 20 and 23, the response was the worst in the new simplex and also worse than the worst response in the previous simplex, so the simplex was contracted and its direction was reversed ($\alpha = -0.5$). However, at vertex 13, the response was the worst in the new simplex but not worse than the worst response in the previous simplex, so the simplex was contracted but its direction was not reversed ($\alpha = 0.5$). It should be noted that experiment 10 was treated as a constraint owing to the inadequate rate of solvent evaporation, and therefore it was considered to produce the worst response in the simplex.

The simplex optimization procedure was stopped after vertex 24 because from vertex 18 onwards insignificant improvements in the response value were obtained, suggesting that the optimum had been attained. Finally, the experimental conditions defining experiment 18 (*i.e.*, sample heating bath temperature 84.2°C, solvent heating bath temperature 18.8°C, coolant temperature −7.7°C, extraction time 93 min, pressure 149 mmHg) should be considered as the most suitable, as they provide the lowest response value. Under these conditions, the sample temperature is actually 60°C.

Table III gives the recoveries and the relative standard deviations (R.S.D.s) obtained for the extracted compounds under the optimized conditions for the SDE operated at reduced pressure. It is worth emphasizing that the high solubility in

TABLE II

SIMPLEX STEPS FOR THE OPTIMIZATION OF THE SDE PROCEDURE AT REDUCED PRESSURE

Vertex No.	Simplex No.	Retained vertices	Experimental variable levels					Response
			T (°C)	T_s (°C)	T_c (°C)	t (min)	P (mmHg)	
1	1	–	75.0	7.0	−7.0	90	206	89 739
2	1	–	84.1	9.0	−6.0	93	196	79 941, 78 852[e]
3	1	–	77.0	16.1	−6.0	93	196	81 138
4	1	–	77.0	9.0	−2.4	93	196	90 929
5	1	–	77.0	9.0	−6.0	104	196	90 070
6	1	–	77.0	9.0	−6.0	93	160	75 651, 75 235[e]
7	2	1,2,3,5,6	79.1	11.1	−9.9	96	186	75 028, 74 074[e]
8[a]	2	1,2,3,5,6	80.1	12.1	−13.7	98	181	–[f]
9	3	1,2,3,6,7	79.9	11.9	−8.0	82	182	75 155, 77 417[e]
10	4	2,3,6,7,9	83.9	15.9	−7.3	93	162	–[g]
11[b]	4	2,3,6,7,9	77.2	9.2	−7.1	91	195	93 772
12	5	2,6,7,9,10	84.5	6.6	−8.9	90	158	75 399, 75 469[e]
13	6	2,6,7,9,12	78.0	3.2	−8.2	89	191	95 535
14[c]	6	2,6,7,9,12	79.5	6.4	−8.0	90	184	96 811
15	7	6,7,9,12,13	75.3	7.7	−10.4	87	155	–[f]
16[b]	7	6,7,9,12,13	81.9	8.7	−7.1	92	186	76 980
17	8	6,7,9,12,16	83.0	15.7	−7.8	92	158	72 879
18[d]	8	6,7,9,12,16	84.2	18.8	−7.7	93	149	72 214, 72 464[e]
19[a]	8	6,7,9,12,16	85.5	22.0	−7.6	94	141	72 949
20	9	6,7,12,16,18	82.8	9.9	−7.8	103	154	85 253
21[b]	9	6,7,12,16,18	80.6	11.4	−7.9	88	175	78 939
22	10	6,7,12,18,20	81.2	13.5	−9.0	99	138	83 611
23	11	6,7,12,18,22	79.6	13.8	−8.8	85	162	85 935
24[b]	11	6,7,12,18,22	82.0	10.8	−8.1	99	156	74 425

[a] Obtained from expansion, $\alpha = 2.0$.
[b] Obtained from contraction, $\alpha = -0.5$.
[c] Obtained from contraction, $\alpha = 0.5$.
[d] Obtained from expansion, $\alpha = 1.5$.
[e] The second response value is the mean value obtained after performing a new run to check a vertex maintained $K + 1$ movements [26], where K is the number of variables.
[f] Constraint. Rejected without experimentation owing to temperature limitation of the equipment (coolant temperature).
[g] Considered as a constraint. Rejected owing to inadequate evaporation of the solvent.

water of 2-phenylethanol might be the cause of its low recovery.

As far as the optimization of the SDE operation in the aeration mode is concerned, the variables considered to be most relevant are given in Table IV. It should be noted that the sample temperature was held constant (40°C) throughout the simplex procedure, as the use intended for the optimized system demands the extraction of thermally unstable substances.

The response function (R') used in this optimization can be expressed as

$$R' = \frac{\sum (C_i - C_i^0)^2}{n} \quad (4)$$

where the symbols are defined as in eqn. 3.

Before starting the experimentation, it was decided to consider coolant temperatures lower than −10°C as a boundary violation, owing to the previously mentioned limitation of the equipment. Table V gives the set of experimental values tested in the optimization of the SDE

TABLE III

RECOVERIES AND RELATIVE STANDARD DEVIATIONS OBTAINED FOR THE COMPOUNDS SELECTED UNDER THE SIMPLEX-OPTIMIZED CONDITIONS CORRESPONDING TO THE SDE OPERATED AT REDUCED PRESSURE

Compound	Recovery (%)[a]	R.S.D. (%)[b]
Isoamyl acetate	94.59	8.87
Ethyl hexanoate	96.14	9.29
Terpinolene	51.98	22.19
1-Hexanol	95.45	10.59
Ethyl octanoate	98.50	14.08
Benzaldehyde	97.07	9.34
Linalool	99.55	10.84
Diethyl succinate	46.18	11.57
α-Terpineol	89.06	11.49
Ethyl dodecanoate	99.15	15.57
2-Phenylethanol	13.39	17.95
β-Ionone	98.83	14.96
Ethyl tetradecanoate	90.86	11.87
γ-Decalactone	48.96	13.43

[a] Recovery as a percentage of initial amount. Mean value of ten replicates.
[b] Calculated from ten replicates.

TABLE IV

VARIABLES, BASE LEVELS AND STEP SIZES CONSIDERED IN THE OPTIMIZATION STUDY OF THE SDE OPERATION IN THE AERATION MODE

Variable	Base level	Step size
Solvent heating bath temperature, T_s (°C)	50	10
Coolant temperature, T_c (°C)	−5	5
Extraction time, t (min)	90	20[a]
Flow-rate of aeration gas, F (ml/min)	100	100

[a] Modified to 60 after vertex 10 (see text for further details).

operation in the aeration mode and the values obtained for the response function. It must be noted that at vertex 11, the step size for the extraction time was changed from 20 to 60 because only during the actual experimentation did it become apparent that either the unit adopted for the mentioned factor was dispropor-

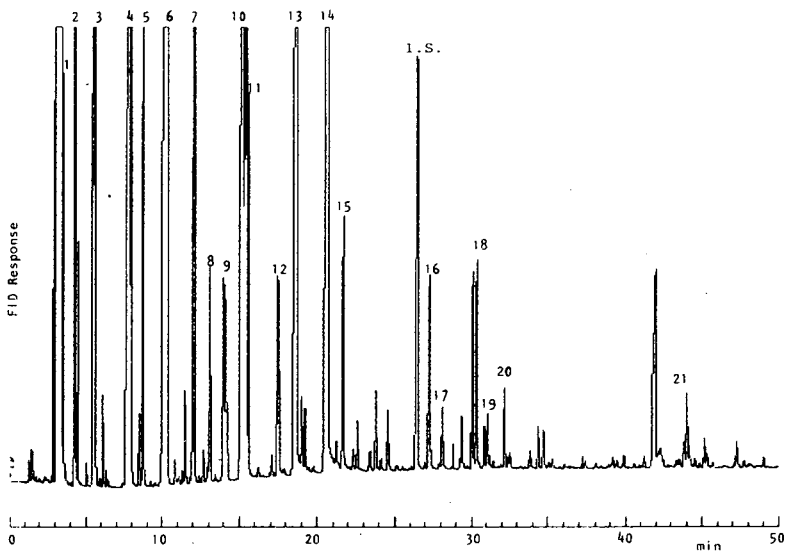

Fig. 1. Chromatogram of the aroma concentrate obtained from simultaneous steam distillation–solvent extraction (SDE) at reduced pressure of a banana by using dichloromethane. Experimental conditions for the SDE procedure corresponds to the simplex-optimized conditions in Table II (experiment No. 18). Column, 30 m × 0.25 mm I.D. Carbowax 20M, film thickness 0.25 μm (Quadrex); temperature 30°C (5 min), then increased at 3°C/min to 170°C; carrier gas, helium (25 p.s.i.g.); injection, split 1:50 (0.5 μl). Peaks: 1 = ethyl acetate; 2 = 2-pentanone; 3 = isobutyl acetate; 4 = ethyl butanoate; 5 = butyl acetate; 6 = isoamyl acetate; 7 = isobutyl butyrate; 8 = heptan-2-one; 9 = butyl butyrate; 10 = isoamyl alcohol; 11 = 2-hexenal; 12 = 4-hepten-2-one; 13 = isopentyl butyrate; 14 = isopentyl 3-methylbutyrate; 15 = 4-hepten-2-ol acetate; 16 = hexyl butyrate; 17 = 3-methylbutyl hexanoate; 18 = 4-hepten-2-ol; 19 = 4-octen-2-ol acetate; 20 = 4-hepten-2-ol butyrate; 21 = 4-octen-1-ol. Internal standard (I.S.): methyl octanoate.

TABLE V

SIMPLEX STEPS FOR THE OPTIMIZATION OF THE SDE PROCEDURE IN THE AERATION MODE

Vertex No.	Simplex No.	Retained vertices	Experimental variable levels				
			T_s (°C)	T_c (°C)	t (min)	P (ml/min)	Response
1	1	–	50.0	−5.0	90	100.0	21 566
2	1	–	59.3	−3.9	94	121.8	19 374, 18 767[d]
3	1	–	52.2	−0.4	94	121.8	18 989, 19 023[d]
4	1	–	52.2	−3.9	108	121.8	23 633
5	1	–	52.2	−3.9	94	192.6	23 655
6	2	1,2,3,4	54.6	−2.7	99	40.2	20 309, 21 138[d]
7	3	1,2,3,6	55.8	−2.1	80	70.1	21 012
8	4	2,3,6,7	61.0	0.5	94	77.0	25 896
9[a]	4	2,3,6,7	52.7	−3.6	91	94.2	21 898
10	5	2,3,6,8	57.7	−1.2	111	110.4	26 625
11	6	2,3,6,11	55.8	−2.1	61	70.1	20 090
12	7	2,3,6,11	50.0	−5.0	90	100.0	18 656
13[b]	7	2,3,6,11	44.5	−7.7	84	111.5	34 822
14[c]	7	2,3,6,11	47.3	−6.4	87	105.8	16 895, 17 731[d]
15	8	2,3,11,14	52.6	−3.7	59	169.6	19 034
16	9	2,3,14,15	49.8	−5.1	115	189.4	22 637
17[a]	9	2,3,14,15	54.3	−2.8	75	99.9	21 073
18	10	2,3,14,16	51.6	−4.2	144	99.9	17 540, 16 695[d]
19	11	2,3,14,18	55.3	−2.3	104	35.3	23 394
20[a]	11	2,3,14,18	51.2	−4.4	112	150.9	20 150
21	12	2,3,14,18	54.0	−3.0	107	73.8	20 875
22[a]	12	2,3,14,18	51.9	−4.1	111	131.6	22 404
23	13	2,14,18,21	53.9	−8.4	117	78.8	22 124
24	14	2,14,18,23	52.0	−8.4	119	129.3	21 316
25	15	2,14,18,24	51.6	−3.1	109	149.6	17 839

[a] Obtained from contraction, $\alpha = -0.5$.
[b] Obtained from expansion, $\alpha = 2.0$.
[c] Obtained from expansion, $\alpha = 1.5$.
[d] The second response value is the mean value obtained after performing a new run to check a vertex maintained $K + 1$ movements [26], where K is the number of variables.

tionately small or the system was relatively independent of its level. As can be seen in Table V, progress in the simplex is achieved through reflections, expansions and contractions performed as already described.

From Table V, it is also clear that the experimental conditions defining vertex 18 (*i.e.*, solvent heating bath temperature 51.6°C, coolant temperature −4.2°C, extraction time 144 min and flow-rate of aeration gas 99.9 ml/min) give the best response, so they were finally selected as the most suitable for the SDE operation which involves the concentration of the dynamic headspace resulting from purging the sample with an inert gas. Under these optimized conditions, the recoveries and R.S.D.s given in Table VI were achieved. It is evident that the recoveries obtained for several compounds (diethyl succinate, α-terpineol, 2-phenylethanol and γ-decalactone) are extremely low and their corresponding R.S.D.s are unsatisfactory. However, the possibility of reliably determining some of the solutes in Table VI suggests that the optimized procedure is of interest for analysing samples avoiding the risk of undesirable chemical processes promoted by the sample temperature.

In order to illustrate the analytical capabilities of the optimized procedures, Figs. 1 and 2 depict

TABLE VI

RECOVERIES AND RELATIVE STANDARD DEVIATIONS OBTAINED FOR THE COMPOUNDS SELECTED UNDER THE SIMPLEX-OPTIMIZED CONDITIONS CORRESPONDING TO THE SDE PROCEDURE IN THE AERATION MODE

Compound	Recovery (%)[a]	R.S.D. (%)[b]
Isoamyl acetate	71.82	9.14
Ethyl hexanoate	72.63	7.65
Terpinolene	70.77	6.69
1-Hexanol	20.84	11.30
Ethyl octanoate	72.42	8.33
Benzaldehyde	24.96	10.13
Linalool	43.76	8.93
Diethyl succinate	1.92	30.90
α-Terpineol	9.24	18.23
Ethyl dodecanoate	66.50	7.62
2-Phenylethanol	1.78	50.24
β-Ionone	51.90	13.56
Ethyl tetradecanoate	20.31	15.96
γ-Decalactone	2.52	26.02

[a] Recovery as a percentage of initial amount. Mean value of ten replicates.
[b] Calculated from ten replicates.

the chromatograms obtained from simultaneous steam distillation–solvent extraction at reduced pressure and in the aeration mode, respectively, of a banana, using dichloromethane as the extraction solvent. It is interesting that the aroma of the extract obtained from the SDE operated in the aeration mode was very similar to that of the original sample, thus suggesting the usefulness of this procedure for extracting volatile compounds from different products. The overall procedure, including sample preparation, steam distillation–extraction under optimized conditions and capillary GC analysis, requires *ca.* 3 h.

CONCLUSIONS

The proposed SDE device has proved to be very versatile as it allows operation at normal pressure and at reduced pressure and the concentration of the dynamic headspace from the sample. Moreover, the design of the new version is such that losses of high-volatility compounds are minimized and only one configuration is

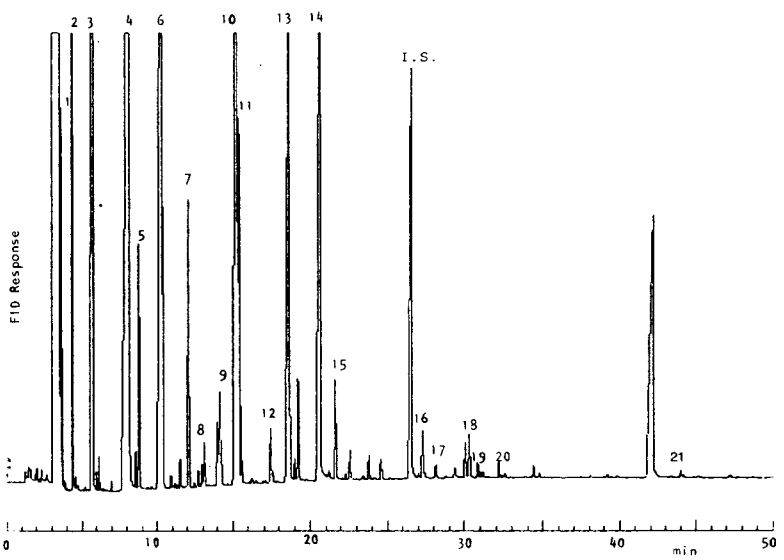

Fig. 2. Chromatogram of the aroma concentrate obtained from simultaneous steam distillation–solvent extraction (SDE) in the aeration mode of a banana by using dichloromethane. Experimental conditions for the SDE procedure correspond to the simplex-optimized conditions in Table V (experiment No. 18). The chromatographic analysis was performed under the same conditions as in Fig. 1. Peaks and internal standard as in Fig. 1.

required for using extraction solvents having densities either higher or lower than that of the sample solvent. A significant improvement in the performance of the SDE procedure was achieved by applying the sequential simplex method.

ACKNOWLEDGEMENTS

Financial support for this work by the Comisión Interministerial de Ciencia y Tecnología (Project ALI 91/0621) is gratefully acknowledged. G.P.B. thanks the Comunidad de Madrid for a grant. The authors are also indebted to Mr. Jesús López Avilés for his skillful assistance with the modified SDE apparatus.

REFERENCES

1 W.G. Jennings and A. Rapp, *Sample Preparation for Gas Chromatographic Analysis*, Hüthig, Heidelberg, 1983.
2 C. Poole and S.A. Schuette, *J. High Resolut. Chromatogr. Chromatogr. Commun.*, 6 (1983) 526.
3 H. Maarse and R. Belz, *Isolation, Separation and Identification of Volatile Compounds in Aroma Research*, Akademie Verlag, Berlin, 1985.
4 I. Liška, J. Krupčik and P.A. Leclercq, *J. High Resolut. Chromatogr.*, 12 (1989) 577.
5 S.T. Likens and G.B. Nickerson, *Am. Soc. Brew. Chem. Proc.*, (1964) 5.
6 G.B. Nickerson and S.T. Likens, *J. Chromatogr.*, 21 (1966) 1.
7 H. Maarse and R.E. Kepner, *J. Agric. Food Chem.*, 18 (1970) 1095.
8 A.J. McLeod and S.J. Cave, *J. Sci. Food Agric.*, 26 (1975) 351.
9 R.A. Flath and R.R. Forrey, *J. Agric. Food Chem.*, 25 (1977) 103.
10 M. Godefroot, P. Sandra and M. Verzele, *J. Chromatogr.*, 203 (1981) 325.
11 M. Godefroot, M. Stechele, P. Sandra and M. Verzele, *J. High Resolut. Chromatogr. Chromatogr. Commun.*, 5 (1982) 75.
12 A.J. Núñez, J.M.H. Bemelmans and H. Maarse, *Chromatographia*, 18 (1984) 153.
13 J. Curvers, T. Noij, C. Cramers and J. Rijks, *Chromatographia*, 19 (1984) 225.
14 J.D. Green and B.P. Payne, *Anal. Chim. Acta*, 226 (1989) 183.
15 M. de Frutos, J. Sanz and I. Martínez-Castro, *Chromatographia*, 25 (1988) 861.
16 G.P. Blanch, G. Reglero, M. Herraiz and J. Tabera, *J. Chromatogr. Sci.*, 29 (1991) 11.
17 G.P. Blanch, J. Tabera, J. Sanz, M. Herraiz and G. Reglero, *J. Agric. Food Chem.*, 40 (1992) 1046.
18 G.P. Blanch, J. Tabera, M. Herraiz and G. Reglero, *J. Chromatogr.*, 628 (1993) 261.
19 C. Hendrix, *Chemtech*, (1980) 488.
20 J.C. Berridge, *Anal. Chim. Acta*, 191 (1986) 243.
21 R.J. Fisher, *Food Technol.*, 43 (1989) 90.
22 J. Tabera, G. Reglero, M. Herraiz and G.P. Blanch, *J. High Resolut. Chromatogr.*, 14 (1991) 392.
23 D.E. Long, *Anal. Chim Acta*, 46 (1969) 193.
24 S. Deming and S.L. Morgan, *Anal. Chem.*, 45 (1973) 278A.
25 J.A. Nelder and R. Mead, *Comput. J.*, 7 (1965) 308.
26 V. Schubert, R. Diener and A. Mosandl, *Z. Naturforsch., Teil C*, 46 (1991) 33.
27 W. Spendley, G.R. Hext and F.R. Himsworth, *Technometrics*, 4 (1962) 441.

Journal of Chromatography A, 655 (1993) 151–154
Elsevier Science Publishers B.V., Amsterdam

CHROM. 25 046

Determination of chlorinated insecticides in blood samples of agricultural workers

M. Gracia Rosell*, Jordi Obiols, M. José Berenguer and Xavier Guardino

Instituto Nacional de Seguridad e Higiene en el Trabajo, Centro Nacional de Condiciones de Trabajo, Dulcet 2-10, E-08034 Barcelona (Spain)

Francesca López and Josep Brosa

Departament de Treball, Generalitat de Catalunya, Centre de Seguretat i Higiene de Barcelona, Avgda. de l'Exercit 39, E-08034 Barcelona (Spain)

ABSTRACT

Lindane, aldrin and *p,p'*-DDT were determined in blood samples from 71 farmers by means of an analytical method which combines a direct whole-blood extraction with *n*-hexane and gas chromatography (GC)–electron-capture detection (ECD), using a capillary column, applied to the organic extract. This technique allowed the determination of pesticides at levels varying from 0.1 to 180 μg per l of blood, the detection limit for every pesticide being 0.1 μg/l. GC–mass spectrometry was used to confirm the identity of each pesticide. The advantage of capillary column GC–ECD for pesticide determination is its sensitivity and high resolution, which makes it possible to separate pesticides from a complex *n*-hexane extract obtained in a very simple pretreatment of the blood sample, which is itself a very complex matrix.

INTRODUCTION

It has long been recognized that chlorinated insecticides may be stored in the body fat and exert a toxic action upon the central nervous system, and as a consequence the determination of such compounds in biological samples, specifically blood, from occupationally exposed populations is considered of high interest. In addition, lindane may produce kidney and liver changes in some experimental animals and, more importantly, there have been several cases of aplastic anaemia in which there was a clear association between erythropoietic depression of the individuals involved and their recent or, less frequently, remote exposure [1]. Occupational overexposure to aldrin produces excitation of the nervous system. In cases of acute poisoning dysrhythmia in the electroencephalogram (EEG) and convulsive fits have occurred. Nevertheless, in these patients there is a marked trend of the EEG towards normality several months after removal of exposure, along with a decrease in blood dieldrin concentrations (also a metabolite of aldrin) [2], which correlate with both intensity and exposure time [3]. The exposure to *p,p'*-DDT may be of occupational origin or strongly related to environmental contamination. Nowadays pesticide blood levels are considered a good indicator of pesticide body burden as close correlations between the concentrations of pesticides in blood and fat have been established, even in the case of non-occupationally exposed individuals [4].

From the analytical point of view, two aspects require comment with regard to pesticide gas chromatography (GC) determination: (1) sample

* Corresponding author.

0021-9673/93/$06.00

treatment and (2) column and analytical conditions. Dale *et al.*'s [5] extraction method with *n*-hexane has been considered a proper procedure for blood sample treatment by many authors [6–8].

Analysis of pesticides has dramatically improved with the use of capillary columns. With this system better sensitivity and resolution, have been achieved [9,10] and it is also a less time-consuming method. In accordance with this, the determinations of blood lindane, aldrin and *p,p'*-DDT in our laboratory were carried out using a method combining direct extraction with *n*-hexane, capillary column GC–electron-capture detection (ECD) and GC–mass spectrometry (MS).

The aims of this paper are: (1) to describe an analytical method that improves the separation of the peaks in the chromatograms and one that requires a shorter analytical time, about 30 min per sample, in comparison with the results obtained with a packed column; and (2) to assess the occupational exposure to pesticides of a group of agricultural workers and compare this group with a group of workers with no occupational exposure.

EXPERIMENTAL

A population group of 71 farmers with mean age of 43 (median = 43) and mean exposure time to pesticides of 12.6 years (median = 12) was studied. The origin of the exposure was the preparation and use of pesticide mixtures on different types of crops: strawberry, large strawberry, market garden crops, flowers and other fruits. Seven unexposed workers of the same age range were studied as controls.

Sample collection

A 5-ml venous blood sample was drawn from each worker under fasting conditions and before a work shift with a vacuum tube containing heparin. Blood samples were immediately frozen and kept at −30°C until they were analysed.

Chemicals

Pesticide-grade *n*-hexane used in the analytical procedure was obtained from Monplet & Esteban (Barcelona, Spain). Aldrin, lindane, *p,p'*-DDT and dieldrin used to prepare standard solutions were obtained from PolyScience (IL, USA).

Calibration

A calibration curve was prepared for every pesticide with standard solutions obtained by weighing and dissolving appropriate quantities of each pesticide in *n*-hexane containing internal standard (dieldrin 40 μg/l) (see Fig. 1).

Analytical conditions

The chromatographic study was carried out using a Hewlett-Packard Model 5890 gas chromatograph equipped with a ^{63}Ni electron-capture detector and a SPB-5 capillary column, 30 m × 0.25 mm I.D., 0.25 μm film thickness, from Supelco (Bellefonte, PA, USA). Temperatures were: column, initial 180°C (1 min), final 270°C; rate 2°C/min; injector 270°C; detector 300°C. Helium was used as the carrier gas at a linear speed of 19 cm/s and 25 cm/s, and nitrogen as the auxiliary at 45 ml/min. The injector was in split mode (1:60) and the injected volume was 2 μl.

The MS study was carried out with a Hewlett-Packard Model 5995 gas chromatograph–mass spectrometer using an SPB-5 capillary column, 30 m × 0.25 mm I.D., 0.25 μm film thickness, from Supelco. Temperatures were: injector, 200°C; transfer line, 220°C; ionization source,

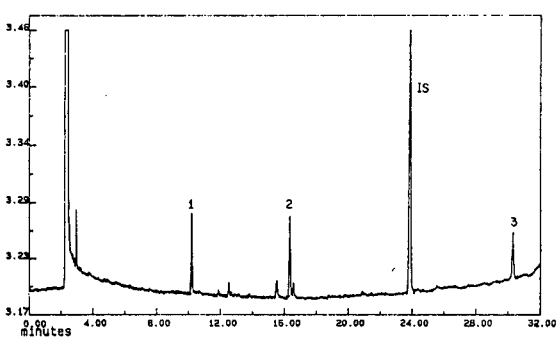

Fig. 1. Chromatogram of a mixture of standards. 1 = Lindane (0.14 pg); 2 = aldrin (0.13 pg); and 3 = *p,p'*-DDT (0.16 pg); IS = internal standard. Linear velocity of helium: 19 cm/s. Detector response: arbitrary units.

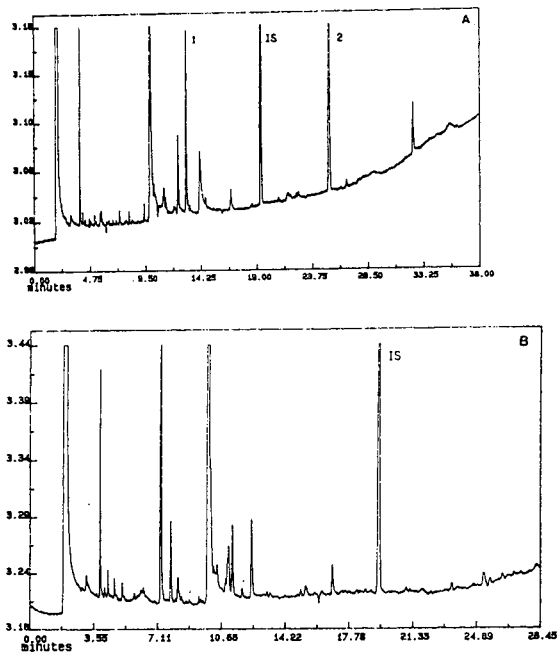

Fig. 2. Chromatograms obtained from blood of (A) an exposed worker and (B) an unexposed worker. 1 = Aldrin; 2 = p,p'-DDT; IS = internal standard. Linear speed of He: 25 cm/s.

220°C; analyser, 220°C. The electron energy was 70 eV.

Qualitative analyses of the samples were carried out with selective ion monitoring (SIM) at the following m/e rates: lindane, 219, 217 and 181; aldrin, 291, 263 and 261; and p,p'-DDT, 237, 235 and 165.

Detection limit

Using the above-mentioned analytical conditions, the detection limit for every pesticide was 0.01 μg per l of whole blood. Fig. 2 shows chromatograms from (A) an exposed worker and (B) an unexposed worker.

RESULTS AND DISCUSSION

Lindane, aldrin and p,p'-DDT were identified in all the samples from the occupationally exposed group. The overall results of the 71 farmers involved in different kinds of exposure are presented in Table I. These results have been divided into two groups in accordance with the type of crops and are presented in Table II along with the results from non-occupationally exposed workers. Samples from non-occupationally exposed people showed neither lindane nor aldrin but p,p'-DDT was present in almost all of them, as is shown in group 3 of Table II.

The levels of lindane and aldrin in the samples from the farmers were very low. The lindane concentrations found should be considered as trace levels, with no differences between groups, while in the case of aldrin the concentrations were also very low but a difference could be established according to the type of crop. The highest values were found in the group of straw-

TABLE I

OVERALL RESULTS

Compound	μg per l whole blood			
	Mean[a]	S.D.	Median[a]	Range
Lindane	0.021	0.021	0.010	<0.01–0.12
Aldrin	0.448	0.817	0.030	<0.01–3.32
p,p'-DDT	3.63	3.54	2.84	0.08–18.0

[a] Mean and median of results obtained from blood samples of 71 farmers.

TABLE II

RESULTS ACCORDING TO CROPS

Compound	μg per l whole blood			
	Mean	S.D.	Median	Range
Group 1 (strawberry, large strawberry, mixed crops)				
Lindane	0.026	0.037	0.010	<0.01–0.12
Aldrin[a]	0.525	0.778	0.040	<0.01–3.19
p,p'-DDT[a]	2.11	2.01	1.06	0.12–8.51
Group 2 (vegetables, ornamental plants, flowers, fruits and mixed crops)				
Lindane	0.015	0.025	0.010	<0.01–0.12
Aldrin[a]	0.015	0.017	0.010	<0.01–0.05
p,p'-DDT[a]	4.58	3.59	3.75	0.08–14.0
Group 3 (non-exposed population)				
Lindane and aldrin <0.01 μg/l				
p,p'-DDT	0.13	0.14	0.04	<0.01–0.41

[a] Differences of concentration between group 1 and group 2 are statistically significant.

berry farmers. The highest pesticide concentrations found in the samples from the farmers are those of *p,p'*-DDT, and they also allow us to distinguish between two groups, strawberry farmers and other crop farmers, the levels found in the former group being higher.

As far as lindane is concerned, it should be considered as a trace compound of uncertain origin (environmental contamination), while aldrin concentrations are higher in the strawberry group as it might have been used for the protection of this crop. *p,p'*-DDT concentrations are markedly higher and also allow us to establish a difference between the two above-mentioned groups. Nevertheless, a full assessment of both findings, *i.e.* higher *p,p'*-DDT concentrations and group differences, could not be carried out because comprehensive information about the impact of environmental contamination upon the studied groups was not available to us.

Whole-blood sample extraction with 5 ml of *n*-hexane is an easy, fast and accurate method, and when used under the conditions described herein allows us to achieve very low detection limits, in agreement with those reported by Mussalo-Rauhamaa *et al.* [11] with a similar, but not fully described extraction procedure.

REFERENCES

1 T.H. Milby, A.J. Samuels and F. Ontobioni, *J. Occup. Med.*, 10 (1968) 584.
2 G. Czegledi-Janko and P. Avar, *Br. J. Industr. Med.*, 27 (1970) 283.
3 V.K.H. Brown, C.G. Hunter and A. Richardson, *Br. J. Industr. Med.*, 21 (1964) 283.
4 J.L. Radomski, W.B. Diechmann, A.A. Rey and T. Merkin, *Toxicol. Appl. Pharmacol.*, 20 (1971) 175.
5 W.E. Dale, A. Curley and C. Cueto, *Life Sci.*, 5 (1966) 47.
6 R.C. Baselt, *Biological Monitoring Methods for Industrial Chemicals*, PSG Publ., Littletown, MA, 1988, p. 15.
7 R.S. Murphy and F.W. Kutz, *Environ. Health Pers.*, 48 (1983) 81.
8 A. Mandes, V. Lodi, G. Ruani, F.S. Violante and G.B. Raffi, *La Difesa delle Piante*, 14 (1991) 13.
9 L. Zenon-Roland, R. Agneessens, P. Naugniot and H. Jacobs, *J. High Resolut. Chromatogr. Chromatogr. Commun.*, 7 (1984) 480.
10 S.H. Kennedy, *Int. Lab.*, March (1987) 44.
11 H. Mussalo-Rauhamaa, H. Pyysalo and K. Antervo, *Arch. Environ. Health*, 46 (1991) 340.

Journal of Chromatography A, 655 (1993) 155–161
Elsevier Science Publishers B.V., Amsterdam

CHROM. 25 308

Evidence obtained by gas chromatography–mass spectrometry of conversion of alkanes into aromatic compounds during coal pyrolysis

R. Moliner*, M. Lázaro, A. Fernández and J. Ibarra

Instituto de Carboquímica, CSIC, Zaragoza Apatdo 589, 50.080 Zaragoza (Spain)

L. Comellas

Institut Quimic de Sarriá, 08017 Barcelona (Spain)

ABSTRACT

Tars obtained under different temperature and pressure conditions from a type III-S coal were analysed by high-resolution capillary gas chromatography. The tar components were identified by means of a selective mass detector. Quantitative analysis was also carried out using a flame ionization detector. It was shown that the tar obtained at low temperature (500°C) and pressure (0.1 MPa) has a higher content of *n*-alkanes and a lower content of aromatic compounds than those obtained at high temperature (700°C) and pressure (1 MPa). This fact is presented as evidence of the conversion, by cyclization secondary reaction, of alkanes into aromatic compounds. Most of the aromatic compounds identified are alkyl derivatives of naphthalene and benzothiophene. The presence of heterocyclic sulphur compounds in the high-temperature tars shows that sulphur released from coal during pyrolysis is involved in the cyclization reactions of the *n*-alkanes. Empirical models correlating the alkane, naphthalene and phenanthrene yields with the temperature and pressure of pyrolysis were obtained.

INTRODUCTION

Heating of coal under inert atmosphere yields variable quantities of a complex mixture of hydrocarbons from C_6 to C_{30}, called tar. The composition of tars depends on the nature of the coal and the pyrolysis conditions. Several analytical methods such as supercritical fluid chromatography (SFC), HPLC and GC have been used for tar characterization. Of these methods, only GC has been successfully interfaced with appropriate identification techniques such as mass spectrometry.

To date GC–MS has proved to be an unrivalled method of identification of individual components in a mixture. This is most valuable when dealing with a complex material such as coal tar since no other method approaches the degree of resolution required to discriminate between the enormous number of compounds involved [1].

For this reason GC–MS has evolved into the most commonly used technique for separation and identification of tar components. Some useful applications of GC–MS to the analysis of hydrocarbon mixtures obtained from different carbonaceous materials can be found in refs. 2–6: Blanco *et al.* [2] studied the volatile fraction of a coal tar pitch; Aceves and Grimalt [3] carried out a screening of aliphatic and aromatic hydrocarbons in urban aerosols; Canton and Grimalt [4] characterized polycyclic aromatic hydrocarbon (PAH) mixtures in polluted coastal sediments; Martín *et al.* [5] studied bituminous material extracted from fossil organic matter with carbon dioxide.

* Corresponding author.

Sinninghe *et al.* [6] carried out an exhaustive identification by GC–MS of the compounds released from "*in situ*" pyrolysis of five Spanish brown coals. It was proposed that, of the coals investigated in this paper, Mequinenza coal, a well known [7] low-rank coal with a very high sulphur content, be classified into a new type of kerogen, type III-S kerogen. The authors reported a high content of long-chain *n*-alkanes and *n*-1-alkenes in the pyrolysates obtained at 610°C from this coal. These results agree with some results that will be presented here. However, tar composition depends on coal nature and pyrolysis conditions. In fact, it has been shown [8] that alkanes can be broken down by secondary reactions into light aromatic compounds. This conversion is desirable because of the higher commercial value of the latter.

On the other hand, sulphur evolved from the pyrolysis of organic sulphur and pyrite of coal could also be involved in secondary cyclization reactions yielding heterocyclic sulphur compounds. The presence of these compounds makes refining of crude tar difficult because of their chemical stability.

In this paper, tars obtained from pyrolysis of Mequinenza coal at different temperatures and pressures are analysed by GC–MS in order to identify the major components and to find evidence of the conversion of heavy alkane from coal into aromatic compounds. Empirical models correlating the yields of alkane, naphthalene and phenanthrene with temperature and pressure were obtained in order to correlate cyclization progress with the pyrolysis conditions. In addition to alkanes and PAHs, heterocyclic sulphur compounds were identified in order to find evidence of the involvement of sulphur in cyclization secondary reactions yielding heterocyclic sulphur compounds.

EXPERIMENTAL

Pyrolysis was carried out in a fluidized bed pyrolysis unit which has been described elsewhere [9]. The coal used was a well known high-sulphur, low-rank coal from Mequinenza (Spain). Its main characteristics are shown in Table I. The coal sample (100 g) was instantaneously fed into the reactor so that a heating rate of 200°C/min was obtained. Volatile matter released was continuously swept out from the reactor by the fluidizing nitrogen. In this way, the residence time of the vapours was very low (*ca.* 10 s). The tar and water formed were cooled in a heat exchanger and recovered by washing the recovering device with methylene chloride. The organic phase was separated from the aqueous phase by sedimentation, filtered on a 5-μm Millipore filter and distilled for solvent elimination.

TABLE I

ANALYSIS OF MEQUINENZA COAL

	Air dried	daf[a]
First analysis		
Moisture (%)	11.55	
Ash (%)	10.32	
Volatile matter (%)	39.96	51.14
Calorific value (kcal/kg)	5552	7106
Ultimate analysis		
Carbon (%)	53.67	68.69
Hydrogen (% dry basis)	4.21	5.39
Nitrogen (%)	0.75	0.96
Sulphur (%)	9.07	11.61

[a] Dry, ash free basis.

Pyrolysis conditions were selected according to an expanded factorial design at two levels. Two variables, temperature and pressure, were investigated. Table II shows the experimental conditions for each run. Three replicate runs were made in order to evaluate the variance of the experimental error. Temperature varied slightly along the run, so an average of the measured values was considered for the calculations.

Tars were chromatographed on a wall-coated open tubular fused-silica capillary column from Chrompack (Middelburg, Netherlands). A column of 50 m × 0.25 mm I.D., covered with a 0.4-μm film of CP-sil-5 CB chemically bonded phase was used.

Quantitative analyses were carried out on a 3400 Varian Chromatograph (Walnut Creek, CA, USA) using flame ionization detection (FID). The chromatographic parameters are

TABLE II

PYROLYSIS CONDITIONS

Run	Temperature (T)		Pressure (P)		Time (t)	
	Coded[a]	Actual (°C)	Coded[b]	Actual (MPa)	Coded[c]	Actual (min)
1	−0.6	540	−1	0.1	−1	10
2	−0.85	515	+1	1	−1	10
3	0.5	650	0	0.5	0	20
4	0.5	650	0	0.5	0	20
5	0.45	645	0	0.5	0	20
6	1.5	750	−1	0.1	−1	10
7	1.4	740	+1	1	+1	30
8	1.5	750	−1	0.1	−1.5	5
9	0.4	640	−1	0.1	−1	10
10	1.1	710	−0.5	0.3	−0.5	15

[a] T(coded) = T(actual) − 600/100.
[b] P(coded) = P(actual) − 0.55/0.45.
[c] t(coded) = t(actual) − 20/10.

shown in Fig. 1. Naphthalene and phenanthrene were used as internal standards in order to delimit the chromatographic zone where the most of the compounds of interest are eluted. Identification of the major chromatographic peaks was carried out by GC–MS. A Hewlett-Packard (Avondale, PA, USA) HP/MS 5989A system was used. Molecules were ionized by electron impact at 70 eV. A quadropole analyser was used for mass spectra analysis. The Wiley computerized library was used for identification.

RESULTS AND DISCUSSION

Fig. 1 shows the FID chromatograms of tars obtained at different temperatures and pressures. Tables III and IV show the peaks identified in each of them. For the rest of the tars, the same peaks were identified, but quantitative differences were observed. The chromatogram of the low-temperature tar presents several peaks which were identified as alkanes. They can be easily identified as a set of sharp peaks, sequentially spaced at the end of the chromatogram. The molecular ion of these peaks was not observed in the mass spectra, however evidence of its nature was obtained. An internal standard of n-alkanes was used to identify these peaks on the FID chromatograms.

The chromatogram of the tar obtained at 700°C and 1 MPa does not have the peaks of

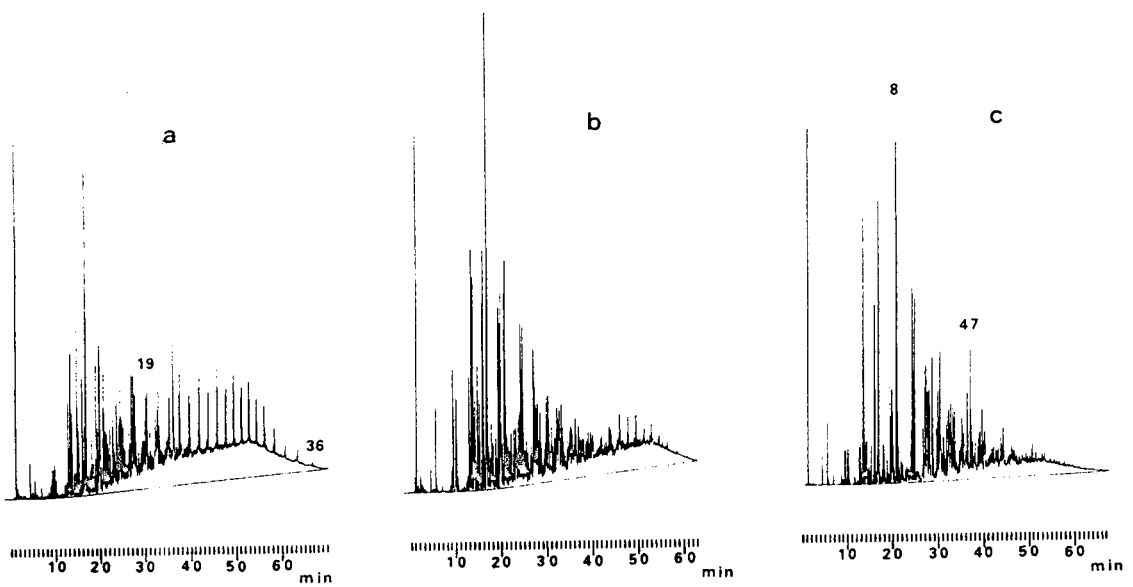

Fig. 1. FID chromatograms of the tars obtained at (a) 500°C, 0.1 MPa; (b) 700°C, 0.1 MPa; (c) 700°C, 1 MPa. For peak references, see Tables III and IV. Chromatographic parameters: Flash injector temperature, 250°C. FID temperature, 350°C. Temperature programme: 50°C; hold time, 5 min; 5°C/min to 300°C. Sample: 1 μl. Split: 1:100. Carrier: hydrogen.

TABLE III

COMPOUNDS IDENTIFIED BY GC–MS IN THE TAR OBTAINED AT 540°C

Peak No.	Compound
1	Phenol
2	2-Methylphenol
3	4-Methylphenol
4	2,5-Dimethylphenol
5	Ethylphenol
6	2,3-Dimethylphenol
7	Naphthalene
8	1,2 Benzenediol + benzo[*b*]thiophene
9	2,5-Diethylthiophene
10	1-Decanol
11	Dodecane
12	4-Ethyl-3-methylphenol
13	4-Propylphenol
14	2-Methylbenzo[*b*]thiophene
15	Tridecane
16	2-Methylnaphthalene
17	2,5-Dimethylbenzothiophene
18	Tetradecane
19	Pentadecane
20	Hexadecane
21	Heptadecane
22	4,8-Dimethyl-1-nonanol
23	Octadecane
24	Nonadecane
25	Eicosane
26	Heneicosane
27	Docosane
28	Tricosane
29	Tetracosane
30	Pentacosane
31	Hexacosane
32	Heptacosane
33	Octacosane
34	Nonacosane
35	Triacontane
36	Dotriacontane

alkanes. Since these compounds must have been distilled from coal at this temperature, we can conclude that alkanes have undergone secondary reactions yielding other compounds. Fig. 2 shows an expanded view of the zone between naphthalene and phenanthrene of the chromatograms in Fig. 1. It can be observed that the high-temperature tar contains many more peaks in this zone. As deduced from Tables III and IV, these peaks correspond mainly to methyl, ethyl, dimethyl and trimethyl derivatives of naphthalene and benzothiophene. These compounds can be produced by a primary cracking of the coal organic matrix, or by a cyclization of the alkane in the vapour phase. Cyprès [8] has shown, by using model compounds, that the cracking of long aliphatic chains, short olefin chains and phenols yields mono- and polycyclic aromatic compounds. The main pathway to aromatic compound formation is the Diels–Alder reaction on short-chain olefins, mainly butadiene and propene. The olefins are formed by cracking of alkane and cyclopentadiene, which is one of the primary cracking products of the phenols.

Primary cracking acts mainly by breaking labile ethylene bridges between aromatic clusters. It is generally accepted that this breaking occurs at temperatures between 500 and 600°C. In fact some compounds, such as methyl benzothiophenes or naphthalenes, are already present in the low-temperature tar. So, if primary cracking were the reaction pathway, the final yield of aromatic compounds should have been achieved at 550°C except if the kinetics of the process is very slow. However, kinetics is not a limiting effect since coal residence time in the reactor varied from 10 to 30 min, and no difference was observed in the aromatic contents of tar obtained at different pyrolysis times.

On the contrary, cyclization of alkane by the Diels–Alder mechanism occurs above 600°C [10]. Consequently, most of the aromatic compounds contained in tars obtained at temperatures higher than 600°C must be formed by secondary cracking and cyclization of alkanes.

Similar reasoning can be applied to the formation of benzothiophene, dibenzothiophene and derivatives. In this case the mechanism of reaction is more complex because a source of sulphur, probably H_2S, must be assumed. H_2S release from the Mequinenza coal starts at 350°C, so H_2S is present when alkanes are distilled from coal at 550°C. However, the fixation of sulphur in tar as benzothiophene derivatives mainly occurs at temperatures higher than 600°C, *i.e.*, where the cracking of alkanes occurs.

Pressure also plays an important role in the cracking process. In fact, increasing the temperature is not enough to complete the cracking of alkanes since they have been identified in the tar

TABLE IV

COMPOUNDS IDENTIFIED BY GC–MS IN THE TAR OBTAINED AT 740°C

Peak No.	Compound	Peak No.	Compound
1	Phenol	30	Dibenzofuran
2	1H-Indene	31	2,3,6-Trimethylbenzothiophene
3	2-Methylphenol	32	2,3,6-Trimethylnaphthalene
4	4-Methylphenol	33	7-Ethyl,2-methylbenzo[*b*]thiophene
5	2,5-Dimethylphenol	34	2,3,5-Trimethylnaphthalene
6	4-Ethylphenol	35	1,4,5-Trimethylnaphthalene
7	2,3-Dimethylphenol	36	Trimethylbenzothiophene
8	Naphthalene	37	9H-Fluorene
9	Benzo[*b*]thiophene	38	9-Methylfluorene
10	6-Methylbenzo[*b*]thiophene	39	2,3-Diethylbenzothiopene
11	4-Methylbenzo[*b*]thiophene	40	2-Methyl-1-naphthanenol
12	2-Methylnaphthalene	41	9-Ethylfluorene
13	4-Methylbenzo[*b*]thiophene	42	4-Methyldibenzofuran
14	5-Methylbenzo[*b*]thiophene	43	3-Methylfluorene
15	1-Methylnaphthalene	44	2-Methylfluorene
16	2,6-Dimethylbenzo[*b*]thiophene	45	4-Methylfluorene
17	2,5-Dimethylbenzo[*b*]thiophene	46	Dibenzothiophene
18	2,6-Dimethylnaphthalene	47	Phenanthrene
19	1,3-Dimethylnaphthalene	48	Anthracene
20	1,7-Dimethylnaphthalene	49	3-Methyldibenzothiophene
21	1,6-Dimethylnaphthalene	50	2-Methylnaphtha[2,1-*b*]thiophene
22	(2,3 + 1,4)-Dimethylnaphthalene	51	3-Methyldibenzothiophene
23	1,5-Dimethylnaphthalene	52	4-Methyldibenzothiophene
24	Acenaphthalene	53	2-Methylnaphthathiophene
25	2-Ethylnaphthalene	54	3-Methyldibenzothiophene
26	1,8-Dihydro-*n*-indene	55	2-Methylanthracene
27	Benzo[*b*]thiophene-4-ol	56	Methyldibenzothiophene
28	Naphthalenol	57	4H-Ciclopenta[*def*]phenanthrene
29	2-Methylphenylthiophene	58	9-Methylphenanthrene

obtained at 750°C under atmospheric pressure. On the other hand, they are not present in the tar of 600°C and 0.3 MPa. Thus, alkanes are more efficiently cracked by increasing pressure and temperature than by increasing temperature only.

In order to quantify these relationships, empirical models correlating temperature (T) and pressure (P) with yields (Y) of some representative compounds, such as naphthalene and phenanthrene, have been obtained. Table V shows the concentration of these compounds in tars, and the yields obtained from 100 g of dry coal. The yields were fitted to the regression equation:

$$Y = a_0 + a_1T + a_2P + a_{12}TP + a_{11}T^2 + a_{22}P^2 \pm e \quad (1)$$

A commercially available computer programme (Statgraphics 5.1) was used for calculations. The effects of the variables and the regression models were statistically tested against the null hypotheses by the F-ratios. In experimental works, significance levels of 99.5 (0.05 for the null hypothesis) are generally accepted. The values of the variables have been introduced as codified values in order to facilitate the comparison between the variable effects. The codified values were calculated according to equations shown in Table II. Table VI shows the regression coefficients and the R^2 for the models.

Fig. 3 shows the alkane yield (Y_a), predicted by the model. Y_a decreases as temperature and pressure increases. The influence of temperature is stronger at low pressure. Under a pressure of 1 MPa, the yield of alkane is very low, even at the

TABLE V

TAR CONCENTRATION AND YIELD OF ALKANES (A), NAPHTHALENE (N) AND PHENANTHRENE (Ph)

Run	Tar concentration (%)			Yield (100 g of dry coal)		
	A	N	Ph	A	N	Ph
1	5.31	0.18	–	0.86	0.029	–
2	2.41	0.24	–	0.20	0.021	–
3	–	0.68	0.19	–	0.066	0.018
4	–	0.69	0.22	–	0.082	0.025
5	–	0.62	0.13	–	0.065	0.014
6	2.04	0.86	0.29	0.27	0.115	0.039
7	–	1.92	0.87	–	0.223	0.101
8	1.14	0.95	0.28	0.16	0.137	0.041
9	2.14	0.31	0.14	0.25	0.036	0.017
10	1.21	0.90	0.26	0.13	0.095	0.027

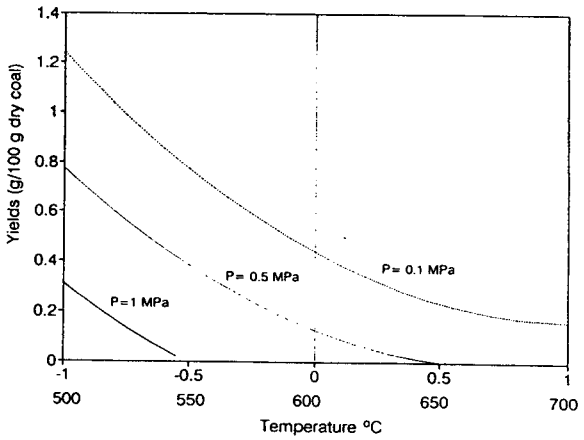

Fig. 3. Predicted yield of alkanes as a function of temperature and pressure.

lower temperature tested. Fig. 4 shows the naphthalene yield, Y_N, predicted as a function of temperature and pressure: Y_N increases as temperature and pressure do. The phenanthrene yields, P_N, predicted by the model are shown in Fig. 5. The trends observed are similar to those of the naphthalene yields.

CONCLUSIONS

Analysis by high-resolution gas chromatography interfaced to a mass selective detector of tars obtained from pyrolysis of a high-sulphur coal has shown that tar composition depends on pyrolysis conditions. Low-temperature, low-pres-

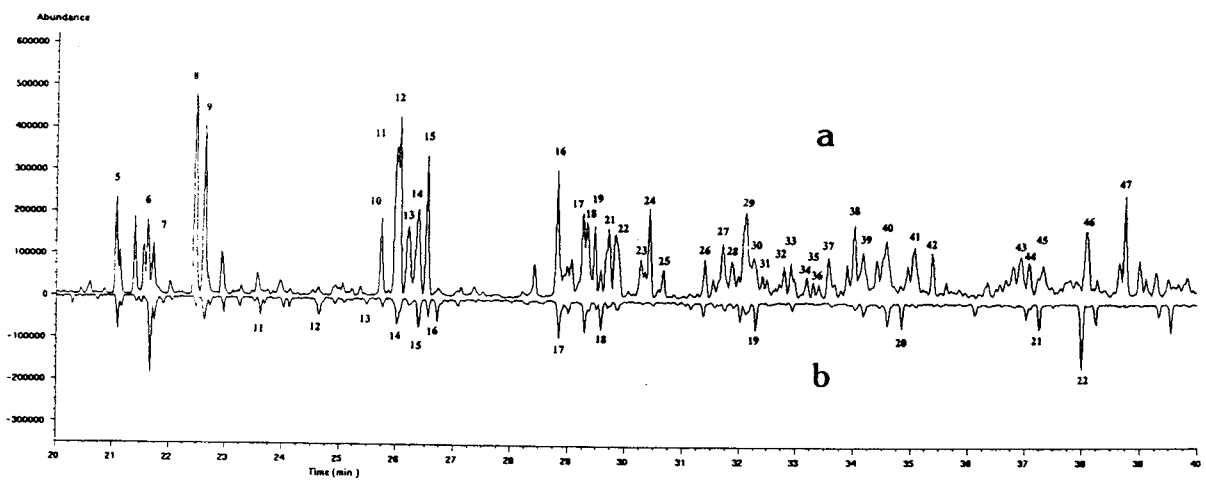

Fig. 2. Total-ion current chromatograms of the tars obtained at (a) 700°C, 1 MPa; (b) 500°C, 0.1 MPa. For peak references, see Tables III and IV. Electron impact: 70 eV. Multiplier: 2200 eV. Source temperature: 220°C. Interface temperature: 280°C. Analyser temperature: 110°C.

TABLE VI

REGRESSION COEFFICIENTS AND SIGNIFICANCE LEVELS

	a_0	a_1	a_2	a_{12}	a_{11}	a_{22}	r^2	Confidence interval
Alkanes	0.137	−0.385	−0.312	0.153	0.263	–	0.98	±0.097
Naphthalene	0.041	0.042	0.015	0.028	0.034	–	0.97	±0.026
Phenanthrene	–	0.033	0.014	0.013	–	0.024	0.99	±0.010

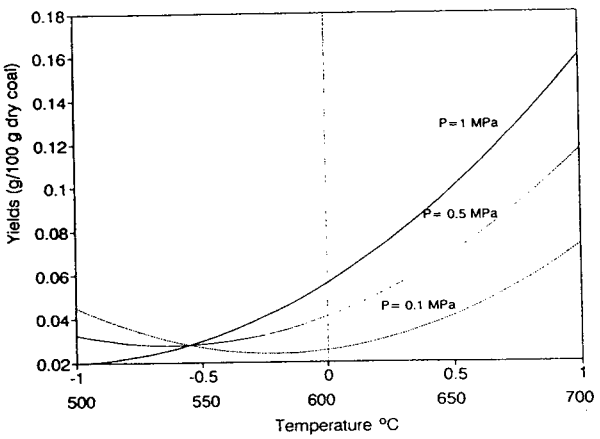

Fig. 4. Predicted yield of naphthalene as a function of temperature and pressure.

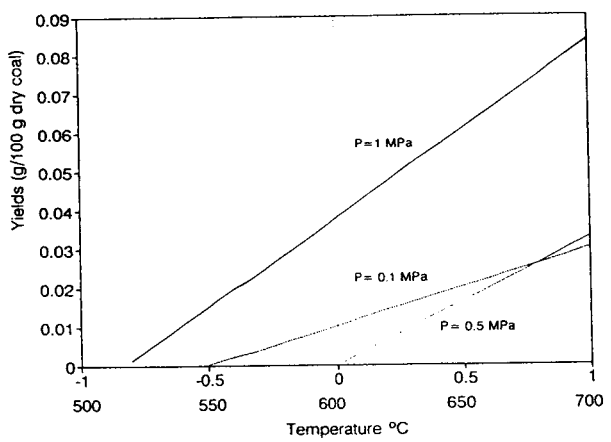

Fig. 5. Predicted yield of phenanthrene as a function of temperature and pressure.

sure tars have higher *n*-alkane concentrations. Evidence of conversion of *n*-alkanes into aromatic compounds, mainly alkyl derivatives of naphthalene and phenanthrene, at high temperature and pressure has been presented. Sulphur released from coal during pyrolysis is involved in cyclization reactions of *n*-alkanes, yielding heterocyclic sulphur compounds, mainly alkyl derivatives of benzothiophene.

ACKNOWLEDGEMENT

This work was supported by the JOULE Programme of the European Community, Contract No. JOUF.0028.C.

REFERENCES

1 J.M. Charlesworth, *Fuel Process. Technol.*, 16 (1987) 99–162.
2 C.G. Blanco, J. Blanco, P. Bernad and M.D. Guillen, *J. Chromatogr.*, 539 (1991) 157–167.
3 M. Aceves and J.O. Grimalt, *J. Chromatogr.*, 607 (1992) 261.
4 L. Canton and J.O. Grimalt, *J. Chromatogr.*, 607 (1992) 279.
5 F. Martin, T. Verdejo and F.J. González-Vila, *J. Chromatogr.*, 607 (1992) 377.
6 J.S. Sinninghe, F.X. de las Heras and J.W. de Leeuw, *J. Chromatogr.*, 607 (1992) 361.
7 J.V. Ibarra, I. Cervero, J.L. Miranda and R. Moliner, in J.A. Moulijn (Editor), *Coal Science and Technology, Vol. 11*, Elsevier, Amsterdam, 1987, pp. 633–636.
8 R. Cyprès, *Fuel Process. Technol.*, 15 (1987) 1–15.
9 *Combined Pyrolysis/Combustion/Electricity Production Cycle, Project JOUF.0028.C, European Community; Progress Report No. I*, European Commission, Brussels, November, 1990.
10 R. Cyprès, *Feasibility study of the hydropyrolysis of coal, Demonstration Project LG 103/84; Final Report*, European Commission, Brussels, 1990.

END OF SYMPOSIUM PAPERS

Capillary Electrophoresis

Principles, Practice and Applications

NOW ALSO IN PAPERBACK

by **S.F.Y. Li**, *National University of Singapore, Singapore*

Journal of Chromatography Library Volume 52

Capillary Electrophoresis (CE) has had a very significant impact on the field of analytical chemistry in recent years as the technique is capable of very high resolution separations, requiring only small amounts of samples and reagents. Furthermore, it can be readily adapted to automatic sample handling and real time data processing. Many new methodologies based on CE have been reported. Rapid, reproducible separations of extremely small amounts of chemicals and biochemicals, including peptides, proteins, nucleotides, DNA, enantiomers, carbohydrates, vitamins, inorganic ions, pharmaceuticals and environmental pollutants have been demonstrated. A wide range of applications have been developed in greatly diverse fields, such as chemical, biotechnological, environmental and pharmaceutical analysis.

This book covers all aspects of CE, from the principles and technical aspects to the most important applications. It is intended to meet the growing need for a thorough and balanced treatment of CE. The book will serve as a comprehensive reference work and can also be used as a textbook for advanced undergraduate and graduate courses. Both the experienced analyst and the newcomer will find the text useful.

Contents:

1. Introduction. Historical Background. Overview of High Performance CE. Principles of Separations. Comparison with Other Separation Techniques. **2. Sample Injection Methods.** Introduction. Electrokinetic Injection. Hydrodynamic Injection. Electric Sample Splitter. Split Flow Syringe Injection System. Rotary Type Injector. Freeze Plug Injection. Sampling Device with Feeder. Microinjectors. Optical Gating. **3. Detection Techniques.** Introduction. UV-Visible Absorbance Detectors. Photodiode Array Detectors. Fluorescence Detectors. Laser-based Thermooptical and Refractive Index Detectors. Indirect Detection. Conductivity Detection. Electrochemical Detection. Mass Spectrometric Detection. **4. Column Technology.** Uncoated Capillary Columns. Coated Columns. Gel-filled Columns. Packed Columns. Combining Packed and Open-Tubular Column. **5. Electrophoretic Media.** Electrophoretic Buffer Systems. Micellar Electrokinetic Capillary Chromatography. Inclusion Pseudophases. Metal-complexing Pseudophases. Other Types of Electrophoretic Media. **6. Special Systems and Methods.** Buffer Programming. Fraction Collection. Hyphenated Techniques. Field Effect Electroosmosis. Systematic Optimization of Separation. **7. Applications of CE.** Biomolecules. Pharmaceutical and Clinical Analysis. Inorganic Ions. Hydrocarbons. Foods and Drinks. Environmental Pollutants. Carbohydrates. Toxins. Polymers and Particles. Natural Products. Fuel. Metal Chelates. Industrial Waste Water. Explosives. Miscellaneous Applications. **8. Recent Advances and Prospect for Growth.** Recent Reviews in CE. Advances in Injection Techniques. Novel Detection Techniques. Advances in Column Technology. Progress on Electrolyte Systems. New Systems and Methods. Additional Applications Based on CE. Future Trends. **References. Index.**

1992 608 pages Hardbound
US$ 225.75 / Dfl. 395.00
ISBN 0-444-89433-0
1993 608 pages Paperback
Price: US$ 114.25 / Dfl. 200.00
ISBN 0-444-81590-2

"Everything seems to be there, any detection system you have ever dreamed of, any capillary coating, enough electrolyte systems to saturate your wits, and more..."

"...by far the most thorough and comprehensive book in the field yet to appear."

P.G. Righetti, Milan

ORDER INFORMATION

For USA and Canada
ELSEVIER SCIENCE PUBLISHERS
Judy Weislogel,
P.O. Box 945
Madison Square Station,
New York, NY 10160-0757
Fax: (212) 633 3880

In all other countries
ELSEVIER SCIENCE PUBLISHERS
P.O. Box 211,
1000 AE Amsterdam
The Netherlands
Fax: (+31-20) 5803 705

US$ prices are valid only for the USA & Canada and are subject to exchange rate fluctuations; in all other countries the Dutch guilder price (Dfl.) is definitive. Customers in the European Community should add the appropriate VAT rate applicable in their country to the price(s). Books are sent postfree if prepaid.

ELSEVIER
SCIENCE PUBLISHERS

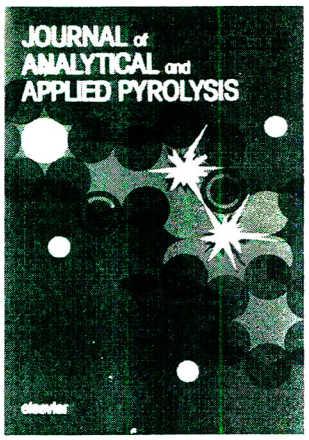

JOURNAL OF ANALYTICAL AND APPLIED PYROLYSIS

Audience

Analytical Chemists; Researchers involved in Chromatography, Mass Spectrometry, and Polymer Science; Geochemists, Technologists in Plastic and Rubber Industries; Bacteriologists; Food and Medical Chemists.

AIMS AND SCOPE

The international *Journal of Analytical and Applied Pyrolysis* is devoted to the publication of qualitative and quantitative results relating to: Controlled thermal degradation and pyrolysis of technical and biological macromolecules; environmental, geochemical, biological and medical applications of analytical pyrolysis; basic studies in high temperature chemistry, reaction kinetics and pyrolysis mechanisms; pyrolysis investigations of energy related problems, fingerprinting of fossil and synthetic fuels, coal extraction and liquefaction products.

ABSTRACTED/INDEXED IN: Analytical Abstracts, Biological Abstracts, Chemical & Earth Sciences, Chemical Abstracts, Current Contents/Physical, Mass Spectrometry Bulletin, Science Citation Index.

SUBSCRIPTION INFORMATION

1993: Volumes 24-26 in 9 issues

Dfl. 1098.00 / US $ 627.50 (including postage)

ISSN 0165-2370

CHROM

I would like ☐ a free sample copy of Journal of Analytical and Applied Pyrolysis.

☐ Instructions to Authors.

☐ to enter a subscription for 1993. Please send me a Proforma Invoice.

Name _____

Address _____

_____

_____

The Dutch Guilder price (Dfl.) is definitive. US$ prices are for your convenience only and are subject to exchange fluctuations. Customers in the European Community should add the appropriate VAT rate applicable in their country to the price(s).

Elsevier Science Publishers
Attn. Carla G.C. Stokman
P.O. Box 330, 1000 AH Amsterdam
The Netherlands
Fax: (+31-20) 5862 845

In the USA & Canada
Attn. Judy Weislogel
P.O. Box 945, Madison Square Station
New York, NY 10160-0757, USA
Fax: (212) 633 3880

711\414\144\178\3

PUBLICATION SCHEDULE FOR THE 1994 SUBSCRIPTION

Journal of Chromatography A and *Journal of Chromatography B: Biomedical Applications*

MONTH	O 1993	N 1993	D 1993	
Journal of Chromatography A	652/1 652/2 653/1	653/2 654/1 654/2 655/1	655/2 656/1 + 2 657/1 657/2	The publication schedule for further issues will be published later.
Bibliography Section				
Journal of Chromatography B: Biomedical Applications				

INFORMATION FOR AUTHORS

(Detailed *Instructions to Authors* were published in Vol. 609, pp. 437–443. A free reprint can be obtained by application to the publisher, Elsevier Science Publishers B.V., P.O. Box 330, 1000 AH Amsterdam, Netherlands.)

Types of Contributions. The following types of papers are published: Regular research papers (Full-length papers), Review articles, Short Communications and Discussions. Short Communications are usually descriptions of short investigations, or they can report minor technical improvements of previously published procedures; they reflect the same quality of research as Full-length papers, but should preferably not exceed five printed pages. Discussions (one or two pages) should explain, amplify, correct or otherwise comment substantively upon an article recently published in the journal. For Review articles, see inside front cover under Submission of Papers.

Submission. Every paper must be accompanied by a letter from the senior author, stating that he/she is submitting the paper for publication in the *Journal of Chromatography A* or *B*.

Manuscripts. Manuscripts should be typed in **double spacing** on consecutively numbered pages of uniform size. The manuscript should be preceded by a sheet of manuscript paper carrying the title of the paper and the name and full postal address of the person to whom the proofs are to be sent. As a rule, papers should be divided into sections, headed by a caption (*e.g.*, Abstract, Introduction, Experimental, Results, Discussion, etc.) All illustrations, photographs, tables, etc., should be on separate sheets.

Abstract. All articles should have an abstract of 50–100 words which clearly and briefly indicates what is new, different and significant. No references should be given.

Introduction. Every paper must have a concise introduction mentioning what has been done before on the topic described, and stating clearly what is new in the paper now submitted.

Experimental conditions should preferably be given on a *separate* sheet, headed "Conditions". These conditions will, if appropriate, be printed in a block, directly following the heading "Experimental".

Illustrations. The figures should be submitted in a form suitable for reproduction, drawn in Indian ink on drawing or tracing paper. Each illustration should have a legend, all the *legends* being typed (with double spacing) together on a *separate sheet*. If structures are given in the text, the original drawings should be supplied. Coloured illustrations are reproduced at the author's expense, the cost being determined by the number of pages and by the number of colours needed. The written permission of the author and publisher must be obtained for the use of any figure already published. Its source must be indicated in the legend.

References. References should be numbered in the order in which they are cited in the text, and listed in numerical sequence on a separate sheet at the end of the article. Please check a recent issue for the layout of the reference list. Abbreviations for the titles of journals should follow the system used by *Chemical Abstracts*. Articles not yet published should be given as "in press" (journal should be specified), "submitted for publication" (journal should be specified), "in preparation" or "personal communication".

Vols. 1–651 of the *Journal of Chromatography*; *Journal of Chromatography, Biomedical Applications* and *Journal of Chromatography, Symposium Volumes* should be cited as *J. Chromatogr.* From Vol. 652 on, *Journal of Chromatography A* (incl. Symposium Volumes) should be cited as *J. Chromatogr. A* and *Journal of Chromatography B: Biomedical Applications* as *J. Chromatogr. B*.

Dispatch. Before sending the manuscript to the Editor please check that the envelope contains four copies of the paper complete with references, legends and figures. One of the sets of figures must be the originals suitable for direct reproduction. Please also ensure that permission to publish has been obtained from your institute.

Proofs. One set of proofs will be sent to the author to be carefully checked for printer's errors. Corrections must be restricted to instances in which the proof is at variance with the manuscript. "Extra corrections" will be inserted at the author's expense.

Reprints. Fifty reprints will be supplied free of charge. Additional reprints can be ordered by the authors. An order form containing price quotations will be sent to the authors together with the proofs of their article.

Advertisements. The Editors of the journal accept no responsibility for the contents of the advertisements. Advertisement rates are available on request. Advertising orders and enquiries can be sent to the Advertising Manager, Elsevier Science Publishers B.V., Advertising Department, P.O. Box 211, 1000 AE Amsterdam, Netherlands; courier shipments to: Van de Sande Bakhuyzenstraat 4, 1061 AG Amsterdam, Netherlands; Tel. (+31-20) 515 3220/515 3222, Telefax (+31-20) 6833 041, Telex 16479 els vi nl. *UK*: T.G. Scott & Son Ltd., Tim Blake, Portland House, 21 Narborough Road, Cosby, Leics. LE9 5TA, UK; Tel. (+44-533) 753 333, Telefax (+44-533) 750 522. *USA and Canada*: Weston Media Associates, Daniel S. Lipner, P.O. Box 1110, Greens Farms, CT 06436-1110, USA; Tel. (+1-203) 261 2500, Telefax (+1-203) 261 0101.

Reversed Phase CHIRAL HPLC Column

NEW CHIRALCEL® OD-R

Indapamide

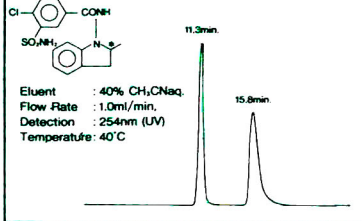

Eluent : 40% CH_3CNaq.
Flow Rate : 1.0ml/min.
Detection : 254nm (UV)
Temperature : 40°C

Verapamil

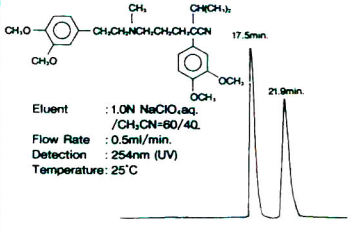

Eluent : 1.0N $NaClO_4$aq. /CH_3CN=60/40.
Flow Rate : 0.5ml/min.
Detection : 254nm (UV)
Temperature : 25°C

Hydroxyzine

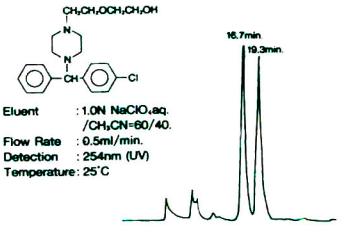

Eluent : 1.0N $NaClO_4$aq. /CH_3CN=60/40.
Flow Rate : 0.5ml/min.
Detection : 254nm (UV)
Temperature : 25°C

Propranolol

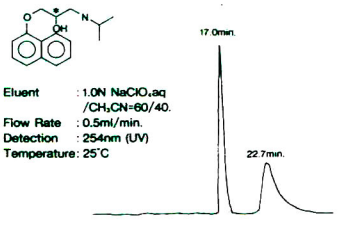

Eluent : 1.0N $NaClO_4$aq /CH_3CN=60/40.
Flow Rate : 0.5ml/min.
Detection : 254nm (UV)
Temperature : 25°C

Pindolol

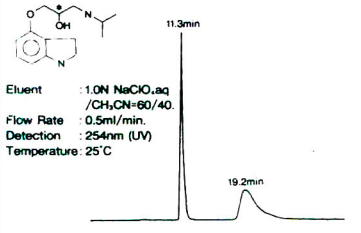

Eluent : 1.0N $NaClO_4$aq /CH_3CN=60/40.
Flow Rate : 0.5ml/min.
Detection : 254nm (UV)
Temperature : 25°C

1-Phenoxy-2-Propanol

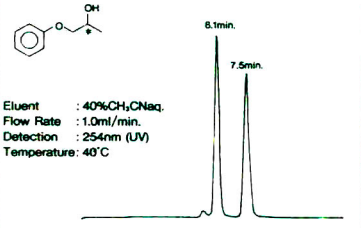

Eluent : 40%CH_3CNaq.
Flow Rate : 1.0ml/min.
Detection : 254nm (UV)
Temperature : 40°C

Alimemazine

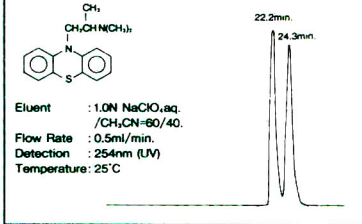

Eluent : 1.0N $NaClO_4$aq. /CH_3CN=60/40.
Flow Rate : 0.5ml/min.
Detection : 254nm (UV)
Temperature : 25°C

Trimepramine

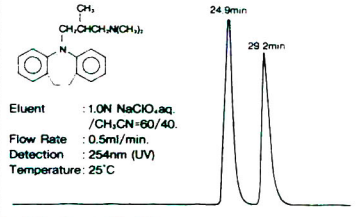

Eluent : 1.0N $NaClO_4$aq. /CH_3CN=60/40.
Flow Rate : 0.5ml/min.
Detection : 254nm (UV)
Temperature : 25°C

4-Pheny-2-butanol

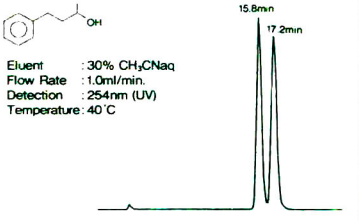

Eluent : 30% CH_3CNaq
Flow Rate : 1.0ml/min.
Detection : 254nm (UV)
Temperature : 40°C

CBZ-Val.

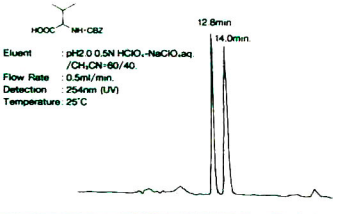

Eluent : pH2.0 0.5N $HClO_4$-$NaClO_4$aq. /CH_3CN=60/40.
Flow Rate : 0.5ml/min.
Detection : 254nm (UV)
Temperature : 25°C

3-Phenylbutyric acid

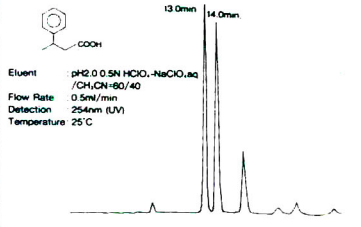

Eluent : pH2.0 0.5N $HClO_4$-$NaClO_4$aq /CH_3CN=60/40
Flow Rate : 0.5ml/min
Detection : 254nm (UV)
Temperature : 25°C

2-Phenylbutyric acid

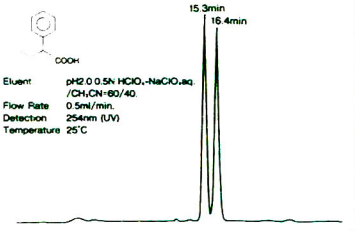

Eluent : pH2.0 0.5N $HClO_4$-$NaClO_4$aq. /CH_3CN=60/40.
Flow Rate : 0.5ml/min.
Detection : 254nm (UV)
Temperature : 25°C

For more information about CHIRALCEL OD-R column, please give us a call.

DAICEL CHEMICAL INDUSTRIES, LTD.
CHIRAL CHEMICALS DIVISION 8-1, Kasumigaseki 3-chome, Chiyoda-ku, Tokyo 100, JAPAN
Phone: +81-3-3507-3151 Facsimile: +81-3-3507-3193

AMERICA
CHIRAL TECHNOLOGIES, INC.
730 SPRINGDALE DRIVE
DRAWER I EXTON, PA 19341
Phone: 215-594-2100
Facsimile: 215-594-2325

EUROPE
DAICEL (EUROPA) GmbH
Ost Street 22
4000 Düsseldorf 1, Germany
Phone: +49-211-369848
Facsimile: +49-211-364429

ASIA/OCEANIA
DAICEL CHEMICAL (ASIA) PTE. LTD.
65 Chulia Street #40-07
OCBC Centre, Singapore 0104.
Phone: +65-5332511
Facsimile: +65-5326454